

“Investigations on gas permeation and related physical properties of structurally architected aromatic polymers (polyphenylene oxides and polyarylates), polyarylate-clay nanocomposites and poly(ionic liquid)”

Thesis submitted to the

UNIVERSITY OF PUNE

For the degree of

DOCTOR OF PHILOSOPHY

IN CHEMISTRY

BY

YOGESH S. BHOLE

Research Guide

Dr. Ulhas K. Kharul

POLYMER SCIENCE AND ENGINEERING DIVISION

NATIONAL CHEMICAL LABORATORY

PUNE-411008, INDIA

June 2007

Dedicated to my mother

Acknowledgements

I take this opportunity to express my respect to my guide Dr. Ulhas Kharul who introduced me to a fascinating world of membrane science and technology. I am grateful to him for giving me liberty in the work and for continuous encouragement during the course of the present study. His technical and personal guidance has been invaluable in making me become a better professional and person. Apart from science I have learned various aspects of life from him. Although this acclamation is insufficient, I preserve an everlasting gratitude for him.

I wish to place on record my sincere thanks to Dr. B. D. Kulkarni, Deputy Director & Head Chemical Engineering Division, for their constant support and encouragement. He has placed a major influence on me during the period of my thesis.

I'm grateful to Dr. S. Sivaram and Dr. P. Ratnasamy, present and past directors of NCL, respectively, for giving me the opportunity to work in this institute and making all the facilities available for my research work.

It gives me great pleasure to thank Dr (Mrs). J. P. Jog, Dr. W. P. Harkare, Dr. C. Ramesh, Mr. K. V. Pandare, Dr. K. R. Patil, Mr. A. B. Gaikwad, Mrs. Dhoble, Dr. (Mrs). Mayadevi, Dr. P. P. Wadgaonkar, Dr. (Mrs). Neelima Bulakh, Dr. S. D. Patil, Dr. Guruswamy for their guidance, valuable suggestions and allowing me to use all facilities.

My thanks are duly acknowledged to CSIR, New Delhi for their valuable support in the form of a Senior Research Fellowship.

Life wouldn't have been better without my closest Harshada, Santosh, Vijay, Dr. Rahul shingte, Dr. Santosh Mhaske, Vivek Borkar, Swaraj Singh. They are and will be always close to my heart. At this moment I can not forget all my lab members Savita, Ganpat, Vahida, Moreshware, Snandeeep, Manoj, Ravi, Pinak, Narayan, Prasad, Anita, Nazrul and Pankaj. Support of Harshada, Santosh and Prasad in terms of various instrumental analyses is unforgettable. With much pleasure I thank to my friends Santosh wangale, Yogesh chendake, Manisha, Sudhir, Nana, Aniruddha, Jiten, Vaishali, Dr. Rodney Fernandez, Dr. Rajesh Pandey, Dr. Jainy kuriakose, Dr. Pankaj Pawar, Dr. Jitendra Pandey for being with me during moments of both success and despair.

I am blessed with a very caring and loving family. The highest recognition goes to my mother, whose hopeful disposition, timely encouragement and deep faith in her god has motivated me to persevere and properly prioritize my life. This thesis was not possible without the love and constant encouragement from my grand parents, little brother Sachin and blessings of my late father.

Certificate of Guide

Certified that the work incorporated in the thesis entitled “**Investigations on gas permeation and related physical properties of structurally architected aromatic polymers (polyphenylene oxides and polyarylates), polyarylate-clay nanocomposites and poly(ionic liquid)**” submitted by Yogesh Suresh Bhole was carried out under my supervision. Such material as has been obtained from other sources has been duly acknowledged in this thesis.

June, 2007

Pune

U. K. Kharul

(Research Guide)

Declaration by the Candidate

I declare that the thesis entitled “**Investigations on gas permeation and related physical properties of structurally architected aromatic polymers (polyphenylene oxides and polyarylates), polyarylate-clay nanocomposites and poly(ionic liquid)**” is my own work conducted under the supervision of Dr. U. K. Kharul, at Polymer Science and Engineering Division, National Chemical Laboratory, Pune. I further declare that to the best of my knowledge, this thesis does not contain any part of work, which has been submitted for the award of any degree either of this University or any other University without proper citation.

Research Guide

(U. K. Kharul)

Student

(Y. S. Bhole)

Contents

*	Abstract	i
*	List of Tables	v
*	List of Schemes	vii
*	List of Figures	viii

Chapter 1 Literature survey: Theoretical considerations, factors affecting gas permeation properties and various methodologies employed to improve gas permeation properties

1.1	Gas transport through polymeric membranes	1
1.2	Gas sorption and transport in glassy polymers	3
1.3	Factors effecting gas permeation properties in glassy polymers	5
1.3.1	Effect of polymer properties	5
1.3.1.1	Free Volume	5
1.3.1.2	Chain Mobility	6
1.3.1.3	Segmental packing	7
1.3.1.4	Polarity	7
1.3.1.5	Crosslinking	7
1.3.1.6	Crystallinity	8
1.3.2	Effect of penetrant properties on permeability and permselectivity	8
1.3.2.1	Condensability of gas molecules	8
1.3.2.2	Size and shape of gas molecules	8
1.3.3	Effects of membrane preparation parameters	9
1.3.4	Effect of temperature and pressure	10
1.4	Various strategies for improving permeation properties	12
1.4.1	Polymer structure modification	12
1.4.1.1	Systematic structural modification of monomers	12
1.4.1.2	Polymer modification	20
1.4.1.3	Membrane surface modification	21
1.4.1.4	Plasma modification	22
1.4.1.5	Crosslinking	23

1.4.2	Polymer blends and composites	23
1.4.2.1	Polymer blends	23
1.4.2.2	Polymer composites containing inorganic fillers	25
1.4.2.3	Polymer composites with low molecular weight organic molecules	27
1.4.2.4	Carbon membranes derived from organic polymers	27
1.4.3	Physical modification of membranes	29
1.4.3.1	Annealing	29
1.4.3.2	Track etching	29
1.4.4	Efforts to selectively improve the permeation properties of desired gas	29
1.4.5	Predictive techniques for gaseous transport in polymers	31
	References	32
<hr/>		
Chapter 2	Scope and objectives of the present work	39
<hr/>		
Chapter 3	Structural modifications in Polyphenylene oxide (PPO): Effects of substituents possessing simultaneous bulk and polarity	
<hr/>		
3.1	Introduction and Literature survey	42
3.1.1	Ring substitution	42
3.1.2	Substitution at -CH ₃	44
3.2	Objectives	45
3.3	Experimental	46
3.3.1	PPO synthesis	47
3.3.2	Benzoylation of PPO	47
3.3.3	Nitration of PPO	48
3.3.4	Amination of PPO	49
3.3.5	Amide group substitution on PPO	49
3.3.6	Dense Membrane preparation	50
3.3.7	Polymer characterization	50
3.3.8	Determination of equilibrium sorption and permeability of gases	51
3.3.8.1	Measurement of gas permeability	51

3.3.8.2	Sorption equipment and procedure	52
3.4	Results and discussion	53
3.4.1	Polymer synthesis and modification	53
3.4.1.1	PPO synthesis	53
3.4.1.2	Benzoylation of PPO	54
3.4.2	Physical properties of benzoylated PPO	55
3.4.2.1	Spectral properties	55
3.4.2.2	Chain degradation after benzoylation	58
3.4.2.3	Solubility	58
3.4.2.4	Thermal characterizations	59
3.4.2.5	Packing density parameters	61
3.4.3	Permeation properties of PPO and benzoylated PPO	62
3.4.4	Nitration, amination and amide group substitution	67
3.4.4.1	Synthesis of nitro and amine group containing PPO	67
3.4.5	Physical properties of nitrated and aminated PPO	69
3.4.5.1	Spectral properties	69
3.4.5.2	Thermal and dynamic mechanical properties	71
3.4.5.3	Packing density parameters	73
3.4.6	Gas sorption properties of PPO-NO ₂ and PPO-NH ₂	74
3.4.7	Permeation properties of nitrated and aminated PPO	77
3.5	Conclusions	82
	References	84

Chapter 4 Investigations in polyarylates: Effect of asymmetric ring substitution on bisphenol and polar/bulky group substitution on acid moiety

4.1	Introduction and Literature survey	87
4.1.1	Effect of substitution on bisphenol moiety	88
4.1.1.1	Effect of bulky non-polar group substitution	88
4.1.1.2	Effect polar group substitution	89
4.1.1.3	Effect of combination of bulky non-polar and polar group substitution	89
4.1.1.4	Effect of bridge substitution	90

4.1.2	Effect of substitution on acid moiety of polyarylate	91
4.1.2.1	Effect of bulky non-polar group substitution	91
4.1.2.2	Effect polar group substituted diacid	91
4.1.2.3	Effect of isomerism in diacid	91
4.1.2.4	Effect of bridge substituted diacid	92
4.2	Objectives	92
4.3	Experimental	93
4.3.1	Monomer synthesis	94
4.3.1.1	Synthesis of dimethylfluorene bisphenol (DMFBP)	94
4.3.1.2	Synthesis of dibromodimethylfluorene bisphenol (DBrDMFBP)	95
4.3.1.3	Synthesis of dibromohexafluorobisphenol-A (DBrHFBisA)	97
4.3.1.4	Synthesis of dibromodimethylbisphenol-A (DBrDMbisA)	98
4.3.2	Structural characterization of as-received bisphenols	99
4.3.3	Preparation of acid chloride	100
4.3.4	Polymer synthesis	101
4.3.4.1	Solution polycondensation	101
4.3.4.2	Interfacial polycondensation	102
4.3.5	Dense membrane preparation	104
4.3.6	Polymer characterizations	104
4.3.7	Determination of equilibrium gas sorption and permeability	105
4.4	Result and discussions	105
4.4.1	Polyarylates bases on asymmetrically substituted bisphenol	105
4.4.1.1	Polyarylates bases on asymmetrically substituted diisopropyl bisphenol-A	106
4.4.1.2	Polyarylates bases on asymmetrically substituted diphenyl bisphenol-A	114
4.4.2	Polyarylates based on fluorene bisphenols and dibromohexafluoro bisphenol-A	121
4.4.2.1	Polyarylates based on systematically substituted fluorene bisphenols	121
4.4.2.2	Polyarylates based on dibromohexafluoro bisphenol-A	127
4.4.3	Polyarylates based on dibromo-terephthalic acid	141
4.4.3.1	Physical properties	141

4.4.3.2 Permeation properties	143
4.5 Conclusions	145
References	148

Chapter 5 Composite membrane materials: Tuning gas permeation properties by using organically modified clay and poly(ionic liquid)

5.1 Polyarylate-clay nanocomposites: preparation, evaluation of physical properties and gas permeability	151
5.1.1 Introduction and literature survey	151
5.1.2 Objectives	152
5.1.3 Experimental	153
5.1.3.1 Materials	153
5.1.3.2 Nanocomposite preparation	154
5.1.3.3 Characterizations	155
5.1.3.4 Permeability determination	155
5.1.4 Results and discussion	156
5.1.4.1 Method of Nanocomposite formation	156
5.1.4.2 X-Ray diffraction and TEM studies	157
5.1.4.3 Dynamic mechanical analysis	160
5.1.4.4 Solution viscosity, nanocomposite density and free volume	161
5.1.4.5 Permeation properties	162
5.1.4.6 Determination of aspect ratio from permeability	165
5.1.5 Conclusions	166
5.2. Poly(ionic liquid): Preparation, sorption analysis and composite membrane investigations	168
5.2.1 Introduction and Literature survey	168
5.2.2 Objectives	169
5.2.3 Experimental	169
5.2.3.1 Materials	169
5.2.3.2 Anion exchange of PVBTMACl	170

5.2.3.3	Characterization	170
5.2.3.4	Dense membrane preparation	171
5.2.3.5	Equilibrium swelling studies	171
5.2.3.6	Preparation of blends	172
5.2.3.7	Preparation of Nafion-PVBTMABF ₄ composite membranes	172
5.2.3.8	Determination of equilibrium gas sorption and permeation	172
5.2.4	Result and discussion	173
5.2.4.1	Preparation of poly(ionic liquid) (PVBTMABF ₄)	173
5.2.4.2	Purification of PIL	173
5.2.4.3	Physical properties of poly(ionic liquid)	174
5.2.4.4	Solvent solubility of PIL	177
5.2.4.5	Gas sorption study of poly(ionic liquid), PVBTMABF ₄	177
5.2.4.6	Comparison of CO ₂ sorption in PIL with other polymers	181
5.2.4.7	Membranes based on PIL	182
5.2.4.8	Permeation properties of nafion and composite membranes	187
5.2.5	Conclusions	189
	References	191
<hr/>		
Chapter 6	Conclusions	195
<hr/>		

Synopsis

List of publications

Abstract

“Investigations On Gas Permeation And Related Physical Properties Of Structurally Architected Aromatic Polymers (Polyphenylene Oxides And Polyarylates), Polyarylate-Clay Nanocomposites and Poly(Ionic Liquid)”

A Thesis submitted by Y.S. Bhole, Univ. of Pune, 2007

This thesis presents investigations in gas permeation properties of polymeric materials while following three promising approaches. The polymer backbone modification in polyphenylene oxide (PPO) and the monomer structural variations in polyarylates enhanced the understanding towards structure-gas permeation property relationship in these polymer families. The polyarylate nanocomposites were examined towards their usefulness in improving selectivity performance. The composite membranes based on polyionic liquid (PIL) were attempted to draw the benefit of high intrinsic CO₂ sorption properties of PILs.

Modification of PPO backbone

Benzoylation of polyphenylene oxide (PPO) was carried out with aromatic acid chlorides bearing specific substituent at *para*-position (methyl, Br, Cl and nitro), which differ in their bulk and polarity. The reaction conditions were optimized individually to simultaneously obtain high degree of substitution and polymer viscosity. The substituted benzoyl group addition on PPO backbone increased T_g, while d-spacing, fractional free volume and thermal stability were decreased. Gas permeability investigations revealed that all the benzoylated PPO exhibited lower permeability, improved O₂/N₂, Ar/N₂ and helium based selectivities, while CO₂ based selectivities were decrease in comparison to unsubstituted PPO. Interestingly, the extent of decrease in permeability followed the trend of increasing molar mass of gases and not the kinetic diameter. The observed trend in variation of permeability by benzoylation was elucidated on the basis of (i) structural variations caused by *p*-substituted benzoyl group and (ii) the degree of benzoylation.

Subsequent to basic inputs obtained after PPO acylation, nitration and amination of PPO were carried out while restricting bulk and maintaining polarity. The nitration reaction of PPO was optimized in such a way that the degree of nitration was high and at

the same time such polymer exhibit high enough viscosity to be able to be transformed into film form to withstand gas pressure during permeability measurements. The reduction of nitro group to amino could be done quantitatively. Both, the nitrated and aminated PPO were amorphous in nature. An increase in chain packing density and chain stiffness, while lowering in fractional free volume and d-spacing in comparison to unsubstituted PPO as a result of induced polarity was observed. Though both, nitro and amino group substitution on PPO led to decrease in gas permeability, selectivity of various gas pairs was increased appreciably. The gas sorption analysis revealed that the reduction in permeability by substitution of NO_2 or NH_2 group was largely contributed by reduction in diffusivity rather than the solubility. Though, solubility selectivity as well as diffusivity selectivity were increased by these polar group substitutions, the nitro group substitution was more effective in improving solubility selectivity while amino group substitution was more effective in improving diffusivity selectivity.

Structural variations in polyarylates using appropriately substituted monomers

The substitution on monomer level in polyarylates examined effects of asymmetric bisphenol substitution (with varying bulk, polarity or flat nature of substituent) and acid substitution (bulk / polarity variations) on physical and gas permeation properties of resulting polyarylates.

The asymmetric substitution by isopropyl or phenyl group on bisphenol-A was studied to evaluate effects of bulky and planar phenyl ring respectively. The polyarylates obtained from these bisphenols with iso/terephthalic acid decreased T_g . The permeability in case of isopropyl substitution increased owing to increase in free volume and d-spacing, while the phenyl substitution led to decrease in gas permeability and increase in selectivity as a result of increased packing density. Effect of incorporation of polar and bulky group in acid moiety in combination with these asymmetric substitution were also investigated.

Fluorene bisphenol based polyarylates were studied for gas permeability and related physical properties to investigate combined effect of bisphenol asymmetric ring substitution and bridge substitution by fused rigid aromatic 9,9'-fluorenylidene group. The nonpolar asymmetric substitution by methyl group in dimethylfluorene bisphenol

based polyarylates led to reduction in permeability, while combination of polar bromine and nonpolar methyl asymmetric group substitution in DBrDMFBP based polyarylate led to increased permeability.

A combination of preferred substitutions to draw an advantage of respective group characteristics was investigated in dibromohexafluoro bisphenol-A based polyarylates. The hexafluoroisopropylidene bridge group of HFBisA is known for improving permeability in various families of polymers. HFBisA was asymmetrically substituted by polar bromine group, to draw an advantage of polar group substitution in asymmetric manner in DBrHFBisA based polyarylates. This bisphenol was polymerized with polar group (NO₂, Br) substituted terephthalic acid, which led to substantial enhancement in selectivity of various gas pairs, while maintaining permeability in such a way that some of these polyarylates lie near Robeson's upper bound.

Dibromo substitution on acid moiety in TPA based polyarylates maintained or slightly decreased T_g in comparison to TPA based polyarylates with same bisphenol. Increased bromine content on the terephthalic acid (i.e. T < DBrT) was accompanied with the decrease in permeability and increase in selectivity.

Composite membranes

Polyarylate-clay nanocomposites were prepared with poly(tetramethylbisphenolA-iso / terephthalate) and two selected clays (montmorillonite 6A and 10A) having different organic modifier by solution intercalation method to investigate effectiveness of nanocomposites towards improving selectivity. With varying clay loading in the polyarylate (3, 5 and 7 % w/w), an increase in disorder of the clay structure, solution viscosity and nanocomposite density indicated polymer-clay interactions. The higher reduction in the T_g of the 10A clay based nanocomposites as compared to 6A based nanocomposites was ascribed to the difference in the clay miscibility with polymer matrix and the nature of organic intercalant present on clay particles. A general decrease in permeability was observed. An increase in He/CH₄ selectivity at 7 % clay loading indicated the usefulness of nanocomposites towards improving selectivity. Aspect ratio for both the types of nanocomposites were estimated based on reduction in He permeability using Neilson's model.

Polymeric ionic liquid (PIL) were prepared by simple ion exchange method. A 95.3 % exchange of chloride anion by BF_4 anion elevated CO_2 sorption capacity. Owing to inability of this PIL to be converted into dense film form, the composite membranes were prepared with dense nafion membrane. A two fold increase in CO_2/N_2 selectivity for this composite membrane in comparison to nafion membrane indicated the usefulness of this approach for improving CO_2 based selectivity while drawing an advantage of high CO_2 sorption capacity of PIL.

List of Tables

Table 3.1	Reaction parameters for PPO benzoylation	55
Table 3.2	Solubility of benzoylated PPO in various solvents at ambient conditions	58
Table 3.3	Physical properties of benzoylated PPO	60
Table 3.4	Permeability (P) ^a coefficients of PPO and benzoylated PPO	63
Table 3.5	Selectivity (α) ^a for different gas pairs of PPO and benzoylated PPO	64
Table 3.6	Properties of gases used for the permeation study of benzoylated PPO	65
Table 3.7	Effect of HNO ₃ : H ₂ SO ₄ volume ratio on nitration of PPO	68
Table 3.8	Physical properties of nitrated and aminated PPO	73
Table 3.9	Dual-mode sorption parameters for PPO, PPO-NO ₂ and PPO-NH ₂ at 6.8 atm pressure and at 35 °C	76
Table 3.10	Apparent solubility coefficient for PPO, PPO-NO ₂ and PPO-NH ₂ at 6.8 atm pressure and at 35 °C	76
Table 3.11	Permeability coefficient (P) of PPO, PPO-NO ₂ and PPO-NH ₂	78
Table 3.12	Selectivity (α) for various gas pairs of PPO, PPO-NO ₂ and PPO-NH ₂	78
Table 3.13	Concentration-averaged diffusivity of PPO, PPO-NO ₂ and PPO-NH ₂ at 6.8 atm pressure and at 35 °C	79
Table 4.1	Monomers used and their abbreviations	93
Table 4.2	Characterization of bisphenols obtained from Aldrich and Honsu chemicals	99
Table 4.3	Structure and abbreviations of acid chlorides used in present investigation	101
Table 4.4	Polyarylates synthesized by solution condensation method	102
Table 4.5	Polyarylates synthesized by interfacial condensation method	103
Table 4.6	Physical properties of DiPrBisA based polyarylates	107
Table 4.7	Gas permeability (P) and selectivity (α) for DiPrBisA based polyarylates	111
Table 4.8	Physical properties of DiPhBisA based polyarylates	115
Table 4.9	Gas permeability (P) and selectivity (α) for DiPhBisA based polyarylates	120
Table 4.10	Physical properties of polyarylates based on fluorene bisphenols	122
Table 4.11	Permeability coefficients (P) and selectivities (α) of polyarylates based on fluorene bisphenols	124

Table 4.12	Physical properties of polyarylates based on DBrHFBisA	127
Table 4.13	Dual-mode sorption parameters of polyarylates at 10 atm and 35 °C	132
Table 4.14	Apparent solubility coefficient and concentration-averaged diffusivity at 10 atm and 35 °C	133
Table 4.15	Permeability (P) coefficients and selectivity (α) for polyarylates based on DBrHFBisA	136
Table 4.16	Physical properties of DBrT based polyarylates	143
Table 4.17	Permeability (P) coefficients and selectivity (α) for DBrT based polyarylates	144
Table 5.1.1	Structural specifications of MMT 6A and 10A	153
Table 5.1.2	Physical properties of nanocomposites with varying percent loading of 6A and 10A clay	156
Table 5.1.3	Permeability coefficient (P) and selectivities (α) for nanocomposites with different percent loading of clays	162
Table 5.2.1	Physical properties of precursor polymer and PIL (PVBTMABF ₄)	176
Table 5.2.2	Solubility of polymers in various solvents	177
Table 5.2.3	Dual-mode sorption parameters for PIL and precursor polymer at 10 atm and at 35 °C	179
Table 5.2.4	Comparison of solubility selectivity of PIL with other glassy polymers	181
Table 5.2.5	Observations of attempted blends of various polymers with PIL	182
Table 5.2.6	Effect of PIL impregnation on weight and dimensional change of nafion membrane	187
Table 5.2.7	Permeability and selectivity of nafion-PIL composite membranes	188

List of Schemes

Scheme 3.1	Oxidative coupling of 2,6-dimethylphenol	47
Scheme 3.2	Benzoylation of polyphenylene oxide	48
Scheme 3.3.	Nitration of polyphenylene oxide	48
Scheme 3.4.	Amination of nitrated polyphenylene oxide	49
Scheme 3.5.	Amidation of aminated polyphenylene oxide	50

List of Figures

Fig.1.1	Time-lag measurement of gas permeation	2
Fig.1.2	Schematic representations of dual-mode sorption	4
Fig.1.3	Pressure dependence of permeability at 35°C [Ghosal (1994)]	11
Fig.3.1	Schematics of gas permeability apparatus	52
Fig.3.2	Schematic of sorption equipment	53
Fig.3.3	¹ H- NMR spectra of benzoylated PPO	56
Fig.3.4	IR spectra of benzoylated PPO (a: PPO, b: PPO-BzH, c: PPO-BzCH ₃ , d: PPO-BzBr, e: PPO-BzCl, f: PPO-BzNO ₂)	57
Fig.3.5	Variation in glass transition temperature (T _g) with the change in solubility parameter (δ) of benzoylated PPO	60
Fig.3.6	TGA spectra of PPO and aryl substituted PPO (a: PPO, b: PPO-BzH, c: PPO-BzCH ₃ , d: PPO-BzBr, e: PPO-BzCl, f: PPO-BzNO ₂)	61
Fig.3.7	Wide angle X- ray spectrum of PPO and benzoyl substituted PPO (a: PPO, b: PPO-BzH, c: PPO-BzCH ₃ , d: PPO-BzBr, e: PPO-BzCl, f: PPO-BzNO ₂)	62
Fig.3.8	Variation of percent reduction in permeability after benzoylation of PPO with degree of substitution (a: PPO-BzBr, b: PPO-BzNO ₂ , c: PPO-BzCl, d: PPO-BzH, e: PPO-BzCH ₃)	66
Fig.3.9	IR spectra of PPO, PPO-NO ₂ , PPO-NH ₂ and PPO-NHCOPh	69
Fig.3.10	¹ H-NMR spectra of PPO and substituted PPO (I: PPO, II: PPO-NO ₂ , III: PPO-NH ₂)	70
Fig.3.11	TGA spectra of PPO-NO ₂ and PPO-NH ₂	71
Fig.3.12	DMA spectra of PPO, PPO-NO ₂ and PPO-NH ₂	72
Fig.3.13	Wide angle X-ray diffraction spectra of PPO, PPO-NO ₂ and PPO-NH ₂	74
Fig.3.14	Sorption isotherms of PPO, PPO-NO ₂ and PPO-NH ₂ for N ₂ , CH ₄ and CO ₂	75
Fig.3.15	Correlation of sorption parameters with Lennard-Jones potential well-depth parameter (— PPO, - - - PPO-NO ₂ , PPO-NH ₂)	77
Fig.3.16	Correlation of diffusivity and solubility with 1/v _f of PPO, PPO-NO ₂ and PPO-NH ₂ (□: CO ₂ , Δ: CH ₄ , ×: O ₂ , o: N ₂)	80
Fig.3.17	Correlation of percent decrease in permeability after PPO substitution	81

	with kinetic diameter of penetrants (\square - PPO-NO ₂ , Δ - PPO-NH ₂)	
Fig.4.1	Repeat unit of polyarylate	87
Fig.4.2	FTIR and ¹ H-NMR spectrum of DMFBP	95
Fig.4.3	FTIR and ¹ H-NMR spectrum of DBrDMFBP	96
Fig.4.4	FTIR and ¹ H-NMR spectrum of DBrHFBisA	97
Fig.4.5	FTIR and ¹ H-NMR spectrum of DBrDMBisA	98
Fig.4.6	WAXD spectra of DiPrBisA based polyarylates	108
Fig.4.7	DMA spectra of DiPrBisA based polyarylates	110
Fig.4.8	Correlation of permeability with v_f of polyarylates (1: DiPrBisA-T, 2: DiPrBisA-NO ₂ I, 3: DiPrBisA-NO ₂ T, 4: DiPrBisA-HFA, 5: DiPrBisA-BuI)	113
Fig.4.9	Correlation of permeability with solubility parameter of polyarylates (1: DiPrBisA-T, 2: DiPrBisA-NO ₂ I, 3: DiPrBisA-NO ₂ T, 4: DiPrBisA-HFA, 5: DiPrBisA-BuI)	114
Fig.4.10	WAXD spectra of DiPhBisA based polyarylates	116
Fig.4.11	DMA spectra of DiPhBisA based polyarylates	118
Fig.4.12	Correlation of gas permeability in DiPhBisA based polyarylates with kinetic diameter of the gas molecules	120
Fig.4.13	WAXD spectra of polyarylates based on fluorene bisphenols	123
Fig.4.14	WAXD spectra of polyarylates based on DBrHFBisA	128
Fig.4.15	DMA spectra of DBrHFBisA based polyarylates	130
Fig.4.16	Sorption isotherms for DBrHFBisA based polyarylates	131
Fig.4.17	Correlation of solubility coefficient with Lennard- Jones potential well depth parameter	134
Fig.4.18	Correlation of solubility coefficient with a) $1/v_f$, b) solubility parameter of polyarylates (1: DBrHFBisA-I+T, 2: DBrHFBisA-BrT, 3: DBrHFBisA-NO ₂ T, 4: DBrHFBisA-HFA, 5: DBrHFBisA-BuI)	135
Fig.4.19	Occurrence of DBrHFBisA based polyarylates on Robeson limiting curve	138
Fig.4.20	Correlation of diffusivity coefficient of different gases with $1/v_f$	139
Fig.4.21	Correlation of diffusivity coefficient of different gases with solubility parameter	140
Fig.4.22	WAXD spectra of DBrT based polyarylates	142
Fig.5.1.1	The structure of monomers and polymer used to prepare	154

polyarylate-clay nanocomposites	
Fig.5.1.2 Wide angle X-ray diffraction spectra for treated and untreated clays	157
Fig.5.1.3a Wide angle X-ray diffraction spectra for polyarylate (PA) and nanocomposites based on 6A clay	158
Fig.5.1.3b Wide angle X-ray diffraction spectra for polyarylate (PA) and nanocomposites based on 10A clay	159
Fig.5.1.4 TEM images of nanocomposites; a: PA-6A ₅ and b: PA-10A ₅	160
Fig.5.1.5 Tan δ curve by DMA of polyarylate (PA) and nanocomposites	161
Fig.5.1.6 Variation of relative permeability (P_c/P_p) with volume fraction (ϕ_f) of 6A based nanocomposites	163
Fig.5.1.7 Variation of relative permeability (P_c/P_p) with volume fraction (ϕ_f) of 10A based nanocomposites	164
Fig.5.2.1 Preparation of poly(ionic liquid)	173
Fig.5.2.2 ESCA of a: PVBTMACl for occurrence of Cl ⁻ in, b: PVBTMABF ₄ for occurrence of boron	174
Fig.5.2.3 FTIR spectra of precursor polymer and PIL	175
Fig.5.2.4 WAXD spectra of 1: PVBTMACl, 2: PVBTMABF ₄ (After water wash)	176
Fig.5.2.5 Gas sorption isotherms of precursor polymer and PIL	178
Fig.5.2.6 Change in solubility and solubility selectivity with respect to pressure	179
Fig.5.2.7 CO ₂ sorption capacities of PVBTMABF ₄ at different pressures a) Present work at (at 35 °C) b) reported literature (at 22 °C)	180
Fig.5.2.8 Chemical structure of Nafion	183
Fig.5.2.9 SEM of cross section of PIL impregnated nafion composite membranes a: Nafion, b: Solvent dipped, c: 24 hours dipped, d: surface image of 36 hours dipped membrane	184
Fig.5.2.10 ATR image of (a) nafion and (b) nafion membrane impregnated with PIL for 36 hours	185
Fig.5.2.11 AFM surface image of a) Nafion b) nafion membrane impregnated with PIL for 36 hours	186

Chapter 1

Literature survey: Theoretical considerations, factors affecting gas permeation properties and various methodologies employed to improve gas permeation properties

1.1 Gas transport through nonporous polymeric membranes

The polymeric materials used for dense membrane preparation are either rubbery (which operate above their glass transition temperature, T_g) or glassy (which operate below their T_g) in nature. It has been noted that the mode of gaseous transport is quite different in the glassy state as compared to the rubbery state. Since at T_g , macromolecules experience increasing cooperative segmental motion along the backbone, elastomers above T_g have increased molecular motion as compared to the glassy polymers. The Henry's Law (Equation 1.1) applies to the gas sorption in rubbery state.

$$C = S \times P \quad (1.1)$$

where C is the concentration of a gas in polymer matrix (cc(STP)/cc polymer), S is the Henry's solubility constant for a given gas-polymer pair (cc(STP)/(cc polymer cmHg) and P is the gas pressure in cmHg. Gas flux through the membrane normally follows Fick's first law.

$$Q = -D(dC/dx) \quad (1.2)$$

where D is the diffusivity and C is the local concentration of a gas in the membrane. The diffusivity normally is concentration independent with some deviations in the case of highly soluble gases. Integration over the membranes thickness, 'Q' yields [Kesting (1993)]:

$$Q = D \frac{(C_1 - C_2)}{l} \quad (1.3)$$

where C_1 and C_2 are the gas concentrations at the high and low pressure surfaces of the membrane, respectively, and l is membrane the thickness. Substituting Equation 1.1 into 1.3 yields:

$$Q = DS \frac{(P_1 - P_2)}{\ell} = P \frac{(p_1 - p_2)}{\ell} \quad (1.4)$$

where p_1 and p_2 are the partial pressures of the gas on the high and low pressure side of the membrane, respectively, and P is the permeability, given by:

$$P = D \times S \quad (1.5)$$

Both, P and D (and thus S) can be determined in a single experiment by measuring the “time lag” for pressure increase on the low pressure side of the membrane.

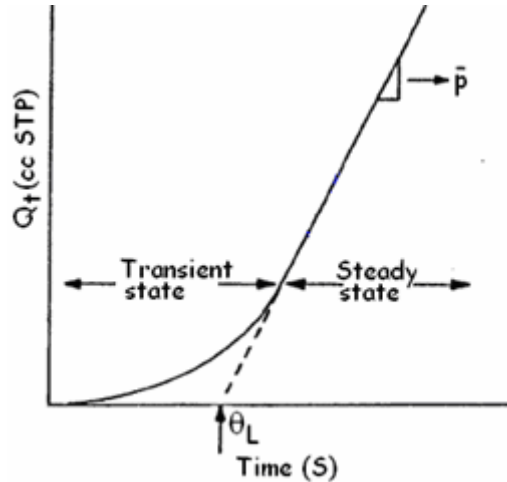


Figure 1.1 Time-lag measurement of gas permeation

The time lag, θ , obtained by extrapolating the linear portion of the pressure versus time function back to the time axis (Figure 1.1) is given by:

$$\theta = \frac{\ell^2}{6D} \quad (1.6)$$

The permeability is given by the slope of the function and solubility can be calculated by equation 1.5. For most permanent gases, the permeability coefficient P is pressure independent for all practical purposes in rubbery polymers. However, for some of the gases with high boiling points at temperatures lower than the critical temperature, permeability increases with pressure due to an increase in the solubility constant. The effects of temperature on diffusivity and solubility of a gas are normally opposite. Usually, diffusivity increases and solubility decreases with increasing temperature. The effect of temperature on permeability is, therefore, a composite of these effects. Under most normally encountered conditions, the effect on diffusivity predominates and

permeability increases with the temperature. However, below some temperature, solubility can become so high, that the effect is reversed. As a rule of thumb, temperature will have a greater effect on the permeability of the gas with the higher diffusion activation energy. Therefore, it is the usual observation that selectivity decreases with increasing temperature. The gas separation selectivity for a given gas pair can be defined as follows:

$$\alpha_{A/B} = P_A / P_B = [D_A / D_B] \times [S_A / S_B] \quad (1.7)$$

where $\alpha_{A/B}$ is the ratio of the permeability of gas *A* to gas *B*. A diffusive and solubility selectivity can also be defined as $[D_A/D_B]$ and $[S_A/S_B]$, respectively.

The gas transport phenomena for rubbery polymers are well defined in terms of Henry's Law of solubility and Fick's laws of diffusion. The relative solubility of the gases is the controlling factor in the selectivity of the rubbery membrane. The mechanical and thermal stabilities of these membranes are not favorable. Moreover, their lower selectivity limits to their use in industrial gas separation application. Though rubbery polymers are not generally used for gas separation, their high permeability is useful to prepare thin film composite membranes with gutter layer between micro porous support and selective layer [Pinnau (1994)].

1.2 Gas sorption and transport in glassy polymers

The process of gaseous diffusion in glassy polymers is known to be more complex than that of rubbery polymers. The reason lies in the inhomogeneity in the polymer matrix due to 'intersegmental packing defects (free volume) frozen into the structure', when the temperature drops below T_g [Kesting (1993)]. A number of statistical models have been developed to explain the transport mechanism in glassy polymers and estimate the parameters *P*, *D* and *S* [(Stern (1994)]. One of the most popular concepts is based on the available free-volume of the system [Vrentas (1977) Petropoulos (1990)]. This type of model suggests that gas permeability not only varies with free volume, but also with its distribution.

The heterogeneity of glassy polymers results in deviations from Henry's Law with respect to linear dependence of concentration with applied pressure. Two types of

sorption sites account for this non-linearity [Vieth (1965)]. The first is called as ‘Henry’s site’ and the second is known as ‘Langmuir’s site’. Henry sorption is the dominant mechanism of sorption into the matrix component and Langmuir sorption dominates in the microvoid region [Tsujita (2003)]. Molecules in Langmuir sites are less mobile than the ones in Henry-type sites. Local equilibrium exists between molecules in Henry and Langmuir sites. The description of gas sorption and diffusion through glassy polymers utilizing two different sites is known as the ‘dual-mode sorption theory’.

Dual-mode sorption is normally described by the sum of these two contributions as follows (Figure 1.2):

$$C = C_D + C_H = k_D p + \frac{C'_H b p}{1 + b p} \quad (1.8)$$

where C = total sorption amount in glassy polymeric membrane, C_D = Henry mode sorption, C_H = Langmuir sorption amount, P = applied gas pressure, k_D = Henry's solubility coefficient, C'_H = Langmuir saturation constant, b = Langmuir affinity constant.

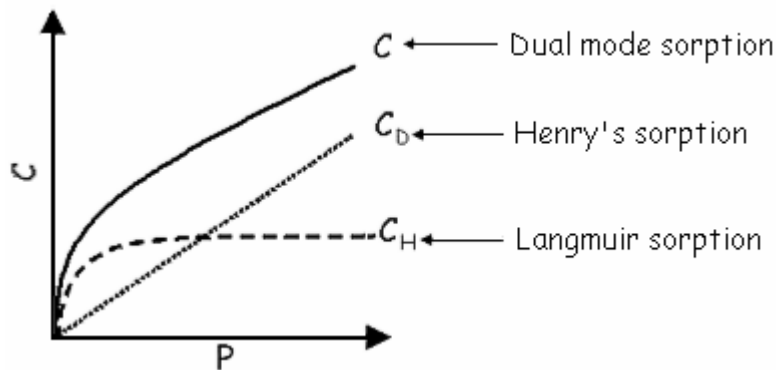


Figure 1.2 Schematic representations of dual-mode sorption

The dual-mode sorption equation (1.8) provides a linear relationship with pressure in the high pressure region [Tsujita (2003)]. The linear slope in the high pressure region corresponds to the Henry's solubility coefficient and the intercept of the extrapolated line to the C axis is the Langmuir saturation constant (Figure 1.2). Based on the gas sorption isotherm obtained experimentally, one can determine the three dual-mode sorption parameters, k_D , C'_H , and b , by curve fitting using a nonlinear least squares method. C'_H is related to the unrelaxed volume (Equation 1.9), which is a measure of the departure from

equilibrium in the glassy state, i.e. the difference between the specific volume of glassy state and liquid states ($V_g - V_l$).

$$C'_H = \left(\frac{V_g - V_l}{V_g} \right) \frac{22400}{V_p} \quad (1.9)$$

where V_p = the molar volume of sorbant gas and C'_H , evaluated from the experimentally determined sorption isotherm. If a gas is polar in nature and condensable, gas sorption may exhibit an anomalous isotherm. For example, some glassy polymers can be plasticized to rubbery state by CO_2 gas owing to their interactions [Wang (1996)]. Thus a linear relationship in the high pressure region does not occur over a wide pressure range, due to the subtle effects of plasticization at high pressure by sorbant gas or vapor.

1.3 Factors effecting gas permeation properties in glassy polymers

Gas permeation and permselectivity performance of polymer depends upon various polymer and penetrant properties as briefed in the following section.

1.3.1 Effect of polymer properties

1.3.1.1 Free Volume

The penetrant diffusivity depends strongly on the polymer fractional free volume, v_f , which is the fraction of total polymer volume that is not occupied by polymer chains themselves. Fractional free volume (v_f) can be estimated by the following equation:

$$v_f = \frac{V - V_w}{V} \quad (1.10)$$

where V ($= M/\rho$) is the molar volume of the structural repeat unit (of molecular weight M) and (ρ) is the measured density. V_w is the van der Waals volume calculated by the group contribution method [Van Krevelen (1972)].

Within a given family of glassy polymers, gas solubility increases with increasing polymer free volume. Solubility is usually a much weaker function of the free volume than diffusivity. Gas diffusion coefficients are typically related to free volume by the following expression [Ghosal (1996)].

$$D = D_0 \exp\left[-\frac{B}{FFV}\right] \quad (1.11)$$

where D_0 and B are constants characteristic of the polymer-penetrant system.

The commonly used methods to determine free volume is based on semi-empirical calculation using experimentally determined density of the polymer and V_w by group contribution method. The positron annihilation lifetime spectroscopy and photochromic and fluorescence technique are also used for determining the v_f [Victor (1987)].

1.3.1.2 Chain Mobility

Chain mobility in the polymer matrix (expressed by various transition temperatures) has direct relationship with penetrant permeability and inverse relationship with selectivity. The emphasis in new material development for gas separation is on improving the selectivity with marginal effects on permeability. It is reported that structural modifications that simultaneously inhibit chain packing and the torsional mobility around flexible linkages in the polymer backbone tend to cause either simultaneous increases in both the permeability and permselectivity, or a significant increase in permeability with negligible loss in permselectivity [Koros (1989)]. Introduction of rigid linkages such as aromatic group decrease the torsional mobility and in turn, reduce penetrant mobility [Ghosal (1994)]. In general, the flexible linkage and the rigid linkage tend to have opposite effect on the diffusivity selectivity of penetrant. Many rigid groups are also polar in nature and act to increase chain-chain cohesive energy density (in addition to increasing intramolecular barriers to segmental motion), which also decreases penetrant diffusion coefficients. Inhibition of the segmental and sub-segmental mobility can be judged by increase in glass transition or sub- T_g temperatures [Koros (1992)]. Typical methods to characterize torsional mobility include dynamic mechanical relaxation spectroscopy, differential scanning calorimetry, dipole relaxation spectroscopy and nuclear magnetic resonance (NMR) [Ghosal (1994)].

1.3.1.3 Segmental packing

Inhibitions to intersegmental packing are reflected by an increase in v_f of the polymer matrix [Koros (1992)]. Sometimes d-spacing obtained from wide angle x-ray diffraction spectra of the amorphous polymer is used to express this effect [Charati (1991)]. The introduction of bulky side groups such as $-CF_3$ in place of $-CH_3$ favors the packing inhibition and therefore increases the diffusion coefficient [Koros (1993)]. Bulky side groups also restrict torsional mobility, which tends to decrease diffusivity.

1.3.1.4 Polarity

Polarity is related to the unevenness of the distribution of electrons about atoms, functional groups or molecules, and cohesive energy density is a measure of expressing the polarity [Kesting (1993)]. The solubility of a polar penetrant such as CO_2 within a polymer is crucial in determining permeation properties and may promote plasticization at high pressure [Koros (1985)]. Van Amerongen et al. [1950] determined gas solubilities in rubbery poly(butadiene-co-acrylonitrile) as a function of polar acrylonitrile group concentration in the polymer. The solubility of non-polar gases such as N_2 , O_2 and H_2 decreased as acrylonitrile concentration increased. However, the solubility of quadrupolar CO_2 increased substantially as acrylonitrile content increased.

Polymer polarity affects quantifiable parameters such as the dielectric constant and the solubility parameter. The solubility parameter (δ) is defined as the square root of the cohesive energy density of the polymer per unit volume [Seymour (1984)]. It can be experimentally determined by either solvent solubility or swelling experiments. It can also be estimated by semi-empirical method [Burrell (1975)] as follows;

$$\delta = \frac{\rho \sum G}{M} \quad (1.12)$$

where ρ is the mass density of the polymer, M is molar mass of the repeat unit and $\sum G$ is the molar attraction constant obtained by the group additivity method.

1.3.1.5 Crosslinking

The crosslinking provide chain irregularity in polymer matrix, since these sites are randomly distributed over the volume of the specimen. This additional constraint

significantly reduces the polymer segmental mobility and thus the diffusion coefficients typically decrease. The effect of crosslinking in various polymers on permeation properties is given in Section 1.4.1.5.

1.3.1.6 Crystallinity

Impermeable crystallites increase the tortuous path for the penetrant molecules through the polymer matrix [Ghosal (1994)]. They may also restrict segmental mobility in the non-crystalline regions of the polymer. Both these effects reduce gas diffusivity. Since crystalline regions reduce both penetrant solubility and diffusivity, thereby reducing permeability. The crystallinity in gas separation membrane materials is generally undesirable. Various techniques have been employed to assess the relative and absolute degree of crystallinity, including X-ray diffraction, density methods, thermal analysis, nuclear magnetic resonance (NMR) and infrared (IR) spectroscopy [He (2000)]. Each technique has its advantages and limitations in terms of crystallinity determination.

1.3.2 Effect of penetrant properties on permeability and permselectivity

1.3.2.1 Condensability of gas molecules

Gas solubility in polymer matrix generally increases with increasing gas condensability [Chern (1985)]. Gas critical temperature, T_c , normal boiling point, T_b or Lennard-Jones force constant represent gas condensability and correlate well with the solubility coefficients of a range of penetrants in a polymer [Ghosal (1994)]. For example, in most polymers, CO_2 ($T_c = 31^\circ\text{C}$) is more soluble than CH_4 ($T_c = -82.1^\circ\text{C}$) and O_2 ($T_c = 118.4^\circ\text{C}$) than N_2 ($T_c = -147^\circ\text{C}$).

1.3.2.2 Size and shape of gas molecules

The diffusion coefficient depends on penetrant size, as characterized by the Van der Waals volume or kinetic diameter of the penetrant. The diffusion coefficients decrease with increasing penetrant size. Diffusion coefficients in polymers are also sensitive to penetrant shape [Ghosal (1994)]. The van der Waals volume can be calculated by geometrical method provided the covalent radius and the van der Waals radius of each atom in the compound are available. However, the van der Waals volume

does not account for the shape of the penetrant. The diffusivity of linear or oblong penetrant molecules such as CO₂ is higher than the diffusivities of spherical molecules of equivalent molecular volume. The Van der Waals volumes of CO₂ and CH₄ are estimated to be 17.5 and 17.2 cm³/mole. These molecular volumes yield equivalent spherical diameters of 3.33 and 3.31 Å for CO₂ and CH₄ respectively. Thus the kinetic diameter is frequently used to characterize the penetrant size [Ghosal (1994)].

1.3.3 Effects of membrane preparation parameters

Owing to non-equilibrium character of glassy polymers, processing conditions employed to make membranes are important while considering the gas transport properties.

Majority of the dense membranes used for evaluation of gas permeation properties are prepared by solution casting technique and the solvent used for making polymer solution can affect the permeation properties. Khulbe et al. [1997] used different solvents for preparing PPO membranes and observed that the permeability increased and the selectivity (O₂/N₂ and CO₂/CH₄) decreased with the increase in the boiling points of the solvents. The membrane morphology and the selectivity performance depends upon properties of the solvents used in preparing polymer solutions, solution concentration, surface (glass, steel, teflon, etc.) on which the membrane is cast, casting techniques (drop casting, blade casting), casting temperature and annealing temperature [Hacarlioglu (2003)]. Small amount of solvent in glassy polymer functions as the plasticizer to increase the chain mobility [Hacarlioglu (2003)]. It was reported that the permeability of PTMSP to helium may vary almost five fold, depending on the solvent used to cast the membrane. In an another example, a melt-extruded polysulfone film was approximately 20% less permeable to CO₂, at 35 °C and 10 atm than a solvent-cast film [Ghosal (1994)]. Previous exposure of a glassy polymer to highly soluble gases (such as CO₂) or organic vapors dilate the non-equilibrium excess volume and, in turn, the Langmuir capacity of glassy polymers, resulting in enhanced solubility [Wonders (1979)]. Upon degassing, the excess volume and excess solubility of the polymer slowly drift back towards their original values. The effect of film casting temperature (from 25-65 °C) in case of PPO using, 1,2-trichloroethylene as solvent was demonstrated [Khulbe (2004)].

The membrane surface morphology and the gas permeation through the membrane were affected by evaporation temperature. The permeation of CO₂, CH₄, O₂ and N₂ decreases as the evaporation temperature increases. However, no significant change was observed on the permeability ratio for gas pairs CO₂/CH₄ and O₂/N₂.

The effect of different film thickness of poly(vinyltrimethyl silane) (PVTMS) and poly(trimethylsilyl norbornene) (PTMSNB) cast from hydrocarbon solutions on permeation properties was demonstrated [Shishatskii (1996)]. For all the gases, diffusion coefficients decreased when film thickness decreased and film density increased. Recently Huang et al. [2007] correlated the effect of film thickness on aging time and consequently gas permeation properties of polysulfone, PPO and Matrimid. The film thickness was varied from 0.4 μm to 60 μm and permeability of O₂, N₂, and CH₄ were monitored for more than a year. Because of volume relaxation due to physical aging, a substantial decrease in permeability was observed with time. The rate of the aging effect was greater with the thinner films.

A sub-T_g, thermal annealing can be used to reduce free volume of glassy polymers, which decreases gas solubility, diffusivity and, in turn, permeability. The annealing temperature and duration of the annealing step controls the amount of excess volume relaxation and, in turn, the attendant decreases in gas solubility and diffusivity [Ghosal (1994)].

1.3.4 Effect of temperature and pressure

The gas diffusivity increases significantly at elevated temperatures. For small gas molecules, such as H₂, N₂, O₂, CH₄; diffusivity is typically more temperature sensitive than solubility. For example, the solubilities of H₂, CH₄ and CO₂ in natural rubber vary less than 30% as temperature changes from 25 to 50 °C [Ghosal (1994)]. Thus, decreases in diffusivity selectivity at higher temperatures often lead to decreases in overall permselectivity. Polyimides are generally regarded as highly thermally stable polymers, but their application temperature is still not high enough. The hydrogen separation from the ammonia synthesis off-gas of Monsanto and Ube Industries demonstrated a H₂ recovery of 90 % with a purity of 95 % can be reached at temperatures up to 120 °C and 150 °C for a top layer of 0.1 and 1.0 μm, respectively [Buys (1990)].

The diffusivity, solubility and, in turn, permeability may vary appreciably as the pressure of penetrant in contact with the polymer changes [Ghosal (1994)]. Examples of permeability isotherms which span the range of typically observed behavior are presented in Figure 1.3 below.

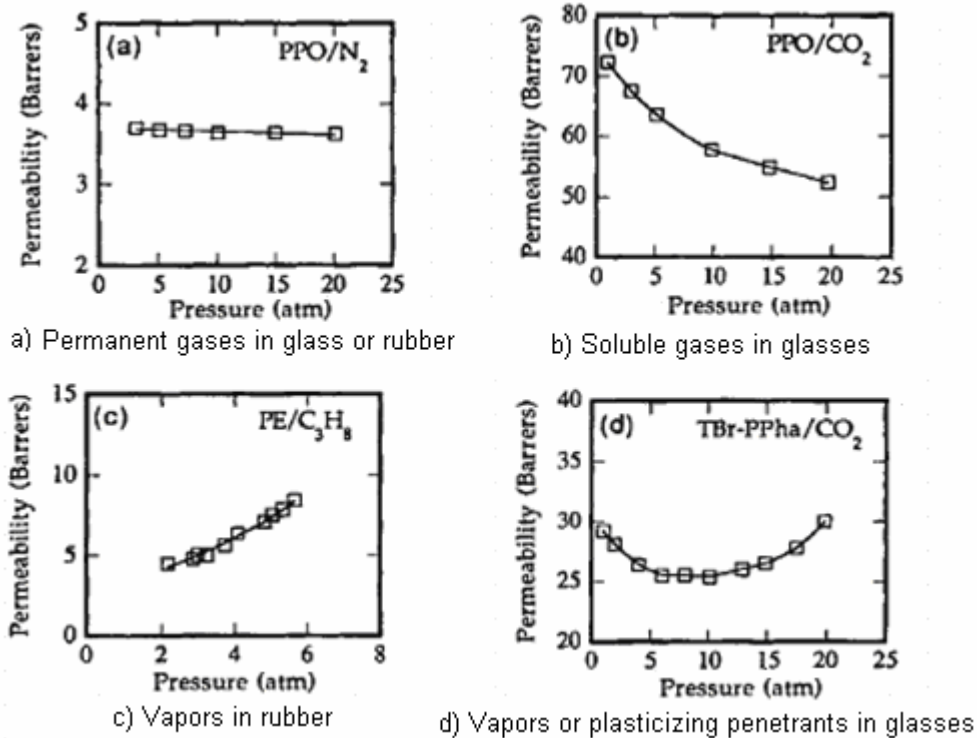


Figure 1.3 Pressure dependence of permeability at 35°C [Ghosal (1994)].

The data presented in Figure 1.3(a) is typical of the pressure dependence on permeability of rubbery or glassy polymers to low sorbing penetrants such as H₂, He, N₂, O₂ and other permanent gases. Figure 1.3(b) shows gas permeability decrease monotonically with increasing pressure as predicted by the dual mode model. This behavior is typically observed in the permeation of glassy polymers to penetrants such as CO₂, which are more soluble in polymers than the other permanent gases.

The permeability of a rubbery polymer to an organic vapor often exhibits an isotherm similar to that presented in Figure 1.3(c). The monotonic increase in permeability is related to concomitant increase in penetrant solubility and diffusivity with increasing pressure,

Figure 1.3(d) may be viewed as a superposition of Figure 1.3(b) and (c) and is typical of the isotherm characterizing the permeability of a glassy polymer to a plasticizing penetrant such as an organic vapor. The polymer permeation properties exhibit dual mode behavior at low pressures and penetrant induced plasticization at high pressures.

1.4 Various strategies for improving permeation properties

A brief overview of various methodologies followed in the literature for improving intrinsic gas permeation properties of polymeric materials is presented in this section. The membrane material investigation for gas separation is directed towards improving intrinsic permeation properties and processability simultaneously; in order to meet current techno-economic challenges and cater diversified demands of separation. Robeson (1991) has proposed correlation between permeability and permselectivity for commercially important gas pairs. A typical inverse relationship between permeability and selectivity (polymers with high permeability tend to have low selectivity and vice versa) though exist, efforts towards betterment of gas permeation properties of various polymers by following various routes are continuously being explored. Some of such efforts are overviewed in the following section.

1.4.1 Polymer structure modification

1.4.1.1 Systematic structural modification of monomers

The structure modifications of the polymer backbone which simultaneously increase chain rigidity and decrease chain packing density have been shown to lead to membranes with improved permeability without significant losses in gas permselectivity [Koros (1989)]. The increase in permeability results from the increases in both diffusivity and solubility, arising from changes in chain packing and torsional mobility. A primary level chemical structure variation of monomers offers a wider spectrum of variation in physical properties of the resulting polymer. Various families of polymers are investigated for effects of monomer level structural variation on physical and gas permeation properties, such as polycarbonate, polysulfone, polyimide, polyarylate, polyamide, etc., as given below.

a) Polycarbonate

In general, polycarbonates have excellent mechanical properties but modest gas separation properties. For example, the permeability of bisphenol-A polycarbonate to CO₂ is 6.8 barrers with CO₂/CH₄ permselectivity of 19 at 35 °C [Hellums (1989)]. The replacement of ortho-aromatic protons of bisphenol with Cl, Br or CH₃ groups resulted in tetrachloro polycarbonate (TCPC), tetrabromo polycarbonate (TBrPC) or tetramethyl polycarbonate (TMPC), respectively [Muruganandam (1987)]. The permeability of TMPC to CO₂ was approximately three times higher than that of unsubstituted PC with marginal decrease in CO₂/CH₄ selectivity. This increase was due to nearly twofold increase in CO₂ diffusivity coupled with a substantial increase in CO₂ solubility. TCPC and TBrPC resulted in reduction of permeability relative to the TMPC, but led to increased selectivity. The decrease in permeability was a consequence of the introduction of stronger cohesive forces owing to polarity, that might resulted in more dense packing and reduced rates of certain group motions [Muruganandam (1987)]. The increased cohesive energy density of the Cl and Br substituted materials relative to TMPC lowers the diffusivity and increases the mobility selectivity with little difference in solubility or solubility selectivity [Koros (1993)]. The solubility selectivities of PC based on tetra-substituted bisphenols were lower than that of unsubstituted PC [Zolandz (1992)].

Hellums et al. [1989] studied gas transport properties of polycarbonates based on hexafluoroisopropylidene moiety at the bisphenol bridge position (TMHFPC). This polymer exhibited CO₂ permeability of 111 barrer vis-à-vis 6.8 barrer for unsubstituted PC coupled with a 26 % increase in permselectivity. The incorporation of the bulky hexafluoroisopropylidene group markedly increased fractional free volume and stiffening of polymer chains, as judged by T_g. Relative to unsubstituted PC, CO₂ diffusivity in TMHFPC was higher by a factor of almost 7. The solubility of CO₂ in this polymer was 2.5 times higher as well, than that in polycarbonate based on nonfluorinated bisphenol.

b) Polysulfone

Effects of structural variations in polysulfone based on ring/bridge substituted bisphenol on their gas permeation and physical properties are well reported. Almost fourfold enhancement in CO₂ permeability of TMPSF relative to the unsubstituted PSF

was observed without an appreciable decrease in selectivity [McHattie (1992)]. The combination of hexafluoroisopropylidene and tetramethyl substituents resulted in further increase in both, CO₂ permeability and CO₂/CH₄ selectivity. On the contrary, dimethyl substitution on bisphenol in polysulfone (DMPSF) resulted in a lower free volume [McHattie (1991a)]. This was attributed to the inability of the methyl groups to increase average chain spacing. As a result of free volume reduction, the permeability of DMPSF was reduced considerably for different gases.

Aitken et al. [1992] reported 4,4'-biphenol based polysulfones (BIPSF) with methyl substitution on phenyl rings of bisphenol (tetramethylbisphenol polysulfone, TMBIPSF and hexamethylbiphenol polysulfone and HMBIPSF). Comparisons were made to unsubstituted bisphenol-A based polysulfone (PSF) and tetramethylbisphenol-A polysulfone (TMPSF). BIPSF and PSF showed very similar transport characteristics. This was attributed to their similar packing behavior. In case of HMBIPSF, permeability increased and the selectivities for some of the gas pairs were higher than those of TMPSF.

In a series of polysulfone, effect of replacement of bisphenol isopropylidene group by hexafluoroisopropylidene (HFPSF), ether (PSF-O) and methylene (PSF-F) linkage on gas permeation properties was reported [McHattie (1991b)]. HFPSF was more permeable than PSF with comparable selectivity. The hexafluoro-isopropylidene sterically hindered both, the bond rotation as well as the intersegmental packing. The packing of HFPSF could also be inhibited by intermolecular repulsive forces between fluorine atoms, which are areas of high electron density. The PSF-F and PSF-O showed similar transport properties due to similarities in size and flexibility of the methylene and ether linkages.

Vega et al. [1993a] reported that replacement of a methyl group at the bridge position by a phenyl ring (PSF-AP) offer a small increase in permeability with similar or slightly higher selectivity compared to unsubstituted PSF. Substitution of two locked phenyl rings (fluorene bisphenol based polysulfone, FBPSF) in place of the methyl groups in the connector unit led to almost two fold increase in permeability and solubility coefficients than those observed for unsubstituted PSF.

Pixton et al. [1995] reported gas permeation properties of PSF based on bisphenol containing adamantylidene connector group. These polymers exhibited higher gas

permeability and some increase in permselectivity in comparison to bisphenol A-based PSF.

c) Polyarylate

Polyarylates are prepared by condensing aromatic diol and aromatic dicarboxylic acid. The effect of substitution on these monomers on gas permeation properties of resulting polyarylates is reviewed at the beginning of chapter 4.

d) Polyimide

Aromatic polyimides have excellent thermo-chemical stability, mechanical strength and low dielectric constants and thus are investigated to a greater extent for effects of structural variations in diamine/dianhydride moiety on gas permeation properties. In polyimides containing 4,4'-(hexafluoro-isopropylidene)diphthalic anhydride (6FDA), gas permeation properties were significantly improved because of the rigid molecular structure and the presence of bulky $-CF_3$ group that inhibited efficient chain packing and reduced local segmental mobility [Cao (2002)].

Polyimides containing $-C(CF_3)_2-$ group in its dianhydride unit increased both selectivity and permeability [Kim (1988)]. Not only do the '6F' groups increase chain stiffness, but they also act as molecular spacer to decrease chain packing, resulting in a polymer with greater free volume [Stern (1994)]. As a result of reduced chain packing, a tendency to form charge transfer complexes (CTCs) also weakened, as could be detected by the disappearance of color of the formed polymer [St. Clair (1987)], leading to increased permeability. Dianhydrides incorporating '6F' are generally more effective at enhancing selectivity versus comparable diamines containing '6F' groups [Stern (1994)].

The pendant methyl group on diamine restricted intramolecular rotation while maintaining a highly rigid structure [Tanaka (1992)]. The methyl substituents restrict internal rotation around the bonds between the phenyl rings and the imide rings. The rigidity and non-planar structure of the polymer chain and the bulkiness of methyl groups make chain packing inefficient, resulting in increases in both diffusion and solubility coefficients of the gases.

Langsam et al. [1993] investigated ortho-substituted alkyl diamines and their

effects on gas permeation properties. They demonstrated that an *o*-methyl substituted 9,9-bis(4-aminoaryl)fluorene when condensed with 6FDA, resulted in 5-fold increase in O₂ permeability.

An incorporation of sulfone bridging units to achieve high permselectivity is documented [Kawakami (1995), Hao (1998)]. The effect of polar substituents such as chlorine and fluorine on aromatic rings of diamine was investigated [Hirayama (1996)]. Stern et al. [1997] reported permselectivity for 6FDA based polyimides in combination with phenol containing diamines. The 6FDA/HAB homopolymer exhibited O₂/N₂ selectivity of 9.3 with 1.61 barrer O₂ permeability.

Effect of isomerization in diamine was reported [Stern (1989), Coleman (1990), Kawakami (1995)]. The *meta*-substitution decreased permeability and increased selectivity due to impeded intra and intersegmental motions than *para*- isomer. A comparison between the two isomers, PMDA-4,4'-ODA (*para*) and PMDA-3,3'-ODA (*meta*) was reported by Mi et al. [1993]. The *para*-isomer exhibited T_g of 400 °C, vis-à-vis 287 °C for *meta*-isomer. The *para*-isomer was twice as permeable as its *meta*-isomer.

Tokuda et al. [1997] developed a polyimide (PI-BT-COOMe), contained CO₂ affinitive methyl-carboxyl functionality, which gave higher CO₂/N₂ selectivity. The CO₂/N₂ permselectivity in this case was 52, with CO₂ permeability of 15 Barrer at 25 °C.

e) Polyamide

As a class, aromatic polyamides offer excellent thermo-mechanical and chemical resistance, and can be easily spun into hollow fibers that are appropriate for gas separation [Singh (1999)]. Because polyamides commonly have high cohesive energy density and show an efficient polymer chain packing, they normally exhibit low permeability to small molecules. These authors reported the gas transport properties of polyamides based on IPC derivatives bearing a pendent phenyl group and a hexafluoroisopropylidene (6F) linkage in the main chain. Polymers containing a phenyl pendent group at the 5-position of the isophthaloyl linkage were more permeable than those bearing only a hydrogen atom at this position. An increase in permeability was generally accompanied by decreases in selectivity. In the SO₂-bearing polymer, the addition of a phenyl pendent group hindered chain packing more than in the 6F

containing polyamides. Consequently, permeability coefficients increased more upon addition of a pendent phenyl group in SO₂-containing rather than 6F-containing polyamide.

The synthesis and gas transport properties of aromatic polyamides (PIPAs) based on isophthaloyl chloride (IPC) derivatives bearing pendent groups and hexafluoroisopropylidene (6F) linkages in the main chain are reported [Morisato (1995)]. Polymers containing 6F groups were markedly more permeable and less selective than their sulfonyl analogs. Polymers containing *t*-butyl pendent group at the 5-position of the isophthaloyl linkage were more permeable and less selective than those bearing only a hydrogen atom at this position. The CO₂/CH₄ solubility selectivity of the 6F-containing polymers was similar to values reported for other polymeric materials with similar concentrations of polar carbonyl linkages.

f) Polytriazole and oxazoles

Polytriazole combine good thermal stability and chemical resistance with processability and expected to be a promising polymer for gas separation at elevated temperature [Gebben (1989)]. High separation factors were found for CO₂/CH₄ (62) and for O₂/N₂ (10), with reasonable permeabilities compared to other thermally stable polymers.

The gas permeation properties of aromatic poly-1,2,4-triazole and poly-1,3,4-oxadiazole have been investigated by Hensema et al. [1994]. Various functional groups were incorporated as pendent groups onto the polymer backbone of poly-1,2,4-triazoles and gas permeation appeared to be dependable on the amount of unclosed triazole groups. The highest permeabilities were found for the fully converted poly-1,2,4-triazole. High permeabilities were also found for poly-1,3,4-oxadiazoles, with a 1,1,3-trimethyl-3-phenylindane (PIDA-POD) and a 4,4'(2,2'-diphenyl)hexafluoro-propane (HF-POD) unit in the polymer backbone. Incorporation of a 4,4'-diphenyl ether unit (DPE-POD) resulted in lower permeability but high selectivity.

g) Polybenzimidazole (PBI)

A series of polyalkylenebenzimidazole having longer flexible chain showed higher gas permeability, but lower selectivity than the polymer containing shorter flexible chain [Zhang (1995)]. Pesiri et al. [2003] reported gas permeation properties of PBI at high temperature. The permeance of H₂ increased from 0.09 Barrer at room temperature to over 18 Barrer at 340 °C. The CO₂ transport was also increased significantly with increased temperature, from 0.01 Barrer at 25 °C to 4 Barrer at 340 °C. The selectivity of the CO₂/CH₄ gas pair was reported to be 33 at 250 °C.

Kumbharkar et al. [2006] reported polybenzimidazoles based on 3,3'-diaminobenzidine and *t*-butyl isophthalic acid (PBI-BuI)/4,4'-(hexafluoroisopropylidene) bis(benzoic acid) (PBI-HFA). The increase in permeability of PBI-HFA and PBI-BuI in comparison to PBI-I for various gases was in the range of 10-40 times, with relatively small reduction in selectivity. Since *t*-butyl substitution did not add more flexibility to the main chain, PBI-BuI possessed better diffusivity based selectivities than for PBI-HFA.

h) Poly(ether ketone)

It is known that wholly aromatic poly(ether ketone) is one of the advanced thermoplastics with excellent mechanical property, high thermal stability, solvent resistance and considerable toughness [Chivers (1994)]. Conversely, the poly(ether ketone) is difficult to process by a solution technique due to poor solubility. It is reported that an incorporation of substituent on phenyl rings of poly(ether ether ketone) can improve the solution processability [Handa (1997)]. Poly(ether ether ketone)s substituted with alkyl group exhibited 5-18 fold increase in permeability, and, in some cases, at no loss in permselectivity in comparison to their unsubstituted analogs [Handa (1997)]. The bisphenol-A based poly(ether ether ketone) (PEEKK) membrane reported to be amorphous in nature when prepared from the solution in chloroform [Mohr (1991a)]. The gas sorption and transport properties of a series of PEEKK containing two isopropylidene groups per repeat unit were reported. The substitution of -C(CF₃)₂- for -C(CH₃)₂- units of bisphenol resulted in a stiffer polymer chain, as evidenced by the increase in glass transition temperature. This also opened up the polymer structure, resulting in a higher free volume, higher sorption, diffusion and permeability coefficients for gases. It was

said that, this may reflect the higher free volume and more attractive interactions of the gas molecules with $-C(CF_3)_2-$ units relative to $-C(CH_3)_2-$ units. The free-volume effect does, however, enhanced the rate of diffusion of some gas molecules more than others, which resulted in greater He/CH₄ and CO₂/CH₄ permselectivity.

i) Polyphenylene oxides (PPO)

Among various glassy polymers, poly(2,6-dimethyl-1,4-phenylene oxide) (DMPPPO) has comparatively high gas permeability and moderate selectivity. Vega et al. [1993b] had compared the gas transport properties of the polyphenylene ethers poly(2,6-dimethyl-1,4-phenylene oxide), DMPPPO, and poly(2,6-diphenyl-1,4-phenylene oxide), DPPPO and the thioether poly(1,4-phenylene sulfide), PPS. The material properties and free volume correlations were used to estimate the behavior of the unavailable poly(1,4-phenylene oxide), PPO. It was observed that symmetrical substitution of phenyl groups on the backbone of polyphenylene ether, PDPPO increased the gas transport properties by one order of magnitude relative to the unsubstituted material, PPO. In case of symmetrical methyl substitution, PDMPO, further increase in permeability, apparent diffusion and sorption coefficients were observed. The gas transport coefficients correlated with the fractional free volume of the polymers. PDMPO exhibited the largest fractional free volume and thus gas transport coefficients followed by PDPPO and then PPS. The modifications on PPO backbone and their effect on gas permeation properties are reviewed at the beginning of chapter 3.

j) Polyacetylene

Polyacetylene-based polymers are widely studied for gas and vapor permeation. These amorphous, highly rigid, glassy polymers are characterized by high glass transition temperatures, typically >200 °C, low densities, high fractional free volume and very high gas permeabilities [Pinnau (2004a)].

Poly(1-trimethylsilyl-1-propyne) [PTMSP], which has a high fractional free volume and thus high gas permeabilities, resulted from very high gas solubility and diffusivity coefficients [Toy (2000)]. These presumably derived in part from a very open

polymer matrix and, for diffusivity, interconnectivity of the free volume elements. The high permeabilities of PTMSP were coupled with very low selectivities.

The pure gas permeation properties for a series of di-substituted, amorphous, glassy poly(2-alkylacetylenes), i.e., poly(2-hexyne), poly(2-octyne), poly(2-nonyne), poly(2-decyne) and poly-(2-undecyne) were determined at 35 °C for H₂, CO₂, O₂, N₂, CH₄, C₂H₆, C₃H₈, and *n*-C₄H₁₀ by Pinnau et al. [2004b]. Gas permeability increased by increasing the (i) side-chain length of the polymers and (ii) size and condensability of the penetrants. For example, the nitrogen and *n*-butane permeabilities of poly(2-undecyne) were 2- and 10-fold higher than those of poly(2-hexyne).

Poly(4-methyl-2-pentyne) [PMP] has highest fractional free volume and therefore the highest gas permeability of all known isopropyl-based poly(dialkylacetylenes) [Pinnau (2004a)]. For example, the N₂ permeability of PMP at 35 °C is 1250 Barrer. The high gas permeabilities of PMP resulted from poor polymer chain packing due to alternating rigid double bonds along the main chain and a very bulky, sterically hindered isopropyl side-chain.

1.4.1.2 Polymer modification

Chemical modification of the polymer is widely studied approach in the view of improvements could be obtained in polymer properties in certain directions. Some of the significant polymer families studies in the direction to improve gas permeation properties include polyphenylene oxide (PPO), polysulfone (PSF), polyethersulfone (PES), polyimide(PI), etc; as described below.

Lee et al. [2003] introduced trimethylsilyl (TMS) group onto the phenylene rings of polysulfone (PSf), hexafluoropolysulfone (HFPSf), tetramethylpolysulfone (TMPSf) and tetramethylpoly(phenylsulfone) (TMPPSf) with controlled degree of substitution (DS). Silylation increased gas permeabilities markedly, whereas, the O₂/N₂ permselectivity decreased slightly. The enhanced gas permeability may be associated with both, the loosened chain packing and the increased small-scale local motion by mobile TMS groups. It was concluded that TMS was very effective in improving gas separation properties and its effect was more pronounced at high degree of substitution.

Kamps et al. [1992] demonstrated nitration of polysulfone (PSf) and polyether-sulfone (PES) leading to decrease in the permeability, solubility and diffusivity of CO₂ and CH₄. The selectivity of CO₂/CH₄ pair was improved for PSf by 28% and for PES by 18% in comparison to their unsubstituted counterparts. An increase in free-volume upon nitration accompanied by a decreasing diffusivity for CO₂ and CH₄ emphasized that not only a single factor like the free-volume or a free-volume distribution affects mass transport through polymeric membranes, but main-chain nitration decreases the segmental mobility also.

Guiver et al. [2002] studied the bromination of Matrimid (polyimide). Compared with unmodified polymer, brominated Matrimid exhibited a lower decomposition temperature but an increased T_g, attributable to the decreased chain mobility in the presence of bulky bromine atoms. The brominated polymer exhibited approximately 1.6-fold increase in gas permeability for O₂ and CO₂, with some concurrent decrease in permselectivity of approximately 7-8 % for the O₂/N₂ and CO₂/CH₄ gas pairs.

The effects of amidation on gas permeation properties of polyimide were investigated by Liu et al. [2003]. Gas permeability results suggested that the amidation lowers the gas permeability for all gases, while it improves the gas permselectivities of He/N₂ and O₂/N₂. For the gas pairs of CO₂/N₂ and CO₂/CH₄, the *N,N*-dimethylaminoethylethylamine (DMEA) modified 6FDA-durene/mPDA (50:50) shows enhanced gas permselectivities, whereas the DMEA modified 6FDA-durene exhibited reduced gas permselectivities. Thus experimental results also implied that the effects of amidation on gas permselectivity strongly depend on the polyimide chemical structure.

1.4.1.3 Membrane surface modification

The formation of ultrathin fluorinated layers on the surface of polymeric materials showed promises in improving gas permeation properties [Borisov (1997)]. This process was employed for polyethylene, poly(4-methyl-1-pentene) (PMP), polysulfone, poly(phenylene oxide), PVTMS, PTMSP and polytrimethyl germlypropyne. The concentration of molecular fluorine in the gas mixtures used for the fluorination of polymeric materials was usually in the range 0.02-2.0 %.

The fluorination of PTMSP films raised the O₂/N₂ selectivity from 1.5 to 4-88 with O₂ permeability decrease by a factor of 5-17 depending on the treatment conditions; while it raised the H₂/CH₄ selectivity from 1 to 109 with H₂ permeability decrease by a factor of 3.3 [Langsam (1987)]. After 15 min of treatment, fluorination of a composite membrane with a PMP skin layer of 1.2 μm thickness, the H₂/CH₄ selectivity was increased from 7 to 85. Little improvement occurs for the O₂/N₂ gas pair because these two gases respond similarly to the fluorine treatment due to their similar molecular size and solubility [Mohr (1991b)].

Surface fluorination however did not improve the gas separation properties of some polymeric materials and certain gas pairs [Le Roux (1994c)]. For instance, fluorinated PVTMS membranes with a skin thickness of 7.5 μm did not show improved O₂/N₂ selectivity when compared to the selectivity of the unfluorinated membrane; while an increase in their He/CH₄ and CO₂/CH₄ selectivities was observed.

The surface bromination of the PTMSP led to increased O₂/N₂ selectivity from 1.5 to 3.5, while the oxygen permeability was decreased [Nagai (2001)].

1.4.1.4 Plasma modification

It is well known that plasma polymerization is a suitable method for the preparation of thin and pinhole free films that adhere well to the substrates. The advantage of plasma polymerization is that a thin, robust permselective membrane could be formed, while the enhanced separation is being caused presumably by the increased solubility of O₂ in the deposited layer [Sarofeim (1994)]. It was demonstrated that plasma polymerization of hexamethyldisiloxane on porous polypropylene as a substrate led to the film with O₂ permeability of 5 x 10⁻⁵ cm³/cm².s.cmHg versus O₂ permeability of 1 x 10⁻⁵ without siloxane [Sarofeim (1994)]. Coatings of 4-vinyl pyridine, 2-vinyl pyridine and perfluoro tri-n-butylamine polymers [(Kawakami (1984)] by plasma were found to be effective in increasing the O₂/N₂ permeability ratios of natural rubber from 2 to 5.8 and polydimethylsiloxane from 1.7 to 3.9 respectively due to 4-vinyl pyridine coating.

Stancell and Spencer [Stancell (1972)] investigated the gas permeabilities of composite films prepared by the deposition of plasma polymers from a number of starting monomers on silicone-carbonate (SC) copolymer film. The monomers were divided into

three groups based on their chemical structures (nitrile, vinyl and aromatic types). The H_2 to CH_4 permeability ratio was increased from 0.87 to 33 and the H_2 permeability was decreased by just 20% when benzonitrile was plasma deposited onto a silicone-carbonate copolymer film.

1.4.1.5 Crosslinking

The polymer cross-linking imparted membranes with anti-plasticization, good chemical resistance and even with good long-term performance [Ismail (2003)]. Dudley et al. [2001] studied the crosslinking of polymer blend membranes containing a reactive additive (ethynyl terminated monomer) using a variety of energy sources into integrally skinned asymmetric membranes. Complete conversion of the ethynyl units resulted in the marked improvements in gas selectivity, resistance to chemicals and thermal stability.

Liu et al. [2001] developed room temperature chemical cross-linking for polyimide films for gas separations. It was found that the gas permeability decreased significantly in the order of $CO_2 > N_2 > O_2 > He$, with an increase in the degree of cross-linking; which were mainly attributed to the significant decreases in diffusion coefficients. The permselectivities of He/N_2 and O_2/N_2 increased from 10 to 86 and from 4.1 to 5.9, respectively; but CO_2/N_2 decreased from 12 to 5.4. This suggested that cross-linking approach could be most useful for the application of He/N_2 and O_2/N_2 separation.

Rezac et al. [1997] found that crosslinking of polyimide blend offered increased chemical resistance without decreasing permeability. Staudt-Bickel et al. [1999] synthesized uncross-linked and cross-linked polyimides to investigate the effect of the degree of cross-linking on swelling and plasticization due to CO_2 . An increase in CO_2/CH_4 selectivity from 58 to 87 with increasing degree of cross-linking was observed.

1.4.2 Polymer blends and composites

1.4.2.1 Polymer blends

The blending of polymers that can result in properties not found in a single polymer has attracted considerable attention and number of polymer pairs that form miscible blends have been increasingly investigated. Polymer-polymer interaction can strongly influence not only the gas sorption and transport properties of blends, but also

their mechanical properties [Li (1995)]. Some of the important blends studied in recent past for gas permeation investigations are briefly reviewed here.

Polyimides by itself are interesting candidates as a material for gas separation membranes because of their relatively high permeability combined with a high selectivity for different gas pairs. However, polyimides tend to plasticize in CO₂ environments at lower feed pressures [Kapantaidakis (2003)] and in propylene environments at pressures as low as 1 bar [Krol (2001)]. Blending of a polyimide that is highly susceptible to plasticization with a polymer that hardly plasticizes (PES) presents a simple method to suppress plasticization [Kapantaidakis (1996)].

Matsuyama et al. [1999a] prepared the polyethylenimine/poly(vinyl alcohol) blend membrane and investigated its CO₂/N₂ separation performance. The CO₂ permeance decreased with an increase in CO₂ partial pressure in feed gas, whereas the N₂ permeance was nearly constant. This result showed that only CO₂ was transported by the facilitated transport mechanism. The CO₂ and N₂ permeabilities increased monotonically with the PEI weight percent in the blend membrane. The selectivity increased remarkably with increasing heat-treatment temperature of the membrane. The highest selectivity obtained reached more than 230 when the CO₂ partial pressure was 0.065 atm.

Recently, Yi et al. [2006] studied poly(vinylamine)/poly(ethylene glycol) blend membranes. The gas permeability results showed that membrane crystallinity decreased as poly(ethylene glycol) content increased (upto 15 %), while the permeation rates of CO₂ and CH₄ were increased. The blend membrane with 10 wt. % PEG has the highest pure CO₂ permeation rate of $5.8 \times 10^{-6} \text{ cm}^3 \cdot (\text{STP}) / \text{cm}^2 \cdot \text{s} \cdot \text{cmHg}$ and the highest selectivity of 63.1 at 25 °C and 96 cmHg of feed pressure.

A different approach of blending was studied by Seo et al. [2006] to prepare hybrid polymeric films including a semi-crystalline polymer (Nylon 6) as a barrier phase for gas diffusion, an amorphous polymer (PPO) as a matrix and a compatibilizer for the two. The selectivity of the ternary blend film containing 2 wt. % PSMA (compatibilizer) showed a 2.6 times increase in CO₂/N₂ selectivity with 5 times decreased CO₂ permeability than PPO.

1.4.2.2 Polymer composites containing inorganic fillers

In molecular separations, efforts to explore the utility of incorporating non porous and porous inorganic fillers, such as clay (layered silicates) [Yano (1993), Messersmith (1995), Yano (1997), Khayankarn (2003), Sinha Ray (2003)], layered aluminophosphate [Jeong (2004)], fumed silica [Merkel (2003a), (2003b)], carbon molecular sieves [Vu (2003)], zeolites [Mahajan (2000), Jia (1991), Duval (1993), Gür (1994), Süer (1994), Rojey (1990)], carbon nanotube [Kim (2006)], etc. were reported.

Vu et al. [2003] incorporated carbon molecular sieves (CMSs) into Matrimid and Ultem by pyrolysis of a polyimide (Matrimid 5218) precursor. The CMS membrane with an intrinsic CO₂/CH₄ selectivity of 200 with CO₂ permeability of 44 Barrers and an O₂/N₂ selectivity of 13.3 with an O₂ permeability of 24 Barrers at 35 °C was reported. For Ultem–CMS membrane, a 40 % increase in CO₂/CH₄ selectivity was observed.

Addition of 4A-type zeolite to poly(vinyl acetate) (PVAc) showed slight decrease in O₂ permeability with good increase in O₂/N₂ selectivity [Mahajan (2000)]. Paul et al. [1973] discovered a delayed diffusional time lag effect for CO₂ and CH₄ when they added zeolite 5A in to PDMS. It was observed that there was an immobilizing adsorption of CO₂ and CH₄ by the zeolite 5A that significantly increased the time lag, but had minor effects on the steady-state permeation. Kulprathipanja et al. [1988] reported that the incorporation of silicalite (25 wt. %) into cellulose acetate improved O₂/N₂ selectivity from 3.36 to 4.06. Jia et al. [1991] examined the permeabilities of various gases with the silicalite–PDMS mixed matrix membrane and observed small increase in the permeabilities of faster permeating gases (e.g. O₂ and CO₂), while permeabilities of slow permeating gases penetrants (e.g. N₂ and CH₄) decreased in comparison to pure PDMS with increasing loading of silicalite. The best selectivity for O₂/N₂ was 2.92. The permeability for O₂, on the other hand, increased from 571 to 655 barrer. Duval et al. [1993] examined an array of both, zeolites (5A, silicalite, 13X) and commercial carbon molecular sieves for a range of rubbery polymers (PDMS, ethylene–propylene rubber, etc.). For the CO₂/CH₄ separation using nitrile butadiene rubber (NBR) mixed matrix films with zeolite KY, significant improvement in CO₂/CH₄ selectivity from 13.5 to 35 at 46 vol. % zeolite loading was observed. The enhancement in O₂/N₂ selectivity from 3.0 to 4.7 for ethylene–propylene rubber mixed matrix film with 53 vol. % silicalite. Gür et

al. [1994] used zeolite 13X as a filler in polysulfone, (loadings up to 20 vol. %) and found no significant effects on gas permeabilities. Sürer et al. [1994] found some success in incorporating zeolite 4A into polyethersulfone and showed enhanced O₂/N₂ selectivity from 3.7 to 4.4. Rojey et al. observed significant selectivity enhancement for H₂/CH₄ using flat-sheet membranes containing zeolite 4A dispersed in an Ultem matrix [Jiang (2006)].

Kim et al. [2006] fabricated nano-composite membranes consisting of single-walled carbon nanotubes embedded in a poly(imide siloxane) copolymer and evaluated their gas permeation properties. He permeability was decreased with the addition of close-ended CNTs. This drop in He permeability suggested that the copolymer adhered well to the CNTs and that the membranes prepared were defect free. However, the permeability of O₂, N₂ and CH₄ increased in proportion to the amount of open-ended CNTs in the polymer matrix.

Two effects of inorganic particles in polymer matrix on permeation properties can be described [Kim (2001a)]. First, the strong interaction between polymer and inorganic particle reduces segmental and subsegmental mobility and inhibits segmental packing of polymer. A change in polymer structures contributes to increase in diffusivity (by disrupting interchain packing) and diffusivity selectivity (by increasing polymer backbone stiffness), which plays more important role than the gas solubility. Second, the interaction between the residual -OH groups on the inorganic component and polar gases (such as CO₂ and SO₂) and the morphological changes can give rise to the increase of solubility associated with an increase of the Henry's contribution.

The polyimide/silica nanocomposite membranes investigated by Kusakabe et al. [1996] exhibited superior gas permeability and selectivity especially at high silica content, compared to pure polyimide. However, the poly(amide-imide)/ TiO₂ nanocomposite material studied by Hu et al. [1997] has demonstrated slight increase in selectivity and decrease in permeability when compared with pure poly(amide-imide).

Poly(ethylene oxide-*b*-amide-6) / silicon oxide or titanium oxide organo-inorganic hybride membranes were prepared by hydrolysis or polycondensation of tetraethoxysilane (TEOS), or titanium tetraisopropoxide (TiOP), respectively [Zoppi (2000)]. For films containing silicon oxide as the inorganic filler, gas permeability

decreased as a function of the inorganic component content. When titanium oxide was used as the filler, gas permeability was considerably lower than that measured for films containing silicon oxide (80/20 polymer/inorganic precursor compositions). In these cases, the morphologies were very similar, but films containing titanium oxide were much more rigid. The CO₂/N₂ selectivity was improved from 37.7 to 52.9, while CO₂/H₂ selectivity was decreased to 7 from 9, for 80/20 polymer/TiOP films.

More literature clay-based polymer nanocomposites and their gas permeation properties is given at the beginning of Chapter 5.

1.4.2.3 Polymer composites with low molecular weight organic molecules

The effect of organic additives on the gas permeability and selectivity of is being explored as an effective alternative to redesign the permeability-selectivity balance shown by high free volume, high permeability polymers [Maeda (1987a), (1987b)]. Though, the incorporation of additives increases their selectivity to certain gases, it is accompanied by reduction in permeability. The addition of tricresyl phosphate, *N*-phenyl-2-naphthylamine and 4,4'-dichlorodiphenyl sulfone to polysulfone caused considerable reductions in sorption of CO₂ and thus the permeability at low additive concentration [Maeda (1987a)].

The propensity for various diluents to cause antiplasticization of PPO was examined by Maeda et al. [1987b]. Addition of diluent decreased the CO₂ sorption and the extent of curvature of the isotherm. The permeabilities of He, CO₂, CH₄ for a constant driving pressure of 10 atm for each gas declined up to 30% addition.

Recently, Qiu et al. [2006] reported the addition of nanosized organic filler, trimethylsilylglucose (TMSG) into high free volume Poly(trimethylsilylpropyne) (PTMSP). It was observed that the increasing TMSG content in PTMSP resulted in substantial reduction in gas permeability of He, H₂, CO₂, O₂, N₂ and CH₄, leading to increased selectivities for some gas pairs.

1.4.2.4 Carbon membranes derived from organic polymers

Carbon molecular sieve membranes have been identified as promising candidates, both in terms of gas separation properties and stability [Ismail (2001)]. Carbon molecular

sieves are porous solids that contain constricted apertures that approach the molecular dimensions of diffusing gas molecules. Carbon molecular sieves that are produced from the pyrolysis of polymeric materials have proved to be very effective for gas separation in adsorption applications [Ismail (2001)]. Molecular sieve carbon can be obtained from many thermosetting polymers such as poly(vinylidene chloride) (PVDC), poly(furfuryl alcohol) (PFA), cellulose, cellulose triacetate, saran copolymer, polyacrylonitrile (PAN), phenol formaldehyde and various coals such as coconut shell [Koresh (1980)]. The pore dimensions of carbon depend on morphology of the organic precursor and the chemistry of pyrolysis.

Carbon molecular sieve membranes with pore diameter of 3–5 Å have ideal separation factor ranging from 4 to more than 170 for various combinations of gases [Hsieh (1990)]. The ideal separation factor reported for N₂/SF₆ and He/CO₂ was 4, while it was in the range of 20–40 for He/O₂, He/N₂ and He/SF₆. The ideal separation factor for O₂/N₂, H₂/N₂ and O₂/SF₆ were 8, 10-20 and more than 170, respectively [Hsieh (1990)].

Hatori et al. [1992] prepared porous carbon films from Kapton-polyimide. The flat carbon films prepared by pyrolysis at 800 °C had O₂/N₂ selectivities of 4.6. In another study, carbon molecular sieve membrane obtained by carbonization of a commercial polyimide (polyetherimide) showed O₂/N₂ permselectivity of 7.4 at 25°C [Fuertes (1998a)].

A solution of poly(furfuryl)alcohol (PFA) in acetone was sprayed onto the porous stainless steel in the form of a fine mist using an external mix airbrush with N₂ gas [Acharya (1999)]. The resulting membranes were found to have O₂/N₂ selectivity up to 4 and O₂ as 10⁻⁹ mol.m⁻².Pa⁻¹.s⁻¹.

The permeabilities of selected gases in CMS derived from pyromellitic dianhydride PMDA and ODA were in the order H₂>He>CO₂>O₂>N₂ for the membranes pyrolysed at 1073 and 1273 K [Suda (1995)]. With increasing pyrolysis temperature, the gas permeability decreased but selectivities of various gas pairs increased. For He/N₂ and H₂/N₂ gas pairs, the selectivity reached up to 498 and 900, respectively, for the membrane pyrolysed at 1273 K.

The gas transport through the CMC membrane based on BPDA-pPDA was reported to occur according to an activated mechanism [Fuertes (1998b)].

1.4.3 Physical modification of membranes

1.4.3.1 Annealing

The effect of thermal hysteresis on the polymer chain packing and permeation properties of two 6FDA based polyimide isomers was investigated by Fuhrman et al. [2004]. Quenching from above the glass-transition temperature resulted in a small increase in the fractional free volume and larger increases in the permeabilities with respect to annealed samples. The *meta*-connected 6FDA–6FmDA exhibited a larger increase in the permeability after quenching than the *para*-connected isomer, 6FDA–6FpDA.

The H₂ and CO₂ transport properties of poly(ethylene-2,6-dicarboxylate naphthalene) (PEN) [Hardy (2003)] decreased for thermally crystallized samples. No change in the sorption properties of the amorphous phase was noticed as a function of the thermal treatment and the evaluation of the diffusion coefficient was related to the tortuosity effect.

The heat treatment of the sodium-neutralized poly(ethylene methacrylic acid) ionomers at 160°C increased the gas permeability for O₂ more than for CO₂ and reduced the CO₂/O₂ permselectivity ratio from 4.1 to 1.6 [Al-Ati (2002)].

1.4.3.2 Track etching

A passage of energetic projectile through polymeric film produces cylindrical zones of irreversible chemical and structural changes. The kind of changes depends on the polymer type and irradiation conditions. The tracks create molecular chains breaking (scissioning), crosslinks, free radicals and other radiolytic processes [Fleischer (1975)]. These damaged zones can be converted into useful ion track pore by controlled chemical etching. Recently, Kulshrestha et al. [2006] has reported the track-etched polymer blends of polycarbonate (PC) and polysulphone (PSF) for gas permeation. Gas permeability of H₂ and CO₂ increased with increases etching time.

1.4.4 Efforts to selectively improve the permeation properties of desired gas

Efforts to selectively improve permeation properties of desired gases such as CO₂ are discussed in this section. Kim et al. [2001b] prepared pore-filled membranes using PAN membrane as a support. Methoxy poly(ethylene glycol)acrylate was used as a

filling material, followed by UV-irradiated photografting. A high CO₂/N₂ permselectivity (32) coupled with CO₂ flux of 5.65 GPU was reported. The high CO₂ permselectivity was attributed to the high solubility selectivity owing to the affinity of CO₂ with PEO. The poly(ether imide) films having PEO content of about 70 % displayed high CO₂ permeance (140 Barrer) with a CO₂/N₂ permselectivity of 70 at 25 °C [Okamoto (1995)].

Facilitated transport membranes (FTM) have received a lot of attention in gas separations because they offer higher selectivities and larger fluxes. In addition to the solution-diffusion mechanism of the polymeric membranes [Shekhawat (2003)], FTMs also involve a reversible complex reaction.

Guha et al. [1990] prepared immobilized liquid membranes consisting of aqueous solutions of 20 % diethanolamine (DEA) immobilized in 25.4 µm microporous polypropylene supports. The CO₂ permeabilities decreased from 4,825 to 974 Barrers as the CO₂ partial pressure increased from 12 to 126 cmHg, while CO₂/N₂ separation factors also decreased from 276 to 56 over the same pressure range. In another study, facilitated transport of CO₂ through a thin solution-cast perfluorosulfonic acid ionomer membrane was demonstrated, wherein ethylenediamine (EDA) immobilized in the ionomer membrane by electrostatic forces acted as a CO₂ carrier [Matsuyama (1999b)].

The plasma-grafted acrylic acid onto a microporous polyethylene membrane with ethylenediamine as a carrier for the facilitated transport of CO₂ had a high stability and high selectivity for CO₂ over N₂ (4700 at 0.047 atm) at 25 °C [Matsuyama (1994)]. The stability was attributable to both, the hydrophilicity of the poly(acrylic acid) membrane and the retention of the carrier by electrostatic force. A membrane with amine moiety prepared by plasma-grafting of 2-(*N,N*-dimethyl)aminoethyl methacrylate (DAMA) onto a microporous polyethylene substrate, which exhibited CO₂/N₂ separation factor as high as 130 [Matsuyama (1996)].

Membranes having facilitated transport were synthesized by Quinn et al. [1997] and shown to selectively permeate CO₂ and H₂S from CH₄ and H₂. The membranes based on the polyelectrolyte poly(vinylbenzyltrimethylammonium fluoride), PVBTAF, exhibited exceptional permselective properties. For example, at 23 °C and 32 cmHg CO₂, a PVBTAF composite membrane displayed a CO₂ permeance of $6 \times 10^{-6} \text{ cm}^3/\text{cm}^2 \cdot \text{s} \cdot \text{cm} \cdot \text{Hg}$ and CO₂/H₂ and CO₂/CH₄ selectivities of 87 and 1000, respectively. The permeance of

both, CO₂ and H₂S increased with decreasing feed partial pressure of the respective gases, a characteristic of facilitated transport membranes.

1.4.5 Predictive techniques for gaseous transport in polymers

A scale of numerical values based on polymer cohesive energy density and fractional free volume has been devised to predict permeability and also to estimate diffusion and solubility properties [Salame (1986)]. The method involves a parameter, permachor (π);

$$(\pi) = -(2.3/S) \cdot \log (P/P^*) \quad (1.13)$$

where P* is permeability of N₂ in natural rubber, P is permeability of N₂ in the test polymer, and S is the scaling factor.

Park and Paul have correlated the permeation data by using an empirical modification of a free volume [Park (1997)]. This method improved the accuracy predicting and correlating gas transport properties of glassy polymer membranes.

Robeson et al. [1997] derived a method for predicting gas permeation behavior for aromatic polymers,

$$\ln P = \sum_{i=1}^n \phi_i \ln P_i \quad (1.14)$$

where P = permeability, ϕ_i = volume fraction of a structural unit i and P_i = the permeability contribution of the structural unit. It is said that using existing data and Equation 1.14, solutions can be generated for a particular system by using a least square fit.

References

- Acharya M., Foley H.C. *J. Membr. Sci.* **161** (1999) 1-5.
- Aitken C.L., Koros W.J., Paul D.R. *Macromolecules* **25** (1992) 3651-3658.
- Al-Ati T., Hotchkiss J.H. *J. Appl. Polym. Sci.* **86** (2002) 2811-2815.
- Borisov S., Khotimsky V.S., Rebrov A.I., Rykov S.V., Slovetsky D.I., Pashunin Yu.M. *J. Membr. Sci.* **125** (1997) 319-329.
- Burrell H. Solubility parameter values, in Brandrup J. and Immergu E.H., (eds.), *Polymer Handbook*, 2nd edn., John Wiley, New York, pp. IV (1975) 338-340.
- Buys H.C.W.M., Van Elven A., Jansen A.E., Tinnemans A.H.A. *J. Appl. Polym. Sci.* **41** (1990) 1261-1270.
- Cao C., Wang R., Chung T.S., Liu Y. *J. Membr. Sci.* **209** (2002) 309-319.
- Charati S.G., Houde A.Y., Kulkarni S.S., Kulkarni M.G. *J. Polym. Sci., Part B: Polym. Phys.* **29** (1991) 921-931.
- Chern R.T., Koros W.J., Hopfenberg H.B., Stannett V.T. in *Material Science of Synthetic Membranes*, D. R. Lloyd, (eds.), American Chemical Society (1985).
- Chivers R.A., Moore D.R. *Polymer* **35** (1994) 110-116.
- Coleman M.R., Koros W.J. *J. Membr. Sci.* **50** (1990) 285-297.
- Dudley C.N., Schöberl B., Sturgill G.K., Beckhamb H.W., M.E. Rezac *J. Membr. Sci.* **191** (2001) 1-11.
- Duval J.-M., Folkers B., Mulder M.H.V., Desgrandchamps G., and Smolders C.A. *J. Membr. Sci.* **80** (1993) 189-198.
- Fleischer R.L., Price P.B., Walker R.M. *Nuclear tracks in solids: principals and applications*. Berkeley, CA: University of California Press; 1975.
- Fuertes A.B., Centeno T.A. *Microporous and Mesoporous Materials* **26** (1998) 23-26.
- Fuertes A.B., Centeno T.A. *J. Membr. Sci.* **144** (1998) 105-111.
- Fuhrman C., Nutt M., Vichtovonga K., Coleman M.R. *J. Appl. Polym. Sci.* **91** (2004) 1174-1182.
- Gebben B., Mulder M.H.V., Smolders C.A. *J. Membr. Sci.* **46** (1989) 29-41.

- Ghosal K., Freeman B.D. *Polym. Adv. Tech.* **5** (1994) 673-697.
- Ghosal K., Chern R.T., Freeman B.D. *Macromolecules* **29** (1996) 4360-4369.
- Guha A.K., Majumdar S., Sirkar K.K. *Ind. Eng. Chem. Res.* **29** (1990) 2093-2100.
- Guiver M.D., Robertson G.P., Dai Y., Bilodeau F., Kang Y.S., Lee K.J., Jho J.Y., Won J. *J. Polym. Sci., Part A: Polym. Chem.* **40** (2002) 4193-4204.
- Gür T.M. *J. Membr. Sci.* **93** (1994) 283-289.
- Hacarlioglu P., Toppare L., Yilmaz L. *J. Appl. Polym. Sci.* **90** (2003) 776-785.
- Handa Y.P., Roovers J., Moulinie P. *J. Polym. Sci., Part B: Polym. Phys.* **35** (1997) 2355-2362.
- Hao J., Tanaka K., Kita H., Okamoto K. *J. Polym. Sci., Part A: Polym. Chem.* **36** (1998) 485-494.
- Hardy L., Espuche E., Seytre G., Stevenson I. *J. Appl. Polym. Sci.* **89** (2003) 1849-1857.
- Hatori H., Yamada Y., Shiraishi M., Nakata H., Yoshitomi S. *Carbon* **30** (1992) 305-306.
- He Y., Inoue Y. *Polym. Int.* **49** (2000) 623-626.
- Hellums M.W., Koros W.J., Husk G.R., Paul D.R. *J. Membr. Sci.* **46** (1989) 93-112.
- Hensema E.R., Sena M.E.R., Mulder M.H.V., Smolders C.A. *Gas Sep. Purif.* **8** (1994) 149-160.
- Hirayama Y., Yoshinaga T., Kusuki Y., Ninomiya K., Sakakibara T., Tamari T. *J. Membr. Sci.* **111** (1996) 169-182.
- Hsieh H.P. *Membr. Mater. Proc.* **84** (1990) 1.
- Hu Q., Marand E., Dhingra S., Fritsch D., Wen J., Wilkes G. *J. Membr. Sci.* **135** (1997) 65-79.
- Huang Y., Paul D.R. *Ind. Eng. Chem. Res.* **46** (2007) 2342-2347.
- Ismail A.F., Ridzuan N., Rahman S.A. *Songklanakarin J. Sci. Technol.* **24** (Suppl.) (2002) 1025-1043.
- Ismail A.F., David L.I.B. *J. Membr. Sci.* **193** (2001) 1-18.
- Jeong H-K., Krych W., Ramanan H., Nair S., Marand E., Tsapatsis M. *Chem. Mater.* **16** (2004) 3838-3845.

- Jia M., Peinemann K-V., Behling R-D. *J. Membr. Sci.* **57** (1991) 289-296.
- Jiang L.Y., Chung T.S., Kulprathipanja S. *AIChE J.* **52** (2006) 2898-2908.
- Kamps K.M.P., Teunis H.A., Wessling M., Smolders C.A. *J. Membr. Sci.* **74** (1992) 193-201.
- Kapantaidakis G.C., Kaldis S.P., Dabou X.S., Sakellaropoulos G.P. *J. Membr. Sci.* **110** (1996) 239-247.
- Kapantaidakis G.C., Koops G.H., Wessling M., Kaldis S.P., Sakellaropoulos G.P. *AIChE J.* **49** (2003) 1702-1711.
- Kawakami M., Yamashita Y., Iwamoto M., Kagawa S. *J. Membr. Sci.* **3** (1984) 249-258.
- Kawakami H., Ansai J., Nagaoka S. *J. Appl. Polym. Sci.* **57** (1995) 789-795.
- Kesting R.E., Fritzsche A.L. *Polymeric Gas Separation Membranes*, John Wiley and Sons, Inc., New York, 1993 19-59.
- Khayankarn O., Magaraphan R., Schwank J.W., *J. Appl. Polym. Sci.* **89** (2003) 2875-2881.
- Khulbe K.C., Matsuura T., Lamarche G., Kim H.J. *J. Membr. Sci.* **135** (1997) 211-223.
- Khulbe K.C., Hamad F., Feng C., Matsuura T., Gumi T., Palet C. *Sep. and Purif. Tech.* **36** (2004) 53-62.
- Kim, T.H., Koros W.J., Husk G.R., O'Brien K.C. *J. Membr. Sci.* **37** (1988) 45-62.
- Kim J. H., Lee Y. M. *J. Membr. Sci.* **193** (2001) 209-225.
- Kim J.H., Ha S.Y., Nam S.Y., Rhim J.W., Baek K.H., Lee Y.M. *J. Membr. Sci.* **186** (2001) 97-107.
- Kim S., Pechar T.W., Marand E. *Desalination* **192** (2006) 330-339.
- Koresh J.E., Soffer A. *J. Chem. Soc., Faraday Trans. I* **76** (1980) 2457-2471.
- Koros W.J. *J. Polym. Sci., Phys. Ed.* **23** (1985) 1611-1628.
- Koros W.J., Hellums M.W. *Fluid Phase Equilibria* **53** (1989) 339-354.
- Koros W.J., Coleman M.R., Walker D.R.B. *Annu. Rev. Mater. Sci.* **22** (1992) 47-89.
- Koros W.J., Fleming G.K. *J. Membr. Sci.* **83** (1993) 1-80.
- Krol J.J., Boerrigter M., Koops G.H. *J. Membr. Sci.* **184** (2001) 275-286

- Kulprathipanja S., Neuzil R., Li N. US Patent, 1998, US 4740219.
- Kulshrestha V., Acharya N.K., Awasthi K., Singh M., Avasthi D.K. Vijay Y.K. *Int. J. Hydro. Energy* **31** (2006) 1266-1270.
- Kumbharkar S.C., Karadkar P.B., Kharul U.K. *J. Membr. Sci.* **286** (2006) 161-169.
- Kusakabe K., Ichiki K., Hayashi J., Maeda H., Morooka S. *J. Membr. Sci.* **115** (1996) 65-75.
- Langsam M. U.S. Patent, 1987, US4657564.
- Langsam M., Burgoyne W.F. *J. Polym. Sci. Part A: Polymer Chemistry*, **31** (1993) 909-921.
- Le Roux J.D., Teplyakov V.V., Paul D.R. *J. Membr. Sci.* **90** (1994) 55-68.
- Lee K.J., Jho J.Y., Kang Y.S., Won J., Dai Y., Robertson G.P., Guiver M.D. *J. Membr. Sci.* **223** (2003) 1-10.
- Li J., Nagai K., Nakagawa T., Wang S. *J. Appl. Polym. Sci.* **58** (1995) 1455-1463.
- Liu Y., Wang R., Chung T-S. *J. Membr. Sci.* **189** (2001) 231-239.
- Liu Y., Chng M.L., Chung T-S., Wang R. *J. Membr. Sci.* **214** (2003) 83-92.
- Maeda Y., Paul D.R. *J. Polym. Sci., Part B: Polym. Phys.* **25** (1987) 957-980.
- Maeda Y., Paul D.R. *J. Polym. Sci., Part B: Polym. Phys.* **25** (1987) 981-1003.
- Mahajan R., Koros W.J. *Ind. Eng. Chem. Res.* **39** (2000) 2692-2696.
- Matsuyama H., Teramoto M., Iwai K. *J. Membr. Sci.* **93** (1994) 237-244.
- Matsuyama H., Teramoto M., Sakakura H. *J. Membr. Sci.* **114** (1996) 193-200.
- Matsuyama, H., Terada A., Nakagawara T., Kitamura Y., Teramoto M. *J. Membr. Sci.* **163** (1999a) 221-227.
- Matsuyama, H., Matsui K., Kitamura Y., Maki T., Teramoto M. *Sep. Purif. Tech.* **17** (1999b) 235-241.
- McHattie J.S., Koros W.J., Paul D.R. *Polymer* **32** (1991a) 840-850.
- McHattie J.S., Koros W.J., Paul D.R. *Polymer* **32** (1991b) 2618-2625.
- McHattie J.S., Koros W.J., Paul D.R. *Polymer* **33** (1992) 1701-1711.

- Merkel T.C., He Z., Pinnau I., Freeman B.D., Meakin P., Hill A.J. *Macromolecules* **36** (2003) 6844-55.
- Merkel T.C., Freeman B.D., Spontak R.J., He Z., Pinnau I., Meakin P., Hill A.J. *Chem. Mater.* **15** (2003) 109-123.
- Messersmith P.B., Giannelis E.P. *J. Polym. Sci., Part A: Polym. Chem.* **33** (1995) 1047-1057.
- Mi Y., Stern S.A., Trohalaki S. *J. Membr. Sci.* **77** (1993) 41-48.
- Mohr J.M., Paul D.R., Tullios G.L., Cassidy P.E. *Polymer* **32** (1991a) 2387-2394.
- Mohr J.M., Paul D.R., Mlsna T.E., Lagow R.G. *J. Membr. Sci.* **55** (1991b) 131-148.
- Morisato A., Ghosal K., Freeman B.D., Chern R.T., Alvarez J.C., de la Campa J.G., Lozano A.E., de Abajo J. *J. Membr. Sci.* **104** (1995) 231-241.
- Muruganandam N., Koros W.J., Paul D.R. *J. Polym. Sci., Part B: Polym Phys.* **25** (1987) 1999-2026.
- Nagai K., Masuda T., Nakagawa T., Freeman B.D., Pinnau I. *Prog. Polym. Sci.* **26** (2001) 721-798.
- Okamoto K., Fujii M., Okamoto S., Suzuki H., Tanaka K., Kita H. *Macromolecules* **28** (1995) 6950-6956.
- Park J.Y., Paul D.R. *J. Membr. Sci.* **125** (1997) 23-39.
- Paul D.R., Kemp D.R. *J. Polym. Sci., Part C: Polym. Symp.* **41** (1973) 79-93.
- Pesiri D.R., Jorgensen B., Dye R.C. *J. Membr. Sci.* **218** (2003) 11-18.
- Petropoulos J.H. *J. Membr. Sci.* **48** (1990) 79-90.
- Pinnau I. *Polym. Adv Tech.* **5** (1994) 733-744.
- Pinnau I., He Z., Morisato A. *J. Membr. Sci.* **241** (2004) 363-369.
- Pinnau I., Morisato A., He Z. *Macromolecules*, **37** (2004) 2823 -2828.
- Pixton M.R., Paul D.R. *Polymer* **36** (1995) 3165-3172.
- Qiu J., Zheng J.-M., Peinemann K.-V. *Macromolecules* **39** (2006) 4093-4100.
- Quinn R., Laciak D.V. *J. Membr. Sci.* **131** (1997) 49-60.
- Rezac M.E., Sorensen E.T., Beckham H.W. *J. Membr. Sci.* **136** (1997) 249-259.

- Robeson L.M., Smith C.D., Langsam M. *J. Membr. Sci.* **132** (1997) 33-54.
- Robeson L.M. *J. Membr. Sci.* **62** (1991) 165-185.
- Salame M. *Polym. Eng. Sci.* **26**, (1986) 1543-1546.
- Sarofeim M.T. Ph.D Thesis University of Ottawa, Canada September 1994.
- Seo Y., Kim S., Hong S.U. *Polymer* **47** (2006) 4501-4504.
- Seymour R.B., Carraher Jr. C.E. Structure property relationship in polymers, Plenum press, New York, (1984).
- Shekhawat D., Luebke D.R., Pennline H.W. A Topical Report submitted to National Energy Technology Laboratory, United States Department of Energy (2003).
- Shishatskii A.M., Yampol'skii Yu.P., Peinemann K.-V. *J. Membr. Sci.* **112** (1996) 275-285.
- Singh A., Ghosal K., Freeman B.D., Lozano A.E., de la Campa J.G., de Abajo J. *Polymer* **40** (1999) 5715-5722.
- Sinha-Ray S., Yamada K., Okamoto M., Ogami A., Ueda K. *Chem. Mater.* **15** (2003) 1456-1465.
- St. Clair A.K., St. Clair T.L., Slemph W.W. Recent Advances in Polyimide Science and Technology Weber W.D., Gupta M.R. (eds), Society of Plastic Engineers, Poughkeepsie, NY 16 (1987).
- Stancell A.F., Spencer A.T., *J. Appl. Polym. Sci.* **16** (1972) 1505-1514.
- Staudt-Bickel, C., Koros W.J. *J. Membr. Sci.* **155** (1999) 145-154.
- Stern S.A., Mi Y., Yamamoto H. *J. Polym. Sci., Part B: Polym Phys.* **27** (1989) 1887-1909.
- Stern S.A. *J. Membr. Sci.* **94** (1994) 1-65.
- Stern S.A., Kawakami H., Houde A., Zhou G. US Patent, 1997, US5591250.
- Suda H., Haraya K. *J. Chem. Soc., Chem. Commun.* (1995) 1179-1180.
- Süer M.G., BaC N., Yilmaz L. *J. Membr. Sci.* **91** (1994) 77-86.
- Tanaka K., Okano M., Toshino H., Kita H., and Okamoto K-I. *J. Polym. Sci., Part B: Polym. Phys.* **30** (1992) 907-914.

- Tokuda, Y., Fujisawa E., Okabayashi N., Matsumiya N., Takagi K., Mano H., Haraya K., Sato M. *Energy Convers. Mgmt.* **38** (1997) S111-S116.
- Toy L.G., Nagai K., Freeman B.D., Pinnau I., He Z., Masuda T., Teraguchi M., Yampolskii Yu. P. *Macromolecules* **33** (2000) 2516-2524.
- Tsujita Y. *Prog. Polym. Sci.* **28** (2003) 1377-1401.
- Van Amerongen G.J. *J. Polym. Sci.* **5** (1950) 307-332.
- Van Krevelen D.W., Hoftyzer P.J., Properties of polymers: correlation with chemical structure, Elsevier Publishing Company, Amsterdam, 1972.
- Vega A.M., Paul D.R. *J. Polym. Sci., Part B: Polym. Phys.* **31** (1993) 1599-1610.
- Vega A.M., Paul D.R. *J. Polym. Sci., Part B: Polym. Phys.* **31** (1993) 1577-1589.
- Victor J.G. and Torkelson J.M. *Macromolecules* **20** (1987) 2241-2250.
- Vieth W.R., Sladek K.J. *J. Colloid Sci.* **20** (1965) 1014-1033.
- Vrentas J.S., Duda, J.L. *J. Polym. Sci., Polym. Phys. Ed.* **15** (1977) 403- 407.
- Vu, D.Q., Koros, W.J., Miller, S.J. *J. Membr. Sci.* **211** (2003) 311-334.
- Wang J.S., Naito Y., Kamiya Y. *J. Polym. Sci., Polym. Phys. Ed.* **34** (1996) 2027-2033.
- Wonders A.G., Paul D.R. *J. Membr. Sci.* **5** (1979) 63-75.
- Yano K., Usuki A., Okada A., Kurauchi T., Kamigaito O. *J. Polym. Sci., Part A: Polym. Chem.* **31** (1993) 2493-2498.
- Yano K., Usuki A., Okada A. *J. Polym. Sci., Part A: Polym. Chem.* **35** (1997) 2289-2294.
- Yi C., Wang Z., Li M., Wang J., Wang S. *Desalination* **193** (2006) 90–96.
- Zhang J., Xiaohuai H. *Gaofenzi Xuebao* **3** (1995) 278-283.
- Zolandz L.R., Fleming G.K. in Membrane Handbook, Ho W.S.W., Sirkar K.K. (eds.) van Nostrand Reinhold, 1992.
- Zoppi R.A., das Neves S., Nunes S.P. *Polymer* **41** (2000) 5461-5470.

Chapter 2

Scope and objectives of the present work

The first large-scale membrane separation plant based on polymer membranes was installed by the Monsanto Co. in 1977 for the recovery of H₂ from an industrial gas stream. Membrane separation processes meeting crucial requirements (e.g. energy efficiency, capital costs, compactness, relatively easy operation and control etc.) for number of industrial applications provide inputs for widening the scope of applicability in more complex mixtures. One of the challenges for applying membrane processes for new applications is membrane material that would fulfill more stringent requirements. Newer membrane material development having appropriate combination of properties (permeability, selectivity, processability, operational stability, etc.) always remained the area of investigation for widening the scope of membranes for gas separation. The combination of appropriate permeability and selectivity by following various methodologies for membrane modification are reviewed in earlier chapter.

Aim of the present work was to improve gas permeation properties by following promising methodologies for selected polymers.

Among various glassy polymers, poly (2,6-dimethyl-1,4-phenylene oxide) (PPO) has high gas permeability and moderate selectivity. Its high permeability stems from larger diffusion coefficients of gases in PPO as compared to other polymers. In addition, PPO is a versatile material for performing chemical modification on its backbone. These potentials were exploited in various literature reports on PPO modification leading to strengthening the relationship between polar or bulky group substitution effects and gas permeation properties. The objective behind present PPO modification was to combine the effects of bulk and polarity in a single type of substitution to draw advantages of both the effects. The methodology adopted was based on Friedel-craft benzoylation using aromatic acids (containing substituents at its *p*-position) as reagent, followed by investigations of physical and gas permeation properties of resulting PPO containing benzoyl groups. An another forethought was to achieve bulky and polar substituent effects by substituting PPO with amide group via nitration, reduction to amination,

followed by amidation with acid chlorides.

The potential of polyarylates as gas separation membrane material is well demonstrated owing to its favorable physical and permeation properties. The structural modifications at both of its monomers (bisphenol and dicarboxylic acid) is relatively easy and led to certain understanding on effects of site (symmetric / asymmetric) and nature (polar / bulky) of substitution on gas permeation properties. The present work on polyarylates was aimed at furthering the understanding towards promising combinations of bulk, polarity, substitution site on either or both of its monomers. The effect of bridge substitution and asymmetric ring substitution by bulky group (methyl, isopropyl, phenyl and bromine) on the bisphenol moiety in combination with effect of acid substitution (bulky, polar and bridge substituted) on gas permeation and related physical properties of resulting polyarylates are described in Chapter 2. The synthetic aspects, physical and gas permeation properties of polyarylates with above types of substitution are categorized in the thesis as follows:

- Polyarylates bases on asymmetrically substituted bisphenol (diisopropyl bisphenol-A, di-*t*-butyl bisphenol-A and diphenyl bisphenol-A) with dicarboxylic acids bearing various groups / substituents.
- Polyarylates based on systematically substituted fluorine-bisphenol and dibromohexafluoro bisphenol-A; addressing combined effects of bridge and ring substitution with dicarboxylic acids containing various substituents.
- Polyarylates based on dibromoterephthalic acid, in which acid moiety was substituted by polar bromine.

The composite materials provide a newer avenue for exploiting them as gas separation membrane materials having promising properties. The objective of this work was to investigate two promising approaches of making composite materials, one based on clay-polyarylate nanocomposites and another with polyionic liquid (PIL) that exhibits high CO₂ sorption capability. The nanocomposites based on clay as an additive is well known to improve the barrier properties of water vapor, O₂ or CO₂. It was thought to investigate effects of lowering in permeability on variation in selectivity of various gas pairs. For this purpose, the polyarylate with relatively high permeability was selected intentionally to form nanocomposites with clay, so that the decrease in permeability as a

result of nanocomposites formation would lead to acceptable permeability, while allowing investigations in selectivity variations.

Poly(ionic liquid)s, PIL possess a potential to be used as membrane material, especially for CO₂ containing gas mixtures, owing to their high CO₂ sorption capacity. The objective of this work was to investigate gas permeation properties of PIL based composite materials while overcoming inherent limitations of PIL of film formation inability that limits its membrane applicability. Due to such limitation, conventional thin film composite membranes would also foresee the similar failure. Thus a different methodology adopting formation of composite membrane while swelling the already cast membrane in to the solution containing PIL was planned. This would result in an impregnation of PIL chains into swollen host matrix. This was anticipated to overcome limitations of film formation inability. The investigations on such composite membrane formation and investigations on permeation properties shed a light on possibility of employing PILs as membrane materials.

Chapter 3

Polyphenylene oxide (PPO) structural modification with substituents possessing simultaneous bulk and polarity

3.1 Introduction and Literature survey

Poly(2,6-dimethyl-1,4-phenylene oxide) (PPO) is known to exhibit high glass transition temperature [Toi (1982), Pan (1996), Percec (1987)] and good thermal stability under nonoxidizing conditions [Pan (1996)]. PPO backbone has a kinked structure owing to its ether linkage. The presence of two methyl groups and kinked ether linkages suppressed the chain packing and densification in PPO backbone. It possesses high gas permeability and moderate selectivity. The high permeability stems from larger diffusion coefficients of gases in PPO [Toi (1982)]. It has been demonstrated to be an attractive membrane material with excellent mechanical properties and resistant to a number of chemical agents [Xu (2002)]. Unfortunately, it has a relatively low selectivity for gases and much lower solubility in common solvents like *N,N*-dimethyl formamide (DMF), *N,N*-dimethyl acetamide (DMAc) and *N*-methyl pyrrolidinone (NMP), which confines its applicability as a membrane material.

PPO is a versatile material for performing chemical modification on its backbone. The chemical characteristics of the PPO repeat unit allows functionalization of this polymer by different mechanisms that can result in wide range of substituted PPO with improved gas permeation properties. This can be classified into two major categories; A) ring substitution and B) substitution at benzylic -CH₃ group. The effect of such substitutions on gas permeation property is briefed in following sections.

3.1.1 Ring substitution

Effects of aromatic electrophilic substitution on permeation and related physical properties were investigated with bromination [Chern (1987), Story (1992)], sulfonation and carboxylation [Polotskaya (1997), Chowdhury (2000)], silylation [Zhang (1994)],

alkynylation [Bonfanti (1994)], acylation and sulfonylation [Percec (1987)] and nitration [Ghosal (1992)].

PPO-aryl bromination was demonstrated to be an effective way of changing the packing state and the torsional motion of the aromatic constituents in the main chain [Chern (1987)]. Bromination of PPO at the aromatic ring position increased CO₂ permeability of the resulting polymer by a factor of 2.5 without hampering CO₂/CH₄ selectivity. A large increase in diffusivity was attributed to steric hindrance imparted by the bromine substituents, resulting in an increase in the length of polymer segments which participated in torsional motions. Overall chain mobility was decreased as indicated by an increase in T_g [Story (1992)]. The solubility of CO₂, CH₄ and N₂ in PPO was increased with an increasing extent of bromination and the change was larger for a gas with lower condensability. The substitution by an ionogenic sulfonate group on PPO rendered more rigidity to the chains and greatly decreased the free volume that determined low gas permeability and high selectivity [Polotskaya (1997)]. Chowdhury et al. [2000] showed that an introduction of polar group such as -COOH or -SO₃H to the aromatic ring of the PPO backbone increased permeability ratio, the effect being stronger for -SO₃H substitution rather than for -COOH substitution. It was also observed that in case of -SO₃H substituted PPO, loss in permeability was compensated by simultaneous substitution of bromine group along with -SO₃H. The silylation [Zhang (1994)] showed that the gas permeability and some permselectivity in trimethylsilyl-substituted PPO increased; but both, the permeability and permselectivity in triphenylsilyl-substituted PPO decreased as the degree of substitution increased. Bonfanti et al. [1994] studied the functionalization of PPO by bromination followed by alkynylation up to 80 % of substituted alkyne units. The alkynylation decreased the separation factor with improved gas permeability up to ten times than for the unmodified PPO. In the case of Friedel-Crafts sulfonylation [Percec (1987)], a small decrease in CH₄ permeability and an increase in CO₂ permeability was reported. In case of acylation by long chain acid, a large increase in CH₄ permeability while maintaining CO₂ permeability led to a large decrease in CO₂ based selectivities. This is a classic example, wherein the effect of chain length on selectivity was prominent. The aryl-nitration (15 %) of PPO decreased the gas permeability, but the selectivity was increased [Ghosal (1992)]. The nitro substituent on

the aryl backbone anticipated to restrict segmental torsional mobility. Excessive chain degradation restricted the study of PPO nitration above 15 % substitution.

Other significant PPO ring substitutions include amination [Pan (1996)], amide group substitution [Mahajan (1988)], etc. wherein, gas permeation was not addressed.

3.1.2 Substitution at -CH₃

Carboxylation [Chowdhury (2000), Story (1992)], esterification [Story (1992)], azidation followed by fullerene substitution [Sterescu (2004)], nucleophilic displacement reaction such as Williamson etherification, cyanide displacement and heterocyclic group transfer [Percec (1988)] etc. can be grouped under this type of substitution.

The carboxylation of PPO increased the selectivity with decrease in permeability [Story (1992)]. With 22 % carboxylation, the CO₂/CH₄ selectivity increased by 29 %, while the CO₂ permeability decreased by 48 %. The methyl esterification of carboxylated PPO eliminated -COOH dimerization by inhibiting hydrogen bonding between hydroxyl groups of -COOH functionality [Story (1992)]. This allowed carbonyl groups on the polymer to selectively interact with CO₂, rather than with each other, thereby causing a slight increase in CO₂/CH₄ solubility selectivity as compared with carboxylated PPO. It was expected that the torsional motions would increase, thereby increasing diffusivity and decreasing diffusivity selectivity slightly. The effect of covalently bonded fullerenes on the PPO backbone studied by Sterescu et al., which showed that the PPO-bonded C₆₀ membranes exhibited significantly higher gas permeability (up to 80 %) in comparison to unsubstituted PPO, without compromise on selectivity [Sterescu (2004)]. Percec et al. [1988] studied nucleophilic displacement reaction on PPO, such as Williamson etherification, cyanide displacement, esterification, and heterocyclic group transfer under phase transfer catalyzed (PTC) conditions. The nucleophilic substitution occurred easily with alcohols when a functional yield was as high as 100 %. The thermal stability of the modified polymers did not change significantly when compared with that of the parent polymer. Permeability for CH₄ and CO₂ was reduced in case of cyanide displacement (KCN), etherification (-O-(CH₂)₈CH₃) and heterocyclic group transfer (carbazole) with a decrease in CH₄/CO₂ selectivity, except in a case of cyanide displacement. The permselective properties of PPO modified with long side groups such as (-O-(CH₂)₈CH₃)

were rather poor. The permeability for CH₄ remained almost unchanged whereas the permeability for CO₂ significantly decreased with respect to unmodified PPO. The modification of their permeation properties was attributed to the changes in polymer chain mobility and packing as well as to changes in the side chain polarity.

The attachment of cyclopentadiene ligands to PPO followed by their conversion to η^5 -cyclopentadiene with cobalt, rhodium, and titanium, and the catalytic reactions of these polymer-supported complexes were studied by Verdet and Stille [1982]. The carboxylation of PPO using a lithiation method [Chalk (1968)] followed by treatment with CO₂ to form various carboxylate derivatives such as esters, salts, amides, anhydrides, etc. was reported.

Above literature reports indicated that, generally the nonpolar substitution like silylation [Zhang (1994)], alkynylation [Bonfanti (1994)], fullerene substitution [Sterescu (2004)] led to the increase in gas permeability, while the polar group substitution like bromination [Chern (1987), Story (1992)], carboxylation [Chowdhury (2000), Story (1992)], sulfonation [Polotskaya (1997), Chowdhury (2000)], nitration [Ghosal (1992)] etc. improved selectivities in compensation with a general decrease in gas permeability. It was also reported that the substituent on the phenylene of the polymer main chain affected gas permeability more significantly than the substituent present on the methyl side group [Zhang (1994)]. Smaller group substitution by the sulfonylation and a long chain containing acylation had opposite effects on CH₄ and CO₂ permeability behavior [Percec (1987)]. Thus, high intrinsic permeability, moderately high T_g and ease of chemical modification of various types made this polymer an attractive material for investigations towards improvement in its gas permeation properties by chemical modification of its backbone.

3.2 Objectives

A polar group substitution on PPO backbone generally led to decrease in permeability and increase in selectivity; while bulky group substitution increased permeability with a decrease in selectivity of various gas pairs. In the view of this observed trend, modification of PPO was planned in such a way that the substituent would possess both, bulk as well as polarity so that the advantages of both types of

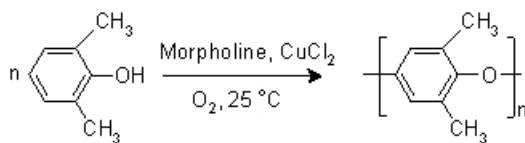
substitutions can be drawn. Such type of combination could be achieved if a substituted aromatic moiety possessing bulk and polarity could be introduced onto PPO backbone. This was aimed to achieve in two ways:

- a) Investigate effects of PPO benzoylation with aromatic carboxylic acids bearing specific groups at *p*-position of the phenyl ring. The advantages of polar group substitution on permeation properties can be drawn from the carbonyl group and also from the one substituted at *p*-position of phenyl ring. The phenyl ring of the benzoyl group was anticipated to impart effects of bulky group.
- b) To substitute PPO by nitro, amino and amide functionality with high degree of substitution, wherein effects of these polar bulky groups towards enhancement in permeation properties can be drawn. Investigations on synthesis protocol for obtaining high degree of substitution, physical property and subsequent investigations of permeation properties were anticipated to enhance understanding towards proposed strategy of withdrawing effects of combined polar and bulky group substitutions on permeation properties of PPO.

3.3 Experimental

The solvents chloroform, dichloromethane, dichloroethane, methanol, petroleum ether, carbon tetrachloride, toluene, ethanol, hexane and *N,N*-dimethyl formamide (DMF) (AR/LR grade) were obtained from S.D. Fine Chemicals, India. Solvents were purified by the standard procedure described in the literature [Perrin, (1981); Vogel, (1973)]. Thionyl chloride, sodium hydroxide, molecular sieves (4A type), hydrochloric acid, sulphuric acid, glacial acetic acid, NaI, SnCl₂.2H₂O, benzoyl chloride, *p*-chlorobenzoic acid, *p*-nitrobenzoic acid, *p*-toluic acid, cupric chloride and anhydrous aluminum chloride (all LR grade) were procured from S.D. fine chemicals (India). The *p*-bromobenzoic acid was procured from Merck (India) Ltd. The 2,6-dimethyl phenol and morpholine were procured from Aldrich Chemicals, USA. 2,6-dimethylphenol was purified by distillation under reduced pressure, while, all other chemicals were used as received. All gases used viz., helium (He), oxygen (O₂), argon (Ar), nitrogen (N₂), methane (CH₄), carbon dioxide (CO₂) with minimum purity of 99.5 % were obtained from Inox (India)/Air liquid (USA).

3.3.1 PPO synthesis

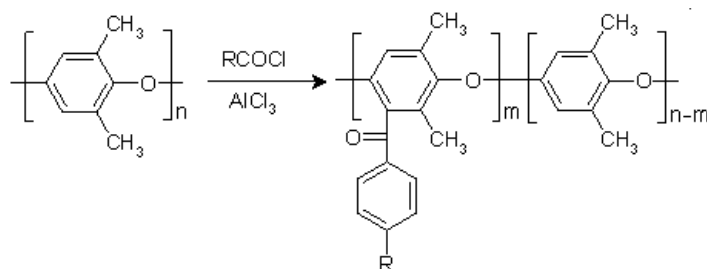


Scheme 3.1 Oxidative coupling of 2,6-dimethylphenol

PPO was synthesized by oxidative coupling of 2,6-dimethyl phenol as shown in Scheme 3.1; following the reported procedure [Penczek (1986)], except a small variation of prolonged period of oxygen blanketing of 14 hours. In a 500 ml three neck round bottom flask, 20 gm of 2,6-dimethyl phenol (0.164 moles) was added to 10 ml of morpholine and stirred until solution became clear at ambient temperature. A 0.34 gm of CuCl₂ (0.00253 mol) and a mixture of toluene-ethanol (160 ml + 40 ml) was added. The oxygen was bubbled into the reaction mixture continuously. The rate of oxygen bubbling was kept as 10 to 15 bubbles per minute. The reaction mixture was stirred for ~ 14 hours with constant string at room temperature. After this time, the reaction mixture was precipitated on to stirred methanol, filtered and washed thrice with methanol. The crude polymer was dried in oven at 60 °C for 12 hours and latter in vacuum oven at 60 °C for 12 hours. The crude polymer was purified by dissolving it into chloroform and again precipitating in methanol. The spectral analysis (IR and ¹H-NMR) and the glass transition temperature of obtained PPO were in agreement with the literature data [Bonfanti (1994), Percec (1987), Pan (1996)]. The intrinsic viscosity of obtained PPO determined by graphical method using toluene as a solvent was 2.3 dl/g and this material was used for benzylation of PPO. For PPO nitration and subsequent reactions, PPO with intrinsic viscosity of 2.6 dl/g was used.

3.3.2 Benzoylation of PPO

The Friedel-Craft benzoylation reactions of PPO were carried with acid chloride as a reagent, AlCl₃ as a Lewis acid catalyst and 1,2-dichloroethane as the solvent, following Scheme 3.2. The aromatic acids used; viz. *p*-chlorobenzoic acid, *p*-nitrobenzoic acid, *p*-toluic acid and *p*-bromobenzoic acid were converted to the respective acid chloride using 4 molar equivalent of thionyl chloride and catalytic amount of DMF at reflux temperature.

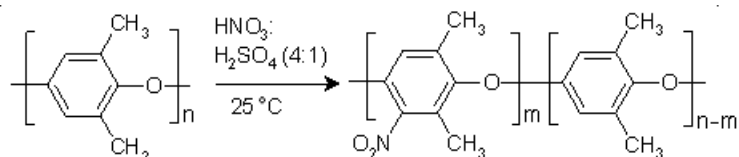


Scheme 3.2 Benzoylation of polyphenylene oxide

The *p*-toluoyl chloride, *p*-bromobenzoyl chloride and *p*-chlorobenzoyl chloride were purified by fractional distillation under reduced pressure; while, *p*-nitrobenzoyl chloride was purified by the recrystallization from the dry petroleum ether. These acid chlorides were stored under dry atmosphere until use.

The reaction conditions for benzoylation of PPO with acid chloride as a reagent were optimized for individual cases as given in Table 3.1. Typically, 2 g of PPO was dissolved in 60 ml of 1,2-dichloroethane with stirring for 6 hrs under N₂ blanketing at ambient. To this solution, already prepared complex of an anhydrous aluminum chloride (1 molar equivalent, 2.22 g, 0.166 mol) and an acid chloride (1.1 molar equivalent, 0.183 mol) in 10 ml of 1,2-dichloroethane was added dropwise for a period of 5 to 10 minutes. Such a reaction mixture was further stirred for a defined time and at temperature as given in Table 3.1. The formed benzoylated product was isolated from the reaction mixture by precipitation onto a stirred methanol followed by the filtration. The obtained material was dried at 60 °C for 12 hours. Further purification was done by its dissolution in chloroform and reprecipitation into methanol. The polymer was dried at 60 °C for 12 hours and finally under vacuum at the same temperature for 24 hours.

3.3.3 Nitration of PPO



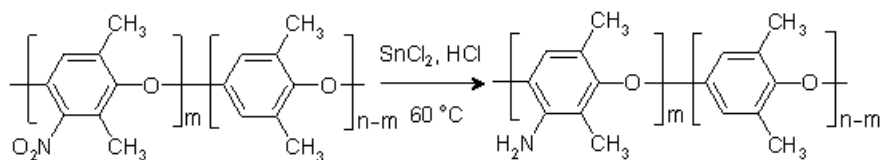
Scheme 3.3 Nitration of polyphenylene oxide

In a typical procedure (Scheme 3.3), 5 g of PPO was dissolved in 125 ml of chloroform at ambient temperature under N₂ flow. To this, a mixture of nitric acid and

sulfuric acid (25 ml, proportions as given in Table 3.7) was added in a drop wise manner for a period of 5 minutes at 25 °C. During the addition, temperature of the reaction mixture was kept constant. The reaction mixture was allowed to stir for 30 minutes. The formed nitrated PPO (PPO-NO₂) was precipitated onto stirred methanol. It was further purified by dissolution in chloroform and reprecipitation into methanol. The volume ratio of nitric acid: sulfuric acid was changed from 1:1 to 4:1 to obtain varying degree of substitution.

3.3.4 Amination of PPO

Amination of nitrated PPO (Scheme 3.4) was performed by following the reported procedure [Pan (1996)] as described below.

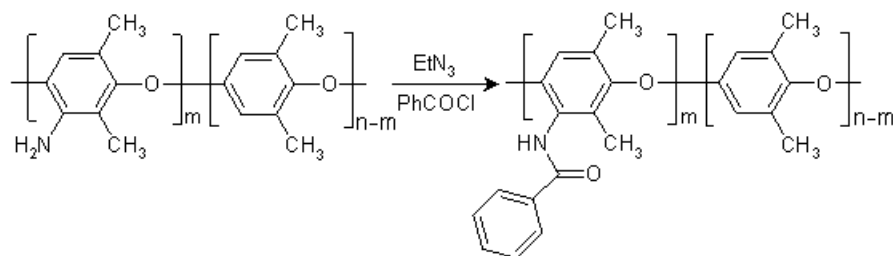


Scheme 3.4 Amination of nitrated polyphenylene oxide

A 3 g of PPO-NO₂ was dissolved in 15 ml chloroform in a two-necked RB flask equipped with a reflux condenser. To this, a solution of 30 g of SnCl₂·2H₂O and 1 g of NaI in 72 ml HCl-glacial acetic acid mixture (2:1) was added in a drop wise manner within 5 minutes at 60 °C while stirring. After 15 minutes of addition of this reducing mixture, the polymer started precipitating. To avoid precipitation, a small quantity of methanol was added till the solution became clear. The resulting mixture was further refluxed for 3 hours and then cooled to room temperature. The polymer was precipitated by pouring reaction mixture onto a 2N NaOH solution. The precipitated polymer was washed with water till free of base. It was air dried for 2 days at room temperature under vacuum. The dried polymer was purified by dissolving in chloroform and precipitation in methanol.

3.3.5 Amide group substitution on PPO

Aminated PPO prepared as above was further used for amide formation following Scheme 3.5.



Scheme 3.5 Amidation of aminated polyphenylene oxide

Aminated PPO (1.5 g) was dissolved in 30 ml of DMAc. After the complete dissolution of the polymer, 4.7 ml of triethylamine (0.034 mol, 3 equivalent) was added. To this stirred solution, 1.58 ml of benzoyl chloride (0.0136 moles, 1.2 equivalent) was added dropwise at ambient temperature. The reaction mixture was stirred for 3h and then precipitated onto stirred methanol. The recovered polymer was dried at 60 °C. It was purified by dissolving in chloroform and precipitation in methanol.

3.3.6 Dense Membrane preparation

A 3-5 % (w/v) polymer solution was prepared either in toluene (in case of benzoylated PPO) or in chloroform (in case of nitrated, aminated or amide group containing PPO). The formed solution was filtered through a 5- μm SS-filter and poured on to a flat glass surface. The solvent was allowed to evaporate at ambient temperature under dry atmosphere. The formed film was peeled off and vacuum dried at 60 °C for a week in order to ensure the complete removal of the solvent, as also confirmed by DSC. The PPO films were prepared using toluene as well as chloroform as the solvent.

3.3.7 Polymer characterization

The intrinsic viscosity $[\eta]$ of PPO as well as substituted PPO was determined by graphical method at 35 °C using toluene (in case of benzoylated PPO) or chloroform (in case of nitrated and aminated PPO) as the solvent and were as given in Table 3.1 and 3.7. The percent degree (DS) of substitution was determined by $^1\text{H-NMR}$ (200 MHz) spectroscopy [Percec (1987)]. The $^1\text{H-NMR}$ spectra with proton assignments were as shown in Figure 3.3 and 3.10. The infrared (IR) spectra were recorded on FTIR-8300 Shimadzu spectrophotometer. The IR spectra for benzoylated PPO were as shown in

Figure 3.4; while spectra for nitrated, aminated and amidated PPO were as shown in Figure 3.9. The thermogravimetric analysis (TGA) was done on a Thermal Analyzer 32 SII model under N₂ atmosphere at the heating rate of 10 °C/minute. The wide-angle X-ray diffraction (WAXD) spectra of these substituted PPO in the film form were performed using Rigaku X-ray diffractometer (D-max 2500) with Cu-K_α radiation in 2θ range of 4-40° and were as shown in Figure 3.7 for benzoylated PPO and in Figure 3.13 for nitrated, aminated and amide containing PPO. The average d-spacing (d_{sp}) for the amorphous peak maxima was calculated using Bragg's equation. The dynamic mechanical analysis (DMA) in case of nitrated and aminated PPO was performed using Rheometrics DMTA III E, in the temperature range of -150 to 300 °C with a heating rate of 5 °C/minute, at the frequency of 10 rads/sec and at 0.1 % strain using a film specimen of ~ 120 μm thick and 2.5 × 0.7 cm² in size. The tan δ curve for PPO and its substituted derivatives were as shown in Figure 3.12. The density of polymers in the film form was obtained by floatation method using aqueous K₂CO₃ solution at 40 °C (Table 3.3 and 3.8). The reproducibility of the density measurements was ± 0.005 g/cm³. The fractional free volume (v_f) and solubility parameter (δ) were estimated using group contribution method [Van Krevelen (1972)] and measured density and given in Table 3.3 and 3.8.

3.3.8 Determination of equilibrium sorption and permeability of gases

3.3.8.1 Measurement of gas permeability

The variable volume method [Stern (1963)] was used for determination of gas permeability. The pure gases used (He, Ar, O₂, N₂, CH₄, CO₂; in the same sequence) had minimum purity of 99.8 %. A schematic diagram of permeation equipment is shown in Figure 3.1. The gas permeability measurements for PPO and all substituted PPO were done at 35 °C using pure gases at 6.8 atm upstream pressure. The average permeability and selectivity of different gas pairs were as summarized in Table 3.4 and 3.5 in case of benzoylated PPO; whereas in case of nitrated and aminated PPO, permeability and selectivity were as given in Table 3.11 and 3.12. The design of the permeation cell, specifications, material of construction, etc. were as discussed elsewhere [Houde (1991)]. One end of the feed side of the cell was connected through valve V₁ to the feed gas cylinder outlet and an electronic pressure gauge (0-999 psi range). The valve V₂ was vent

and used to control the feed pressure. On the permeate side of the permeation cell, a calibrated borosilicate glass capillary (I.D. = either 1.5725 or 1.9995 mm) containing a small mercury slug (~ 4-6 mm in length) was connected. The displacement of mercury slug was monitored against time using cathetometer. The permeability (P) was calculated using the Equation (3.1).

$$\text{Permeability (P)} = \frac{14.7 \times d \times \text{F.C.} \times l}{76 \times A \times t \times \Delta P} \quad (3.1)$$

where d = distance traveled by mercury slug (cm), F.C. = flow meter constant [volume of the flow meter capillary per unit length (cm^3/cm)], l = thickness of the membrane (cm), A = effective membrane area (cm^2), t = time t (sec), ΔP = pressure (psi). The permeability was expressed in Barrer, where $1 \text{ Barrer} = 10^{-10} [\text{cm}^3 (\text{STP}).\text{cm}/\text{cm}^2.\text{s.cm Hg}]$. The ideal selectivity of various gases was calculated using the Equation (3.2).

$$\text{Selectivity } (\alpha) = \frac{P_x}{P_y} \quad (3.2)$$

where P_x and P_y are the permeability of respective pure gas.

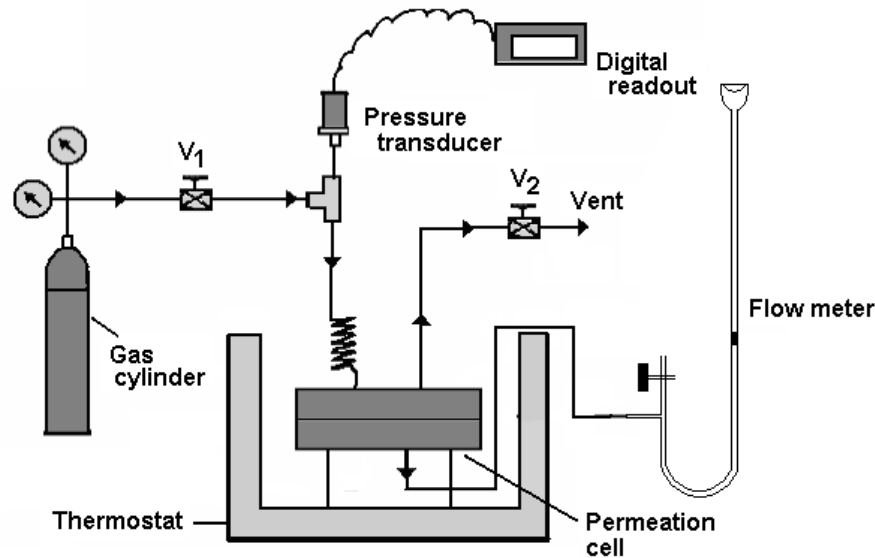


Figure 3.1 Schematics of gas permeability apparatus

3.3.8.2 Sorption equipment and procedure

The equilibrium sorption isotherms for N_2 , CH_4 , and CO_2 were obtained using pressure-decay method as described by Vieth et al. [1966] at 35°C over the pressure

range of 1-20 atm. The schematic of sorption equipment was as given in Figure 3.2. The polymer sample in film form was placed in the sorption cell, evacuated and flushed with gas several times. Then the system was evacuated to 0.00001 mbar using oil diffusion pump. The gas was introduced rapidly and initial pressure recorded. As the sorption proceeds, the pressure starts decreasing and ultimately remains constant after the equilibrium is established. To increase the efficiency of experimentation, sequential sorption runs were made by incremental raise in pressure of the equilibrated system until about 20 atm was attained. The amount of gas sorbed in the sample at each equilibrium pressure was determined from the initial and final pressure. The resulting sorption isotherms were as given in Figure 3.14.

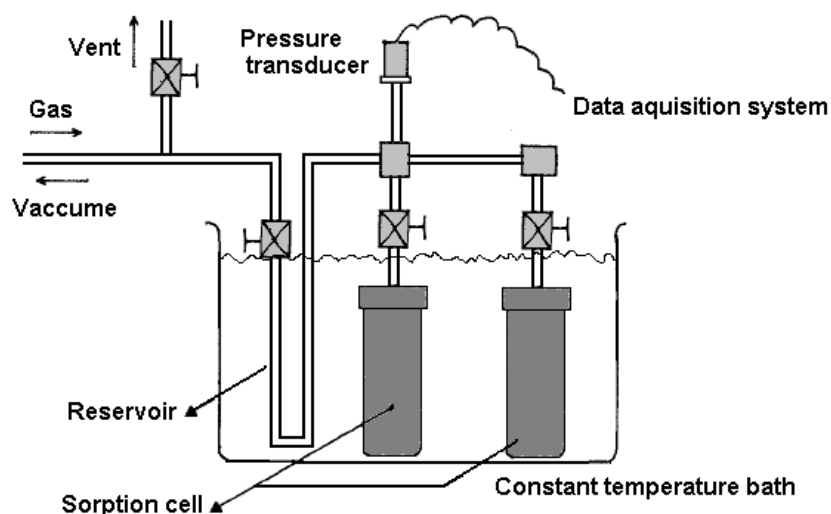


Figure 3.2 Schematic of sorption equipment

3.4 Results and discussion

3.4.1 Polymer synthesis and modification

3.4.1.1 PPO synthesis

Initially, PPO benzylation was performed with commercial PPO sample (gifted by GE) having inherent viscosity of 0.53 dl/g in TCE). The benzyolated product obtained with this PPO could not be transformed into the film form. The brittleness could be attributed to the chain degradation, which is known to occur in Lewis acid environment [Vollmert (1969)] and also during nitration of PPO [Ghosal (1992)]. It was thus decided to perform benzyolation and nitration on PPO having high enough viscosity (molecular

weight). In these cases, though the chain degradation was inevitable, it was anticipated that the film of formed product would withstand pressure during permeation measurements. The PPO synthesis was carried out using the reported procedure [Penczek, US 4607085(1986)]. The prolonged period of oxygen blanketing helped in elevating the viscosity of formed PPO. The duration of O₂ blanketing was optimized as 14 hours. The intrinsic viscosity was determined by graphical method using toluene/chloroform as the solvent. The PPO having intrinsic viscosity of 2.3 dl/g (viscosity-averaged molecular weight of 5,56,400) was used for the benzylation reactions, while for nitration; the intrinsic viscosity of the PPO was 2.6 dl/g (viscosity-averaged molecular weight of 6,75,600).

The benzylation and nitration (and subsequent reactions of amine and amide formation) were performed using PPO with high molecular wt. The films of thus formed product could withstand pressure of at least 7 kg/cm² during the permeation measurement. The benzylation was performed to obtain systematic variation in the *p*-position of benzoyl group using different carboxylic acids. The nitration reactions were optimized to meet criterion of high degree of substitution while maintaining the film formation capability. The synthesis, physical and permeation properties of both these types are discussed separately in following sections.

3.4.1.2 Benzoylation of PPO

Benzoylation of PPO was performed via Friedel-Craft route using AlCl₃ as the catalyst and acid chloride as a reagent. In all the cases of benzoylation, the mole ratio of AlCl₃ and acid chloride with PPO could be kept same (i.e. PPO: acid chloride: AlCl₃ = 1: 1.1: 1); while, the reaction temperature and the time were optimized for each acid chloride individually so as to meet two requirements for the formed product; viz, (i) its ability to form a film by the solution casting method that would withstand upstream gas pressure while mounted in permeation cell and (ii) a material thus obtained should have an appreciable degree of substitution. These reaction conditions were given in Table 3.1. In the present investigation, the reaction with *p*-nitrobenzoyl chloride could be performed within half an hour at 40 °C (Table 3.1); but reaction with *p*-toluoyl chloride took 10 hours duration at 80 °C in order to get an appreciable degree of substitution. The reaction

conditions required with other acid chlorides were intermediate between above two cases. This required variation in reaction conditions is in accordance with the reactivity of these acid chlorides having *para*-substitution. The Hammett substituent constants for the parent acids [Sykes (1998)] as given in Table 3.1 are indicative of their reactivity. The reaction conditions thus set could offer considerable degree of substitution; a minimum of 54.5 % for PPO-BzBr and a maximum of 74 % for PPO-BzCH₃.

Table 3.1 Reaction parameters for PPO benzylation

Polymer abbreviation	Acid chloride Used	Reaction conditions			[η] (dl/g)	DS ^a (mol%)	Hammett substituent constant for <i>p</i> -substituted acids ^b
		PPO:RCOCl: AlCl ₃ (mol:mol:mol)	Time (h)	Temp. (°C)			
PPO-BzH	C ₆ H ₅ COCl	1.0 : 1.0 : 1.1	5	60	0.36	68.9	0
PPO-BzCH ₃	<i>p</i> -CH ₃ C ₆ H ₄ COCl	1.0 : 1.0 : 1.1	10	80	0.34	74	- 0.17
PPO-BzBr	<i>p</i> -BrC ₆ H ₄ COCl	1.0 : 1.0 : 1.1	6	40	0.41	54.5	0.23
PPO-BzCl	<i>p</i> -ClC ₆ H ₄ COCl	1.0 : 1.0 : 1.1	4	35	0.38	68	0.23
PPO-BzNO ₂	<i>p</i> -O ₂ NC ₆ H ₄ COCl	1.0 : 1.0 : 1.1	0.5	40	0.30	60	0.78

^a: Degree of substitution obtained by ¹H-NMR as described below; ^b: [Sykes (1998)]

3.4.2 Physical properties of benzoylated PPO

3.4.2.1 Spectral properties

Various substituted PPO prepared in this study were characterized by H¹-NMR and IR spectroscopy. The percent degree of substitution (DS) in all the cases was calculated based on the proton H¹-NMR spectrum. The spectra were as presented in Figure 3.3, together with an assignment of their proton resonances. The protons due to unsubstituted PPO repeat unit appeared at 6.4-6.5 δ , while the protons due to substituted PPO repeat unit appeared at 6.1-6.2 δ . Similar peak positions for acylation, sulfonylation and amide group incorporation on PPO were reported [Percec (1987), Mahajan(1988)]. The percent degree of substitution was determined from the ratio of integrals of the proton resonances due to the unsubstituted PPO units (signal H_b at $\delta \approx 6.4$ ppm, as shown in Figure 3.3) and those for the substituted units (signal H_c at $\delta \approx 6.1$ ppm). Equation (3.3) was used to calculate the molar degree of substitution [Percec (1987)].

$$\% \text{ Degree of substitution} = \frac{I_c}{\frac{I_b}{2} + I_c} \times 100, \quad (3.3)$$

where I_b and I_c represent the integrals of protons designated as 'b' and 'c' in Figure 3.3.

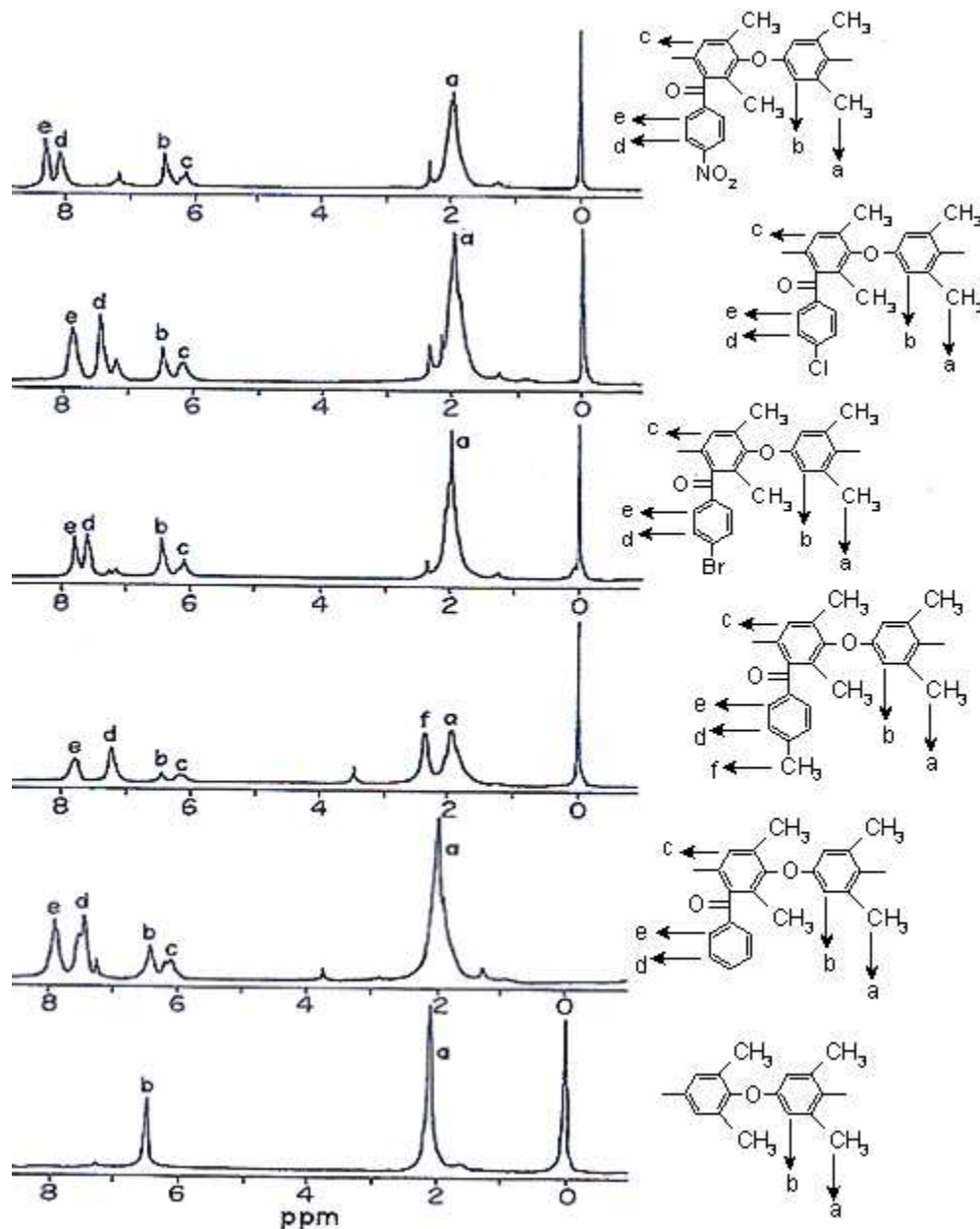


Figure 3.3 ^1H - NMR spectra of benzoylated PPO

The Friedel-Craft acylation of PPO is a feasible reaction under milder conditions [Percec (1987)]. The substitution at first available position occurs easily, but the acylation of second available position is difficult because of deactivation of the aromatic ring by

carbonyl of first acyl group [Percec (1987)]. This carbonyl group due to its electron withdrawing nature decreases the nucleophilicity of the remaining unsubstituted position [Percec (1987), Mahajan(1988)]. Similar phenomenon could be anticipated in the present cases of benzylation.

Figure 3.4 represents the IR spectra of unmodified PPO (a) and various benzylated PPO (b-f). Appearance of a peak at 1670 cm^{-1} , responsible for $>\text{C}=\text{O}$ stretching was seen for all the cases of benzylation. A band at 1188 cm^{-1} was ascribed to the symmetric stretch vibration for the C-O-C of aromatic ether, while absorption bands at 896 cm^{-1} and 1378 cm^{-1} were responsible for the deformation vibration peaks for the hydrogen on the aromatic ring and the methyl groups, respectively. Similar peak assignments were reported by Percec et al. [1987] for the acylated PPO.

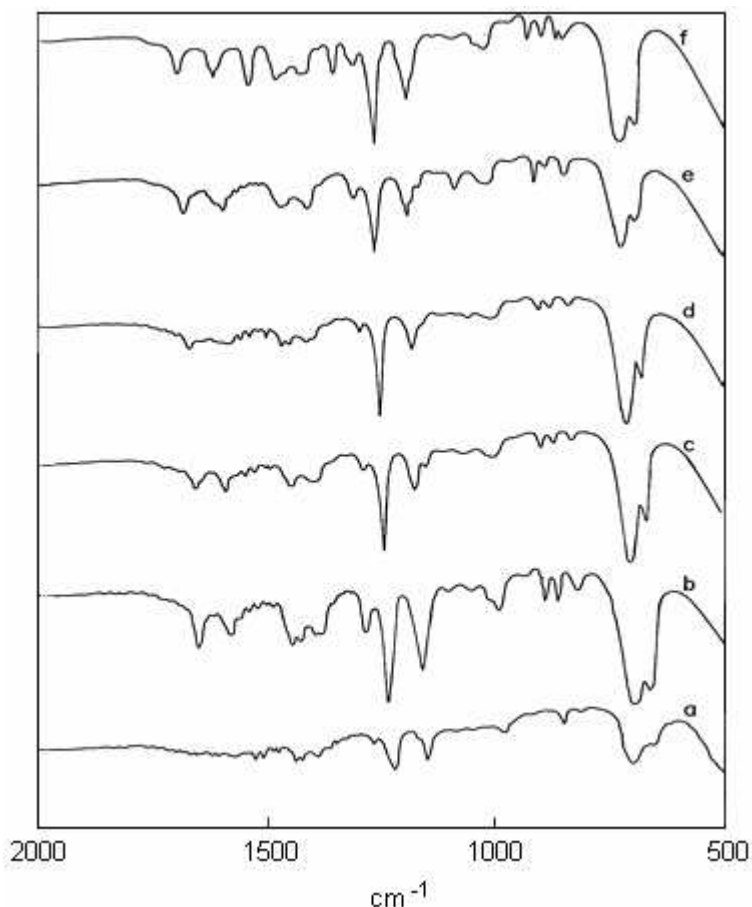


Figure 3.4 IR spectra of benzylated PPO (a: PPO, b: PPO-BzH, c: PPO-BzCH₃, d: PPO-BzBr, e: PPO-BzCl, f: PPO-BzNO₂)

3.4.2.2 Chain degradation after benzylation

The intrinsic viscosity after modification was decreased considerably in comparison to the viscosity of the unsubstituted PPO (Table 3.1). This could be attributed to the degradation of polymer chains during the course of benzylation. Similar observations indicating chain degradation in Lewis acid environment [Vollmert(1969)] and reduction in viscosity at higher degrees of nitration of PPO [Ghosal(1992)] were documented. Though PPO modifications using $AlCl_3$ as the catalysis was reported by Percec [Percec (1987)] and Mahajan et al. [1988], a comparison of molecular weight or viscosity of a formed product with that of initial PPO was not revealed.

3.4.2.3 Solubility

The solubility of the substituted PPO in various organic solvents was as presented in Table 3.2. PPO, though, was soluble in many common solvents [Percec (1987)], it was found to be insoluble in dipolar aprotic solvents like *N,N*-dimethyl formamide (DMF), *N,N*-dimethyl acetamide (DMAc) and *N*-methyl pyrrolidinone (NMP). These solvents are generally used for the asymmetric membrane preparation by phase inversion method, wherein; water is used as a nonsolvent. Though asymmetric membranes of PPO were investigated for the gas separation application [Tan(2000)], chloroform was used as the solvent and alcohol was needed as the nonsolvent. It is interesting to note that the benzylation rendered solubility in DMAc and NMP (Table 3.2) in the present case.

Table 3.2 Solubility of benzylated PPO in various solvents at ambient conditions

Polymer	DCM (9.7)	Chloroform (9.3)	THF (9.1)	Acetone (9.9)	Toluene (8.9)	NMP (11.3)	DMF (12.1)	DMAc (10.8)
PPO	±	+	+	-	+	-	-	-
PPO-BzH	+	+	+	S	+	+	-	+
PPO-BzCH ₃	+	+	+	S	+	+	-	+
PPO-BzBr	+	+	+	S	+	+	-	+
PPO-BzCl	+	+	+	S	+	+	-	+
PPO-BzNO ₂	+	+	+	S	+	+	-	+

where + : Highly soluble, - : Insoluble, ± : Tendency of crystallization, S: swelling;

Values in the parenthesis indicate solubility parameter δ (cal/cm³)^{1/2} of the solvent [Brandrup1989]

The improvement in solubility could be attributed to the increased polarity after the benzoyl group incorporation on PPO backbone. An increase in polarity is further supported by an observed increase in the solubility parameter (Table 3.3) after benzylation.

3.4.2.4 Thermal characterizations

The thermal analysis of these polymers was performed by differential scanning calorimetry and by thermogravimetric analysis (TGA) in order to investigate the effect of substitution on T_g and degradation behavior of resulting polymer, respectively. Though, these properties are dependant on the degree of substitution, the qualitative comparison was made in view of the relatively higher degree of substitution obtained in all the cases (a minimum of 54.5 % and a maximum of 74 %). The T_g of all benzyolated polymers was increased in comparison to the unsubstituted PPO. A similar increase in T_g was observed in the case of sulfonylation by various groups [Percec (1987)]. The T_g of the benzoyl PPO (DS = 88 %) was reported [Schauer (1992)] to be 238.9 °C; while in the present case, it was found to be 235 °C (DS = 68.9 %). This difference could be attributed to the variation in degree of substitution. In the present series, T_g increased in the order: PPO < PPO-BzH \cong PPO-BzCH₃ \cong PPO-BzBr < PPO-BzCl < PPO-BzNO₂. A comparatively larger increase in T_g for PPO-BzNO₂ can be explained on the basis of higher electrostatic interactions present in this material, induced by polar nitro group; though the degree of substitution in this case was comparatively lower than the other cases of benzyolation (except for PPO-BzBr). This was also supported by the highest estimated solubility parameter for this polymer in comparison to the other benzyolated PPO in the series (Table 3.3). It was said that the increased T_g of nitrated PPO could be because of increased interchain interactions and increased rotational energy barrier [Ghosal (1992)]. The T_g in the case of PPO-BzCl was lower than for the PPO-BzNO₂, but was slightly higher than for the other candidates. Though the T_g of PPO-BzH, PPO-BzCH₃ and PPO-BzBr appeared similar, the degree of substitution in the case of bromobenzoyl substitution was considerably lower than for the other two cases. It could thus be inferred that the *para*-substituted halogen on benzoyl group imparted additional rigidity owing to electrostatic interactions. This speculation could further be supported by

a higher observed T_g in case of the PPO-BzCl than for PPO-BzH or PPO-BzCH₃, though their degree of substitution was comparable.

Table 3.3 Physical properties of benzoylated PPO

Polymer	d_{sp} Å	ρ (g/cm ³)	v_f (cm ³ /cm ³)	δ (cal/cm ³) ^{1/2}	T_g (°C)	TGA	
						DT (°C)	T_{10} (°C)
PPO	7.713, 5.901	1.0517	0.3923	8.6	213	425	445
PPO-BzH	6.758, 4.670	1.1572	0.3525	9.8	235	410	435
PPO-BzCH ₃	6.487	1.1335	0.3532	9.7	235	400	420
PPO-BzBr	5.965, 4.29	1.2410	0.4019	9.2	236	380	420
PPO-BzCl	6.194, 4.332	1.2338	0.3471	10.0	239	390	430
PPO-BzNO ₂	6.325	1.2011	0.3638	10.0	249	280	415

It was interesting to note that some correlation was observed between the solubility parameter and the glass transition temperature (Figure 3.5) of various substituted PPO. Thus increased polarity caused by the substituted benzoyl group contributed to an increase in T_g , at least to some extent.

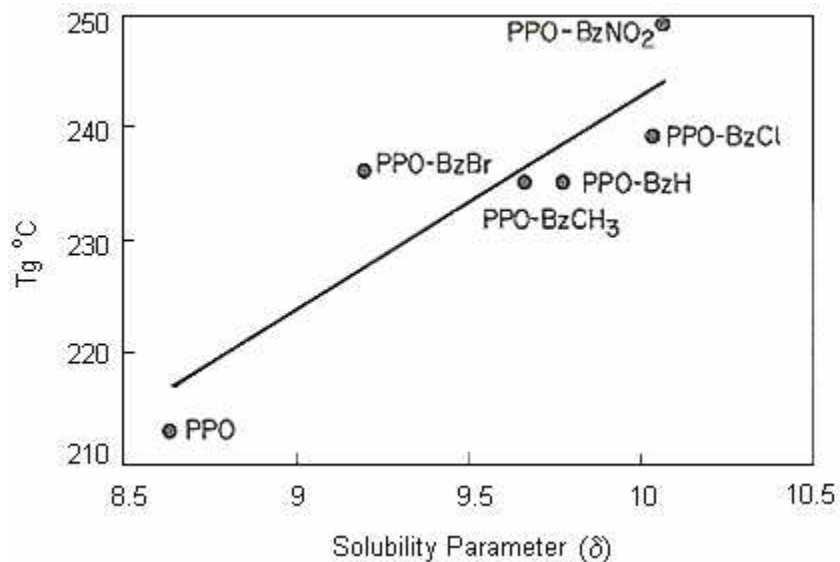


Figure 3.5 Variation in glass transition temperature (T_g) with the change in solubility parameter (δ) of benzoylated PPO

The TGA spectra of PPO and benzoylated derivatives were shown in Figure 3.6. The degradation temperature and the temperature for 10 % weight loss (Table 3.3) indicated that all the benzoylated PPO, in general, have lower thermal stability than unsubstituted PPO; PPO-BzNO₂ being the least stable.

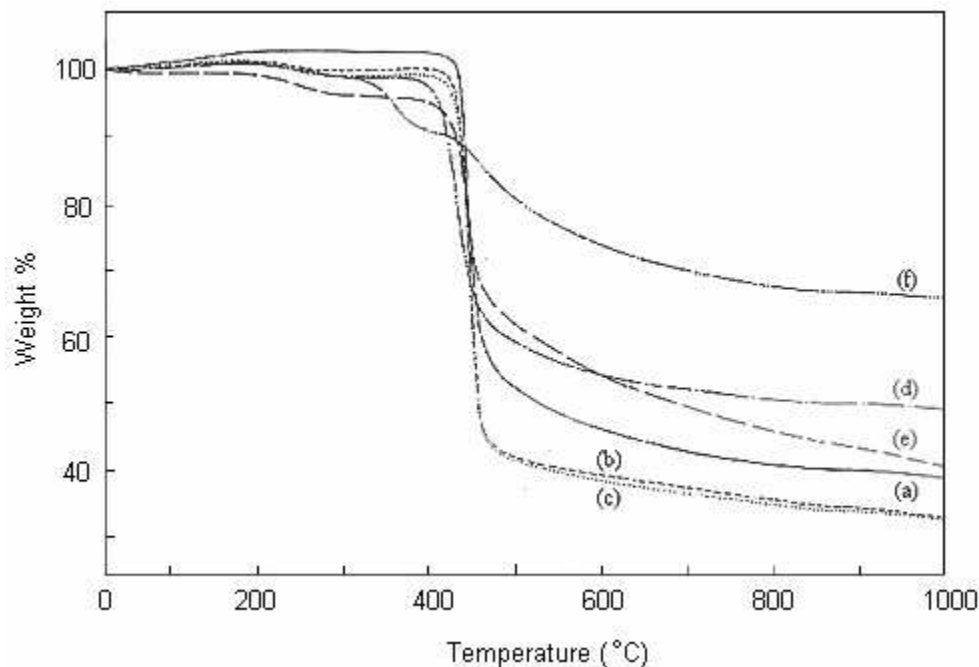


Figure 3.6 TGA spectra of PPO and aryl substituted PPO (a: PPO, b: PPO-BzH, c: PPO-BzCH₃, d: PPO-BzBr, e: PPO-BzCl, f: PPO-BzNO₂)

The thermal stability of PPO-BzCl and PPO-BzBr was intermediate between those for PPO-BzNO₂ and for PPO-BzH or PPO-BzCH₃. The trend observed by TGA was almost opposite than the trend observed for T_g . The temperature at 10 % weight loss (T_{10}) was lower for all the substituted PPO than for the unsubstituted PPO and the lowest being for the nitro-containing polymer. Thus, though the substitution by a polar benzoyl group on PPO led to the increased chain stiffness, it lowered the thermal stability.

3.4.2.5 Packing density parameters

The packing density was characterized by fractional free volume (v_f) estimated by density measurement and d-spacing (d_{sp}) calculated from the WAXD spectra (Figure 3.7). As seen from Table 3.3, with an exception of PPO-BzBr, the v_f for all the substituted PPO decreased in comparison to the unsubstituted PPO. In case of PPO-BzBr, though the degree of substitution was 54.5 %, the v_f was estimated to be slightly higher than even

for the unsubstituted PPO. Such an increase in fractional free volume by bromination was reported for PPO [Chern 1987].

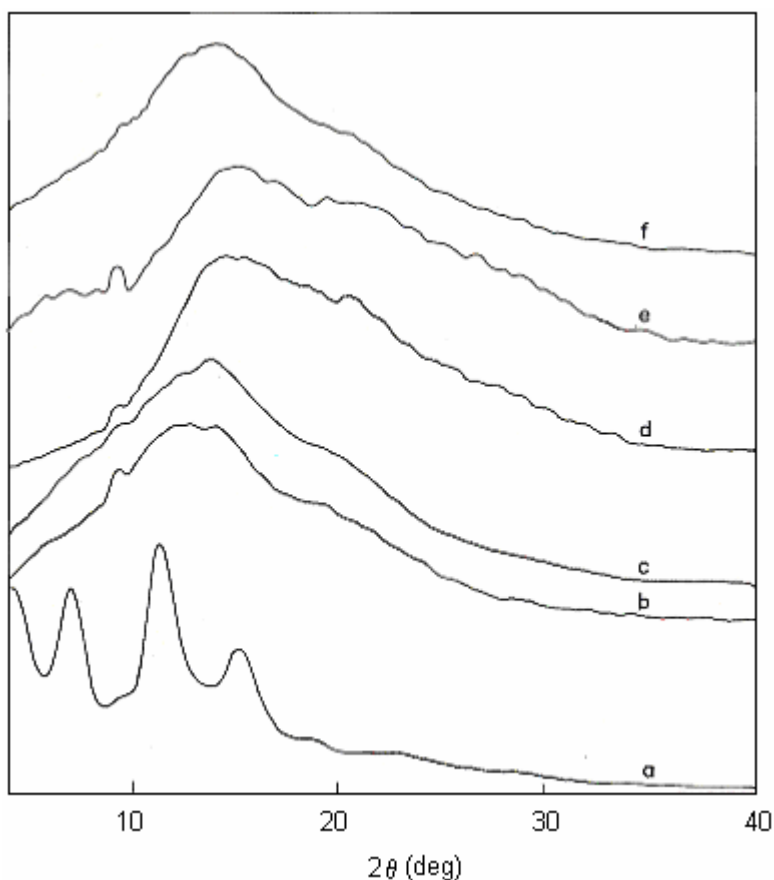


Figure 3.7 Wide angle X- ray spectrum of PPO and benzoyl substituted PPO (a: PPO, b: PPO-BzH, c: PPO-BzCH₃, d: PPO-BzBr, e: PPO-BzCl, f: PPO-BzNO₂)

The WAXD spectra showed that these polymers were mostly amorphous in nature as distinct crystalline peak was absent. While the unsubstituted PPO showed some crystallinity (as also observed by Khulbe et al. [2000]), the benzylation rendered a non-uniform packing eliminating crystalline domain formation in spite of the polar nature of the introduced benzoyl group.

3.4.3 Permeation properties of PPO and benzoylated PPO

The gas permeability of unsubstituted PPO (Table 3.4) was in qualitative agreement with the data reported by Khulbe et al. (except for CO₂ permeability), with toluene as the casting solvent [Khulbe (1997a)]. The high CO₂ permeability observed by

Khulbe was attributed to the pinholes or unknown defects owing to gel type solution of PPO in toluene. In the present investigation, no gel formation was observed when PPO was dissolved in toluene. The helium and other gas permeability reported by Poloskaya [Polotskaya (1996)] were considerably higher than observed in present case. The permeation properties of the PPO are well reported in the literature and differ considerably [Polotskaya (1996), Chowdhury (2000), Chern (1987), Story (1992), Zhang (1994), Percec (1987), Khulbe (1997a), Khulbe (1997b)]. It is known that various factors are responsible for the observed variations in gas permeabilities of PPO. These include physical properties of solvent used for PPO dissolution [Khulbe (1997a)], casting temperature [Khulbe (1997b)], molecular weight of PPO [Chowdhury (2000)], etc.

It could be seen from Table 3.4 and 3.5 that the benzylation of PPO resulted, in general, lowered permeability and a similar or increased selectivity (except for a decrease in CO₂ based and N₂/CH₄ selectivities) than for the unsubstituted PPO. The lowering in permeability could be attributed to the better packing of the polymer chains as a result of polar benzoyl group substitution. The flat nature of the phenyl ring of the benzoyl group may also contribute to the closer packing. This could be further supported by the reduced d-spacing (d_{sp}) and the fractional free volume (v_f) of the benzyolated PPO as seen from the Table 3.3, with an exception of the higher observed v_f for bromine containing PPO-BzBr. Such a behavior of observed higher fractional free volume when bromine is present on the polymer backbone was also reported in other cases of bromination, such as PPO [Chern (1987)] and in case of polyarylates [Kharul (1997)].

Table 3.4 Permeability (P)^a coefficients of PPO and benzyolated PPO

Gas	PPO	PPO-BzH	PPO-BzCH ₃	PPO-BzBr	PPO-BzCl	PPO-BzNO ₂
P(He)	92.0	47.7	50.6	51.4	52.7	41
P(Ar)	6.2	2.6	3.57	4.1	4	2.45
P(N ₂)	4.6	1.59	2.42	2.13	1.8	1.27
P(O ₂)	13.7	6	7.36	8.45	8.6	5.04
P(CO ₂)	51	14.3	21.4	18	16.8	11.4
P(CH ₄)	2.3	0.95	1.49	1.13	0.98	0.76

^a In units of 10⁻¹⁰ [cm³(STP).cm/(cm².s.cm Hg)] at upstream pressure of 6.8 atm and at 35 °C.

Table 3.5 Selectivity (α)^a for different gas pairs of PPO and benzoylated PPO

Gas pair	PPO	PPO-BzH	PPO-BzCH ₃	PPO-BzBr	PPO-BzCl	PPO-BzNO ₂
$\alpha(\text{He}/\text{Ar})$	14.8	18.3	14.2	12.5	13.2	16.7
$\alpha(\text{He}/\text{N}_2)$	20	30	21	24.1	29.3	32.3
$\alpha(\text{He}/\text{CH}_4)$	40	50	34	45.5	53.8	53.9
$\alpha(\text{Ar}/\text{N}_2)$	1.35	1.42	1.48	1.92	2.2	1.93
$\alpha(\text{O}_2/\text{N}_2)$	2.98	3.8	3.0	4.0	4.8	4.0
$\alpha(\text{CO}_2/\text{N}_2)$	11.1	9	8.8	8.5	9.3	9.0
$\alpha(\text{CO}_2/\text{CH}_4)$	22	15.1	14.4	15.9	17.1	15.0
$\alpha(\text{N}_2/\text{CH}_4)$	2	1.67	1.62	1.88	1.83	1.67

^a Ratio of pure gas permeability.

The substitution of the benzoyl group on PPO was done in an anticipation of increase in selectivity owing to the increased polarity (as also supported by the increased solubility parameter). The sulfonylation of PPO offered an increase in the CO₂ based selectivity [Percec (1987)], while the acylation incorporating long alkyl chain drastically reduced these selectivity. Though both these substitutions are of Friedel-Crafts type, the permeation behavior was highly dependant on the nature of the substituent. In the present work, though the permeability coefficients for all the gases were found to be decreased, the selectivity for various gas pairs did not show general increase. In all the substituted PPO, the helium-based selectivity was either increased or remained comparable with the unsubstituted PPO within experimental limits. The O₂/N₂ selectivity was increased after benzoylation except for PPO-BzCH₃. The CO₂ permeability was reduced to a greater extent than the reduction observed in the case of N₂ or CH₄. This led to an overall decrease in CO₂ based selectivities in all the cases of benzoylation. This was in contrary to the earlier case of acylation [Percec (1987)], where the CO₂ permeability was either increased or remained same. An overall increase in CO₂ based selectivities by various polar group substitutions was reported in the literature. This includes carboxylation [Story (1992)], sulfonation [Polotskaya (1997), Chowdhury (2000)], nitration [Ghosal (1992)] and bromination [Chowdhury (2000), Chern (1987)] of PPO. It could be inferred in present case that, the closer packing of polymer chains could

lead to the decreased permeability for all gases including CO₂. Based on this behavior of reduction in permeability, it could be speculated that the gas diffusivity becomes more dominant than the solubility and governs observed variation in the permeation properties. It would have been more informative to evaluate the solubility and diffusivity parameters, which could not be made possible. The Ar/N₂ selectivity was improved, while the N₂/CH₄ selectivity was decreased in all the cases.

The observed complex trend in permeability by benzylation can be elucidated on the basis of (i) the nature of the benzoyl group (and the group present at *para*-position of the >C=O of the benzoyl group) and (ii) the degree of benzylation. Though Table 3.4 shows a general decrease in permeability coefficients for all the benzyolated PPO, the variation was not monotonous. This could be better explained with the help of Figure 3.8. The reduction in gas permeability for different gases was in the order He < CH₄ < N₂ < CO₂ for a particular case of benzylation, which is in the order of their increasing molar mass (Table 3.6). It is interesting to note that the extent of decrease in permeability followed the trend of increasing molar mass of gases and not the kinetic diameter. The decrease in helium permeability was lowest, which was in agreement with its lowest kinetic diameter and molar mass as well. Though the kinetic sieving diameter of N₂ is smaller than that for CH₄, the reduction in permeability for the former was more. The percent decrease in the CO₂ permeability was even higher than for N₂ and CH₄, though its kinetic diameter is lower than for the other two. Thus, the trend in percent decrease in permeability for CO₂, N₂ and CH₄ was actually reversed than the trend for their kinetic sieving diameter. This behavior holds true for all the cases of benzylation (with an exception of reduction in He permeability for PPO-BzCH₃), irrespective of their degree of substitution.

Table 3.6 Properties of gases used for the permeation study of benzyolated PPO

Gas	He	CH ₄	N ₂	CO ₂
Kinetic Sieving diameter (Å)	2.6	3.8	3.64	3.3
Molar mass gm/cm ³	4	16	28	44

It could be seen from Figure 3.8 that the group present at the *p*-position to >C=O of benzoyl group has a role in governing gas permeation. For example, observed

reduction in permeability for a particular gas was highest in the case of PPO-BzNO₂, though its degree of substitution was 60 %.

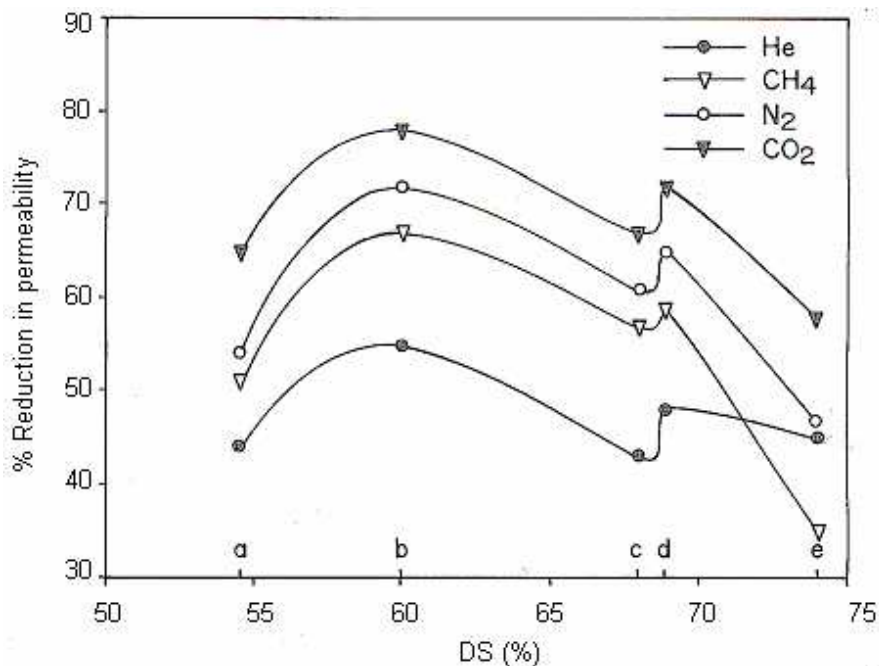


Figure 3.8 Variation of percent reduction in permeability after benzoylation of PPO with degree of substitution (a: PPO-BzBr, b: PPO-BzNO₂, c: PPO-BzCl, d: PPO-BzH, e: PPO-BzCH₃)

The nitro group being most polar than the other groups at *para*-position, the maximum reduction in permeability was observed in this case even though the degree of substitution was comparatively lower than other cases of benzoylation. Whilst the degree of substitution was highest (74 %) for PPO-BzCH₃, it showed the lowest reduction in permeability (except for He). This could be because of the nonpolar nature of the *para*-methyl group, which does not contribute to further enhance the polar interactions induced by benzoyl group.

The permeability of various gases for PPO-BzBr and PPO-BzCl were closer to that of PPO-BzCH₃ than of PPO-BzNO₂, indicating the bulk of Cl and Br may also be contributing in governing permeation properties in addition to their polar nature. This could be supported by the combined higher permeability and good selectivity shown by PPO-BzBr in spite of its lower degree of substitution, wherein the bulk could be contributing towards higher permeability and polarity contributing towards selectivity. Interestingly though the degree of substitution in case of PPO-BzH and PPO-BzCl was

similar, the percent reduction in permeability was more in the former case (Figure 3.8). This could be explained on the basis of flat nature of benzoyl-phenyl ring of PPO-BzH, that does not have *para*-substituent. The similar effect of lowering in permeability was reported for triphenylsilyl PPO [Zhang (1994)] and diphenyl PPO [Alentiev (1998)] in comparison with their methyl counterparts. Thus it could be speculated that the diffusivity of gases was greatly affected by benzoyl group substitution on PPO.

3.4.4 Nitration, amination and amide group substitution

The benzoyl group substitution on PPO offered general decrease in permeability of different gases with considerable increase in He based selectivities and reduction in CO₂ based selectivities (Section 3.4.3). It is known that presence of amide/amine functionality enhanced permeation properties of acid gas like CO₂ in poly(N-vinyl- γ -sodium aminobutyrate) [Zhang (2002)]. In view of high intrinsic permeability of PPO, it was thought to substitute bulky amide group via nitration followed by amination of PPO, to draw effects of bulky and polar amide group simultaneously, on permeation properties of resulting substituted PPO. The nitration and amination could be successfully achieved with high degree of substitution as elaborated in Section 3.4.4.1. An amide formation was investigated with benzoyl chloride to quickly assess the feasibility of transformation of the product to film form. Though the amide formation took place as revealed by disappearance of -NH₂ group in IR spectra (Section 3.4.5.1), the formed film was brittle owing to further chain degradation as assessed by decrease in viscosity. The viscosity of PPO-NH₂ was 0.33 dl/g, which reduced to 0.30 dl/g after amide formation. This material could not be transformed to the film that would withstand the gas pressure in permeation cell. This made us to withdraw investigations with amide substituted PPO. Since nitration was achieved with high degree of substitution, its conversion to amine and investigations of physical and gas permeation properties were performed as given in following sections.

3.4.4.1 Synthesis of nitro and amine group containing PPO

The gas permeation properties of nitrated PPO though were reported in the literature [Ghosal (1992)], the degree of nitration was merely 15 %. It was said that at higher degree of nitration, chain degradation had taken place [Ghosal (1992)]. Since

nitration makes the phenyl ring more susceptible to nucleophilic cleavage [Ghosal (1995)], nitration using PPO of high viscosity thought to be worthwhile. Though the chain degradation is inevitable during nitration, using precursor PPO of high viscosity (2.6 dl/g) and by careful monitoring nitration reaction parameters, nitrated PPO with enough viscosity and degree of substitution (57 %) was obtained, so that its film could withstand the gas pressure during permeation measurement to ably investigate the effects of nitration and amination.

The nitration of PPO was done while varying volume ratio of nitrating mixture ($\text{HNO}_3\text{:H}_2\text{SO}_4$) from 1:1 to 4:1. Though effects of variation of other reaction parameters like time and temperature on improving degree of nitration is also known [Pan (1996)], these parameter variations in present case could not offer the polymer that would withstand pressure on its film during gas permeation measurements. The variation of viscosity and degree of nitration (DS, obtained from $^1\text{H-NMR}$ spectra) with the variation in this volume ratio of nitrating mixture is given in Table 3.7. The reaction time (30 minutes) and temperature (25 °C) were carefully monitored. Beyond 57 % DS, the material with sufficient viscosity (that lead to good film formation) could not be obtained. The nitration is known to be restricted to a level of monosubstitution of PPO phenyl ring, as this group deactivates the aromatic ring towards further electrophilic substitution, strongly inhibiting the introduction of a second nitro group on a ring that already contains a nitro group [Morrison (1989)].

Table 3.7 Effect of HNO_3 : H_2SO_4 volume ratio on nitration of PPO

Volume ratio	(% DS)	$[\eta]$ dl/g
0:0	0	2.6
1:1	17	0.53
2:1	35	0.42
4:1	57	0.36

The amination (conversion of NO_2 to NH_2) was done using PPO- NO_2 having 57 % degree of substitution. The complete conversion of $-\text{NO}_2$ to $-\text{NH}_2$ was obtained as revealed by spectral analysis (IR and $^1\text{H-NMR}$).

3.4.5 Physical properties of nitrated and aminated PPO

3.4.5.1 Spectral properties

IR spectra of unmodified PPO, PPO-NO₂, PPO-NH₂ and PPO-NHCOPh were as shown in Figure 3.9.

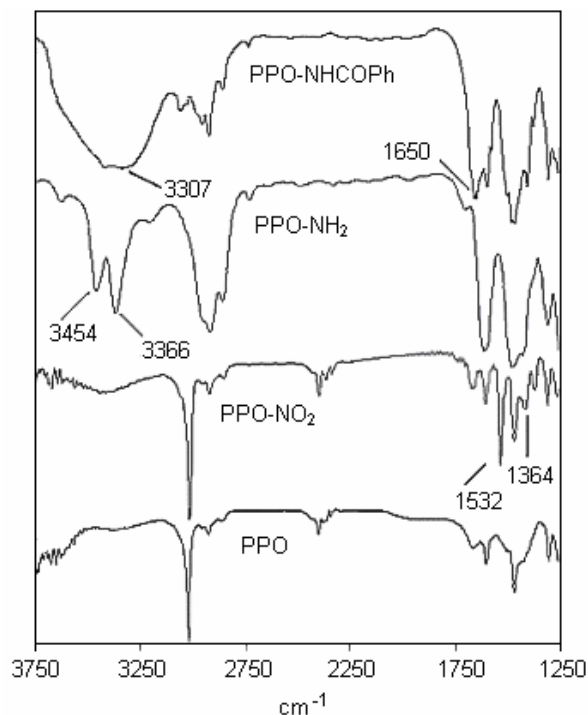


Figure 3.9 IR spectra of PPO, PPO-NO₂, PPO-NH₂ and PPO-NHCOPh

The IR spectra of unmodified PPO exhibited a band at 1214 cm⁻¹ attributable to the symmetric stretch vibration for the C–O–C of aromatic ether. The spectra of the PPO-NO₂ exhibited two additional absorption bands at 1532 cm⁻¹ and 1364 cm⁻¹, corresponding to the aromatic -NO₂ antisymmetric stretch and the -NO₂ symmetrical stretch, respectively [Ghosal (1995)]. A peak at 1532 cm⁻¹ disappeared after reduction of PPO-NO₂ to PPO-NH₂, suggesting complete conversion of nitro group to the amino. The IR spectrum of PPO-NH₂ exhibited absorption bands at 3366 cm⁻¹ and 3454 cm⁻¹ corresponds to the N-H anti-symmetric and symmetric stretch while peak at 1625 cm⁻¹ corresponding to the NH₂ deformation [Lambert (1987)]. A peak at 1650 cm⁻¹ (C=O stretch) in case of PPO-NHCOPh confirmed the conversion of -NH₂ group to -NHCOPh.

The ¹H-NMR spectra of the PPO, PPO-NO₂, and PPO-NH₂ were as presented in Figure 3.10 together with the assignment of their proton resonances.

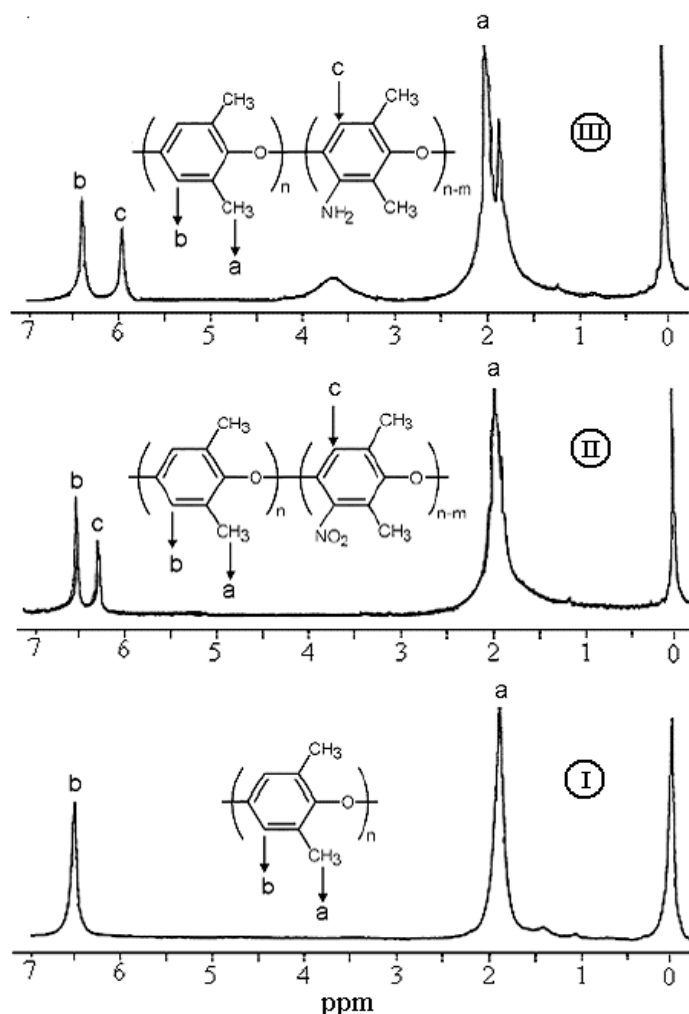


Figure 3.10 $^1\text{H-NMR}$ spectra of PPO (I), PPO- NO_2 (II) and PPO- NH_2 (III)

The $-\text{CH}_3$ protons in NMR spectra of all the three PPO appeared at 2 ppm. The NMR spectrum of PPO- NH_2 exhibited a new peak at 3.5 ppm, which was ascribed to the protons of amine group. The degree of substitution (DS) in both, PPO- NO_2 and PPO- NH_2 was calculated based on peak positions in the $^1\text{H-NMR}$ spectrum. The aromatic protons due to unsubstituted PPO repeat unit appears at 6.4-6.5 ppm, while the protons due to substituted PPO repeat unit appears at 6.1-6.2 ppm; as typically observed for other types of PPO substitutions, viz., acylation and sulfonylation [Percec (1987)]. The percent degree of substitution (DS) was determined from the ratio of integrals of the proton resonances due to the unsubstituted PPO units (signal H_b at $\sim 6.4/6.55$ ppm, as shown in Figure 3.10) and those for the substituted units (signal H_c at $\sim 5.95/6.3$ ppm). The DS was calculated using Equation 3.3.

3.4.5.2 Thermal and dynamic mechanical properties

The degradation temperature as obtained by TGA indicated that both, PPO-NO₂ and PPO-NH₂ possess lower thermal stability than unsubstituted PPO (Table 3.8). The order of stability was PPO >> PPO-NO₂ > PPO-NH₂. The presence of -NO₂ group reduced thermal stability of polymer chains, as also indicated by lowering in viscosity during the nitration reaction. The PPO-NH₂ also exhibited lower thermal stability, with degradation temperature at 306 °C. A lowering of thermo-oxidative stability by amination is known in case of PSF [Son (2002)] also. The TGA spectra of PPO-NO₂ and PPO-NH₂ were as shown in Figure 3.11. A similar reduction in thermal stability by benzoylation of PPO was observed (Section 3.4.2.4), though benzoylation led to an increased chain stiffness as revealed by their glass transition temperature, T_g.

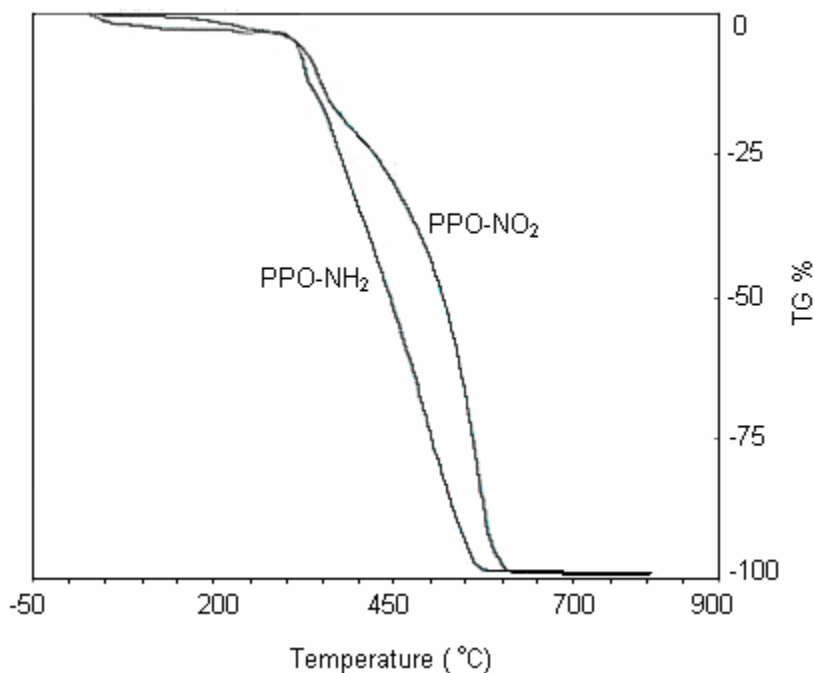


Figure 3.11 TGA spectra of PPO-NO₂ and PPO-NH₂

Unfortunately, T_g of PPO-NO₂ and PPO-NH₂ could not be recorded on Thermal instrument DSC-Q10 under N₂ atmosphere with the heating rate of 10 °C/minute. It was still possible to conclude that the chain stiffness is elevated by either the nitration or amination (as a result of added polarity) by DMA analysis. The tan δ curve in DMA spectra as shown in Figure 3.12 indicated that the α -transition temperature of PPO was lower than that for PPO-NH₂ or PPO-NO₂. The DMA could not be recorded beyond 300

°C, since these materials degrade beyond this temperature, as revealed by TGA. The α -transition temperature for PPO, PPO-NH₂ and PPO-NO₂ was 268 °C, > 300 °C and 286 °C respectively. This peak is usually assigned to thermal excitation of cooperative motions in the chains wherein the polymer is transformed from glassy to rubbery state.

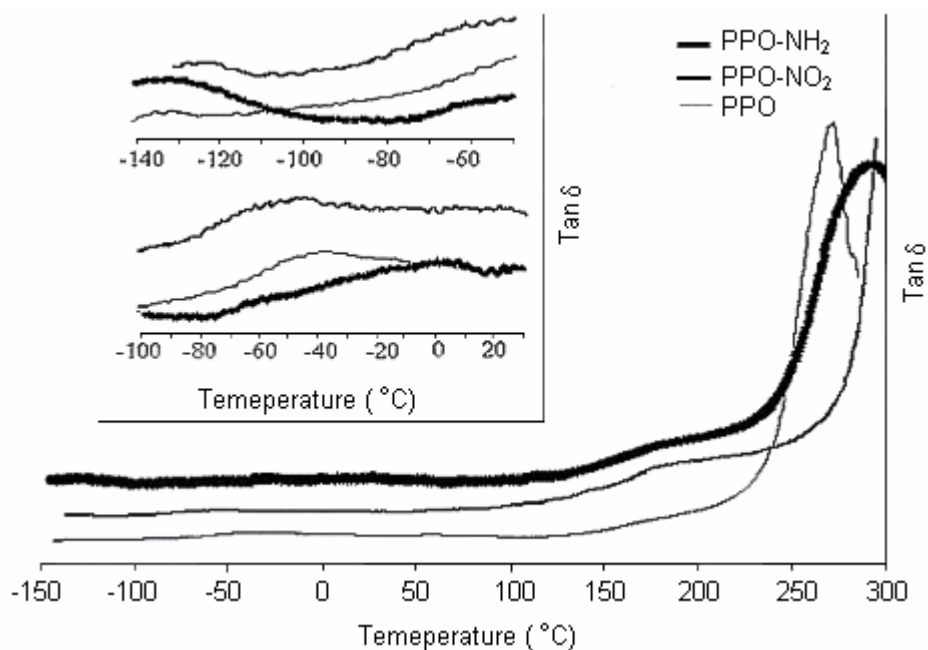


Figure 3.12 DMA spectra of PPO, PPO-NO₂ and PPO-NH₂

The T_g of PPO as determined by DSC in the present case is 220 °C. It is known that the T_α by DMA is usually higher than T_g obtained by DSC [Acuilar-vega (1993), McHattie (1992)]. The variation in frequency can be a reason for shifting the peak position in DMA spectra [Poathan (2003)].

The α -transition peak temperature at 268 °C for PPO is increased to higher temperature in case of PPO-NO₂ and PPO-NH₂ due to induced polar interactions after substitution of nitro and amino groups. A smaller shoulder was observed in all three cases at ~ 170 °C, termed here as β' . This peak could be originating from the defects in packing or less specific cooperative or local mode motions as observed in case of polycarbonates [Yee (1981)]. The long range β transition centered at -40 °C and -45 °C in case of PPO and PPO-NO₂ were observed, which was increased to 7 °C in case of PPO-NH₂, probably due to the presence of H-bonding in this polymer. The β transition for PPO is observed at 5 °C by Chung and Sour [Chung (1971)] and was ascribed to the local cooperative

motions of several monomer units. The low temperature wide range relaxation originating from test temperature of -140 °C till -120 °C was observed in all the three polymers. Chung and Sour [Chung (1971)] observed similar peak in case of PPO at -133 to -148 °C and was ascribed to reorientation of the phenylene group about C-O bond.

Table 3.8 Physical properties of nitrated and aminated PPO

Polymer	d_{sp} Å	ρ g/cm ³	v_f^a cm ³ /cm ³	δ^b (cal/cm ³) ^{1/2}	DMA relaxation				TGA(°C)	
					temperature (°C)				DT	T ₁₀
					α	β'	β	γ		
PPO	11.06, 6.95	1.05	0.392	8.60	268	165	-40	-135	425	445
PPO-NO ₂	6.76	1.16	0.377	9.44	> 300	185	-45	-124	313	338
PPO-NH ₂	6.58	1.11	0.369	-	286	172	7	-136	306	331

3.4.5.3 Packing density parameters

The chain packing in polymer matrix can be characterized by either fractional free volume (v_f) estimated from the density measurement or by d-spacing (d_{sp}) calculated from the WAXD spectra. As presented in Table 3.8, the v_f of the PPO-NO₂ and PPO-NH₂ is significantly lower than that of unmodified PPO. This could be due to the added polar interactions because of the presence of -NO₂ or -NH₂ groups. The increased solubility parameter (δ) of PPO-NO₂ also indicated the added polarity. The decrease in v_f in case of the nitro-substituted polysulfone was ascribed to an increase in polymer cohesive energy density caused by the polar nature of these group [Chern (1985)]. A 192 % nitration of PSF is also known to reduce v_f by 23 % in comparison to unsubstituted PSF [Ghosal (1995)].

The WAXD spectra (Figure 3.13) showed that PPO-NO₂ and PPO-NH₂ are amorphous in nature since a distinct crystalline peak was absent. While the unsubstituted PPO exhibited a pattern for a typical semicrystalline polymer (which is known for PPO), the nitration and amination rendered a non-uniform packing eliminating crystalline domain formation in spite of the polar nature of the -NO₂ and -NH₂ groups. A better chain packing as revealed by decreased d-spacing (d_{sp}) by both, nitro and amine

substitution (Table 3.8) can be ascribed to the attractive polar interactions caused by these groups. The slightly lower d_{sp} of PPO-NH₂ than for PPO-NO₂ in spite of the larger size of nitro group ($V_w = 16.8 \text{ cm}^3/\text{mol}$) than that of amino group ($V_w = 10.54 \text{ cm}^3/\text{mol}$) suggested that the H-bonding interactions by -NH₂ are more effective in bringing chains together than that the polar interaction of -NO₂ would do.

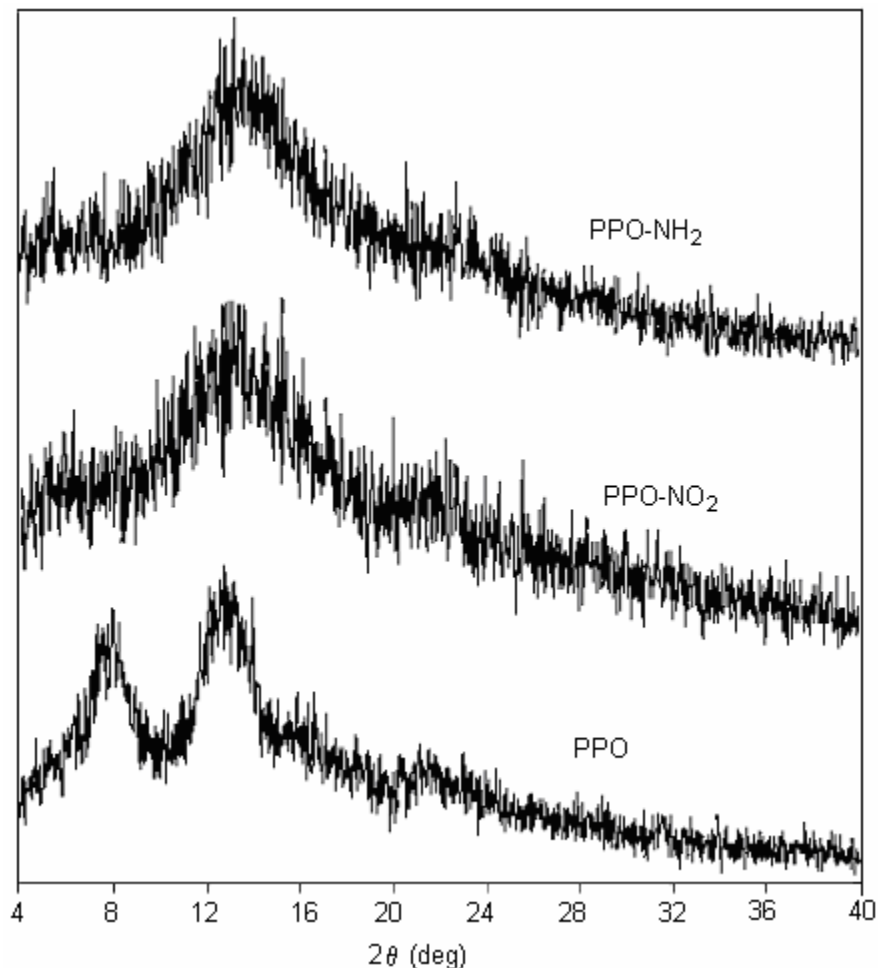


Figure 3.13 Wide angle X-ray diffraction spectra of PPO, PPO-NO₂ and PPO-NH₂

3.4.6 Gas sorption properties of PPO-NO₂ and PPO-NH₂

The sorption experiments were carried out with unsubstituted PPO, PPO-NO₂ and PPO-NH₂ at 35 °C using pure gases: N₂, CH₄ and CO₂. The sorption of O₂ is performed only at 6.8 atm pressure. The sorption isotherms are as shown in Figure 3.14. The isotherms show a shape typical of the dual-mode sorption behavior for gases in glassy polymers as described by Equation 1.8 [Vieth (1966)].

$$C = k_D p + \frac{C'_H b p}{1 + b p} \quad (1.8)$$

where C is the total concentration of the penetrant in the polymer, k_D is the Henry's law constant, C'_H is the Langmuir hole saturation constant, b is the Langmuir affinity constant and p is the pressure.

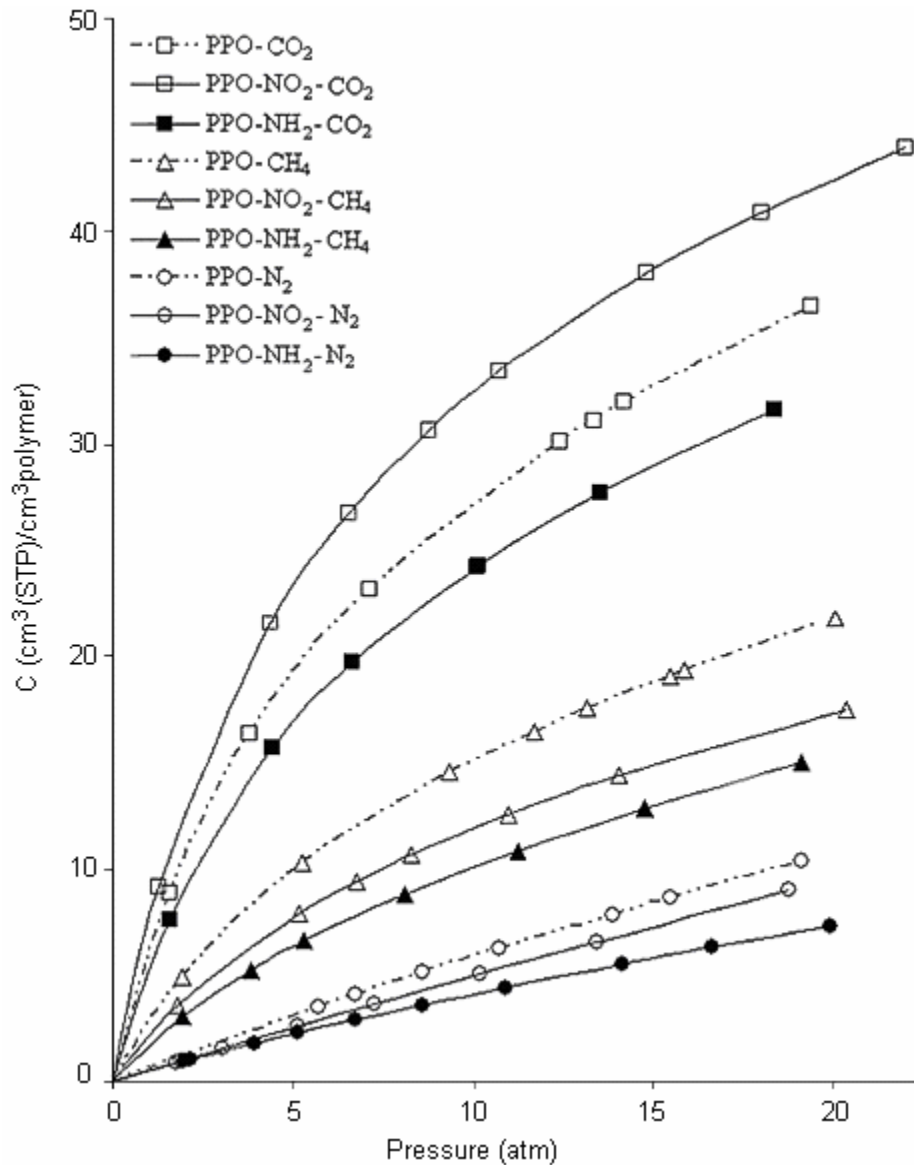


Figure 3.14 Sorption isotherm of PPO, PPO-NO₂ and PPO-NH₂ for N₂, CH₄ and CO₂

The dual mode parameters, which characterize sorption in PPO, PPO-NO₂ and PPO-NH₂ as determined by regression analysis, are given in Table 3.9.

Table 3.9 Dual-mode sorption parameters for PPO, PPO-NO₂ and PPO-NH₂ at 6.8 atm pressure and at 35 °C

Polymer	Gas	k_D (cm ³ (STP) /cm ³ .atm)	C'_H (cm ³ (STP) /cm ³ polymer)	B (l/atm)
PPO	N ₂	0.356	8.45	0.037
	CH ₄	0.377	19.07	0.146
	CO ₂	0.513	33.49	0.197
PPO-NO ₂	N ₂	0.375	6.13	0.025
	CH ₄	0.305	15.30	0.137
	CO ₂	0.4319	42.35	0.199
PPO-NH ₂	N ₂	0.232	5.65	0.046
	CH ₄	0.343	11.80	0.129
	CO ₂	0.453	30.17	0.186

The gas solubility at 6.8 atm (the pressure used for determining gas permeability) and solubility selectivity of various gas pairs are tabulated in Table 3.10.

Table 3.10 Apparent solubility coefficient for PPO, PPO-NO₂ and PPO-NH₂ at 6.8 atm pressure and at 35 °C

Polymer	Apparent solubility coefficient (S) ^a						
	S(N ₂)	S(O ₂)	S(CH ₄)	S(CO ₂)	S(O ₂ /N ₂)	S(CO ₂ /CH ₄)	S(CO ₂ /N ₂)
PPO	0.61	0.75	1.77	3.33	1.24	1.88	5.47
PPO-NO ₂	0.50	0.70	1.39	4.01	1.40	2.88	7.94
PPO-NH ₂	0.43	0.58	1.15	2.93	1.34	2.54	6.82

^a Solubility coefficient in [cm³(STP)/cm³(polymer) atm].

The nitration and amination of PPO generally lowered the sorption of gases studied, with an exception of increase in CO₂ sorption (by ~ 20 %) in case of PPO-NO₂. The C'_H for N₂ and CH₄ in case of polymers investigated here decrease in the order PPO > PPO-NO₂ > PPO-NH₂, following the order of decrease in free volume or d_{sp} for the series. The C'_H for CO₂ in PPO-NO₂ is higher than for PPO and PPO-NH₂, owing to its higher sorption as seen from Figure 3.15.

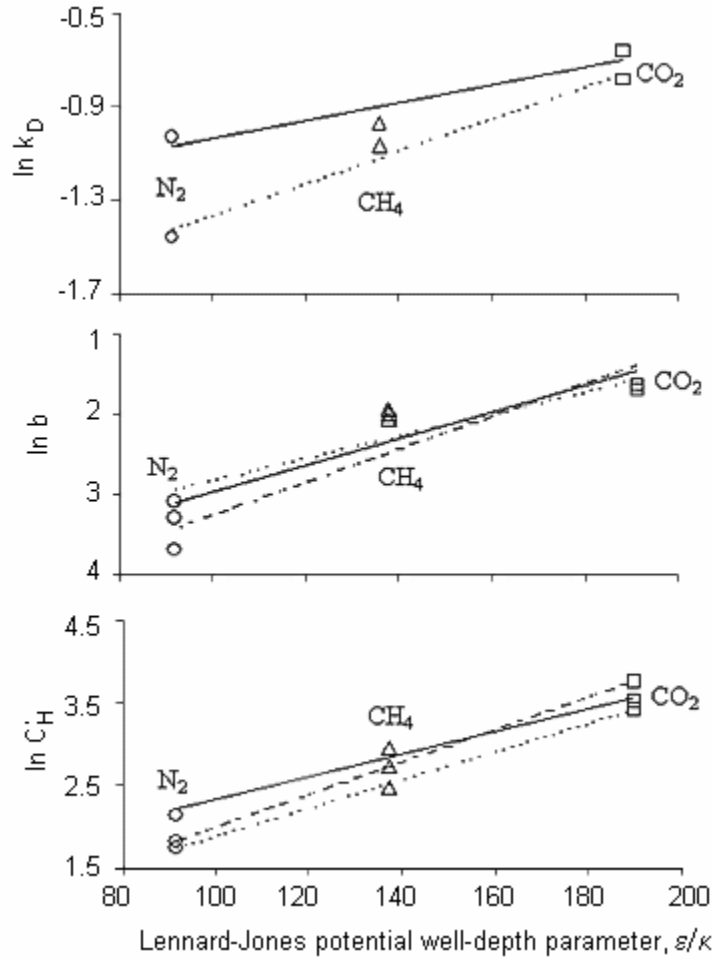


Figure 3.15 Correlation of sorption parameters with Lennard-Jones potential well-depth parameter (— PPO, - - - PPO-NO₂, PPO-NH₂)

In case of condensable gases: CO₂ and CH₄, the Henry's law coefficient, k_D , which characterizes gas sorption in the dissolved state, is higher for PPO-NH₂ than that for PPO-NO₂. The Henry's law constant k_D , Langmuir hole saturation constant C'_H and affinity constant b correlate well with Lennard-Jones potential well-depth parameter, ϵ/κ (which characterizes the tendency of a gas to get sorbed) for N₂, CH₄, CO₂ as shown in Figure 3.15, except for N₂ in PPO-NO₂. These parameters decreased with gas condensability in the order N₂ < CH₄ < CO₂, for a particular polymer.

3.4.7 Permeation properties of nitrated and aminated PPO

The gas permeability and selectivity for various gas pairs were as presented in Table 3.11 and 3.12. The gas permeability in case of unsubstituted PPO was higher than

that of given in Table 3.4. This difference primarily stem from the solvent used for membrane preparation. During present PPO investigations, CHCl_3 was used as the casting solvent; while during investigating PPO-benzoylation, toluene was used as casting solvent. The permeation properties of the PPO are known to differ considerably based on the solvent used for PPO dissolution [Khulbe (1997a)], casting temperature [Khulbe (1997b)], molecular weight of PPO [Chowdhury (2000), Polotskaya (1996)], etc.

Table 3.11 Permeability coefficient (P) of PPO, PPO-NO₂ and PPO-NH₂

Gas	PPO	PPO-NO ₂	PPO-NH ₂
P(He)	127.5	85.2	36.1
P(N ₂)	9.6	3.64	1.3
P(O ₂)	29.6	14.1	5
P(CH ₄)	7.2	2.14	0.76
P(CO ₂)	97.2	45.4	25.9

Table 3.12 Selectivity (α) for various gas pairs of PPO, PPO-NO₂ and PPO-NH₂

Gas	PPO	PPO-NO ₂	PPO-NH ₂
$\alpha(\text{He}/\text{N}_2)$	13.3	23.4	27.8
$\alpha(\text{He}/\text{CH}_4)$	17.8	39.8	47.6
$\alpha(\text{O}_2/\text{N}_2)$	3.1	3.9	3.8
$\alpha(\text{CO}_2/\text{N}_2)$	10.1	12.5	20
$\alpha(\text{CO}_2/\text{CH}_4)$	13.6	21.2	34
$\alpha(\text{N}_2/\text{CH}_4)$	1.3	1.7	1.7

Gas permeability after PPO substitution by either -NO₂ or -NH₂ group reduced considerably due to increase in packing density as revealed by a reduction in v_f and d_{sp} after the substitution. The reduced torsional mobility as revealed by increase in T_α in $\tan \delta$ curve of DMA could also contribute to this lowering in permeability. This reduction is associated with an increase in selectivity for various gas pairs in comparison to the unsubstituted PPO. The trend of reduction in permeability and increase in selectivity

follow the general order: PPO-NH₂ > PPO-NO₂ > PPO. The larger decrease in PPO-NH₂ permeability than that for PPO-NO₂ is a result of higher packing density in earlier case.

The “concentration averaged” diffusivity has been calculated using permeability and solubility coefficients as presented in Table 3.13. As a result of polar group substitution leading to an increase in packing density and decrease in chain / subgroup motions, a large reduction in diffusivity is observed in both the cases, PPO-NO₂ and PPO-NH₂; the effect being more pronounced in later case. A larger decrease in diffusion coefficients in case of PPO-NH₂ can be ascribed to its better packing density. The diffusion coefficient in case of PPO-NO₂ and PPO-NH₂ decreased in the order: O₂ > CO₂ > N₂ > CH₄, also typically observed in other studies for polycarbonates, polyimides and polysulfones [Ghosal (1995)].

Table 3.13 Concentration-averaged diffusivity of PPO, PPO-NO₂ and PPO-NH₂ at 6.8 atm pressure and at 35 °C

Polymer	Diffusivity (D) ^a						
	D _{N₂}	D _{O₂}	D _{CH₄}	D _{CO₂}	D _{O₂} /D _{N₂}	D _{CO₂} /D _{CH₄}	D _{CO₂} /D _{N₂}
PPO	11.98	29.9	3.09	22.16	2.50	7.18	1.85
PPO-NO ₂	5.48	15.2	1.17	8.61	2.77	7.36	1.57
PPO-NH ₂	2.30	6.58	0.50	6.71	2.86	13.42	2.92

^a Diffusivity in 10⁻⁸ cm²/s

Typically, diffusion coefficients of small molecules in polymers are inversely proportional to the penetrant size. The gas diffusivity, D, is often assumed to dependant on free volume as described by the Fujita’s relationship,

$$D = A \exp(-B/v_f) \quad (3.4)$$

where constants A and B are characteristics of the polymer-penetrant system [Ghosal (1996)]. This relation holds good for variation in gas diffusivity within a given family of polymer [Ghosal (1996)]. A good correlation of gas diffusion coefficients with free volume is seen also in the present case as shown in Figure 3.16a following Fujita’s relationship. Typically, in the absence of strong polymer-gas interactions, solubility is a weak function of v_f and increases with increasing v_f [Ghosal (1996)]. As seen from Figure

3.16b, a correlation of gas solubility is seen with v_f , with an exception of CO_2 in PPO- NO_2 . The enhancement in CO_2 solubility is ascribed to interactions between CO_2 and - NO_2 group. Such behavior is consistent with the notion that gases are more soluble in materials with which they have specific interactions. The solubility coefficients for PPO- NO_2 and PPO- NH_2 decreased in the order: $\text{CO}_2 > \text{CH}_4 > \text{O}_2 > \text{N}_2$ as seen from Figure 3.16b.

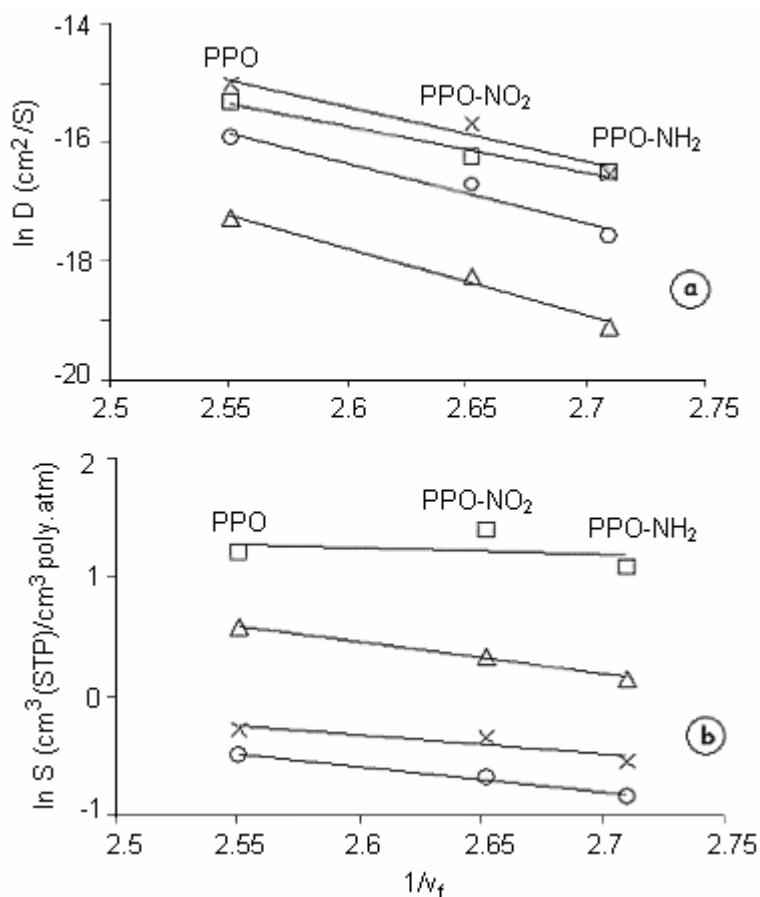


Figure 3.16 Correlation of diffusivity and solubility with $1/v_f$ of PPO, PPO- NO_2 and PPO- NH_2 (\square : CO_2 , Δ : CH_4 , \times : O_2 , \circ : N_2)

The increase in overall selectivity by either nitration or amination is contributed by increase in both, solubility selectivity and diffusivity selectivity (Table 3.10-3.12). It could be seen that the increase in diffusivity selectivity in case of PPO- NH_2 is considerably higher. The amination of PSF [Ghosal (1996)] and carboxylation [Story (1992)] of PPO are also known to increase diffusivity selectivity.

The extent of reduction in He gas permeability with respect to unsubstituted PPO by either $-\text{NO}_2$ or $-\text{NH}_2$ group substitution is lowest among all the gases studied. The percent reduction in permeability of all gases for either PPO- NO_2 or PPO- NH_2 with respect to unsubstituted PPO followed the order of kinetic diameter of the penetrant and showed a good correlation ($R^2 = 0.95$ and 0.78 respectively) as observed from Figure 3.17.

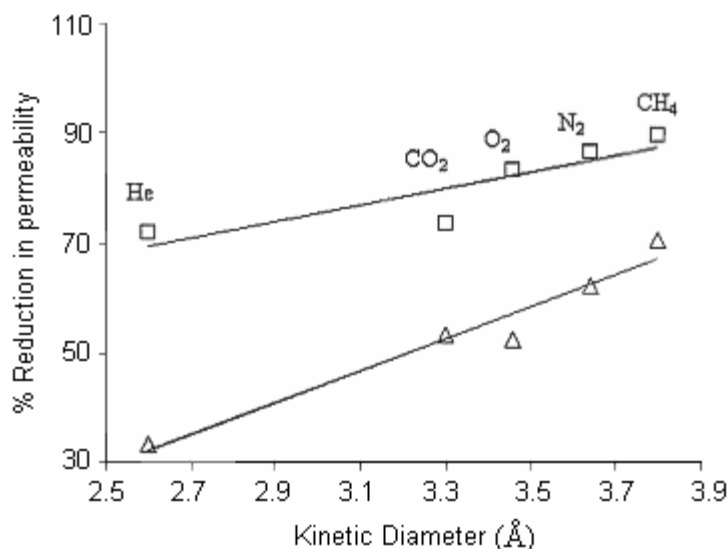


Figure 3.17 Correlation of percent decrease in permeability after PPO substitution with kinetic diameter of penetrants (\square - PPO- NO_2 , Δ - PPO- NH_2)

This indicated that both these substitutions linearly decreased the permeability with kinetic diameter of O_2 , N_2 or CH_4 , with an exception for CO_2 . Owing to this, the extent of increase in CH_4 based selectivity is higher than N_2 based selectivity in case of either PPO- NO_2 or PPO- NH_2 . The decrease in solubility and diffusivity is not monotonous as the inclusion of S_{CO_2} or D_{CO_2} in above correlations disturbs the correlation coefficient, R^2 . This is also supported by observed higher solubility selectivity in case of PPO- NO_2 , while PPO- NH_2 exhibited better diffusivity selectivity; depicting peculiarity of these substitution types.

In case of PPO- NH_2 , it could be expected that there would be some acid-base interaction between acidic CO_2 and the basic $-\text{NH}_2$ group of PPO- NH_2 leading to improved CO_2 solubility. Unfortunately, experimental results do not support this speculation. The amine group is located on aromatic ring leading to the delocalization of

the lone pair of electrons of nitrogen with the aromatic ring, which lowers the availability of this lone pair for interactions with CO₂. The reduction in basicity of the amine attached to aromatic ring of PSF is known [Ghosal (1996)]. On the other hand, in case of PPO-NO₂, the partial charge distribution in -NO₂ group between N and O atoms leading to favorable interactions with CO₂ could be a reason for increased CO₂ sorption in this polymer. It is known that the solubility of a gas in a polymer is determined, in part, by polymer-gas interaction [Ghosal (1994)]. It is reported that increase in polymer polarity appear to enhance CO₂ solubility, whereas decrease in fractional free volume would decrease CO₂ solubility [Ghosal (1995)]. Since CH₄ or N₂ do not possess polarity, S_{CH_4} and S_{N_2} would depend primarily on packing density. This would explain the increase in CH₄ or N₂ based solubility selectivity (CO₂/N₂ or CO₂/CH₄) for PPO-NO₂ and PPO-NH₂ in comparison to the unsubstituted PPO.

3.5 Conclusions

The benzylation of PPO led to an increase in T_g and lowering of thermal stability than unsubstituted PPO. This variation was dependant on the nature of the substituent. A substitution by the nitrobenzoyl group showed the maximum increase in T_g and the lowest thermal stability. All the benzoylated PPO were amorphous in nature and showed solubility in a wide range of solvents.

The nitration of PPO could be obtained with 57 % degree of substitution by optimizing reaction conditions while varying the volume ratio of nitrating mixture and beginning with PPO having high viscosity. The nitro group could be further quantitatively converted to amination as revealed by spectral analysis. The presence of both these groups on PPO backbone increased chain stiffness, lowered thermal stability and increased packing density (lowering in v_f and d_{sp}) than unsubstituted PPO. These variations in physical properties could be ascribed mainly to the added polar interactions. In case of PPO-NH₂, the presence of H-bonding further enhanced packing density than that for PPO-NO₂. In spite of added polarity, nitration and amination of PPO rendered amorphous polymer, though the starting PPO exhibited a pattern for a typical semicrystalline polymer.

PPO benzoylation led to decreased gas permeability owing to induced polarity by benzoyl group. An extent of decrease in the helium permeability was smaller than for the other gases. The percent decrease in permeability of various gases followed the order of their molar mass than the kinetic diameter. The O₂/N₂, Ar/N₂ and helium based selectivities increased, while CO₂ based selectivities decreased. The effect of the group present at the *para*-position of the >C=O of benzoyl had its marked effect on permeation properties. The substitution by the nitrobenzoyl group showed the lowest permeability in this series, while the *p*-chlorobenzoyl substitution showed highest selectivities.

The gas sorption of PPO, PPO-NO₂ and PPO-NH₂ followed a typical dual mode sorption. The nitration and amination of PPO lowered the sorption of gases studied, with an exception of increase in CO₂ sorption (by ~ 20 %) in case of PPO-NO₂. The dual mode sorption parameters C'_H and b decreased in the order PPO > PPO-NO₂ > PPO-NH₂, which is also an order of decreasing v_f or d_{sp} . The sorption parameters of these polymers correlated well with Lennard-Jones potential well-depth parameter, ϵ/κ . The decrease in permeability in case of PPO-NO₂ and PPO-NH₂ as a result of higher packing density and reduced chain motions than that of unsubstituted PPO led to increase in selectivity of various gas pairs up to 2.5 times. The increased packing density in PPO-NH₂ further reduced permeability and improved selectivity in comparison to PPO-NO₂. The reduction in permeability by substitution of NO₂ or NH₂ group was largely contributed by reduction in diffusivity than the solubility. Interestingly, NO₂ group substitution was better effective in improving solubility selectivity while NH₂ group substitution was more effective in improving diffusivity selectivity. The correlation was observed between v_f and gas diffusivity or solubility.

References

- Acuilar-vega M., Paul D.R. *J. Polym. Sci., Part A: Polym. Phys.* **31** (1993) 1577-1589.
- Alentiev A., Drioli E., Gokzhaev M., Golemme G., Ilinich O., Lapkin A., Volkov V., Yampolskii Y. *J. Membr. Sci.* **138** (1998) 99-107
- Bonfanti C., Lanzini L., Roggero A., Sisto R. *J. Polym. Sci., Part A: Polym. Chem.* **32** (1994) 1361-1369.
- Brandrup J., Immergut E.H., Polymer Handbook, 3rd edition, New York: John Wiley & Sons, Inc. 1989. Vol. VII. pp.526-533.
- Chalk A.J., Hay A.S. *J. Polym. Sci., Part A-1: Polym. Chem.* **7** (1969) 691-705.
- Chowdhury G., Vujosevic R., Matsuura T., Laverty B. *J. Appl. Polym. Sci.* **77** (2000) 1137-1143.
- Chern R.T., in Material Science of Synthetic Membranes, D. R. Lloyd (eds.), American Chemical Society, Washington, DC, 1985
- Chern R.T., Shew F.R., Jia R., Stannett V.T., Hopfenberg H.B. *J. Membr. Sci.* **35** (1987) 103-115.
- Chung C.I., Sauer J.A. *J. Polym. Sci., Part A-2* **9** (1971) 1097-1115.
- Daly W.H., Lee S., Rungaroonthaikul C., in Chemical Reaction in Polymers, Benham J.L., Kinstle J.F., (eds.) ACS Symp. Ser., vol. 364, American Chemical Society, Washington, DC, 1988, pp 4-23.
- Ghosal K., Chern R.T. *J. Membr. Sci.* **72** (1992) 91-97.
- Ghosal K., Freeman B.D. *Poly. Adv. Tech.* **5** (1994) 673-697.
- Ghosal K., Chern R.T., Freeman B.D., Savariari R. *J. Polym. Sci., Part B: Polym. Phys.* **33** (1995) 657-666.
- Ghosal K., Chern R.T., Freeman B.D. *Macromolecules* **29** (1996) 4360-4369.
- Houde A.Y., Sorption and permeation of gases in polymers, Ph.D. dissertation (1991), University of Pune, India.

- Khulbe K.C., Matsuura T., Lamarche G., Kim H.J. *J. Membr. Sci.* **135** (1997a) 211-223.
- Khulbe K.C., Chowdhury G., Kruczek B., Vujosevic R., Matsuura T., Lamarche G. *J. Membr. Sci.* **126** (1997b) 115-122.
- Khulbe K.C., Matsuura T., Lamarche G., Lamarche A.M. *J. Membr. Sci.* **170** (2000) 81-89.
- Lambert J.B., Shurvell H.F., Lightner D.A., Cooks R.G., Introduction to organic spectroscopy, Macmillan Publishing Company, New York, 1987.
- Mahajan S.S., Serwade B.D., Wadgaonkar P.P. *Polym. Bull.* **20** (1988) 153-160.
- McHattie J.S., Koros W.J., Paul D.R. *Polymer* **33** (1992) 1701-1711.
- Morrison, R.T. Boyd R.N., Organic Chemistry, Prentice Hall of India, New Delhi, 1989.
- Muruganandam N., Koros W.J., Paul D.R., *J. Polym. Sci. Part: B Polym. Phys.*, **25** (1987) 1999-2026.
- Pan Y., Huang Y., Liao B., Cong G. *J. Appl. Polym. Sci.* **61** (1996) 1111-1115.
- Penczek I., Bialy J., Zbingniew D. US Patent, 1986, US 4607085.
- Percec S. *J. Appl. Polym. Sci.* **33** (1987) 191-203.
- Percec S. *J. Appl. Polym. Sci.* **36** (1988) 415-427.
- Perrin D.D., Armarego W.L.F., Purification of laboratory chemicals, 3 rd edn., Pergamon Press, London.
- Plate N.A., Yampol'skii Yu., in: Paul D.R., Yampol'skii Yu. (Eds.), Polymer Gas Separation Membranes, CRC Press, London, (1994), pp. 156.
- Polotskaya C.A., Acranova S.A., Cazdina N.V., Kuznetsov Yu. P, Nesterov V.V. *J. Appl. Polym. Sci.*, **62** (1996) 2215-2218.
- Polotskaya G.A., Agranova S.A., Antonova T.A., Elyashevich G.K. *J. Appl. Polym. Sci.* **66** (1997) 1439-1443.
- Pothen L.A., Oommen Z., Thomas S. *Comp. Sci. and Tech.* **63** (2003) 283-293.
- Schauer J., Bleha M. *J. Appl. Polym. Sci.* **46** (1992) 1807-1811.

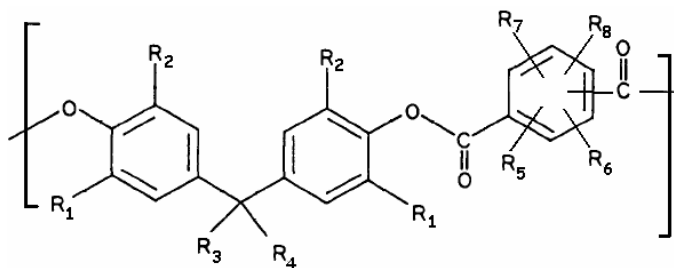
- Son W-K., Song H-Y., Kim S-H., Kim H-J., Kim W-G. *J. Polym. Sci., Part A: Polym. Chem.* **40** (2002) 4281-4287.
- Sterescu D.M., Bolhuis-Versteeg L., Van der Vegt N.F.A., Stamatialis D.F., Wessling M. *Macromol. Rapid Comm.*, **25** (2004) 1674-1678.
- Stern S.A., Gareis P.J., Sinclair T.F., Mohr P.H. *J. Appl. Polym. Sci.* **7** (1963) 2035-2051.
- Story J.B., Koros W.J. *J. Membr. Sci.*, **67** (1992) 191-210.
- Sykes P., A guidebook to mechanism in organic chemistry, 6th Edn., Orient Longman, New Delhi (1988) p. 362–363.
- Tan J.M.A., Noh S.H., Chowdhury G., Matsuura T. *J. Membr. Sci.* **174** (2000) 225-230.
- Toi K., Morel G., Paul D.R. *J. Appl. Polym. Sci.* **27** (1982) 2997-3005.
- Van Krevelen D.W., Hoftyzer P.J., Properties of polymers: correlation with chemical structure, Elsevier Publishing Company, Amsterdam, 1972.
- Verdet L., Stille J.K. *Organometallics* **1** (1982) 380-384.
- Vieth W.R., Tam P.M., Michaels A.S. *J. Colloid and Interface Sci.* **22** (1966) 360-370.
- Vogel A.I., A text book of practical organic chemistry including qualitative organic chemistry, 3rd edn., ELBS, (1973) pp. 71-73.
- Vollmert V.B., Schoene W. *Die Angew. Makromol. Chemie* **7** (1969) 15-28.
- Xu T-W., Yang W-H., He B-L. *Chinese J. of Polym. Sci.* **20** (2002) 53-57.
- Yee A.F., Smith S.A. *Macromolecules* **14** (1981) 54-64.
- Zhang J., Hou X. *J. Membr. Sci.* **97** (1994) 275-282.
- Zhang Y., Wang Z., Wang S.C. *Desalination* **145** (2002) 385–388.

Investigations in polyarylates: Effect of asymmetric ring substitution on bisphenol and polar/bulky group substitution on acid moiety

4.1 Introduction and Literature survey

The potential of using polyarylates as a membrane material can be seen in the study of five types of polymers based on bisphenol-A (Bis-A), viz. polyarylate (PA), polycarbonate (PC), polysulphone (PSF), polyetherimide (PEI) and polyhydroxyether (PH) [Barbari (1989)]. The permeability coefficient for various gases decreased in the order PA > PC > PSF > PEI > PH. The physical properties, especially, the glass transition temperature of PA was appreciable. Their selectivity-permeability combination for gas pairs such as O₂/N₂ falls on close to the so-called “attractive industrial region” [Villegas-Coss (2006)]. They are easily synthesized by conventional solution or interfacial polymerization methods.

Both the monomers of polyarylates, viz., bisphenol and dicarboxylic acid can be conveniently substituted with various substituents. Thus there exists a wide scope for the structural variation of polyarylates by substitution of different types of groups on aromatic ring of either of its monomers. These substituents can be categorized on the basis of their nature (polar, nonpolar, bulky, planer, etc.) and position of the substitution (on diol/diacid with suitable substitution site/symmetry). The repeat unit of polyarylate (Figure 4.1) describes such possibilities of structural variations. Various investigators documented the structure-permeation property relationship as presented in following section [Pessan (1993), Kharul (1998), Houde (1995), Kharul (1997), Pixton (1995a,b)].



Where, R₁ to R₈ = -H, -CH₃, -CF₃, -CH(CH₃)₂, -C(CH₃)₃, Phenyl, -Cl, -Br, -NO₂, etc.

Figure 4.1 Repeat unit of polyarylate

4.1.1 Effect of substitution on bisphenol moiety

The placement of substituent group on bisphenol phenyl rings can have a marked effect on the gas transport as well as other physical properties of the resulting polymer [McHattie (1991), Pixton (1995a), Kharul (1998)]. Bisphenol phenyl ring could be substituted by various groups (bulky, polar, planner, etc.) at the ortho position in symmetric/asymmetric manner. Similarly, dicarboxylic acid may be comprised of single aromatic ring/multiple ring/fused ring system, etc., containing appropriate type/number of substituents. Effects of such substitutions on gas permeation properties of resulting polyarylates explored in the literature are briefed below.

4.1.1.1 Effect of bulky non-polar group substitution

The effects of bisphenol substituent groups with different size, symmetry and polarity on the gas transport properties of resulting polyarylates were examined [Charati (1991), Chen (1993a), Pixton (1995a), Kharul (1997), Kharul (1998)]. The polyarylates synthesized by asymmetrically (dimethyl and diisopropyl) as well as symmetrically (tetramethyl) substituted methyl groups on bisphenol-A, condensed with isophthalic acid [Pixton (1995a)]. The tetramethyl substitution led to increased permeability while maintaining selectivity as that of unsubstituted bisphenol based polyarylate. The dimethyl (asymmetric) substitution on bisphenol resulted in more selective but less permeable polymer, while diisopropyl substitution yielded polymer with similar permeabilities but lower selectivities than the polyarylate based on unsubstituted bisphenol-A.

Chen et al. [1993a] reported gas permeation properties of polyarylates prepared from asymmetrically substituted alkyl groups (methyl, ethyl and isopropyl) on bridge substituted bisphenol (4-*t*-butyl-cyclohexane group at the bridge position). The dimethyl substituted bisphenol resulted in a polyarylate with 2.4 barrer O₂ permeability and O₂/N₂ selectivity of 5.6. When methyl group was replaced by ethyl, marginal increase in O₂ permeability and O₂/N₂ selectivity was reported. As the bulk increased further in case of diisopropyl substituted bisphenol, the O₂ permeability increased by 2-fold with decrease in O₂/N₂ selectivity in comparison to methyl group substitution.

4.1.1.2 Effect polar group substitution

Pixton and Paul [(1995c)] reported gas transport properties of a series of polyarylates based on isophthalic acid and tetrabromo- substituted bisphenols (bisphenol-A, hexafluorobisphenol-A, phenolphthalein and fluorene bisphenol). Tetrabromination maintained or increased permeability with increase in the selectivity for the O₂/N₂ gas pair as compared to nonbrominated analog. The increases in permselectivity were due to the more size selective nature of the brominated polymers [Pixton (1995c)].

In case of aryl-halogenation (polyarylates based on chlorinated and brominated bisphenol A), the permeability to smaller gases (CO₂, Ar, O₂, and N₂) was increased, but the permeability to larger gases (CH₄ and C₂H₆) was decreased [Chern (1991)]. As a result, in the absence of “gas-induced plasticization”, permselectivity of the halogenated polymer was higher than that of the unmodified polymer. The lower gas diffusivity in the halogenated polymer before the onset of plasticization was thought to have resulted from the reduction in local chain mobility upon halogenation.

Polyarylates prepared from tetrabromohexafluorobisphenol-A and tetrachlorohexafluorobisphenol-A with isophthalic acid exhibited O₂ permeability as 5.25 and 5.64 barrer respectively, with O₂/N₂ selectivity more than 6 [Kawakami (1991a)].

4.1.1.3 Effect of combination of bulky non-polar and polar group substitution

Chen et al. [1993a] reported gas permeation properties of polyarylates based on bridge-substituted bisphenol (4-*t*-butyl-cyclohexane group at the bridge position) and alkyl (methyl, ethyl and isopropyl) or nitro group substituted on phenyl ring. Polyarylate based on dinitrodimethyl substitution gave high O₂ permeability (4.4 barrer) than dimethyl substituted (2.4 barrer) polyarylate, without variation in O₂/N₂ selectivity. In comparison to diisopropyl substitution, dinitrodiisopropyl substitution led to decreased O₂ permeability with increase in O₂/N₂ selectivity.

Gas permeability of dibromodimethyl bisphenol-A (DBrDMbisA) based polyarylates were reported to be higher than that for tetrabrominated analog, but were lower than that for tetramethyl substituted analog [Pixton (1995a), Kharul 1998]. The selectivity for various gas pairs were higher than either of the tetrabromo- or tetramethyl-substituted polyarylates.

4.1.1.4 Effect of bridge substitution

Gas permeation properties of polyarylates synthesized from bisphenol with one bridge methyl group replacement was reported by Houde et al. [1995]. The polyarylate based on Bis-MIBK showed 2.5 times higher O₂ permeability than that based on Bis-A, coupled with a higher selectivity for O₂/N₂. The phenyl group substitution led to 50% increase in the gas permeability in comparison to polyarylate based on Bis-A. The effect of disubstitution at bisphenol bridge position on gas permeation properties was reported [Kharul (1994)]. In case of CF₃- disubstitution, d-spacing increased resulting in increase in permeability and reduced selectivity in comparison with unmodified bisphenol-A polymer. The diphenyl substitution decreased phenyl ring mobility, increased permeability and selectivity.

The effects of varying the bisphenol connector group size and shape on gas permeation properties was reported by Pixton et al. [1995b]. The HFBPA based polymers showed high permeability and selectivities similar to their BPA-based analogs. The PhTh and HFBPA-based polymers showed higher He/CH₄ selectivities than either the BPA or FBP-based polyarylates.

Pessan et al. [1995] studied polyesters based on 6,6'-dihydroxy-3,3,3',3'-tetramethyl-1,1'-spirobiindane (SBI). The inhibition of chain packing due to the SBI moiety yielded 5.9-fold higher O₂ permeability with 13% increase in O₂/N₂ selectivity in comparison to polyarylate based on bisphenol-A. The higher He and CO₂ permeabilities were accompanied with lower He/CH₄ and CO₂/CH₄ selectivities.

Polyarylates based on 9,9-bis(4-hydroxyphenyl) anthrone and isophthalic acid or *t*-butyl isophthalic acid were examined by Pixton et al. [1995d]. Substitution of a *t*-butyl group on the isophthalate ring increased permeability, primarily due to higher diffusion coefficients. The physical properties of these materials were similar to fluorine-bisphenol based analogues; however, the former were more permselective.

Tien et al. [1991] reported polyarylates based on 4,4'-norbornyldine-bis(2,6-dibromophenol). The resulting polyarylates showed high O₂/N₂ selectivity with high O₂ permeability. Permeability of O₂ increased with decrease in O₂/N₂ selectivity as terephthalic content increased.

4.1.2 Effect of substitution on acid moiety of polyarylate

4.1.2.1 Effect of bulky non-polar group substitution

Substitution of *t*-butyl group on isophthalic acid increased gas permeability by 2-6 fold, but lowered permselectivity in polyarylates obtained from various bisphenols viz., bisphenol A, hexafluorobisphenol A, phenolphthalein, and fluorene bisphenol [Pixton (1995a)] Increase in permeability was mainly due to increase in diffusion coefficient.

4.1.2.2 Effect polar group substituted diacid

Kawakami reported the effect of bromo substitution on isophthalic acid moiety on gas permeation properties of resulting polyarylate [Kawakami (1991a)]. Tetrabromo-hexafluorobisphenol and bromoisophthalic acid based polyarylate showed reduction in O₂ permeability while O₂/N₂ selectivity increased marginally with respect to polymer based on isophthalic acid and same bisphenol.

Chen et al. [1993b] reported effects of nitro group substitution in diacid. Polyarylates prepared from condensation of 9,9'-bis(2,6-dibromophenol) fluorene and bis(2,6-dibromophenol)-4-*t*-butyl cyclohexane with 2-nitroterephthaloyl dichloride showed O₂/N₂ selectivity 6.73 and 6.34, respectively, which was higher than the polyarylates prepared with unsubstituted diacid.

Kharul et al. [Kharul (2002)] has reported the effect on gas permeation properties in case of polyarylates based on nitro and bromo group substituted diacids. Gas permeability decreased with respect to the polyarylates prepared from unsubstituted diacids, while improvement in O₂/N₂ and CO₂/CH₄ selectivity was noted.

4.1.2.3 Effect of isomerism in diacid

Sheu et al. [1989] studied polyarylates based on phenolphthalein (PPha) with terephthaloyl chloride, isophthaloyl chloride and 50:50 mixture of these acid chlorides. The permeability of PPha-tere was ~25 % higher than that of PPha-50:50, and roughly 100 % higher than that of PPha-iso. The higher permeability of PPha-tere was because of much larger gas diffusivity.

Pessan et al. [1993] also studied the effect of isomerism in dicarboxylic acid. The polyarylates based on isophthalic acid shows lower permeability and higher permselectivity than polyarylates based on terephthalic acid. The ideal selectivity of

O₂/N₂ was increased by 33 % when terephthalic acid was replaced by isophthalic acid. The polyarylate based on pure terephthalic acid exhibited 75 % higher O₂ permeability and 1.1 fold CO₂ permeability than the isophthalic acid based polyarylate.

Kawakami et al. [1991b] reported that polyarylate based on BrI was more permeable and less selective than polyarylate based on BrT.

4.1.2.4 Effect of bridge substituted diacid

Jadhav et al. [1997] has reported polyarylates based on silicon containing diacid [bis(carboxyphenyl)-1,1-dimethyl silane]. Polyarylates prepared using silicon diacid and dimethyl substituted bisphenol (dimethyl bisphenol-A) showed good combination of permeability and selectivity, For example, permeability of O₂ was 1.2-1.7 barrer with high (8-9.3) O₂/N₂ selectivity.

4.2 Objectives

The objective of the present work was to investigate gas permeation and related physical properties of structurally architected aromatic polyarylates.

Effect of bulk as well effect of polar group substitution is documented in the literature for various aromatic polymers based on bisphenol. Generally, in case of polyarylates, bulky group substitution increases the permeability while polar group substitution reduces the permeability. By combining such types of substitutions while analyzing effect of nature (bulky or polar) substituent site (on acid / bisphenol moiety) and symmetry (symmetric / asymmetric) would lead to the polyarylate having attractive combination of permeability and selectivity and thus thought to be addressed.

The effect of bridge substitution and asymmetric ring substitution by bulky group (methyl, isopropyl, phenyl and bromine) on the bisphenol moiety and the effect of acid substitution (bulky, polar and bridge substituted) on gas permeation and related physical properties was aimed. The gas sorption analysis in case of polyarylates based on asymmetrically bromine substituted hexafluoro bisphenol-A was planned to obtain insight into the effects of this substitution on permeation properties. Investigations in polyarylate structural architecture attempted is categorized as;

- 1) Polyarylates based on asymmetrically substituted bisphenol (diisopropyl

- bisphenol-A, di-*t*-butyl bisphenol-A and diphenyl bisphenol-A).
- 2) Polyarylates based on systematically substituted fluorene bisphenol and dibromohexafluoro bisphenol-A; addressing combined effects of bridge and ring substitution.
 - 3) Polyarylates based on dibromoterephthalic acid.

4.3 Experimental

The details about common solvents and gases used are given in Section 3.3. Triethylamine and molecular bromine were obtained from S.D. Fine Chemicals, India. Fluorenone, β -mercaptopropionic acid and benzyltriethylammonium chloride (BTEAC) were obtained from Aldrich chemicals, USA and were used as received. The triethylamine was stored over anhydrous KOH. The monomers and their abbreviations used are given in Table 4.1.

Table 4.1 Monomers used and their abbreviations

Bisphenol		Dicarboxylic acid used	
Common Name	Abbreviation	Common Name	Abbreviation
Fluorene bisphenol ^a	FBP	Terephthalic acid ^a	T
Dimethylfluorene bisphenol ^c	DMFBP	Isophthalic acid ^a + Terephthalic acid	I+T (1:1)
Dibromodimethylfluorene bisphenol ^c	DBrDMFBP	2-Bromoterephthalic acid ^a	BrT
Dibromohexafluoro bisphenol-A ^c	DBrHFBisA	5-Nitroisophthalic acid ^a	NO ₂ I
Diisopropyl bisphenol-A ^b	DiPrBisA	2-Nitroterephthalic acid ^a	NO ₂ T
Di- <i>t</i> -Butyl bisphenol-A ^b	DiBuBisA	4,4'-hexafluoroisopropylidene bis(benzoic acid) ^a	HFA
Diphenyl bisphenol-A ^b	DiPhBisA	5- <i>t</i> -Butyl isophthalic acid ^a	BuI
Bisphenol-A ^a	BisA	Dibromoterephthalic acid ^a	DBrT
Dimethyl bisphenol-A ^a	DMBisA		
Tetramethyl bisphenol-A ^a	TMBisA		
Dibromodimethyl bisphenol-A ^c	DBrDMBisA		
Hexafluorobisphenol-A ^a	HFBisA		

^a Procured from Aldrich Chemicals, USA., ^b Gifted by Honshu Chemicals, Japan, ^c Synthesized in the laboratory.

4.3.1 Monomer synthesis

4.3.1.1 Synthesis of dimethylfluorene bisphenol (DMFBP)

10 g of 9-fluorenone (0.055 mol) was dissolved in 23.8 g of *o*-cresol (0.22 mol) with stirring at ambient temperature. β - mercaptopropionic acid (1 ml) was added as the catalyst and then dry HCl was bubbled in the reaction mixture for about 10 minutes and stirred for 3 hours. It was allowed to stand for 2 days with occasional stirring and then diluted with water to offer a white solid. It was subsequently washed with hot water until free of acid. The crude product was allowed to stir for 1 hour in hot water (70 °C) and filtered. The hot water washing was repeated thrice to remove unreacted phenol. The product was further purified by dissolving in an alkali, reprecipitation with 2N HCl followed by water wash. The obtained product was recrystallized from acetic acid: water mixture (1:1 v/v). The recrystallized white needles were separated on a Buchner funnel and thoroughly washed with water till free of acid. The crystals, after grinding were dried under vacuum at 40 °C for 3 days. The yield of the final product was 17 g (81 %). The chemical structure was confirmed by spectral analysis [IR and ¹H-NMR (Figure 4.2)]. Melting point = 195 °C, literature mp = 214-216 °C [Hergenrother (1998)].

FTIR (nujol): 3600-3170 cm⁻¹(b,-OH stretch); 1610, 1446 cm⁻¹(aromatic C=C stretch); 1263-1114 cm⁻¹ (C-H plane bending).

¹H NMR (DMSO-d₆) : δ 2.05 (s, 6H, -CH₃ at phenyl ring); δ 6.5–6.92 (m, 6H, aromatic protons of -OH containing phenyl ring); δ 7.15–7.44 (m, 6H, aromatic protons on positions 2-7 of cardo group); δ 7.62–7.8 (d, 2H, aromatic protons on positions 1 and 8 of cardo group); δ 8.65–8.93 (b, phenolic -OH).

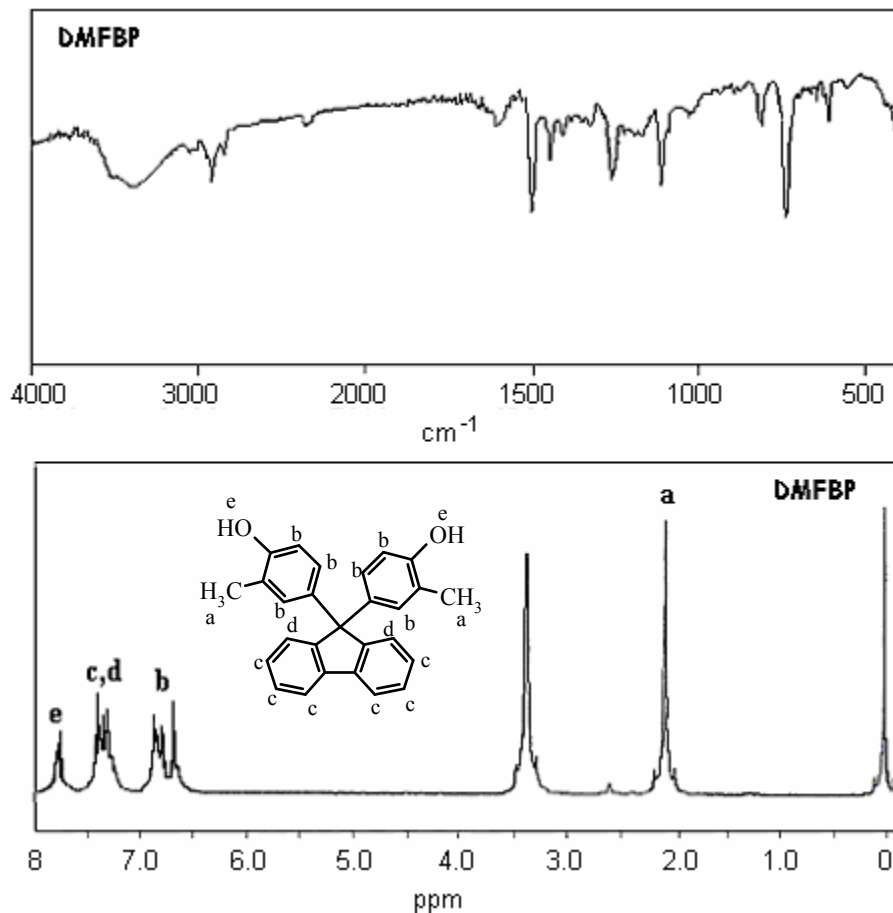


Figure 4.2 FTIR and $^1\text{H-NMR}$ spectrum of DMFBP

4.3.1.2 Synthesis of dibromodimethylfluorene bisphenol (DBrDMFBP)

The DBrDMFBP was synthesized by bromination of DMFBP using molecular bromine. 3 g of DMFBP (0.00793 mol) was dissolved in 30 ml of dry methanol while stirring. The temperature of the reaction mixture was lowered to below $10\text{ }^\circ\text{C}$. Then 8.3 ml of bromine solution (10 % v/v in carbon tetrachloride, 0.016 mol, 2.02 equivalents) was added drop-wise over a period of 45 minutes with continuous stirring and while maintaining the temperature. After complete addition of the bromine solution, temperature of the reaction mixture was allowed to rise to ambient and stirred for 45 minutes. It was then refluxed for 1 hour, added water until the reaction mixture turned white. It was further refluxed until the solution became clear and then allowed to cool to ambient temperature. The formed solid was separated by filtration and thoroughly washed with water. The product obtained was recrystallized from toluene. Yield of the

final product was 4.0 g (94 %). The chemical structure was confirmed by spectral analysis [IR and $^1\text{H-NMR}$ (Figure 4.3)]. Melting point = 225 °C.

FTIR (nujol): 3514 cm^{-1} (-OH stretch); 1630–1570, 1479 cm^{-1} (aromatic C=C stretch); 1265, 1117 cm^{-1} (C-H plane bending); 1020 cm^{-1} (C-Br plane bending).

$^1\text{H NMR}$ (CDCl_3): δ 2.18 (s, 6H, $-\text{CH}_3$ at phenyl ring); δ 5.48 (s, 2H, phenolic -OH); δ 6.83–6.93 (d, 2H, aromatic proton at *o*-position to $-\text{CH}_3$ group); δ 6.98–7.08 (d, 2H, aromatic proton at *p*-position to $-\text{CH}_3$ group); δ 7.16–7.48 (m, 6H, aromatic protons on positions 2-7 of cardo group); δ 7.65–7.81 (d, 2H, aromatic protons on position 1 and 8 of cardo group).

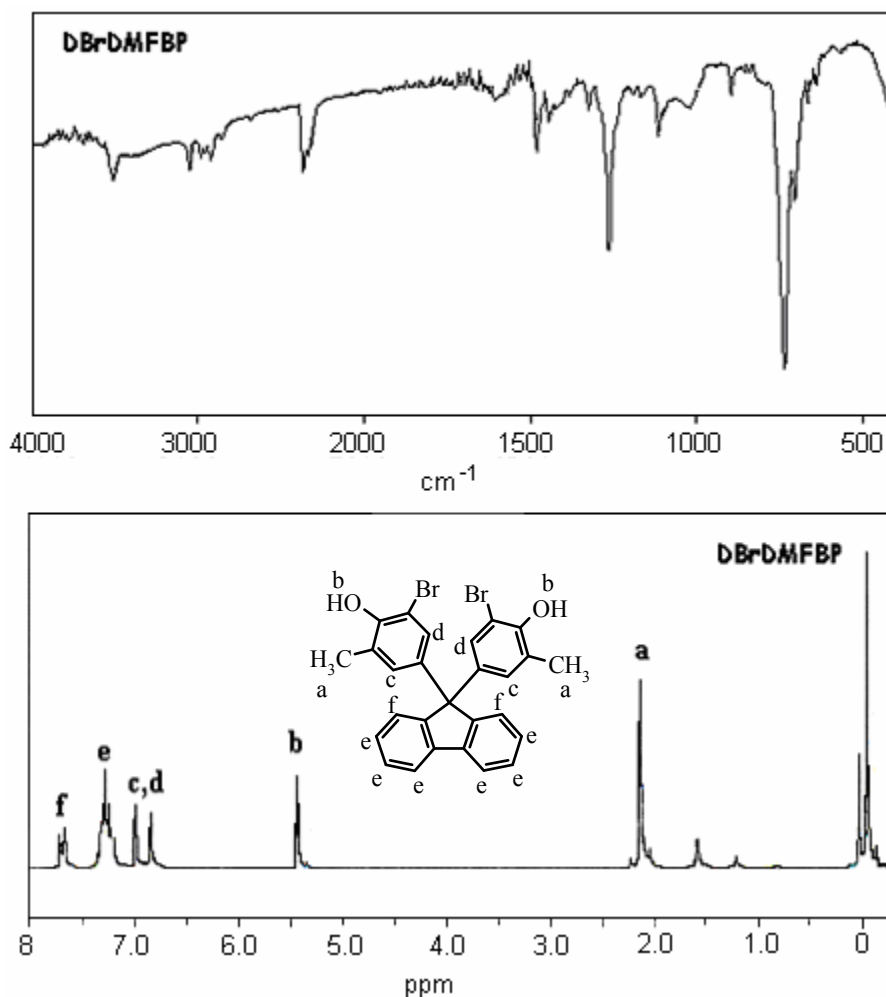


Figure 4.3 FTIR and $^1\text{H-NMR}$ spectrum of DBrDMFBP

4.3.1.3 Synthesis of dibromohexafluorobisphenol-A (DBrHFBisA)

The DBrHFBisA was obtained by the bromination of HFBisA using molecular bromine while following the similar procedure, as described in section 4.3.1.2. The obtained product was purified by recrystallization from toluene. The yield of the product was 65 %. The chemical structure was confirmed by spectral analysis [IR and $^1\text{H-NMR}$ (Figure 4.4)]. Melting point = 93 °C.

FTIR (KBr): 3500 cm^{-1} (-OH stretch); 1604-1499 cm^{-1} (m, aromatic C=C stretch); 1254-1172 cm^{-1} (m, C-H plane bending); 737 cm^{-1} (s, C-H out of plane bending).

$^1\text{H-NMR}$ (CDCl_3): δ 5.66 (b, 2H, phenolic -OH), δ 6.93-7.42 (m, 6H, aromatic protons).

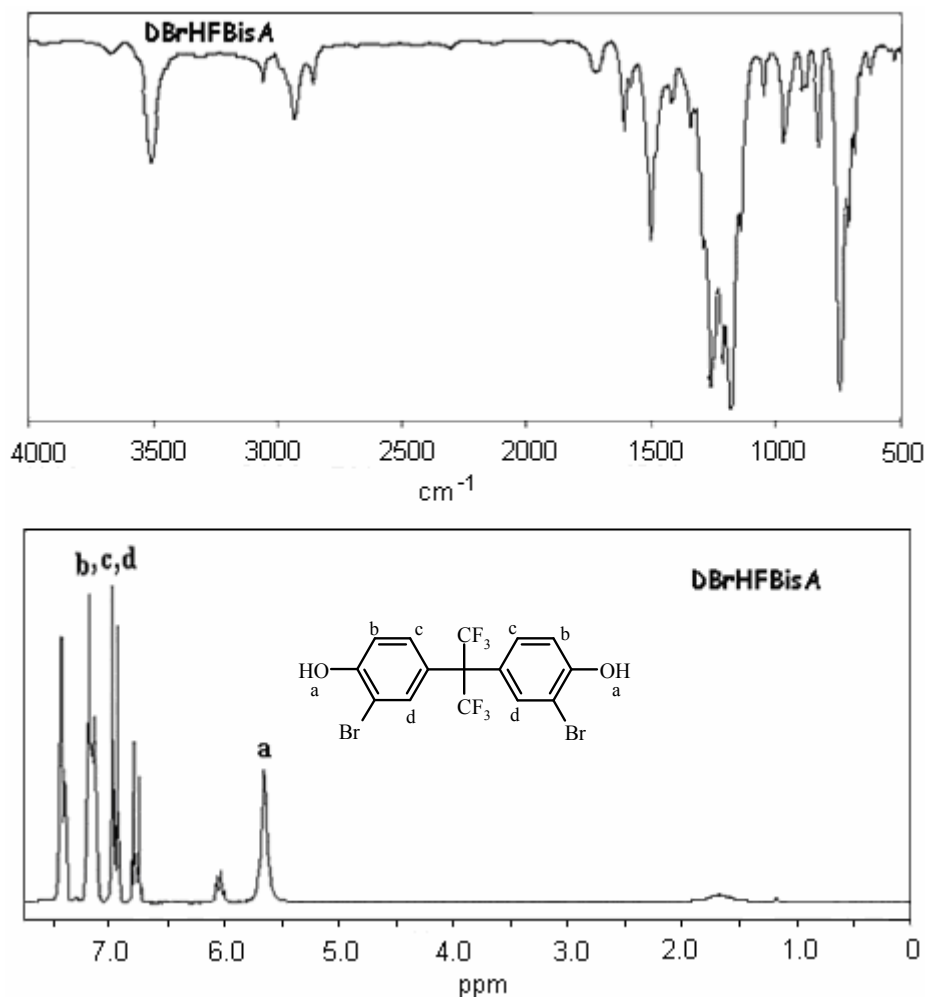


Figure 4.4 FTIR and $^1\text{H-NMR}$ spectrum of DBrHFBisA

4.3.1.4 Synthesis of dibromodimethylbisphenol-A (DBrDMbisA)

The DBrDMbisA was synthesized by the bromination of DMbisA using molecular bromine while following the similar procedure as described in section 4.3.1.2. The obtained product was purified by recrystallization from toluene. The yield of the product was 89.2 %. The chemical structure was confirmed by spectral analysis [IR and $^1\text{H-NMR}$ (Figure 4.5)]. Melting point = 118 °C, literature mp = 120-121 °C [Pixton (1995e)].

FTIR (KBr): 3461-3258 cm^{-1} (broad, -OH stretch); 1570-1402 cm^{-1} (m, aromatic C=C ring stretching); 1257-1101 cm^{-1} (m, C-H in plane bending); 771 cm^{-1} (s, C-H out of plane bending).

$^1\text{H-NMR}$ (CDCl_3): δ 1.62 (s, 6H, protons of bridge - CH_3), δ 2.29 (s, 6H, protons of - CH_3 at phenyl ring), δ 5.49 (b, 2H, phenolic -OH), δ 6.91-7.20 (m, 4H, aromatic protons).

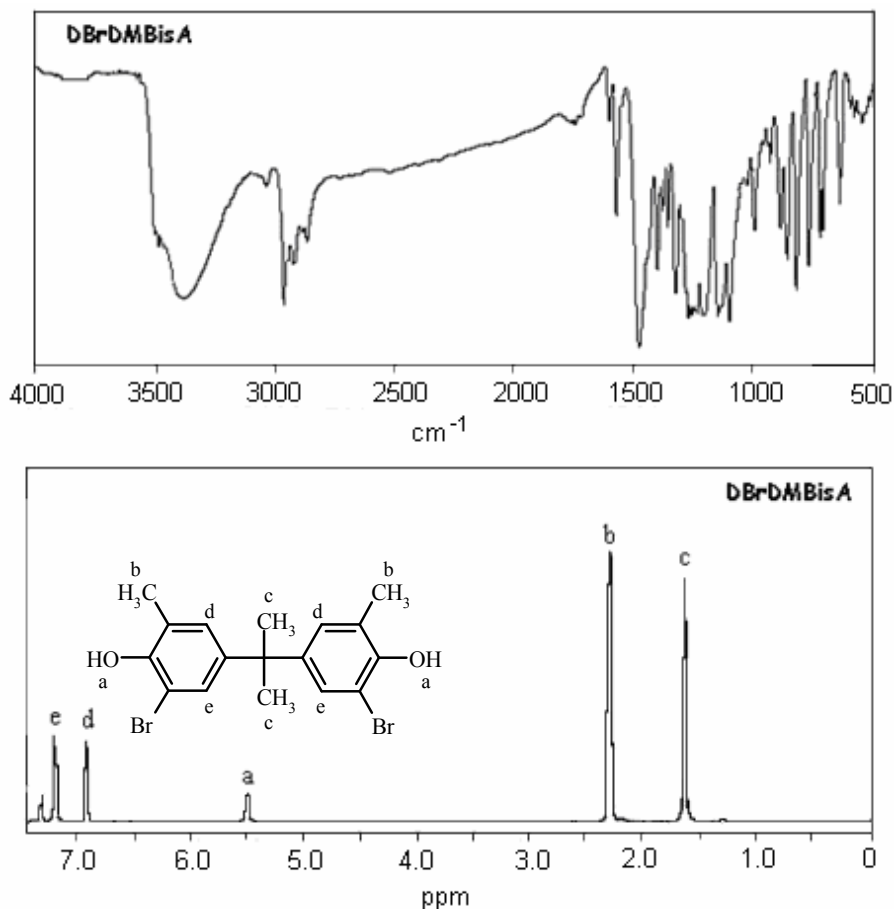
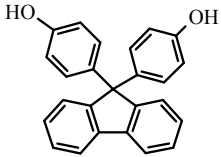
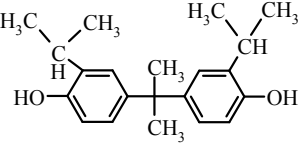
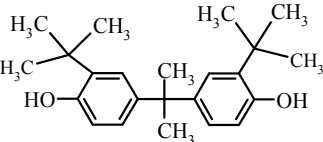
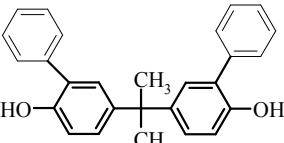
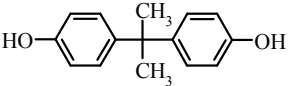


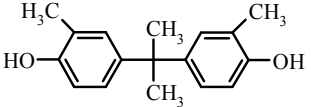
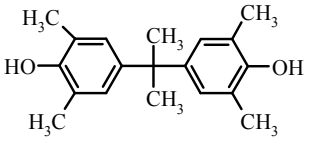
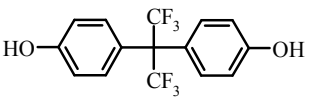
Figure 4.5 FTIR and $^1\text{H-NMR}$ spectrum of DBrDMbisA

4.3.2 Structural characterization of as-received bisphenols

The structural characterization of procured / gifted bisphenols used in the present study was done by melting point, $^1\text{H-NMR}$ and FTIR. The characteristic IR frequencies and $^1\text{H-NMR}$ chemical shift of these bisphenols are presented in Table 4.2.

Table 4.2 Characterization of bisphenols obtained from Aldrich and Honshu chemicals

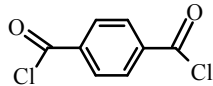
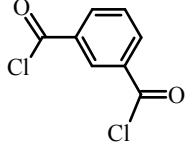
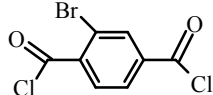
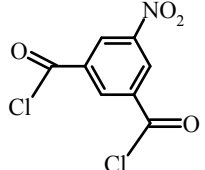
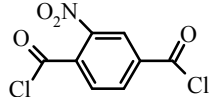
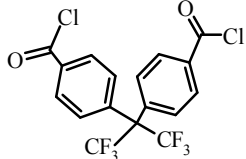
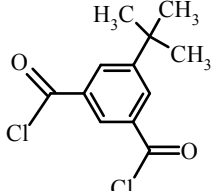
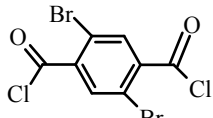
Bisphenol	Structural Identification
 <p>FBP</p>	$^1\text{H NMR}$ (Acetone- d_6): δ 6.67-7.04 (m, 8H, arom. protons of -OH containing phenyl ring); δ 7.19-7.77 (m, 8H, arom. protons of cardo group); δ 8.06 (m, phenolic -OH). FTIR (KBr): 3340-3226 cm^{-1} (b, -OH stretch); 1508-1438 cm^{-1} (m, arom. C=C stretch); 1233-1172 cm^{-1} (m, C-H in plane bending); 822 cm^{-1} (s, C-H out of plane bending). M.P.= 224 $^{\circ}\text{C}$, literature M.P. = 225-227 $^{\circ}\text{C}$ [Pixton (1995b)]
 <p>DiPrBisA</p>	$^1\text{H-NMR}$: δ 1.25-1.28 (s, 12H, protons of <i>i</i> -Pr group - CH_3), δ 1.7 (s, 6H, protons of bridge - CH_3), δ 3.13-3.34 (s, 2H, protons of <i>i</i> -Pr group -CH phenyl ring), δ 4.47 (b, 2H, phenolic -OH), δ 6.67-7.12 (m, 6H, arom. protons). FTIR (KBr): 3461-3258 cm^{-1} (b, -OH stretch); 1609-1492 cm^{-1} (m, arom. C=C stretch); 1240-1154 cm^{-1} (m, C-H in plane bending); 817, 782 cm^{-1} (s, C-H out of plane bending). M.P. = 98 $^{\circ}\text{C}$, literature M.P. = 97.5-98.5 $^{\circ}\text{C}$ [Pixton (1995e)]
 <p>DiBuBisA</p>	$^1\text{H-NMR}$ (Acetone- d_6): δ 1.35 (s, 18H, protons of <i>t</i> -butyl group - CH_3), δ 1.63 (s, 6H, protons of bridge - CH_3), δ 4.71 (b, 2H, phenolic -OH), δ 6.51-7.13 (m, 6H, arom. protons). FTIR (KBr): 3537-3584 cm^{-1} (b, -OH stretch); 1484-1335 cm^{-1} (m, arom. C=C stretch); 1236-1171 cm^{-1} (m, C-H in plane bending); 815 cm^{-1} (s, C-H out of plane bending). M.P. = 115 $^{\circ}\text{C}$, literature M.P. = 115-116 $^{\circ}\text{C}$ [Pixton (1995e)]
 <p>DiPhBisA</p>	$^1\text{H-NMR}$: δ 1.59 (s, 6H, protons of bridge - CH_3), δ 5.04 (b, 2H, phenolic -OH), δ 6.75-7.2 (s, 6H, arom. protons), δ 7.23-7.37 (s, 10H, arom. protons of substituted phenyl group). FTIR (KBr): 3518-3400 cm^{-1} (b, -OH stretch); 1596-1485 cm^{-1} (m, arom. C=C stretch); 1260-1173 cm^{-1} (m, C-H in plane bending); 733, 699 cm^{-1} (s, C-H out of plane bending). M.P. = 116 $^{\circ}\text{C}$, literature M.P. = 114-116.5 $^{\circ}\text{C}$ [Product broacher, Honshu Chemicals]
 <p>BisA</p>	$^1\text{H-NMR}$: δ 1.6 (s, 6H, protons of bridge - CH_3), δ 4.75 (s, 2H, phenolic -OH), δ 6.7-7.3 (m, 8H, aromatic protons). FTIR (KBr): 3352-3257 cm^{-1} (b, -OH stretch); 1509-1353 cm^{-1} (m, arom. C=C stretch); 1220-1176 cm^{-1} (m, C-H in plane bending); 826 cm^{-1} (s, C-H out of plane bending). M.P. = 160 $^{\circ}\text{C}$, literature M.P. = 158-159 $^{\circ}\text{C}$ [Pixton (1995b)]

<i>Continued Table 4.2</i>	
 DMBisA	¹ H-NMR: δ 1.5 (s, 6H, protons of bridge -CH ₃), δ 2.1 (s, 6H, protons of -CH ₃ at phenyl ring), δ 4.7 (b, 2H, phenolic -OH), δ 6.3-6.9 (m, 4H, arom. protons). FTIR (KBr): 3500-3100 cm ⁻¹ (b, -OH stretch); 1660-1440 cm ⁻¹ (m, arom. C=C stretch); 1260-1120 cm ⁻¹ (m, C-H in plane bending); 770 cm ⁻¹ (s, C-H out of plane bending). M.P. = 138 °C, literature M.P. = 139-140 °C [Pixton (1995a)]
 TMBisA	¹ H-NMR: δ 1.6-1.65 (s, 6H, protons of bridge -CH ₃), δ 2.2-2.3 (s, 12H, protons of -CH ₃ at phenyl ring), δ 4.55 (s, 2H, phenolic -OH), δ 6.9 (s, 4H, arom. protons). FTIR (KBr): 3540-3250cm ⁻¹ (b, -OH stretch); 1609-1421 cm ⁻¹ (m, arom. C=C stretch); 1242-1079 cm ⁻¹ (m, C-H in plane bending); 782 cm ⁻¹ (s, C-H out of plane bending). M.P.=164-166 °C, literature M.P. = 165-167 °C [Pixton (1995a)]
 HFBisA	¹ H-NMR (Acetone-d ₆): δ 6.8-7.24 (m, 6H, arom. protons) δ 8.55 (m, 2H, phenolic -OH). FTIR (KBr): 3468-3024 cm ⁻¹ (b, -OH stretch); 1614-1516 cm ⁻¹ (m, arom. C=C stretch) 1243-1171 cm ⁻¹ (m, C-H in plane bending); 828 cm ⁻¹ (s, C-H out of plane bending). M.P. = 161-162 °C, literature M.P. =161-163 °C [Pixton (1995b)]

4.3.3 Preparation of acid chloride

All the dicarboxylic acids used (Table 4.1) were converted to their respective acid chlorides by refluxing the acid in an excess (4 molar equivalent) of thionyl chloride in presence of few drops of pyridine as a catalyst. After complete dissolution of the acid, the reaction mixture was refluxed for an additional hour to ensure completion of reaction. An excess of thionyl chloride was distilled off and the crude product was recrystallized from the dry petroleum ether twice to obtain white crystalline acid chloride. In case of 2-bromoterephthalic acid and nitroterephthalic acid, toluene was added to the formed acid chloride and distilled off to remove traces of SOCl₂. The IR spectra of acids used were recorded and the absence of -COOH peak was confirmed prior to their use. The abbreviations and structure of acid chlorides used is given in Table 4.3.

Table 4.3 Structure and abbreviations of acid chlorides used in present investigation

Acid chloride	Abbreviations	Chemical structure
Terephthoyl chloride	TPC	
Isophthoyl chloride	IPC	
2-Bromoterephthoyl chloride	BrTPC	
5-Nitroisophthoyl chloride	NO ₂ IPC	
2-Nitroterephthoyl chloride	NO ₂ TPC	
4,4'-hexafluoroisopropylidene bis(benzoyl chloride)	HFC	
5- <i>t</i> -Butyl isophthoyl chloride	BuIPC	
2,5- dibromoterephthoyl chloride	DBrTPC	

4.3.4 Polymer synthesis

4.3.4.1 Solution polycondensation

In a typical procedure, 5 mmol of bisphenol was dissolved in 15 ml of dichloromethane (DCM) containing 2.2 molar equivalent of triethylamine with stirring. 1.05 equivalent of acid chloride (1.066 g, 5.2 mmol, equimolar mixture of isophthaloyl

and terephthaloyl chloride) was dissolved in 10 ml of DCM and then added to above bisphenol solution in a drop-wise manner over a period of 15 minutes with continuous stirring. The reaction mixture was stirred for additional 45 minutes and then poured on to stirred methanol. The precipitated polymer was dried in an oven at 50 °C and the residual solvent was removed under vacuum at 60 °C. The polymer was purified by dissolving in chloroform followed by precipitation in stirred methanol. The precipitated polymer was collected on the Buchner, dried in oven at 60 °C for 12 hours and finally in vacuum oven at 60 °C for 24 hours. Polyarylates prepared by solution polycondensation method and the abbreviations used are given in Table 4.4.

Table 4.4 Polyarylates synthesized by solution condensation method

Monomers used		Polymer abbreviation	Yield (%)	[η] (dL/g)
Bisphenol	Diacid chloride			
Fluorene bisphenol	IPC:TPC (1:1)	FBP-I+T	89	0.80
Dimethylfluorene bisphenol	IPC:TPC (1:1)	DMFBP-I+T	91	0.74
Dibromodimethylfluorene bisphenol	IPC:TPC (1:1)	DBrDMFBP-I+T	88	0.35

4.3.4.2 Interfacial polycondensation

In a typical procedure, 0.022 mol of bisphenol was dissolved in 18.4 ml aq. 10 % NaOH solution (0.046 mol, 2.1 equivalent) with stirring and further diluted to 120 ml with water. 0.165 g (0.087 mmol, 0.04 equivalent) of benzyltriethylammonium chloride was added to the solution as a phase transfer catalyst, 30 ml of DCM was added as an organic phase and the mixture was vigorously stirred at ~2000 rpm. 0.023 mol (1.05 equivalents of bisphenol) of acid chloride(s) was dissolved in 30 ml of DCM and this solution added drop-wise to the above vigorously stirred emulsion containing bisphenol over a period of 10 minutes. The mixture was further stirred for 1 hour and then allowed to separate. The aqueous layer was discarded and the organic layer was added slowly to 500 ml stirred methanol. The precipitated polymer collected on Buchner and dried in an oven at 50 °C followed by drying under vacuum at 60 °C to remove residual solvent. All

polymers thus synthesized were finally purified by dissolving in chloroform followed by precipitation in methanol. Polyarylates prepared by interfacial polycondensation method are listed in Table 4.5 along with the abbreviations used.

Table 4.5 Polyarylates synthesized by interfacial condensation method

Monomers used		Polymer abbreviation	Yield (%)	[η] (dL/g)
Bisphenol	Diacid chloride (Abbreviation)			
Diisopropyl bisphenol-A	TPC	DiPrBisA-T	95	0.61
Diisopropyl bisphenol-A	IPC+TPC (1:1)	DiPrBisA-I+T	99	0.27
Diisopropyl bisphenol-A	BrTPC	DiPrBisA-BrT	94	0.29
Diisopropyl bisphenol-A	NO ₂ IPC	DiPrBisA-NO ₂ I	97	0.42
Diisopropyl bisphenol-A	NO ₂ TPC	DiPrBisA-NO ₂ T	98	0.43
Diisopropyl bisphenol-A	HFC	DiPrBisA-HFA	99	0.36
Diisopropyl bisphenol-A	BuIPC	DiPrBisA-BuI	98	0.4
Diphenyl bisphenol-A	IPC+TPC (1:1)	DiPhBisA-I+T	94	0.39
Diphenyl bisphenol-A	BrTPC	DiPhBisA-BrT	94	0.49
Diphenyl bisphenol-A	NO ₂ IPC	DiPhBisA-NO ₂ I	98	0.53
Diphenyl bisphenol-A	NO ₂ TPC	DiPhBisA-NO ₂ T	96	0.49
Diphenyl bisphenol-A	HFC	DiPhBisA-HFA	94	0.63
Diphenyl bisphenol-A	BuIPC	DiPhBisA-BuI	93	0.39
Dibromohexafluoro bisphenol-A	IPC+TPC (1:1)	DBrHFBisA-I+T	96	0.53
Dibromohexafluoro bisphenol-A	BrTPC	DBrHFBisA-BrT	95	0.49
Dibromohexafluoro bisphenol-A	NO ₂ TPC	DBrHFBisA-NO ₂ T	97	0.48
Dibromohexafluoro bisphenol-A	HFC	DBrHFBisA-HFA	99	0.54
Dibromohexafluoro bisphenol-A	BuIPC	DBrHFBisA-BuI	95	0.67
Bisphenol-A	DBrTPC	BisA-DBrT	92	0.73
Dimethyl bisphenol-A	DBrTPC	DMbisA-DBrT	99	0.44
Tetramethyl bisphenol-A	DBrTPC	TMbisA-DBrT	94	0.42
Dibromodimethyl bisphenol-A	DBrTPC	DBrDMbisA-DBrT	98	0.9

4.3.5 Dense membrane preparation

The solvent used for dense membrane preparation of fluorene bisphenol based polyarylates was TCE, while for all other polymers; CHCl_3 was used as solvent. A 2-3 % (w/v) solution of these polyarylates was prepared with stirring for 12 hours at ambient, filtered through a 5- μm SS-filter to remove particulate matter, if any; degassed for ~ 1-3 minutes and then poured on to a flat glass surface. The solvent was allowed to evaporate at 40 °C under dry atmosphere in case of CHCl_3 as a solvent or at 65 °C; in case of TCE as a solvent. The formed film was peeled off and vacuum dried at 60 °C for a week in order to ensure the complete removal of the solvent. Five films of each polymer for gas permeability analysis were casted at identical conditions as mentioned above with ~40 μm thickness (variation of $\pm 3 \mu\text{m}$). The films casted were clear and transparent in nature except for the films of DBrHFBisA-HFA, which was slight hazy. The thick films of ~100-120 μm were casted for density and dynamic mechanical analysis while following the same procedure as above. The formed films were vacuum dried at 80 °C for 12 days in order to ensure the complete removal of the solvent, as confirmed by DSC.

4.3.6 Polymer characterizations

The intrinsic viscosity $[\eta]$ was determined by graphical method at 35 °C using tetrachloroethane (TCE) as the solvent and were as given in Table 4.4 and Table 4.5. The glass transition temperature (T_g) was determined by DSC on Thermal instrument DSC-Q10 under N_2 atmosphere with the heating rate of 10 °C/min. The thermogravimetric analysis (TGA) was performed on a Thermal Analyzer 32 SII model under N_2 atmosphere at heating rate of 10 °C/minute. The wide-angle X-ray diffraction (WAXD) spectra of all polymers in the film form were performed using Rigaku X-ray diffractometer (D-max 2500) with Cu-K_α radiation in 2θ range of 4-40°. The average d-spacing (d_{sp}) for amorphous peak maxima was calculated using Bragg's equation. The dynamic mechanical analysis was performed using Rheometrics DMTA III E with a heating rate of 5 °C/minute, at the frequency of 10 rads/sec and at 0.1 % strain using a film specimen of ~ 120 μm thick and $2.5 \times 0.7 \text{ cm}^2$ in size. The density of polymers in the film form was obtained by the floatation method using an aqueous K_2CO_3 or ZnCl_2

solution at 40 °C. The density measurement of halogenated polymers was performed using aqueous ZnCl₂; while for all other polyarylates, aqueous K₂CO₃ solutions were used. The reproducibility of the density measurements was ± 0.004 g/cm³. Using this density, the fractional free volume (v_f) and solubility parameter (δ) were estimated using group contribution method [Van Krevelen (1972)]. The physical properties thus measured are given in Section 4.4.1.1a, 4.4.1.2b, 4.4.2.1a, 4.4.2.2a and 4.4.3.1.

4.3.7 Determination of equilibrium gas sorption and permeability

The pure gas sorption measurements were carried out at varying pressure, upto 20 atm absolute, and at 35 °C for polyarylates based on DBrHFBisA using equipment as describe in Section 3.3.8.2. The gases used were O₂, CH₄, and CO₂.

The pure gas permeability measurements for all the polyarylates were made at 35 °C using variable volume method using pure gases at 10 atm upstream pressure. The equipment used for the gas permeation analysis is described in Section 3.3.8.1. The permeability for each polymer was repeated on three different membrane coupons prepared individually under identical conditions and the consistent data averaged. The selectivity of different gas pairs was the ratio of pure gas permeability of individual gas pair.

4.4 Result and discussions

4.4.1 Polyarylates bases on asymmetrically substituted bisphenol

In view of the potential of bisphenol substitution symmetry in improving gas permeation properties viz., increase in selectivity by asymmetric substitution [Schmidhauser (1990), McHattie 32 (1991), Pixton (1995a)] and symmetric substitution in increasing permeability [Muruganandam (1987), McHattie 32 (1991), Pixton (1995a)], it was thought that benefits of the bulky group substitution on bisphenol in asymmetric manner can be drawn in simultaneous increase of permeability and selectivity. In case of polyarylates, the isopropyl group substitution on bisphenol was reported with dicarboxylic acid as isophthalic and *t*-butyl isophthalic acid [Pixton (1995a)]. Asymmetric substitution on bisphenol can be coupled with appropriate acid substitution

by polar / bulky group for further advancement in permeation properties of resulting polyarylates.

The substituents on bisphenol moiety chosen in present case were isopropyl, *t*-butyl and phenyl groups. The dicarboxylic acids containing polar (Br and NO₂) and bulky (*t*-butyl and hexafluoroisopropylidene) groups were polymerized with above bisphenols. Though di-*t*-butyl bisphenol-A could be polymerized with above dicarboxylic acids, the viscosity of the resulting polyarylates was low. These materials could not be transformed in to the film form. The film formation attempted by solution casting method resulted in cracked films. The failure to obtain higher molecular weight polymer could be attributed to the lower reactivity of bisphenol substituted with bulky *t*-butyl group. The following discussion is thus restricted to the polyarylates based on diisopropyl bisphenol-A and diphenyl bisphenol-A.

4.4.1.1 Polyarylates bases on asymmetrically substituted diisopropyl bisphenol-A

(a) Physical Properties

The diisopropyl bisphenol-A (DiPrBisA) was initially polymerized with equimolar mixture of iso- and terephthalic acids. Though the film formation was possible with this material, it could not withstand the pressure in gas permeation cell. On the other hand, its polyarylate with terephthalic acid could be prepared with high enough viscosity (Table 4.5). The DiPrBisA was polymerized with NO₂I and NO₂T to investigate the effect of polarity, while its polymerization with HFA and *t*-butyl was performed to assess the effect of added bulk in the acid moiety. These polyarylates were synthesized by interfacial polycondensation (Section 4.3.4.2) with appreciable yield and viscosity as given in Table 4.5. The intrinsic viscosities of these polyarylates were in the range of 0.36-0.61 dl/g in TCE at 35 °C. The films formed by solution casting from their CHCl₃ solution (2-3 %) at ambient temperature were tough and transparent that could allow measurement of gas permeability at 10 atm upstream pressure. The effect of increased bulk on bisphenol-A moiety of DiPrBisA was assessed by comparing its properties with those of polyarylates based on unsubstituted bisphenol-A (BisA-T) and dimethyl bisphenol-A (DMBisA-T). The physical properties of DiPrBisA based polyarylates are given in Table 4.6.

Table 4.6 Physical properties of DiPrBisA based polyarylates

Polymer	d_{sp} (Å)	ρ (g.cm ⁻³)	v_f (cm ³ .cm ⁻³)	δ (cal.cm ⁻³) ^{1/2}	T_g (°C)	TGA (°C)	DMA relaxation temperature (°C)		
							α	γ	δ
DiPrBisA -T	4.92, 6.32	1.095	0.3659	9.08	130	392	-	-	-
DiPrBisA -NO ₂ I	5.15	1.160	0.3538	9.57	126	327	160	24	-35
DiPrBisA -NO ₂ T	4.8, 5.94	1.171	0.3480	9.66	116	310	148	44	3
DiPrBisA -HFA	6.00	1.213	0.3730	8.71	156	415	186	37	-
DiPrBisA -BuI	5.04	1.056	0.3663	8.75	130	435	143	-2	-

All these polyarylates were amorphous in nature as evident from their WAXD spectra (Figure 4.6). Based on the 2θ position of the amorphous peak maxima, average d_{sp} was calculated as given in Table 4.6. The v_f and d_{sp} increased in comparison to BisA-T or DMbisA-T indicating that the bulk of isopropyl group was effective in rendering loose chain packing. This was not affected by methyl group substitution in DMbisA based polyarylates when compared with unsubstituted BisA-T [Pixton (1995a), Kharul (1998)]. DiPrBisA-T showed two intermixed amorphous peaks corresponding to d_{sp} of 4.92 Å and 6.32 Å. Similarly, NO₂-T also showed two peaks at 4.8 Å and 5.94 Å. Such occurrence of two amorphous peaks was also reported for DiPrBisA based polyarylate [Pixton (1995a)]. The solubility parameter (δ) in DiPrBisA-T was found to decrease than that of BisA-T or DMbisA-T as a result of increased alkyl content in the polyarylate. The polar nature of the nitro substituent in DiPrBisA-NO₂I and DiPrBisA-NO₂T was reflected into increased density and reduced v_f than those for DiPrBisA-T. This reduction in v_f can be attributed to the increased chain interactions as also revealed by increased solubility parameter (δ), than that of polyarylate based on unsubstituted diacid (DiPrBisA-T). The observed variations in physical properties between DiPrBisA-NO₂I and DiPrBisA-NO₂T can be explained on the basis of substitution position of -NO₂ as well as carboxylic groups. In case of -NO₂T, the carboxylic acid groups are placed at *para*-position (1,4) to each other and NO₂ group is placed at 2-position. In case of NO₂I,

the carboxylic acid groups are substituted at *meta*-position (1,3) to each other and NO₂ group is placed at 5-position of the phenyl ring. Thus the effect of bulk of added NO₂ on the chain packing could be anticipated more in case of NO₂I than in case of NO₂T. This was reflected by the observed v_f , which was higher in the case of DiPrBisA-NO₂I (0.3538) than in the case of DiPrBisA-NO₂T (0.348). The v_f was increased in case of polyarylates based on HFA and BuI as well, indicating usefulness of these acids in reducing chain packing density of polyarylates. The d_{sp} in present case was unable to correlate with packing density due to the presence of more than one amorphous peak. It is said in the literature that d_{sp} data have limitations as a measures of the extent of “openness” of the matrix [Hellums (1989)].

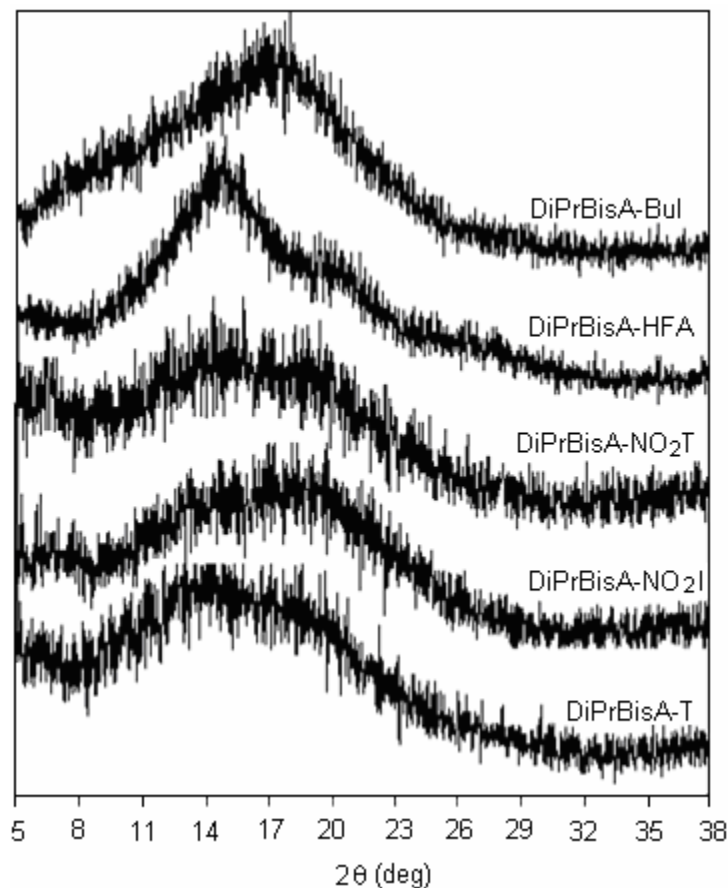


Figure 4.6 WAXD spectra of DiPrBisA based polyarylates

The polyarylates based on unsubstituted bisphenol-A exhibited T_g at 210 °C, while it was reduced to 130 °C in case of DiPrBisA-T. This suggested the plasticizing ability of the isopropyl group. The nature of bisphenol substitution (asymmetric) might

also be contributing to this reduction, which was reported earlier in case of polyarylates [Pixton (1995a)] and polysulfone [McHattie (1991)]. A polar $-\text{NO}_2$ group substitution on dicarboxylic acid decreased the T_g of the resulting polyarylates (DiPrBisA- NO_2I , DiPrBisA- NO_2T) in comparison to the polyarylate without this group (DiPrBisA-T). The effect of decrease in T_g was smaller ($4\text{ }^\circ\text{C}$) in the case of DiPrBisA- NO_2I ; whereas in case of DiPrBisA- NO_2T , the T_g was reduced by $14\text{ }^\circ\text{C}$. The polar $-\text{NO}_2$ group substitution on other types of polymers such as PPO or PSF [Ghosal (1992), (1995)] led to an increase in T_g , attributable to increased inter chain interactions. While, the reduction in T_g by NO_2 group substitution was also reported earlier and said to be because of random distribution of dipolar nitro groups in the polymer chain, which may reduce the thermal transitions due to the repulsive forces [Jin (1997)]. The thermal stability in case of DiPrBisA- NO_2I and DiPrBisA- NO_2T was lower than that of DiPrBisA-T. It was stated that [Jin (1987)] such behavior could be due to the strong substituent effect (electron withdrawing) of the $-\text{NO}_2$ group, which increases the acidity of 2-nitro terephthalic acid based polyesters and make the acid moiety more thermally labile.

The T_g for DiPrBisA-HFA was $26\text{ }^\circ\text{C}$ higher than that of DiPrBisA-T, which may be ascribed to the presence of larger hexafluoroisopropylidene group in the backbone that inhibits molecular motions. Similar increase in T_g was reported by Hellums et al. [1989] in case of the bulky hexafluoroisopropylidene group containing polycarbonates, which markedly increased fractional free volume while hindering torsional motion. In case of DiPrBisA-BuI, the T_g remained similar with that of DiPrBisA-T. The degradation temperature obtained by TGA for DiPrBisA-HFA was higher than that of DiPrBisA-BuI, both being higher than that of DiPrBisA-T.

The DMA spectra ($\tan \delta$ curve) for DiPrBisA based polyarylates were as shown in Figure 4.7. The α -relaxation temperature (T_α) observed for all the polymers were higher than the T_g observed by DSC. It is known that the T_α by DMA can be higher than T_g obtained by DSC [Vega (1993), McHattie (1992)]. The variation observed in T_α was similar to the trend observed in T_g . The T_γ peak is related to motions of the phenylene rings [Yee (1981)]. The observed T_γ transition temperature for DiPrBisA-I+T was much higher than that for BisA-T (by $111\text{ }^\circ\text{C}$). This improvement may be attributed to the restricted motion of phenyl ring due to the presence of bulky isopropyl group. The T_γ

transition temperature in bisphenol substituted polyarylates was assigned mainly to the bisphenol phenyl ring flip [Charati (1994)]. Introducing substituents onto backbone phenylene rings caused large increases in T_γ . These substituents can cause rotational interference between adjacent monomer units within a chain or with adjacent chains.

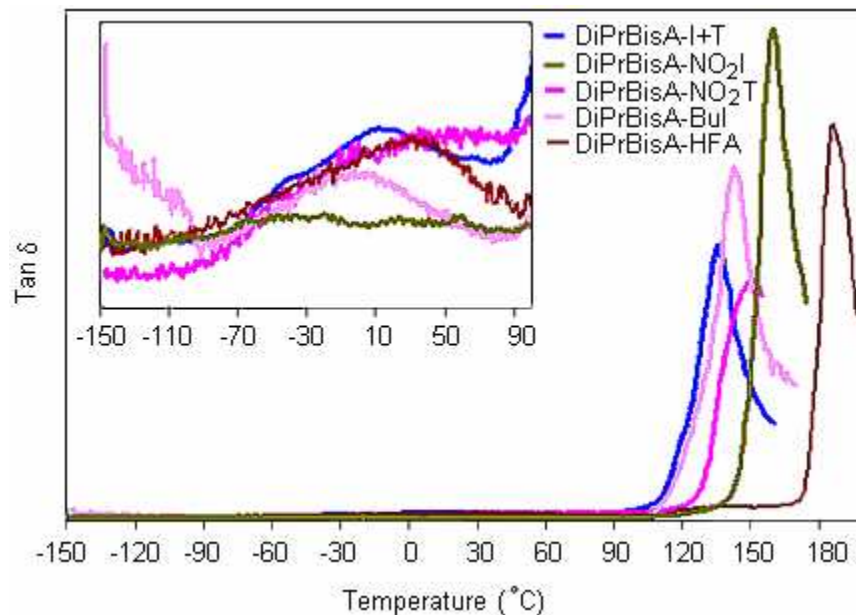


Figure 4.7 DMA spectra of DiPrBisA based polyarylates

The T_γ temperature for DiPrBisA-NO₂T was found to be 20 °C higher than that of DiPrBisA-NO₂I, which can be ascribed to its higher increased intermolecular attractions than the later as evidenced by higher solubility parameter and packing density (lower ν_f). In the case of DiPrBisA-Bul, T_γ was lower than that of DiPrBisA-I+T, which may be ascribed to the increased ν_f . The loose chain packing may reduce the rotational interference between adjacent monomer units within a chain or with adjacent chains, leading to the decrease in T_γ in this case. It was stated that the bulky *t*-butyl substitution, which simultaneously increase ν_f and hinder phenyl ring rotational mobility through steric interactions, may raise or lower the measured T_γ , depending upon which effect is dominant [Pixton (1995a)]. In case of DiPrBisA-HFA, due to the bulky hexafluoroisopropylidene linkage, T_γ transitions temperature was increased by 23 °C in comparison to DiPrBisA-I+T. Thus in this case, though the chain packing is reduced, the steric interactions became dominant. The increased intermolecular attractions as indicated by increase in solubility parameter may also be responsible to increased rotational barrier.

An another low temperature relaxation termed as δ was observed for the polar group substituted (DiPrBisA-NO₂I and DiPrBisA-NO₂T) polyarylates at -35 and to 3 °C respectively, which could be assigned to small scale motions of substituents.

(b) Permeation properties

Pure gas permeability and selectivities of gas pairs are given in Table 4.7. The asymmetric substitution by isopropyl group in DiPrBisA-T resulted into higher permeability for various gases than unsubstituted BisA-T except for CO₂ and CH₄.

Table 4.7 Gas permeability (P) and selectivity (α) for DiPrBisA based polyarylates

Permeation property	DiPrBisA -T	DiPrBisA -NO ₂ I	DiPrBisA -NO ₂ T	DiPrBisA -HFA	DiPrBisA -BuI
P(He)	21.4	18.6	18.0	44.5	36.2
P(N ₂)	0.52	0.40	0.27	1.01	1.09
P(O ₂)	2.0	1.3	1.0	4.2	3.8
P(CO ₂)	6.7	5.0	4.1	14.7	12.9
P(CH ₄)	0.25	0.15	0.10	0.64	0.56
α (He/N ₂)	41	46	66	44	33
α (He/CH ₄)	85	127	180	70	64
α (O ₂ /N ₂)	3.9	3.2	3.8	4.2	3.5
α (CO ₂ /N ₂)	27	41	34	23	23
α (CO ₂ /CH ₄)	13	15	12	15	12
α (N ₂ /CH ₄)	2.06	2.74	2.74	1.58	1.93

A general increase in permeability for DiPrBisA-T was in accordance with its increased v_f . The lowered permeability for CO₂ and CH₄ may be because of the decreased gas solubility in DiPrBisA-T. The lowered CO₂ solubility in case of DiPrBisA based polymer than unsubstituted BisA-T was reported by Pixton et al. [1995a]. In general, selectivities of DiPrBisA-T with respect to DMBisA-T were decreased (as could be anticipated by an increase in permeability) except that for N₂/CH₄.

The polar $-\text{NO}_2$ group substitution decreased the gas permeability, while it was increased in case of polyarylates based on bulky group containing dicarboxylic acids (HFA and *t*-BuI) in comparison to DiPrBisA-T (possessing no substituent on acid). In DiPrBisA- NO_2 T case, the reduction in permeability for various gases was more than in the case of DiPrBisA- NO_2 I, which is in accordance with its higher chain packing density. The polymers based on isophthalic acid normally have lower permeability than terephthalic acid based polyarylates [Pessan (1993)]. In the present case, the observed reversal in the permeation trend was due to the placement of $-\text{NO}_2$ group its 5-position, leading to the increase in v_f . The selectivities for various gas pairs in $-\text{NO}_2$ containing polyarylates were elevated than that of DiPrBisA-T case, except for O_2/N_2 . The selectivities were higher for DiPrBisA- NO_2 T than DiPrBisA- NO_2 I as could be anticipated from the permeability trend. Among these two polyarylates, the He/ CH_4 selectivity was improved notably by 111 % and 47 % for DiPrBisA- NO_2 T and DiPrBisA- NO_2 I, respectively, than that for DiPrBisA-T.

The gas permeability for polyarylates based on bulky group containing dicarboxylic acid (HFA and *t*-BuI) was elevated than that of DiPrBisA-T, owing to increased free volume. The DiPrBisA-HFA was found to be more effective in improving the gas permeability than DiPrBisA-BuI. In general, increased permeability for DiPrBisA-HFA and DiPrBisA-BuI was associated with the simultaneous decrease in selectivity for various gas pairs than that of DiPrBisA-T. The CO_2 and CH_4 permeability were improved to a larger extent in case of DiPrBisA-HFA than for DiPrBisA-BuI case. Similar effect by the $-\text{CF}_3$ group substitution on CO_2 permeability was reported for hexafluoroisopropylidene group containing polycarbonates [Hellums (1989)].

It was observed that for the present polyarylates, decrease in permeability coefficient followed the order $\text{He} > \text{CO}_2 > \text{O}_2 > \text{N}_2 > \text{CH}_4$. A good correlation ($R^2 = 0.93-0.96$) was observed between the gas permeability and the kinetic diameter of the gas molecules. The permeability increased linearly as the kinetic diameter of the gases decreased.

Previous studies have shown an approximate correlation between gas permeability (P) and v_f :

$$P = A \exp\left(\frac{-B}{v_f}\right) \quad (4.1)$$

where the parameters A and B depend on temperature and gas type [Pixton (1995a), Houde (1995)]. For present series, a correlation ($R^2 = 0.69-0.78$) of permeability was also observed with v_f (Figure 4.8). It was stated that some of the effects associated with polarity may not be fully accounted for in this approach [Pixton (1995a)]. This may be a reason for weaker observed correlation of permeability with v_f than that with kinetic diameter of gases.

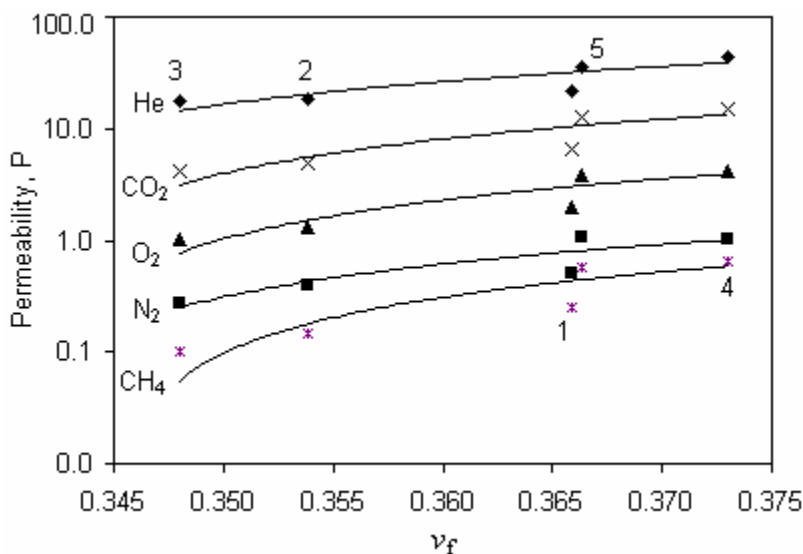


Figure 4.8 Correlation of permeability with v_f of polyarylates (1: DiPrBisA-T, 2: DiPrBisA-NO₂I, 3: DiPrBisA-NO₂T, 4: DiPrBisA-HFA, 5: DiPrBisA-BuI)

A correlation ($R^2 = 0.81-0.92$) between solubility parameter and permeability of polyarylates was also observed (Figure 4.9), indicating the polarity has a role in governing permeation properties of present polyarylates and the substituent effects are not monotonous.

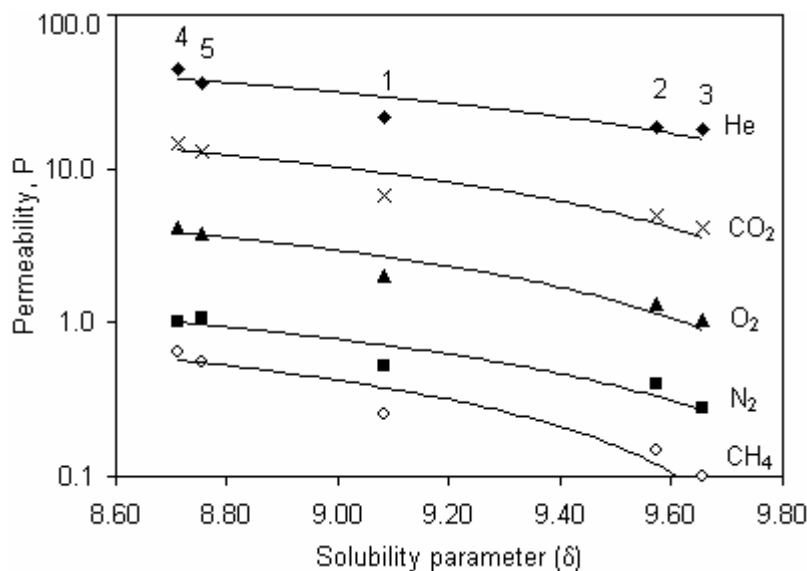


Figure 4.9 Correlation of permeability with solubility parameter of polyarylates (1: DiPrBisA-T, 2:DiPrBisA-NO₂I, 3: DiPrBisA-NO₂T, 4: DiPrBisA-HFA, 5: DiPrBisA-BuI)

4.4.1.2 Polyarylates bases on asymmetrically substituted diphenyl bisphenol-A

The effect of bulky and planner phenyl group substitution on bisphenol moiety in asymmetric manner was investigated in polyarylates based on diphenyl bisphenol-A (DiPhBisA). The effect of diphenyl substitution was evaluated by comparing physical and gas permeation properties of DiPhBisA-I+T vis-à-vis the properties of unsubstituted BisA-I+T and dimethyl substituted DMBisA-I+T. The equimolar mixture of iso and terephthalic acid was chosen intentionally as these individual acids are known to have their own effects on permeation properties [Pessan (1993)]; which could be balanced by taking their equimolar mixture. The DiPhBisA was also polymerized with substituted dicarboxylic acids (BrT, NO₂I, NO₂T, HFA, BuI) containing either polar or bulky groups; to assess the effect of these groups in addition to the effects of diphenyl substitution on bisphenol moiety. These polyarylates were synthesized by interfacial polycondensation (Section 4.3.4.2) with appreciable yield. The intrinsic viscosities of the resultant polyarylates were in the range of 0.39-0.63 dl/g in TCE at 35 °C. The films formed by solution casting from CHCl₃ at ambient temperature were tough and transparent that could allow measurement of gas permeability at 10 atm upstream pressure and at 35 °C.

(a) Physical properties

The physical properties DiPhBisA based polyarylates are given in Table 4.8.

Table 4.8 Physical properties of DiPhBisA based polyarylates

Polymer	d_{sp} (Å)	ρ (g.cm ⁻³)	v_f (cm ³ .cm ⁻³)	δ (cal.cm ⁻³) ^{1/2}	T_g (°C)	TGA (°C)	DMA relaxation temperature (°C)			
							α	β	γ	δ
DiPhBisA -I+T	5.61	1.162	0.3630	9.63	152	459	162	-	15	-98
DiPhBisA -BrT	5.34	1.308	0.3504	9.94	131	434	149	-	30	-61
DiPhBisA -NO ₂ I	4.92, 13.92	1.208	0.3586	9.96	159	353	175	-	23	-53
DiPhBisA -NO ₂ T	5.10, 10.40	1.225	0.3493	10.11	143	347	161	87.9	8.4	-40
DiPhBisA -HFA	5.54, 17.67	1.247	0.3750	9.08	157	431	196	85.6	27	-32
DiPhBisA -BuI	5.54, 12.63	1.094	0.3771	9.06	154	434	181	67.7	-	-23

The WAXD spectra of these polyarylates were as shown in Figure 4.10. All these polymers were amorphous in nature and exhibited two broad peaks (except that for DiPhBisA-I+T and DiPhBisA-BrT), indicating two types of chain packing. The another peak could result from the stacking of phenyl rings present on the bisphenol moiety. The diphenyl substitution on bisphenol in DiPhBisA-I+T increased the v_f than in case of unsubstituted BisA-I+T or dimethyl substituted DMBisA-I+T [Kharul (1998)]. This indicated the capability of phenyl group present on the bisphenol in reducing packing density, though it is flat in nature and the type of substitution being asymmetric.

The polar -Br and -NO₂ group substitution on dicarboxylic acid moiety in these polyarylates led to the increase in chain packing density as evident from lowering in their

ν_f . In case of bulky group substituted DiPhBisA-HFA and DiPhBisA-BuI, the ν_f values were increased than that of DiPhBisA-I+T, rendering looser chain packing.

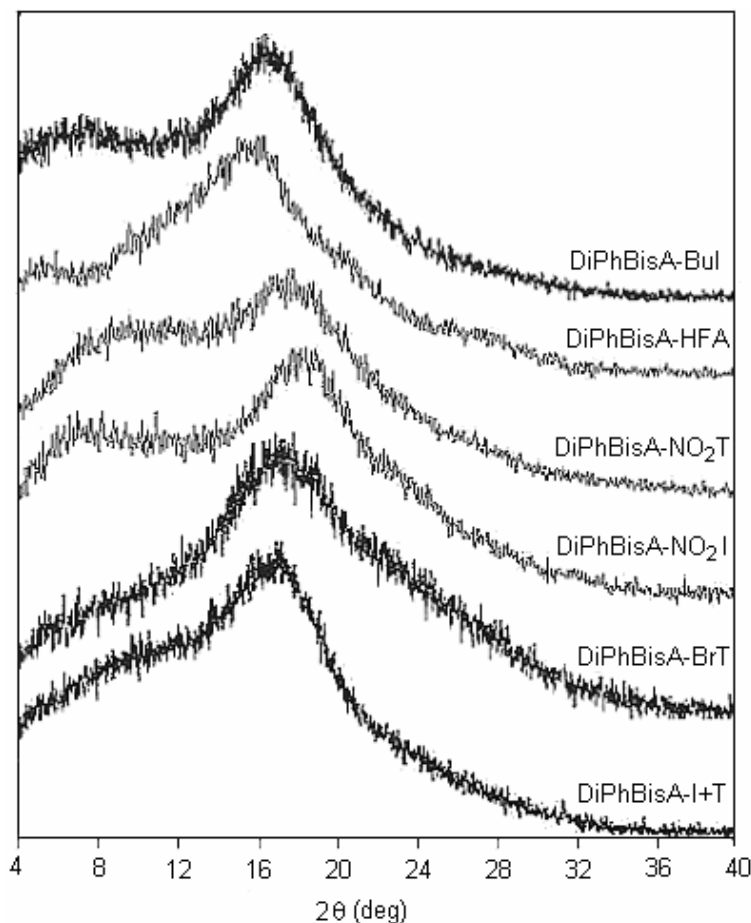


Figure 4.10 WAXD spectra of DiPhBisA based polyarylates

The solubility parameter (δ) of DiPhBisA-I+T decreased in comparison to unsubstituted BisA-I+T or asymmetric methyl substitution in DMBisA-I+T case, due to added aromatic phenyl group (which ultimately leads to lowering of polar group density, especially ester linkages). The addition of polarity by -Br or -NO₂ group introduction on acid moiety increased solubility parameter, while it was decreased in case of polyarylates based on HFA and BuI, as could be anticipated from the nature of these groups.

The T_g reported for BisA-I+T was 198 °C, which was reduced to 161 °C in case of DMBisA-I+T [Kharul (1998)]. It was further reduced to 152 °C in case of DiPhBisA-I+T. Such reduction in T_g by asymmetric type substitution though is well reported in other types of polymers also like PC [Schmidhauser (1990)] and PSF [McHattie (1991)] and also observed in earlier case of isopropyl group substitution on bisphenol in earlier

section; the lowering in T_g in present case by phenyl ring substitution was surprising since the phenyl ring is rigid in nature. This indicates that the lowering in T_g is primarily due to the nature of substitution, which is asymmetric, rather than the nature of substituent. The -Br group substitution on dicarboxylic acid in DiPhBisA-BrT also decreased the T_g in comparison to the DiPhBisA-I+T by 13 °C. Its thermal stability (by TGA) was also decreased by 25 °C than that of DiPhBisA-I+T. The T_g was marginally decreased in DiPhBisA-NO₂T, while it was increased by 7 °C in DiPhBisA-NO₂I than that of DiPhBisA-I+T. The thermal stability by TGA after -NO₂ group substitution on acid moiety was decreased than that of DiPhBisA-I+T. This reduction in thermal stability by polar group substitution could be anticipated from the increased acidity of the phenyl ring of dicarboxylic acid [Jin (1987)]. The bulky group containing DiPhBisA-HFA and DiPhBisA-BuI exhibited marginal increase in T_g than that of DiPhBisA-I+T (by 5 and 2 °C respectively). The increase in T_g for DiPhBisA-HFA may be attributed to the inhibited molecular motions due to the presence of polarizable hexafluoroisopropylidene group, as observed previously [Pixton (1995b)]. A small increase in T_g for DiPhBisA-BuI than that of DiPhBisA-I+T may be due to the increased barriers to molecular motion. Since the ν_f was also increased considerably in both these cases, the barrier to rotational motion may not be that high, resulting in only small increase in T_g . The thermal stability by TGA was found to decrease in both these bulky group containing polymers than that of DiPhBisA-I+T. This lowering in DiPhBisA-HFA may be attributed to the generation of reactive F[·] and CF₃[·] during the thermal degradation of the hexafluoroisopropyl moiety, followed by a cascade of secondary reactions [Choi (1997)]. Similar phenomenon could be anticipated by alkyl group (*t*-butyl) present in DiPhBisA-BuI that resulted in lowering of thermal stability.

The $\tan \delta$ curve by DMA analysis for DiPhBisA based polyarylates is shown in Figure 4.11. The α -relaxation temperature (T_α) observed for all the polymers were higher than the T_g observed by DSC and followed the similar trend in all the polyarylates. The T_γ transition temperature in polyarylates has been assigned mainly to the bisphenol phenyl ring flip [Charati (1994)]. The observed T_γ peak for DiPhBisA-I+T was considerably higher than that of BisA-T, which could be similarly attributed to the

restricted motion of substituted bisphenol phenyl rings. Polar (-Br, -NO₂) group substitution on dicarboxylic acid moiety increased the γ -transitions temperature further, attributable to the increased intermolecular attractions, as also evidenced by increased solubility parameter. The T_γ transition temperature was increased by 15 and 8 °C in case of DiPhBisA-BrT and DiPhBisA-NO₂I, respectively, than that of unsubstituted DiPhBisA-I+T. This transition was probably too weak to be observed in case of DiPhBisA-BuI.

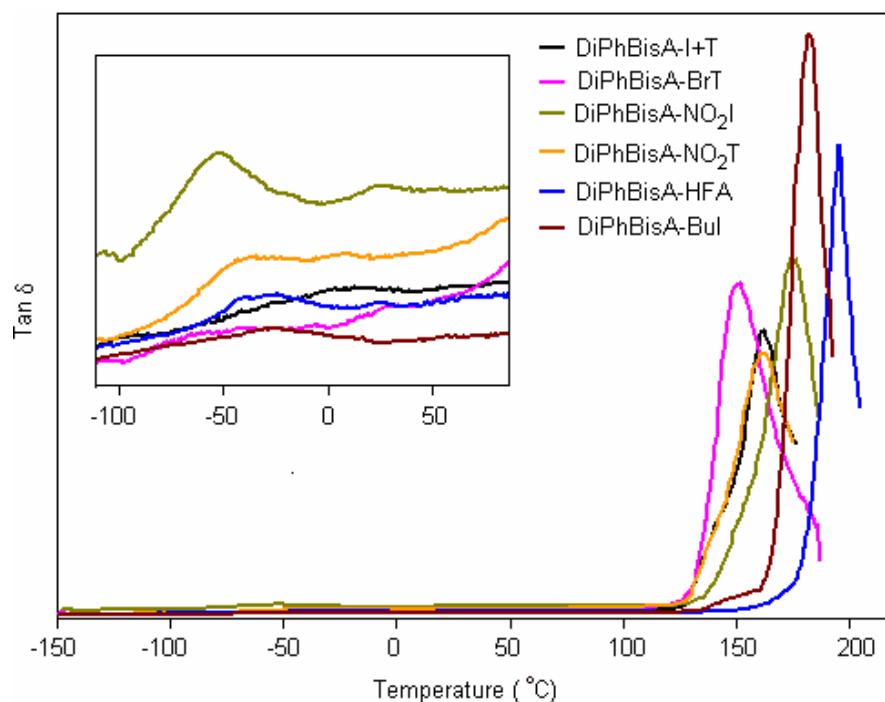


Figure 4.11 DMA spectra of DiPhBisA based polyarylates

(b) Permeation properties

Asymmetric substitution by bulky but flat phenyl group in DiPhBisA-I+T resulted into lowering of permeability for various gases than for unsubstituted BisA-I+T, while the variation was marginal in comparison to permeation in DMbisA-I+T [Kharul (1998)]. The decreased permeability in DiPhBisA-I+T was associated with the increased selectivities for various gas pairs, except for CO₂/N₂. The lowering in permeability for PPO containing phenyl group than that containing methyl group was demonstrated [Vega (1993b)].

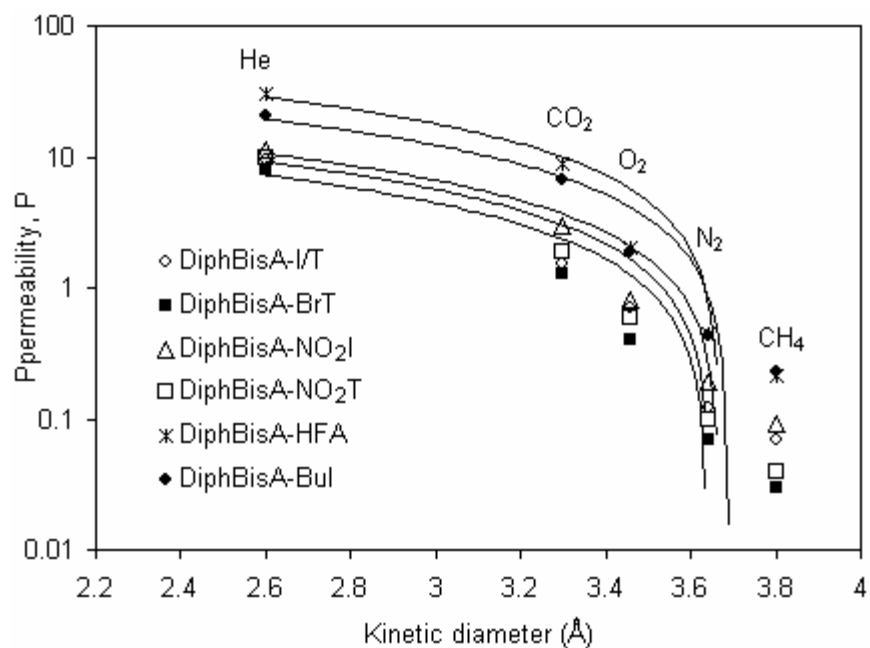
The variation in gas permeability in case of polar group substituted on acid moiety of polyarylates was in accordance with the nature and position of the substituents.

Polymer containing -Br substitution (DiPhBisA-BrT) showed decreased gas permeability than that of DiPhBisA-I+T for all the gases, with simultaneous improvement in selectivities of various gas pairs (Table 4.9) except for Ar/N₂ and O₂/N₂. The He/CH₄ selectivity in DiPhBisA-BrT was improved by 92 % than that of DiPhBisA-I+T. The -NO₂ group substitution on acid moiety in DiPhBisA-NO₂I resulted into increased gas permeability, while this group substitution in DiPhBisA-NO₂T decreased the permeability (except for CO₂), when compared with the permeability of DiPhBisA-I+T. The improved gas permeability in case of DiPhBisA-NO₂I was associated with the decreased selectivities for various gas pairs, except for CO₂ based selectivities. The CO₂ permeability in case of DiPhBisA-NO₂T was increased by 27 % than that of DiPhBisA-I+T. The higher CO₂ permeability in case of DiPhBisA-NO₂I than that of DiPhBisA-NO₂T, though the substituent is same (-NO₂) can be justified on the basis of its higher degree of chain openness (as reflected by ν_f). The CO₂/CH₄ selectivity in case of DiPhBisA-NO₂I and DiPhBisA-NO₂T was improved by 56 and 121 %, respectively, than that of DiPhBisA-I+T.

The gas permeability for polyarylates based on bulky group containing dicarboxylic acid (HFA and *t*-BuI based) was found to be elevated than that of DiPhBisA-I+T. The improvement in permeability in DiPhBisA-HFA was from 2-4.8 times, while that for and DiPhBisA-BuI was upto 1.1-3.4 times. This increase was associated with the decrease in selectivities, except for CO₂ based selectivities; when compared with unsubstituted DiPhBisA-I+T case. In case of DiPhBisA-HFA, higher extent of improvement in CO₂ permeability than for other gases resulted into elevated CO₂/N₂ and CO₂/CH₄ selectivities by 55 and 93 %, respectively. These improvements were by 23 and 34 %, respectively, in case of DiPhBisA-BuI, when compared with the similar properties for DiPhBisA-I+T. In both these cases of bulky group containing polyarylates, the Ar/N₂ and O₂/N₂ selectivities were decreased by 4-24 %. Among these two polymers, DiPhBisA-HFA exhibited larger improvement in permeability with good improvement in CO₂ based selectivities than that for DiPhBisA-BuI case. The increased permeability for CO₂ in case DiPhBisA-HFA may be due to the interaction of CO₂ with -CF₃ group of HFA, as observed previously for polycarbonates and silicon rubbers [Hellums (1989)].

Table 4.9 Gas permeability (P) and selectivity (α) for DiPhBisA based polyarylates

	DiPhBisA -I+T	DiPhBisA -BrT	DiPhBisA -NO ₂ I	DiPhBisA -NO ₂ T	DiPhBisA -HFA	DiPhBisA -BuI
P(He)	9.6	7.9	11	9.9	30.1	20.2
P(Ar)	0.3	0.14	0.33	0.23	1	0.82
P(N ₂)	0.1	0.07	0.19	0.1	0.45	0.43
P(O ₂)	0.7	0.4	0.8	0.6	2	1.9
P(CO ₂)	1.5	1.3	3	1.9	8.7	6.6
P(CH ₄)	0.1	0.03	0.09	0.04	0.21	0.23
α (He/N ₂)	80	113	59	99	67	47
α (He/CH ₄)	137	263	124	248	143	88
α (Ar/N ₂)	2.33	2.00	1.74	2.30	2.22	1.91
α (O ₂ /N ₂)	5.8	5.7	4.2	6.0	4.4	4.4
α (CO ₂ /N ₂)	13	19	16	19	19	15
α (CO ₂ /CH ₄)	21	43	33	48	41	29
α (N ₂ /CH ₄)	1.71	2.33	2.11	2.50	2.14	1.87

**Figure 4.12 Correlation of gas permeability in DiPhBisA based polyarylates with kinetic diameter of the gas molecules**

A good correlation ($R^2 = 0.92-0.96$) of gas permeability in DiPhBisA based polyarylates was observed with kinetic diameter of the gas molecules (Figure 4.12). The permeability increased linearly as the kinetic diameter of the gases decreased.

4.4.2 Polyarylates based on fluorene bisphenols and dibromohexafluoro bisphenol-A

In view of the demonstrated potential of asymmetric substitution on bisphenol moiety, it was decided to substitute fluorenone bisphenol by dimethyl and dibromodimethyl groups in asymmetric manner. The investigations of physical and gas permeation properties of resulting bisphenol based polyarylates would enhance the understanding towards combined effect of bisphenol asymmetric and bridge substitution by flat fused ring of fluorenone simultaneously. The capability of enhancing permeability by hexafluoroisopropylidene group is well demonstrated in several cases, not only in polyarylates, but other polymers as well. It was thought to be interesting to analyze the effects of polar bromine substitution on bisphenol in asymmetric manner on gas permeation and related physical properties of polyarylates based on this bisphenol and polar / bulky group substituted aromatic dicarboxylic acids.

4.4.2.1 Polyarylates based on systematically substituted fluorene bisphenols

This study was aimed at the simultaneous investigations of bridge and asymmetric phenyl ring substitutions in the bisphenol moiety of polyarylates. The equimolar mixture of iso and terephthalic acids was used in the preparation of polyarylates by a solution polycondensation method using trimethylamine as the base. It is known that the reaction of bisphenol and diacid chloride in the presence of a strongly basic tertiary amine is fast, and possibly proceeds by the phenoxide mechanism [Morgan (1965)]. In the present work, addition of acid chloride during polymerization was made in a drop-wise manner over a period of 15 min in anticipation of the formation of a statistical copolymer with high enough intrinsic viscosity. The high yield of the polymer obtained ensured the incorporation of almost all monomers in appropriate proportions. It is well known that polyarylates obtained from the same bisphenol but with isomeric acids (isophthalic or terephthalic acid) have different permeation properties owing to isomerization effect [Pessan (1993), Kharul (1997), Kharul (1998)]. It was anticipated that if an equimolar

mixture of acid is used instead of individual acids, the effects of bisphenol substitution can better be visualized. The effect of the bridge connector group (9, 9'-fluorenylidene) was examined in this series of polyarylates in view of its rigid but flat nature. This group consists of two phenyl rings fused together. It was of interest to study the effect of such a large flat group on gas permeability and selectivity. The effect of asymmetric substitution in addition to this bridge substitution was compared with that of similar ring substitutions in bisphenol-A.

(a) Physical properties

The physical properties of the fluorene bisphenol based polyarylates prepared were as presented in Table 4.10.

Table 4.10 Physical properties of polyarylates based on fluorene bisphenols

Polymer abbreviation	ρ (g/cm ³)	d_{sp} (Å)	v_f (cm ³ /cm ³)	T_g (°C)
FBP-I+T	1.2950	4.36	0.3240	239
DMFBP-I+T	1.2425	4.61	0.3332	224
DBrDMFBP-I+T	1.4050	4.57, 6.28	0.3737	264

All the polymers investigated in this study were amorphous in nature, as revealed by the WAXD spectra as shown in Figure 4.13. Polyarylates based on FBP and DMFBP showed a single amorphous peak, while the DBrDMFBP-based polyarylate showed two diffused amorphous peaks. Such multiple peaks were shown by different types of polymers. The FBP-based polysulfone exhibited one peak, while polycarbonate and isophthalic acid-based polyarylate are known to have two peaks [Pixton (1995b)]. In the case of ring bromine substitution, two WAXD peaks were reported for polyarylates [Pixton (1995c), Kharul (1997)]. Appearance of two peaks in brominated polyarylates was attributed to much higher X-ray scattering ability of bromine [Pixton (1995c)]. The d-spacing (d_{sp}) for the present polyarylates was slightly lower than for corresponding bisphenol-A-based polyarylates bearing corresponding ring substitution [Kharul (1997), Kharul (1998)].

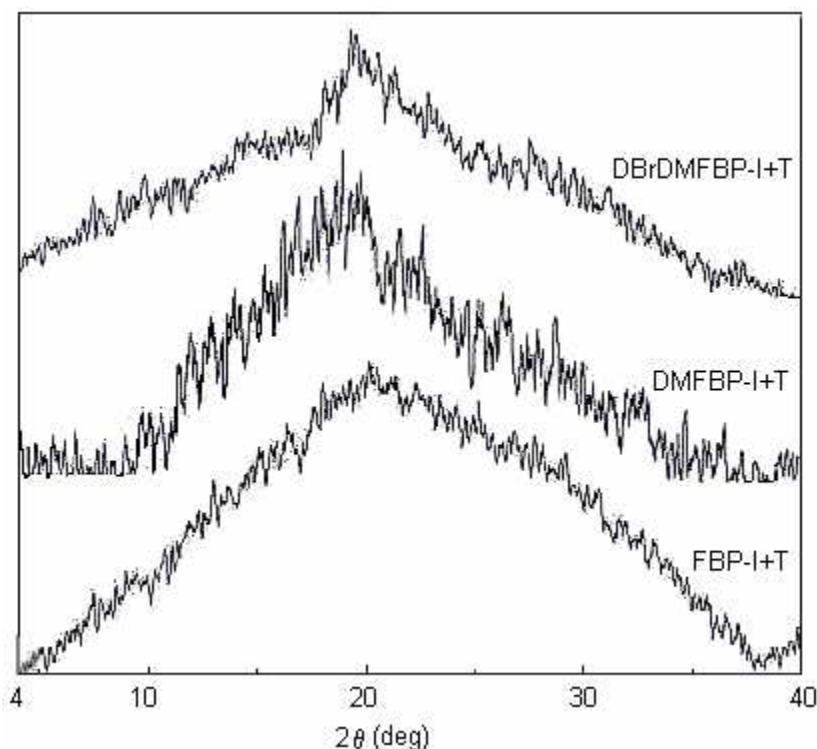


Figure 4.13 WAXD spectra of polyarylates based on fluorene bisphenols

In addition to d_{sp} , the fractional free volume, v_f , was also considered as another way of expressing chain packing in the polymer matrix, which can be estimated by a semi-empirical method [Van Krevelen (1972)], based on measured density of the polymer. An increase in v_f observed in this series was in accordance with the number of substituents on the phenyl ring. The similar trend in v_f variation was noted for BisA, DMBisA and DBrDMBisA-based polyarylates [Kharul (1997), Kharul (1998)]. The remarkable increase in the value of v_f for DBrDMFBP-I + T by bromine substitution was noted.

The glass transition temperature (T_g) for these polymers was found to be higher than that of respective substituted bisphenol-A-based polyarylates obtained with the same acid composition [Kharul (1997), Kharul (1998)]. This increase in T_g could be attributed to a 9,9'-fluorenylidene connector group at the bisphenol bridge position, which is flat but rigid in nature. The T_g for the present polyarylates increased in the order: DMFBP-I + T < FBP-I + T < DBrDMFBP-I + T. Polymers prepared using asymmetrically substituted dimethyl bisphenol are known to exhibit a lower glass transition temperature than the unsubstituted bisphenol-based polymers, though there is an addition of methyl group on the phenyl ring in the earlier case. This behavior was

reported previously by polyarylate [Pixton (1995a), Kharul (1998)], polysulfone [McHattie (1991)], polycarbonate [Schmidhauser (1990)], etc. The bromine substitution on aromatic ring of bisphenol increased T_g for DBrDMFBP-I + T, as also observed for other types of polyesters [Pixton (1995c), Kharul (1997)] and polycarbonate [Muruganandam (1987)]. Though bromine substitution increased chain stiffness due to interchain polar interactions in the corresponding polyarylate, it also has appreciable free volume. This indicates that bulk effects were not shadowed by polar attraction leading to chain collapse that would have been resulted in reduction of free volume.

(b) Gas permeability

Pure gas permeability and selectivities of gas pairs of particular interest were as given in Table 4.11. The variation in gas-permeation properties was assessed in two ways. Firstly, the effect of ring substitution in the FBP series was examined. Secondly, the effect of ring substitution in combination with bridge substitution is discussed. The comparison was made with polyarylates prepared from other ring- as well as bridge-substituted bisphenols.

Table 4.11 Permeability coefficients (P) and selectivities (α) of polyarylates based on fluorene bisphenols

Property	FBP-I+T	DMFBP-I+T	DMDBrFBP-I+T
P(He)	15.616	14	29.830
P(Ar)	0.75	0.6	2.3
P(N ₂)	0.38	0.35	1.4
P(O ₂)	1.72	1.5	4.3
P(CH ₄)	0.41	0.23	1.0
α (He /Ar)	20.821	23.323	13.113
α (He /N ₂)	41	40	21.321
α (He /CH ₄)	38	61	29.630
α (Ar /N ₂)	1.972.0	1.71	1.6
α (O ₂ /N ₂)	4.52	4.3	3.1
α (N ₂ /CH ₄)	0.93	1.52	1.4

(i) *Effect of asymmetric ring substitution*

Gas-permeation properties of FBP-I+T are considered as the base case to compare ring substitution effects. Asymmetric substitution by the non-polar methyl group in DMFBP-I+T gave slightly less permeability for various gases than unsubstituted FBP-I+T. The decrease in CH₄ permeability was larger than for any other gas. This led to ~50% increase in CH₄ based selectivities, while selectivities for other gas pairs were practically similar to the unsubstituted FBP base case. In the case of the isopropylidene linkage at the bridge (bisphenol-A), this type of asymmetric ring substitution by methyl gave marked increase in selectivity of various gas pairs [Pixton (1995a), Kharul (1998)]. The substitution by bromine atom on DMFBP leading to DBrDMFBP resulted in a 2-3.8 times increase in permeability for various gases. The added bulk of the bromine substituent could impose constraint on chain packing as revealed by its higher ν_f , leading to the observed increase in permeability. This increase in the gas permeability was associated with the decrease in selectivity. In the case of isopropylidene linkage at the bridge and asymmetric ring substitution by methyl and bromine in (DBrDMBisA), an increase in permeability as well as selectivity was noted [Kharul (1997)]. It is thus evident that, in the case of DBrDMFBP, effects due to the polar nature of the bromine were possibly suppressed by looser packing, which stem from the bulk of the bromine as well as that of the bulky and flat bridge connector group. In addition, the polymer chains were made stiffer as revealed by its increased T_g by bromine substitution. The flat nature of 9,9-fluorenylidene (though it is rigid and bulky) may be unable to enhance the penetrant-discriminating capability of the polymer during looser chain packing, leading to normal trend of lowering of selectivity as the permeability was increased for this polyarylate.

(ii) *Effect of rigid group incorporation at the bridge position*

This effect could better be assessed by comparing the permeation performance of this series of polyarylates (rigid bridge position) with that of bisphenol-A-based (flexible isopropylidene bridge) polyarylates having a similar type of ring substitution. Other than for the ring-unsubstituted case (FBP), the permeability for asymmetric non-polar substitution (in DMFBP) as well as for asymmetric non-polar plus polar substitution

(DBrDMFBP) increased by almost 2-3 times (except for He) in comparison with corresponding bisphenol-A polyarylates [Kharul (1997), Kharul (1998)], while in the case of unsubstituted FBP, the permeability was only slightly increased. The isophthalic acid-based polyarylate of FBP was reported to be \sim 1.6-2.3 times more permeable than the bisA-polyarylate with the same acid [Pixton (1995b)]. This extent of increase in permeability was lowered when this isophthalic acid was replaced by *t*-butyl isophthalic acid with same bisphenol. Such an increase in permeability was observed in this study only for substituted bisphenols; in other words, the effect of rigid bridge group substitution is more marked when the bisphenol ring of FBP is substituted.

In the case of isopropylidene bridge bisphenol based polyarylates, dimethyl substitution on the phenyl ring led to marked decrease in permeability and increase in selectivity [Kharul (1998)], while dibromodimethyl substitution led to an increase in permeability as well as selectivity [Kharul (1997)]. In the present case, where the rigid but flat 9,9'-fluorenylidene was situated at the bridge position of bisphenol, the ring substitution by methyl (DMFBP) led to a very small decrease in permeability with similar or increased (CH₄ based) selectivities, while dibromodimethyl substitution (DBrDMFBP) led to increased permeability and lowering of selectivity. This variation in permeation properties was more significant in the case of ring substitution in fluorene bisphenol than in the bisphenol-A case. Thus, substitution by 9,9'-fluorenylidene at the bridge position of bisphenol in combination with ring substitution offered an increase in permeability associated with a general decrease in selectivity (DBrDMFBP) or slight variation in permeability and selectivity (DMFBP). The ineffectiveness of the 9,9'-fluorenylidene group at the bridge to increase selectivity can be attributed to its rigid but flat nature. In the case of the hexafluoroisopropylidene bridge on bisphenol, a similar increase in permeability and decrease in selectivity was noted for the resulting polyarylate [Kharul (1994)]. The present work thus supports that the bridge substitution by rigid group though result in stiffer chain (higher T_g), may not be sufficient to increase the selectivity. This could be attributed to the chain conformation. It is known that the substituents on the bisphenol play an important role in governing the chain conformation of the resulting polyarylate [Kharul (1998)]. In the case of fluorenone-based bisphenols, the bridge structure is rigid, which might impose restrictions on the bisphenol phenyl ring flip

leading to more disordered packing. Such a disorder may be the reason for inability to improve penetrant-discriminating ability.

4.4.2.2 Polyarylates based on dibromohexafluoro bisphenol-A

(a) Physical properties

All the polyarylates were obtained with good yield (> 95 %) and viscosity to be able to be transformed into transparent and mechanically stable film so that it could withstand the gas pressure during permeation measurement. Their WAXD spectra indicated amorphous nature and exhibited more than one amorphous peak, typical of brominated polymers [Pixton (1995a), Pixton (1995c), Kharul (1997)] and was ascribed to higher scattering ability of bromine [Pixton (1995a)]. Since X-ray spectra reflect scattering features rather than the average distance between polymer chains and, thus, have limited usefulness for interpreting transport properties [Pixton (1995a)]. The 2 θ -peak position of major amorphous peaks were used to calculate average d-spacing as given in Table 4.12. All present halogenated polymers showed higher density (Table 4.12) as compared to their non-halogenated analogs reported in the literature [Pixton (1995c), Kharul (1998)].

Table 4.12 Physical properties of polyarylates based on DBrHFBisA

Polymer	d_{sp} (Å)	ρ (g.cm ⁻³)	v_f^a (cm ³ .cm ⁻³)	δ^b (cal.cm ³) ^{1/2}	T_g (°C)	TGA (°C)	DMA relaxation temperature (°C)			
							α	β	γ	δ
DBrHFBisA-I+T	4.77, 3.52	1.646	0.3873	9.42	195	391	232	192	54	-52
DBrHFBisA-BrT	4.87, 3.79	1.802	0.3711	9.79	181	400	217	165	63	-58
DBrHFBisA-NO ₂ T	4.90	1.701	0.3707	9.97	207	306	250	182	79	-60
DBrHFBisA-HFA	5.87	1.603	0.3935	8.86	227	387	264	212	52	-
DBrHFBisA-BuI	6.76, 4.77, 3.62	1.502	0.3925	8.90	207	406	244	205	61	-60

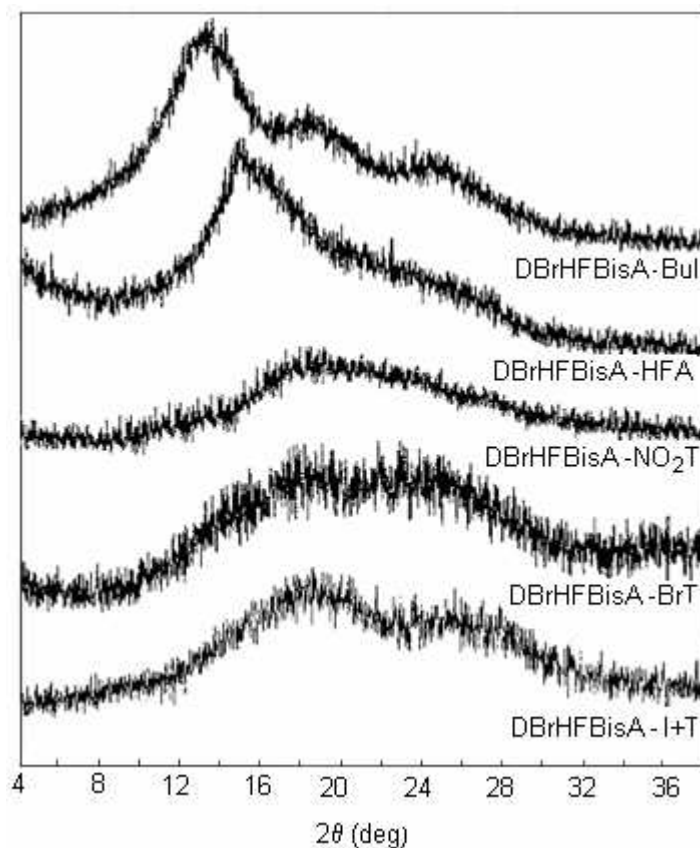


Figure 4.14 WAXD spectra of polyarylates based on DBrHFBisA

The trend observed in fractional free volume (v_f) and solubility parameter (δ) of the polymers investigated was presented in Table 4.12. Asymmetric polar (-Br) group substitution on bisphenol moiety increased density with increase in v_f in comparison to the polymer based on unsubstituted HFBisA-I+T. Normally, increase in density is associated with the decrease in v_f but in the present case increased density is associated with the increased v_f , this anomalous behavior could be better ascribed to the polar and bulky nature of bromine group.

In this series based on DBrHFBisA as the common bisphenol, the polymer solubility parameter (δ) followed the order: $\text{NO}_2\text{T} > \text{BrT} > \text{I+T} > \text{BuI} > \text{HFA}$; while density (ρ) decreased for polyarylates by varying dicarboxylic acids in the following order: $\text{BrT} > \text{NO}_2\text{T} > \text{I+T} > \text{HFA} > \text{BuI}$. Consequently, the order of fractional free volume (v_f) was reversed (except that the v_f of BuI and HFA based polyarylates was almost similar). The higher density and lower v_f in case of BrT and NO_2T based polyarylates indicated that the presence of polar groups (Br/ NO_2) rendered closer chain packing than I+T based

polyarylates owing to increased interchain interactions. The lower density and higher v_f of the polyarylates based on BuI and HFA in comparison to their unsubstituted analog based on I+T indicated lower chain packing. These variations in v_f , density, solubility parameter and WAXD behavior were as anticipated based on literature reports on substitution of these groups in polymer matrix belonging to different families [Muruganandam (1987), Hellums (1989), Chern (1991), Pixton (1995a), Pixton (1995b)].

(i) *Thermal properties*

The asymmetric substitution by polar -Br group on bisphenol moiety in DBrHFBisA-I+T lowered T_g in comparison to the polymer based on unsubstituted bisphenol (HFBisA-I+T) [Maruyama (1986)]. The reduction was by 38 °C. Similar reduction of T_g in comparison to the unsubstituted polymers is known for asymmetric substitution on bisphenol phenyl ring by methyl group in case of polyarylates [Pixton (1995a)] and polysulfone [McHattie (1991)].

In the present series, variation in acid moiety generally led to an increase in T_g , except for the polyarylate derived from BrT; while compared with that obtained from unsubstituted dicarboxylic acid (DBrHFBisA-I+T, Table 4.12). Similar comparison for thermal stability showed that variation in acid had marginal effect, except that for NO₂T, wherein DBrHFBisA-NO₂T exhibited considerably lower degradation temperature. Such reduction in thermal stability of NO₂T based aromatic polyesters was related to the fairly strong substituent effect of the NO₂ group, which increased the acidity of terephthalic acid and made the acid moiety more thermally labile [Jin (1987)].

(ii) *Dynamic mechanical analysis*

The $\tan \delta$ curves for these polyarylates were as shown in Figure 4.15 and the various transition temperatures observed are listed in Table 4.12. The α relaxation temperature (T_α) observed for all the polymers were higher than the T_g observed by DSC. It is known that the T_α by DMA is usually higher than T_g obtained by DSC [McHattie (1992), Vega (1993)]. The trend observed in variation of T_α was similar to that observed for T_g by varying acid moiety in polyarylates. A smaller shoulder in the temperature range of ~165-205 °C was observed in these polyarylates, termed as β transition,

responsible to the non-equilibrium packing defects in the glass or of stresses introduced during fabrication, as noted previously [LeGrand (1969), Charati (1994)].

The γ transition observed in the temperature range of 52-79 °C for different polymers was due to phenyl ring flip [Charati (1994), Kharul (1998)] and introducing substituents onto backbone phenylene rings leads to increases in T_γ .

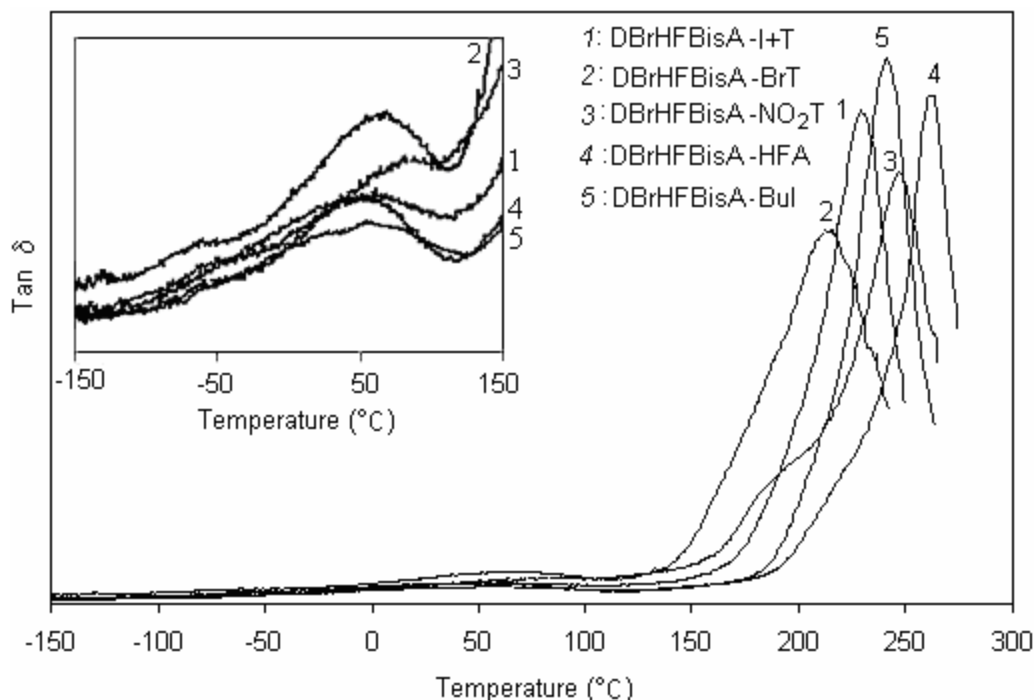


Figure 4.15 DMA spectra of DBrHFBisA based polyarylates

These substituents can cause rotational interference between adjacent monomer units within a chain or with adjacent chains. In present series, polar (-Br, -NO₂) group substitution on dicarboxylic acid moiety increased the γ transitions temperature to a larger extent than for other polyarylates. These polyarylates also exhibited higher chain packing density. This also could be contributing to an increase in T_γ . The bulky *t*-butyl substitution, which simultaneously increases v_f and hinders phenyl ring rotational mobility through steric interactions, may raise the observed T_γ rather than that for DBrHFBisA-HFA, though the chain packing density (v_f) is almost similar in both the cases. Another low temperature relaxation, termed as δ peak was also observed in the temperature range of -50 to -60 °C in all the polymers, except in case of DBrHFBisA-HFA. This transition can be ascribed to the small scale subgroup mobility.

(b) Gas transport properties**(i) Equilibrium sorption**

Equilibrium sorption isotherms for N₂, O₂, CH₄ and CO₂ in polyarylates exhibited dual mode nature (Figure 4.16), as typically observed for glassy polymers and represented by Equation 1.8.

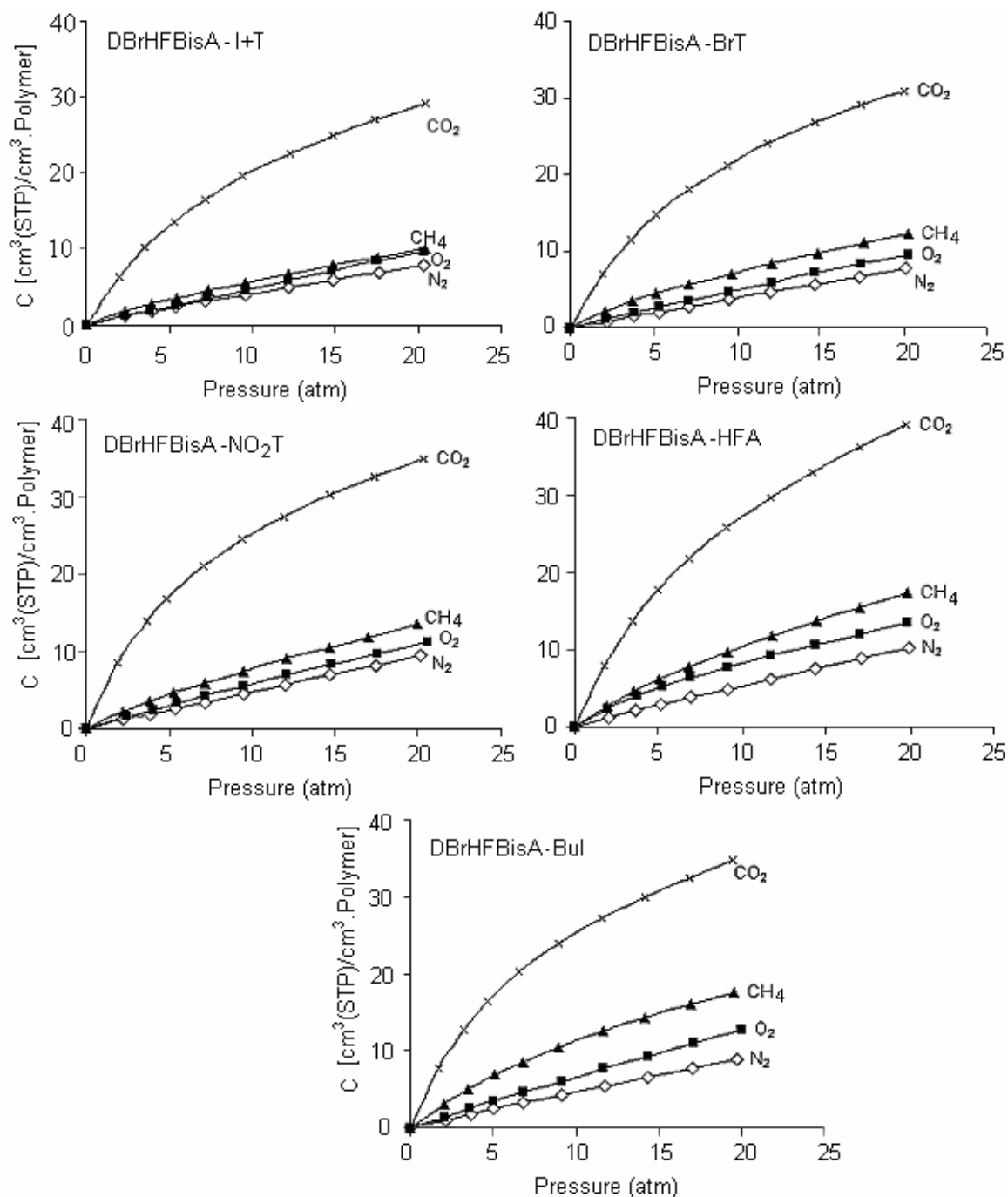


Figure 4.16 Sorption isotherms for DBrHFBisA based polyarylates

The order for sorption of different gases in present polyarylates was $N_2 < O_2 < CH_4 < CO_2$. A nonlinear curve fitting of the sorption data to the dual-mode sorption model (Equation 1.8) using the genetic algorithm (GA) [Goldberg (1989)] yielded parameters, k_D , C'_H and b were as tabulated in Table 4.13.

Table 4.13 Dual-mode sorption parameters of polyarylates at 10 atm and 35 °C

Polymer	Gas	k_D ($cm^3(STP)/cm^3 \cdot atm$)	C'_H ($cm^3(STP)/cm^3 polymer$)	b (l/atm)
DBrHFBisA-I+T	N ₂	0.30	3.02	0.06
	O ₂	0.47	4.22	0.001
	CH ₄	0.37	3.26	0.17
	CO ₂	0.36	31.68	0.11
DBrHFBisA-BrT	N ₂	0.38	0.72	0.0003
	O ₂	0.38	3.66	0.04
	CH ₄	0.44	4.06	0.22
	CO ₂	0.33	34.79	0.12
DBrHFBisA-NO ₂ T	N ₂	0.46	4.02	0.001
	O ₂	0.45	3.92	0.04
	CH ₄	0.48	5.79	0.10
	CO ₂	0.40	35.35	0.15
DBrHFBisA-HFA	N ₂	0.43	3.34	0.04
	O ₂	0.45	5.70	0.18
	CH ₄	0.52	10.60	0.10
	CO ₂	0.61	37.71	0.13
DBrHFBisA-BuI	N ₂	0.40	2.25	0.04
	O ₂	0.55	4.46	0.04
	CH ₄	0.38	16.67	0.08
	CO ₂	0.46	34.62	0.15

The Henry's solubility coefficients, k_D , is known to be a function of both, gas-polymer and polymer-polymer interactions [Barbari (1988)]. This coefficient for N₂ and

O₂ in all the polyarylates was nearer to each other. The k_D , of CH₄ (interacting gas), rank the order of polyarylates as DBrHFBisA-I+T < DBrHFBisA-BuI < DBrHFBisA-BrT < DBrHFBisA-NO₂T < DBrHFBisA-HFA. The k_D for CO₂ in DBrHFBisA-HFA was highest than for other polyarylates, which could be because of stronger interaction of -CF₃ groups with CO₂. Hellums et al. [1989] reported interaction of CO₂ with -CF₃ groups in TMHF-PC. The Langmuir saturation constant C'_H was largest for gases with higher condensability and follow the order: CO₂ > CH₄ > O₂ > N₂ for a polyarylate. The C'_H of less interacting O₂ followed the trend of T_g . The C'_H is known to increase with the order of polymers having higher T_g [Chiou (1989)]. The C'_H for CO₂ in high v_f and high T_g material, viz., DBrHFBisA-HFA was higher than that for other polymers studied.

Solubility coefficient and solubility selectivity

Solubility coefficient and solubility selectivity for polyarylates at 10 atm were as tabulated in Table 4.14.

Table 4.14 Apparent solubility coefficient and concentration-averaged diffusivity at 10 atm and 35 °C

Permeation property	DBrHFBisA-I+T	DBrHFBisA-BrT	DBrHFBisA-NT	DBrHFBisA-HFA	DBrHFBisA-BuI
S(N ₂)	0.42	0.38	0.46	0.53	0.47
D(N ₂)	0.84	0.24	0.36	2.3	2.13
S(O ₂)	0.48	0.49	0.57	0.82	0.66
D(O ₂)	4.47	1.08	1.6	6.69	7.69
S(CH ₄)	0.57	0.72	0.77	1.04	1.13
D(CH ₄)	0.24	0.05	0.07	0.59	0.32
S(CO ₂)	2.02	2.2	2.51	2.72	2.54
D(CO ₂)	3.9	0.86	1.5	6.5	4.6
S(O ₂ /N ₂)	1.14	1.29	1.23	1.54	1.42
D(O ₂ /N ₂)	5.33	4.54	4.44	2.91	3.61
S(CO ₂ /N ₂)	4.84	5.73	5.42	5.12	5.44
D(CO ₂ /N ₂)	4.65	3.61	4.17	2.83	2.16
S(CO ₂ /CH ₄)	3.52	3.06	3.28	2.62	2.26
D(CO ₂ /CH ₄)	16.39	16.23	21.65	11.09	14.51

The substitution of bromo, nitro, hexafluoroisopropylidene and *t*-butyl group on acid moiety of polyarylate increased solubility of various gases upto 25 %, 33 %, 80 % and 96 % respectively, in comparison to I+T based polyarylate, with 7-34 % increased $S(\text{O}_2/\text{N}_2)$, 5-18 % increased $S(\text{CO}_2/\text{N}_2)$ and 7-36 % decreased $S(\text{CO}_2/\text{CH}_4)$. The order for increase in $S(\text{CO}_2)$ in these polyarylates was: DBrHFBisA-I+T < DBrHFBisA-BrT < DBrHFBisA-NO₂T < DBrHFBisA-BuI < DBrHFBisA-HFA. This order reveals that though all the present substituents increased solubility, those leading to increased v_f (BuI and HFA based polyarylates), exhibited higher solubility than those leading to lowering in v_f due to polar interactions (BrT and NO₂T based polyarylates). This suggested that rather than the polarity, an increased v_f was more effective in increasing sorption capacity of CO₂. The solubility coefficient depends primarily on three factors; the penetrant condensability, the free volume in glassy polymer matrix and polymer-penetrant interactions [Qiu (2006)]. The penetrant condensability is an intrinsic property of each gas and usually expressed in terms of Lennard-Jones potential well depth parameter ϵ/κ . It suggests that in an environment of stronger molecular interaction, more condensable the gas is, higher would be the gas solubility. In present work also, the solubility coefficient S , correlated well with Lennard-Jones potential well-depth parameter, ϵ/κ , for N₂, O₂, CH₄, CO₂, as shown in Figure 4.17.

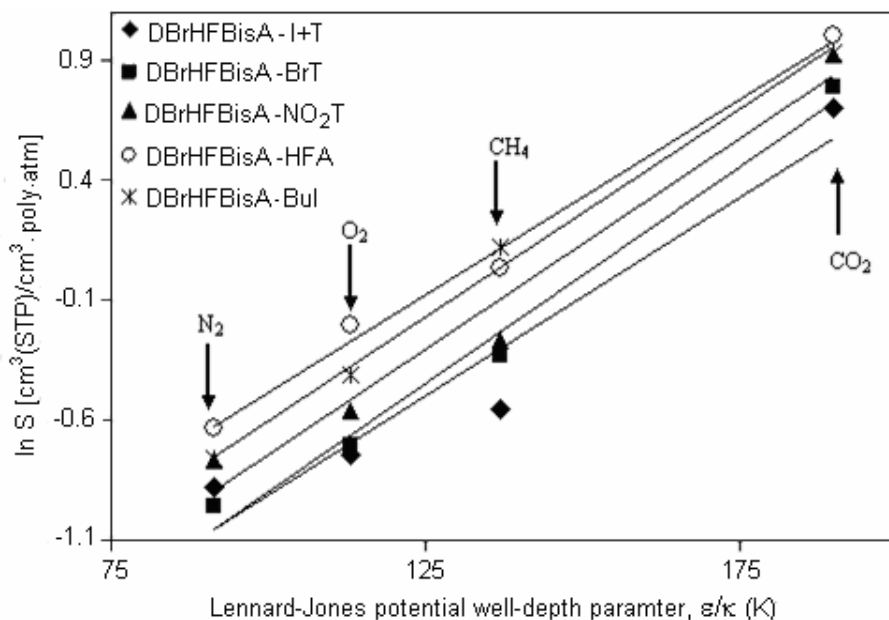


Figure 4.17 Correlation of solubility coefficient with Lennard- Jones potential well depth parameter

The correlation of solubility coefficient with $1/v_f$ for N_2 , O_2 , CH_4 and CO_2 in present polyarylates was as plotted in Figure 4.18a.

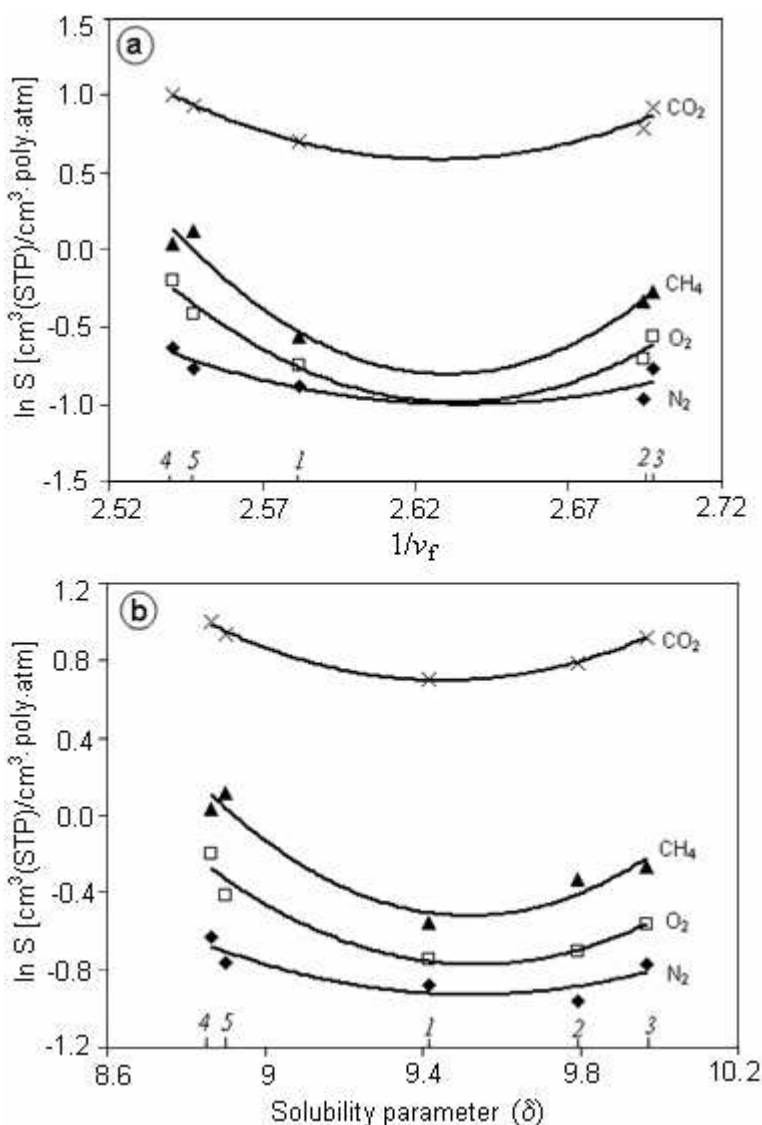


Figure 4.18 Correlation of solubility coefficient with a) $1/v_f$, b) solubility parameter of polyarylates (1: DBrHFBisA-I+T, 2: DBrHFBisA-BrT, 3: DBrHFBisA-NO₂T, 4: DBrHFBisA-HFA, 5: DBrHFBisA-BuI)

The substitution of bulky hexafluoroisopropylidene and *t*-butyl group increased solubility coefficient as ascribed by increased v_f . The asymmetric polar bromine and nitro group substitution though decreased v_f , led to a smaller increase in solubility coefficient than for unsubstituted case. Figure 4.18b shows variation of gas solubility with solubility parameter of the polyarylate and essentially exhibited the similar nature as that of Figure

4.18a. This figure shows that not only increased v_f (than base case of DBrBisA-I+T), but also the increased polymer polarity, as indicated by solubility parameter responsible for elevating the gas sorption, irrespective of the nature of gas.

(ii) *Permeation properties*

The gas permeation and selectivity performance of the polyarylates based on DBrHFBisA and substituted dicarboxylic acids studied in present work are presented in Table 4.15. It would be worth to assess the effect of polar group substitution on bisphenol in asymmetric manner by comparing the permeation properties of DBrHFBisA-I+T with that of HFBisA-I+T reported previously [Kharul (1994)].

Table 4.15 Permeability (P) coefficients and selectivity (α) for polyarylates based on DBrHFBisA

	DBrHFBisA - I+T	DBrHFBisA -BrT	DBrHFBisA - NO ₂ T	DBrHFBis A-HFA	DBrHFBisA - BuI
P(He)	39.0	16.8	24	79.5	75.2
P(Ar)	1.0	0.28	0.36	3.04	2.9
P(N ₂)	0.46	0.12	0.22	1.61	1.31
P(O ₂)	2.8	0.7	1.2	7.2	6.7
P(CO ₂)	10.4	2.5	4.8	23.4	15.5
P(CH ₄)	0.18	0.05	0.07	0.8	0.47
α (He/Ar)	39	60	67	26	26
α (He/N ₂)	85	145	109	49	57
α (He/CH ₄)	217	339	343	99	160
α (Ar/N ₂)	2.17	2.41	1.64	1.89	2.21
α (O ₂ /N ₂)	6.1	5.9	5.5	4.5	5.1
α (CO ₂ /N ₂)	23	21	22	15	12
α (CO ₂ /CH ₄)	58	50	69	29	33
α (N ₂ /CH ₄)	2.56	2.34	3.14	2.02	2.78

The decrease in permeability for various gases was from 24 to 87 %, while the selectivity enhancement was upto 575 %. A marked decrease of permeability of larger

gases (N_2 , CH_4) elevated the selectivity to a larger extent. For example, $\alpha(O_2/N_2)$ and $\alpha(He/CH_4)$ were elevated from 3.8 to 6.1 and from 37.7 to 217 respectively. The permeability of He and CO_2 in DBrHFBisA-I+T was 39.0 and 10.4; vis-à-vis 51 and 35 in case of HFBisA-I+T, respectively. This variation in permeation property was affected by not only the polar bromine atom, but also by the asymmetric type of substitution. Thus the effects of polar group substitution coupled with type of substitution in highly open polymer backbone (offered by hexafluoroisopropylidene linkage) led to observed improvements in permeation properties. It was thought to further enhance the substituent effect on permeation properties by suitably varying the acid moiety. Thus, BrT and NO_2T were chosen to further enhance polarity related effects, while HFA and BuI would further enhance bulky group related effects. The permeation properties of polyarylates based on these acids and DBrHFBisA as given in Table 4.15 signify the importance of attempted structural variations.

As could be anticipated, the polyarylates derived from BrT and NO_2T led to overall decrease in permeability and substantial improvements in selectivity. For example, the He and CO_2 permeability of 16.8 and 2.5 coupled with $\alpha(He/N_2)$, $\alpha(He/CH_4)$ and $\alpha(CO_2/CH_4)$ of 145, 50 and 339, respectively, in DBrHFBisA-BrT clearly indicated the effect of bromine substitution on acid moiety towards reduction in permeability and increase in selectivity. The small reduction in CO_2 based selectivities and $\alpha(O_2/N_2)$ were noted.

The effect of nitro group in DBrHFBisA- NO_2T was rather different than that of Br group in DBrHFBisA-BrT. The earlier exhibited higher permeability for all gases than for the later, although the effect on selectivity was not monotonous. This can be evident based on increased selectivity of some of the gas pairs (He/Ar and CO_2 based). This indicated that not just the polarity of nitro group, but its bulk and chain stiffness also played a role in determining permeation properties though both exhibited almost similar v_f . The chain stiffness was higher in DBrHFBisA- NO_2T rather than that for DBrHFBisA-BrT as indicated by its higher DMA transition temperature (especially T_α and T_γ) than that for later.

The effects of incorporating bulky groups in HFA and BuI based polyarylates in increasing permeability of various gases than that for DBrHFBisA-I+T though was

anticipated, the decrease in selectivity was to a smaller extent. The He permeability of 79.5 and 75.2 in DBrHFBisA-HFA and DBrHFBisA-BuI coupled with He based selectivities (e.g. He/CH₄ of 99 and 160) suggests the potential of these substitutions. The $\alpha(\text{O}_2/\text{N}_2)$ and CO₂ based selectivities were decreased, owing to larger increase in N₂ or CH₄ permeability than that for either O₂ or CO₂; when compared with DBrHFBisA-I+T. The Ar/N₂ selectivities varied marginally, while an increase in $\alpha(\text{N}_2/\text{CH}_4)$ in DBrHFBisA-BuI than that of DBrHFBisA-I+T was noted. When the permeation properties of DBrHFBisA-HFA and DBrHFBisA-BuI were compared, it was seen that butyl group containing polyarylate exhibited lower permeability and some variation in selectivity. The polyarylates investigated in this series lie on Robeson Curve. He permeability and $\alpha(\text{He}/\text{CH}_4)$ as presented in Figure 4.19 for HFBisA-I+T and DBrHFBisA-I+T indicated the potential of asymmetric -Br substitution on HFBisA. The nature of dicarboxylic acid used for obtaining polyarylate was also crucial, as DBrHFBisA-BuI and DBrHFBisA-HFA approached nearer to the curve in comparison to HFBisA-I+T. Additionally, excellent solubility of these polyarylates in common solvents could be advantageous in their applicability as membrane material with high P and α .

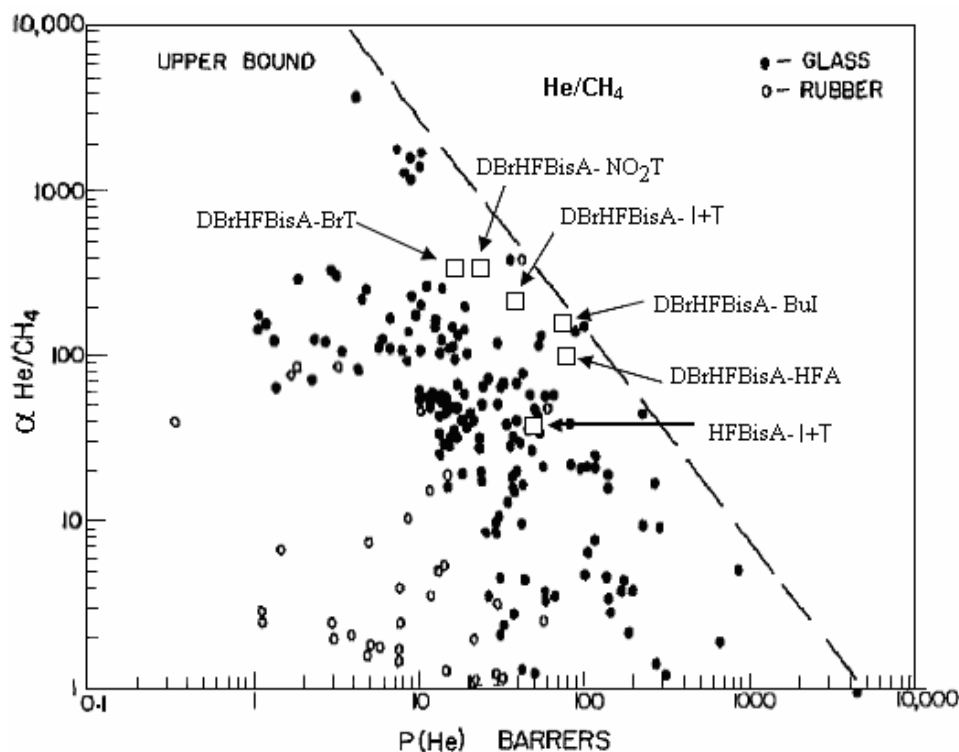


Figure 4.19 Occurrence of DBrHFBisA based polyarylates on Robeson limiting curve

(iii) Diffusivity and diffusivity selectivity

The calculated diffusivity for N_2 , O_2 , CO_2 , and CH_4 are given in Table 4.14. A large decrease in diffusion coefficients (55-78%) in case of DBrHFBisA-BrT and DBrHFBisA- NO_2 T, and increase in diffusivity in case of DBrHFBisA-HFA and DBrHFBisA-BuI can be ascribed to the packing density of polymer. The -Br substitution on acid moiety was more effective in decreasing the diffusivity than that of - NO_2 substitution. It should be noted here that both these polymers exhibited almost similar chain packing density as indicated by v_f (Table 4.12). In case of DBrHFBisA-HFA, the presence of bulky hexafluoroisopropylidene group increased the diffusivity from 18-154 % for different gases than that of DBrHFBisA-IT. It was found that for a particular gas, increase in diffusivity was more in case of DBrHFBisA-HFA than that of DBrHFBisA-BuI following the trend of v_f , when compared with the base case of DBrHFBisA-I+T. The change in diffusion coefficient for different gases followed the order: $O_2 > CO_2 > N_2 > CH_4$, also typically observed in other studies for polycarbonates [Hellums (1989)], polyimides [Coleman (1990)] and polysulfones [McHattie (1992)].

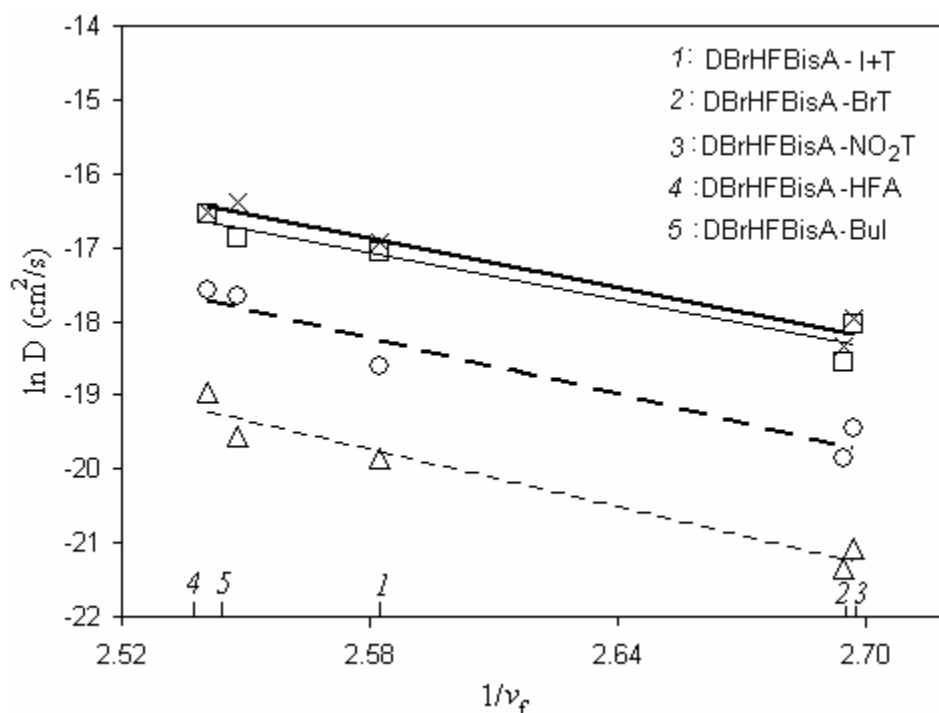


Figure 4.20 Correlation of diffusivity coefficient of different gases with $1/v_f$

Figure 4.20 demonstrated a good correlation between diffusivity and v_f of the polymers studied in the present series. Typically, diffusion coefficients of small

molecules in polymers are inversely proportional to the penetrant size. The gas diffusivity, D , is often assumed to be dependant on free volume as described by the Fujita's relationship (Equation 3.4). This relation holds good for variation in gas diffusivity within a given family of polymer [McHattie 33(1992)]. In the present case, a linear relation was observed between diffusivity and v_f (Figure 4.20).

A good correlation ($R^2 = 0.80$ to 0.93) was also observed between diffusivity the solubility parameter of polymer (Figure 4.21). As the solubility parameter increased the diffusivity decreased as the consequence of increased polymer-polymer chain interactions.

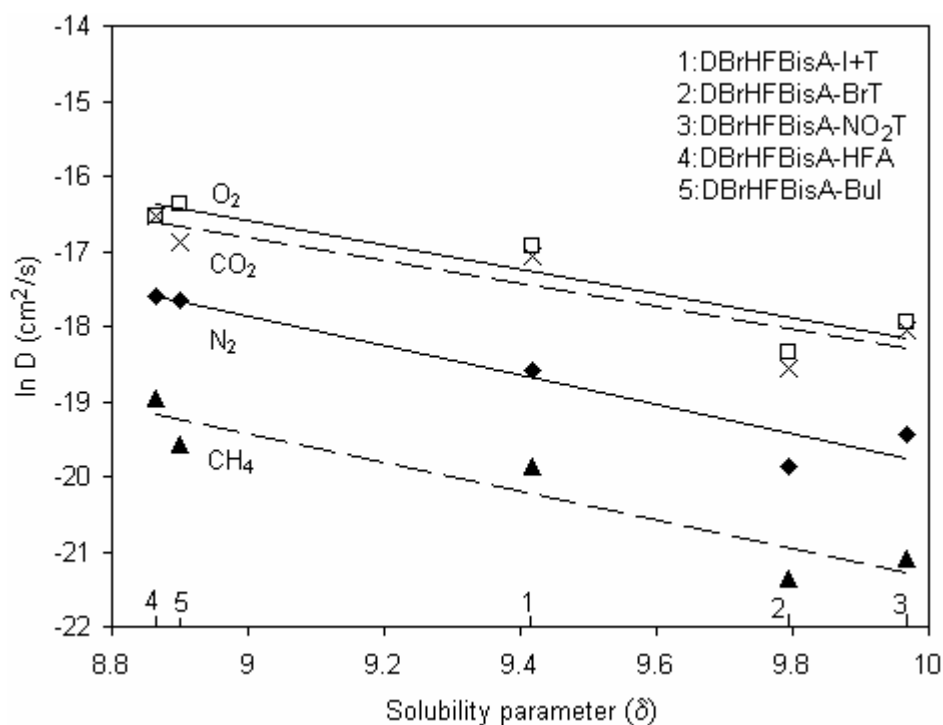


Figure 4.21 Correlation of diffusivity coefficient of different gases with solubility parameter

The diffusivity selectivity for O_2/N_2 and CO_2/N_2 was decreased by 10-22 % in DBrHFBisA-BrT and DBrHFBisA- NO_2 T when compared with the unsubstituted case (DBrHFBisA-I+T). The CO_2/CH_4 selectivity remained almost similar for DBrHFBisA-BrT, while it improved by 32 % in case of DBrHFBisA- NO_2 T when compared with DBrHFBisA-I+T. The diffusivity selectivity in case of bulky group containing DBrHFBisA-HFA and DBrHFBisA-Bul was found to be decreased than that of DBrHFBisA-I+T as a result of increased v_f . Similar failure to improve in O_2/N_2

diffusivity selectivity was reported by Pixton et al. [1995c] for brominated polymers with *t*-butyl substituent on dicarboxylic acid moiety. This behavior was attributed to the dilution of the bromination effect due to bulky *t*-butyl substitution.

4.4.3 Polyarylates based on dibromo-terephthalic acid

The substitution of bromine in acid moiety was found to be beneficial in improving the permeation properties in above cases. It was thus thought to analyze the effect of dibromo- substitution in acid moiety on resulting polyarylates. Four bisphenols, namely, BisA (without substitution on phenyl ring), DMBisA (dimethyl substitution in asymmetric manner), TMBisA (tetramethyl substitution in symmetric manner) and DBrDMBisA (combination of methyl and bromine substitution in asymmetric manner) were polymerized with dibromoterephthalic acid by interfacial condensation. These bisphenols were chosen in order to draw the typical benefits of these substitution types on gas permeation properties of resulting polyarylates. The abbreviations used and the physical properties of these polyarylates are given in Table 4.5. All these polyarylates were synthesized by interfacial polycondensation (Section 4.3.4.2) with appreciable yield and are listed in Table 4.5. The intrinsic viscosities of the resultant polyarylates were in the range of 0.42-0.90 dl/g in TCE at 35 °C. The films formed by solution casting from CHCl₃ at ambient temperature were tough and transparent.

4.4.3.1 Physical properties

The WAXD spectra for these polyarylates were as shown in Figure 4.22 and were amorphous in nature. These polyarylates though exhibited multiple amorphous peaks, as also seen previously in brominated polyarylates [Section 4.4.2.1.1]; their nature and the 2θ position (especially at lower 2θ) is distinctly different. Pixton et al. (1995a) reported that appearance of two distinct WAXD peaks for polymers with pendant phenyl rings or aromatic connector groups can be attributed to pendant or connector group “stacking” [Pixton (1995a)].

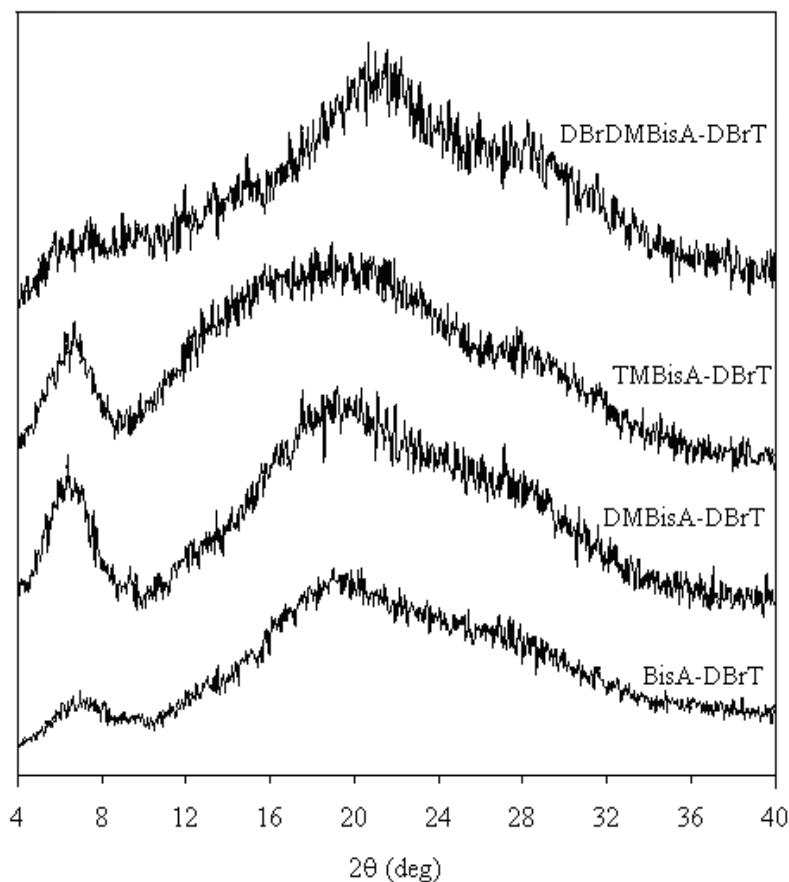


Figure 4.22 WAXD spectra of DBrT based polyarylates

The 2θ position of peak maxima for major amorphous peak was used to compare average chain d-spacing (d_{sp}), as listed in Table 4.16. The observed variation in d_{sp} with change in bisphenol structure was followed the order; TMBisA-DBrT > BisA-DBrT \geq DMBisA-DBrT > DBrDMBisA-DBrT. Another packing density parameter, v_f as given in Table 4.16 indicated that DMBisA-DBrT exhibited the lowest v_f (and thus highest packing density), while highly brominated polyarylate (DBrDMBisA-DBrT) exhibited the highest v_f . It was previously observed that brominated polyarylates exhibit higher v_f than their non-brominated analogs, though the permeation properties do not follow the same trend [Pixton (1995a), Kharul (1997)].

The T_g for DBrDMBisA-DBrT was highest in the series, followed by TMBisA-DBrT, containing symmetric methyl substitution on bisphenol moiety. The T_g DMBisA-DBrT was lower than that for BisA-DBrT, following the trend observed in earlier cases for asymmetric bisphenol substitution type, wherein lowering of T_g was consistently

observed. The variation in T_g within this series followed the same trend as that of polyarylates based on these bisphenols and terephthalic acid [Kharul (1997)]. If the T_g of individual polymer from this series is compared with the polyarylate based on unsubstituted terephthalic acid and the same bisphenol, the T_g in present case was found to be decreased. Intuitively, based on polar group interactions, the T_g could have been expected to be increased. This contradictory observation could be correlated with the chain packing, wherein, a peak in WAXD spectra at lower 2θ leading to very high d-spacing ($> 12 \text{ \AA}$) was observed. Such high d-spacing rendering localized loose packing may result from interchain repulsions rather than the interchain attractions because of presence of bromine group. This could lead to lowering in T_g .

Table 4.16 Physical properties of DBrT based polyarylates

Polymer	d_{sp} (\AA)	ρ (g/cm^3)	v_f (cm^3/cm^3)	δ (cal/cm^3) ^{1/2}	T_g ($^{\circ}\text{C}$)	TGA ($^{\circ}\text{C}$)
BisA-DBrT	4.67, 12.81	1.515	0.3680	10.08	175	406
DMBisA-DBrT	4.66, 13.7	1.484	0.3470	10.04	135	387
TMBisA-DBrT	4.92, 14.02	1.355	0.3843	9.30	201	387
DBrDMBisA-DBrT	4.23	1.565	0.4160	9.32	219	334

4.4.3.2 Permeation properties

Pure gas permeability and selectivities of gas pairs of interest are given in Table 4.17. The effects of dibromo- substitution in an acid moiety on gas permeation properties of resulting polyarylates were initially examined by comparing the gas permeability of polyarylates based on bisphenol and unsubstituted terephthalic acid. The variation in gas-permeation properties can also be assessed in terms of the effect of bisphenol ring substitution type in these polyarylates.

The permeability coefficients for all of the gases of polyarylates studied in present series rank in the order; TMBisA-DBrT $>$ DBrDMBisA-DBrT $>$ BisA-DBrT $>$ DMBisA-DBrT. This is also the order of permeability observed in polyarylates obtained from these bisphenols and unsubstituted terephthalic acid [Kharul (1997), Kharul (1998)].

Table 4.17 Permeability (P) coefficients and selectivity (α) for DBrT based polyarylates

	BisA -DBrT	DMBisA - DBrT	TMBisA - DBrT	DBrDMBisA - DBrT
P(He)	8.4	5.6	18.0	12.2
P(N ₂)	0.12	0.02	0.24	0.10
P(O ₂)	0.6	0.1	1.0	0.6
P(CO ₂)	2.7	0.6	4.6	2.0
P(CH ₄)	0.07	-	0.23	0.06
α (He/N ₂)	70	280	75	122
α (He/CH ₄)	120	-	78	203
α (O ₂ /N ₂)	5.00	5.00	4.17	6.00
α (CO ₂ /N ₂)	22.50	30.00	19.17	20.00
α (CO ₂ /CH ₄)	38.57	-	20.00	33.33
α (N ₂ /CH ₄)	1.71	-	1.04	1.67

A comparison within the series indicated that DMBisA-DBrT exhibited lowest permeability. The permeability of CH₄ was so low that it could not be accurately measured by the variable volume method employed here. He permeability was found to be least affected (33 %), that resulted into 4 times enhancement in He/N₂ selectivity than BisA-DBrT. Similarly, though the permeability of CO₂ was reduced by 78 %, the CO₂/N₂ selectivity by improved by 33 %. In case of TMBisA-DBrT, 67-229 % increase in permeability in comparison to BisA-DBrT was noted. This resulted into a generally decreased selectivity by 15-48 %, with an exception of a small (7 %) increase in He/N₂ selectivity. Muruganandam et al. [1987] found three times higher permeabilities and similar selectivities in TMBisA-PC, as compared to BisA-PC.

The permeability in DBrDMBisA-DBrT was marginally decreased in comparison to BisA-DBrT, with an exception of 45 % increase in He permeability. These variations in permeability were associated with some of the good selectivity, especially He based.

Thus He permeability of 12.2 in this polymer coupled with He/N₂ or He/CH₄ selectivity of 122 or 203, respectively, is an attractive combination of permeation properties.

A good correlation between the gas permeability and kinetic diameter ($R^2 = 0.92-0.96$) of the gas molecules for present polyarylates series was observed. The permeability increased linearly as the kinetic diameter of the gases decreased. The correlation of permeability with other physical properties was not satisfactory.

4.5 Conclusions

- *Polyarylates based on asymmetrically substituted bisphenol*

The packing density parameters indicated that bulk of the isopropyl group in DiPrBisA based polyarylate was effective in rendering loose chain packing in comparison to BisA or DMBisA based polyarylates. When DiPrBisA was polymerized with dicarboxylic acids containing polar groups (NO₂), an increase in density and reduction in v_f was observed in resulting polyarylates. Conversely, v_f was increased in case of polyarylates based on HFA and BuI, indicating usefulness of these acids in reducing chain packing density. The T_g , as indicated by DSC as well as DMA was reduced, as observed in asymmetric substitution cases. Plasticizing effect of isopropyl group might have also added its contribution in reducing T_g of DiPrBisA based polyarylates. Comparison of permeation properties DiPrBisA-T with that of DMBisA-T revealed that bulk of isopropyl group led to increased permeability and decrease in selectivity, except for $\alpha(N_2/CH_4)$. The importance of isopropyl group substitution could be observed in polyarylates based on DiPrBisA and polar group substituted dicarboxylic acids. This could be evident from He permeability of 18 Barrer coupled $\alpha(He/CH_4)$ of 180 in case of DiPrBisA-NO₂T.

The polymers based on DiPhBisA exhibited two broad amorphous peaks, indicating two types of chain packing due to the stacking of phenyl rings present on the bisphenol moiety. The packing density was reduced by diphenyl substitution in DiPhBisA-I+T (increased v_f) than in case of unsubstituted BisA-I+T or dimethyl substituted DMBisA-I+T. The polar -Br or -NO₂ group substitution on dicarboxylic acid moiety increased chain packing density while it was decreased in bulky group substituted DiPhBisA-HFA and DiPhBisA-BuI. The lower T_g in case of DiPhBisA-I+T than

unsubstituted BisA-I+T was attributed to the nature of substitution, which is asymmetric, rather than the nature of substituent. The permeability in case of DiPhBisA-I+T was lower than for unsubstituted BisA-I+T, while the variation was marginal in comparison to that for DMBisA-I+T. This decreased permeability in DiPhBisA-I+T was associated with the increased selectivities for various gas pairs, except for CO₂/N₂.

A Br substitution on acid moiety (DiPhBisA-BrT) showed decreased gas permeability than that of DiPhBisA-I+T for all the gases, with simultaneous improvement in selectivities of various gas pairs. The higher CO₂ permeability in case of DiPhBisA-NO₂I than that of DiPhBisA-NO₂T, was due to higher v_f for earlier case.

- *Polyarylates based on substituted fluorene bisphenol and DBrHFBisA*

The bridge substitution by 9,9-fluorenylidene in fluorene bisphenol based polyarylates increased chain stiffness as indicated by an increase in T_g for these polymers in comparison to polyarylate with respective substitution on bisphenol-A. The effect of bridge substitution on gas permeability and selectivity was more marked when the bisphenol ring positions were substituted. The asymmetric ring substitution by bromine, though increased permeability, showed a lowering of selectivity.

The polar (-Br) group substitution in DBrHFBisA in asymmetric manner resulted showed that the packing density was increased; while the T_g was 38 °C lower than for the polyarylate based on unsubstituted HFBisA. The substitution of various polar as well as bulky groups on diacid moiety increased sorption for almost all the gases in resulting polyarylates. The trend observed for CO₂ sorption suggested that the effect of v_f was more effective than the polarity in improving sorption. The gas permeability was reduced by 24 to 87 % for various gases, while the selectivity was enhanced up to 575 %, attributed to the polar nature of bromine as well as its substitution type. The variation in acid moiety generally led to an increase in T_g, except for the polyarylate derived from BrT; in comparison to unsubstituted dicarboxylic acid based polyarylate: DBrHFBisA-I+T. The packing density by polar group substitution on acid was increased in comparison to DBrHFBisA-I+T. This led to overall decrease in permeability and substantial improvements in selectivity. The v_f was increased in case of polyarylates

based on HFA and BuI, which led to increased permeability of various gases than that for DBrHFBisA-I+T and decreased selectivity to a smaller extent.

- *Polyarylates based on dibromoterephthalic acid*

These polyarylates were amorphous in nature. The DMBisA-DBrT exhibited the lowest v_f (and thus highest packing density), while highly brominated polyarylate (DBrDMBisA-DBrT) exhibited the highest v_f in the series. The T_g was found to be decreased in comparison to the polyarylates based on unsubstituted terephthalic acid and the same bisphenol. The permeability coefficients for all of the gases of polyarylates rank in the order; TMBisA-DBrT > DBrDMBisA-DBrT > BisA-DBrT > DMBisA-DBrT. In case of DBrDMBisA-DBrT, the He permeability of 12.2 coupled with He/N₂ or He/CH₄ selectivity of 122 or 203, respectively, is attractive.

References

- Aitken C.L., Koros W.J., Paul D.R. *Macromolecules* **25** (1992) 2910-2922.
- Barbari T.A., Koros W.J., Paul D.R. *J. Polym. Sci. Part B: Polym. Phys.* **26** (1988) 709-727.
- Barbari T.A., Koros W.J., Paul D.R. *J. Membr. Sci.* **42** (1989) 69-86.
- Charati S.C., Houde A.Y., Kulkarni S.S., Kulkarni M.G. *J. Polym. Sci. Part B: Polym. Phys.* **29** (1991) 921-931.
- Charati S.G., Jog J.P., Kulkarni S.S., Kulkarni M.G. *J. Appl. Polym. Sci.* **54** (1994) 1093-1101.
- Chen N., Tien C-F., Patton S.M., Langsam M. Burgoyne W.F. *Polym. Mater. Sci. Eng.* **69** (1993a) 161-163.
- Chen N., Tien C.F., Patton S.M. US Patent, (1993b) US 5232471.
- Chern R.T., Provan C.N. *J. Membr. Sci.* **59** (1991) 293-304.
- Chiou J.S., Paul D.R. *J. Membr. Sci.* **45** (1989) 167-189.
- Choi E-J., Hill D.J.T., Kim K.Y., O'Donnell J.H., Pomery P.J. *Polymer* **38** (1997) 3669-3676.
- Coleman M.R., Koros W.J. *J. Membr. Sci.* **50** (1990) 285-297.
- Ghosal K., Chern R.T. *J. Membr. Sci.* **72** (1992) 91-97.
- Ghosal K., Chern R.T., Freeman B.D., Savariari R. *J. Polym. Sci., Part B: Polym Phys.* **33** (1995) 657-666.
- Ghosal K., Chern R.T., Freeman B.D. *Macromolecules* **29** (1996) 4360-4369.
- Goldberg D.E. Genetic algorithms in search, optimization and machine learning, Addison-Wesley, Reading, MA 1989.
- Hellums M.W., Koros W.J., Husk G.R., Paul D.R. *J. Membr. Sci.* **46** (1989) 93-112.
- Hergenrother P.M., Jensen B.J., Havens S.J. *Polymer* **29** (1988) 358-369.

- Houde A.Y., Kulkarni, S.S.; Kharul, U.K.; Charati, S.G.; Kulkarni, M.G. *J. Membr. Sci.* **103** (1995)167-174.
- Jadhav A.S., Jayarani P., Kulkarni S.S., Vernekar S.P. US Patent (1997) US 5606000.
- Jin J-I., Choi E-J., Jo B-W. *Macromolecules* **20** (1987) 934-939.
- Jin J-I., Kang C-S. *Prog. Polym. Sri.* **22** (1997) 931-913.
- Kawakami J.H, Muruganandam N., Brode G.L. US Patent (1991a) US 5055114.
- Kawakami J.H, Muruganandam N., Brode G.L. US Patent (1991b) US 4994095.
- Kharul U.K., Kulkarni S.S. *Bull. Mater. Sci.* **17** (1994)1071-1077.
- Kharul U.K., Kulkarni S.S. *Macromol. Chem. Phys.* **198** (1997)1909-1919.
- Kharul U.K., Kulkarni S.S., Kulkarni M.G., Houde A.Y., Charati S.G., Joshi S,G.,
Polymer **39** (1998) 2011–2022.
- Kharul U.K, Kulkarni S.S. US Patent (2002) US 6420511.
- Legrand D.G., Erhardt P.F. *J. Appl. Polym. Sci.* **13** (1969) 1707-1719.
- Maruyama Y., Kakimoto M-A., Imai Y. *J. Polym. Sci., Part A: Polym. Chem. Ed.* **24**
(1986) 3555-3558.
- McHattie J.S., Koros W.J., Paul D.R. *Polymer* **32** (1991) 840-850.
- McHattie J.S., Koros W.J., Paul D.R. *Polymer* **33** (1992) 1701-1711.
- Morgan P.W. *Condensation polymers: by interfacial and solution methods*, Interscience
Publishers, New York, p 153 (1965).
- Muruganandam N., Koros W.J., and Paul D.R. *J. Polym. Sci. Part B: Polym. Phys.* **25**
(1987) 1999-2026.
- Pessan L.A., Koros W.J. *J. Polym. Sci. Part B: Polym. Phys.* **31** (1993) 1245-1252.
- Pessan L.A., Koros W.J., Schmidhauser J.C., Richards W.D. *J. Polym. Sci., Part B:*
Polym Phys. **33** (1995) 487-494.
- Pixton M.R., Paul D.R. *Macromolecules* **28** (1995a) 8277–8286.
- Pixton M.R., Paul D.R. *J. Polym. Sci. Part B: Polym. Phys.* **33** (1995b) 1135-1149

- Pixton MR and Paul DR, *J. Polym. Sci. Part B: Polym. Phys.* **33** (1995c) 1353–1364.
- Pixton M.R., Paul D.R. *Polymer* **36** (1995d) 2745-2751.
- Pixton M.R. Gas Transport Properties of Aromatic Polyester and Polysulfone Materials, Ph.D. Dissertation, The University of Texas at Austin, (1995e).
- Product broacher, Honshu Chemicals, Japan.
- Qiu J., Zheng J-M., and Peinemann K-V. *Macromolecules* **39** (2006) 4093-4100.
- Rutherford S.W., Kurtz R.E., Smith M.G., Honnell K.G., Coons J.E. *J. Membr. Sci.* **263** (2005) 57–65.
- Schmidhauser J.C., Longley K.L. *J. Appl. Polym. Sci.* **39** (1990) 2083–2096.
- Sheu F.R., Chern R.T. *J. Polym. Sci., Part B: Polym Phys.* **27** (1989) 1121-1133.
- Tien C-F., Surnamer A.D. US Patent (1991) 5007945
- Van Krevelen D.W., Hoftyzer P.J. *Properties of polymers: Correlation with chemical structure*, Elsevier, Amsterdam, p 378 (1972).
- Vega A.M., Paul D.R. *J. Polym. Sci., Part B: Polym. Phys.* **31** (1993a) 1599-1610.
- Vega A.M., Paul D.R. *J. Polym. Sci., Part B: Polym. Phys.* **31** (1993b) 1577-1589.
- Vieth W.R., Tam P.M., Michaels A.S. *J. Colloid and Interface Sci.* **22** (1966) 360-370.
- Vega-A.M., Paul D. R. *J. Polym. Sci., Part A: Polym. Phy.* **31** (1993)1577-1589.
- Yee A.F., Smith S.A. *Macromolecules* **14** (1981) 54-64.

Chapter 5

Composite membrane materials: Tuning gas permeation properties by using organically modified clay and poly(ionic liquid)

5.1 Polyarylate-clay nanocomposites: preparation, evaluation of physical properties and gas permeability

5.1.1 Introduction and literature survey

Use of nano-sized particles to form polymer composites has attracted much attention in recent years because of their advantages that could create new technological opportunities. Several reviews on polymer nanocomposites formed from layered silicates have been appeared in the literature [Sinha, (2003), Giannelis (1998), Giannelis (1996)]. The key issue is to obtain an effective dispersion and exfoliation of the platelets into the polymer matrix to yield well-aligned, high-aspect ratio particles for mechanical reinforcement or for a tortuous diffusion pathway to have improved barrier properties. The literature contains numerous reports on variations in different properties caused by addition of layered silicates to various polymer matrices e.g. increased modulus and dimensional stability, increased strength and heat resistance, decreased penetrant permeability, etc [Takahashi (2006)]. Generally, a property benefits of adding plate-like fillers to polymers would enhance both, the volume fraction (ϕ) and the aspect ratio (α) of platelets increase [Takahashi (2006)].

The permeation properties of nanocomposites are known to be greatly different than the pristine polymer. The addition of clay showed reduction in water vapor permeability in poly(vinyl alcohol) [Strawhecker (2000)], poly(urethane urea) [Xu (2001)], polyimide [Yano (1993)], poly(ϵ -caprolactone) [Messersmith (1995)] etc. The oxygen permeability is known to be reduced in case of polyimide [Yano (1993), Khayankarn (2003)] and poly(lactic acid) [Chang (2003)]. The reduction in CO₂ permeability in polyimide [Lan (1994)] is also documented. Jeong et al. [2004] has reported incorporation of layered aluminophosphate (AlPO) with a porous net layer as a

selective phase and a polyimide as a continuous phase. As the percentage of the AIPO flakes increased, a marked decrease in permeability was observed. This was attributed to a large aspect ratio of the AIPO flakes that increased the tortuosity of the transport path of the gas molecules. The permeability reduction was more pronounced as the size of the penetrating gas molecule increased. Nanocomposite membranes with 10 wt. % layered aluminophosphate showed substantial enhancement in selectivity (α (O₂/N₂) = 8.9, vis-à-vis 3.6 for pristine polymer and α (CO₂/CH₄) = 40.9, vis-à-vis 13.4 for pristine polymer).

Recently, Takahashi et al. [2006] has reported reduction in gas permeability of nanocomposites based on butyl rubber and vermiculite. Diffusion coefficients (computed from time lag data) were reduced by two orders of magnitude. The gas sorption isotherm for CO₂ on butyl rubber compositions with 0 and 30 wt % vermiculite showed larger solubility in the nanocomposite than in the neat butyl rubber. The excess sorption appeared to be the result of gas adsorption by the vermiculite.

On the other hand, addition of fumed silica in poly(1-trimethylsilyl-1-propyne) [Merkel (2003a)] and poly(4-methyl-2-pentyne) [Merkel (2003b)] is known to improve gas permeation properties owing to increased free volume in the resulting nanocomposites. For example, the permeability of PTMSP containing 40 wt. % fume silica to methane was 1.8 times higher than that of the unfilled polymer, whereas the permeability of PMP containing 40 wt. % fumed silica to methane is 2.3 times higher than that of respective unfilled polymer.

Traditionally, the incorporation of nonporous fillers, such as clay, metal oxides, silicas, or carbon blacks, into polymers reduces gas or vapor permeability. This decreased permeability is the result of increase in the diffusion path length that penetrant molecules experience [Barrer (1968), Amerongen (1964)] and a reduction in the amount of polymer through which transport occur.

5.1.2 Objectives

Though the permeability of nanocomposites is known to be reduced in several cases and has been successfully used for improving barrier properties of polymeric materials, the effect on selectivity among different penetrates is almost unaddressed. A trade-off relationship while modifying permeation properties of polymers, i.e. an effort to

increase gas permeability generally leads to reduced selectivity and vice-versa [Ghosal (1994)]; is generally observed. The objective of this work was to analyze feasibility of employing such trade-off relationship in improving selectivity profile of high permeating material by formation of its nanocomposites. A glassy polyarylate: poly(tetramethyl-bisphenolA-iso/terephthalate) exhibited appreciable gas permeability [Kharul (1998)] and good solvent solubility. By solvent intercalation, the nanocomposites with two different types of clay (MMT 6A and 10A, that differ in organic modifier) with varying clay loading were prepared to analyze physical and gas permeation properties of resulting nanocomposites.

5.1.3 Experimental

5.1.3.1 Materials

Pristine Na⁺ clay and organically modified montmorillonite (MMT), Cloisite 6A and 10A (specifications as given in Table 5.1.1) were supplied by Southern Clay Products, USA. The monomer and polymerization details to obtain polyarylate (structures as given in Figure 5.1.1) were as given in section 4.3. The obtained polymer was purified by reprecipitation of its CHCl₃ solution into methanol.

Table 5.1.1 Structural specifications of MMT 6A and 10A

Clay used	Ammonium cation	Density (g.cm ⁻³)	Modifier concentration (meq/100 g)	Basal spacing of as received clay (001) (nm)	Basal spacing of toluene treated clay (001) (nm)
Cloisite 6A	(CH ₃) ₂ (HT ^a) ₂ N ⁺	1.71	140	3.4	2.75
Cloisite 10A	(CH ₃) ₂ (HT ^a) (CH ₂ C ₆ H ₅)N ⁺	1.9	125	2.0	1.94

^a T = tallow (65% C18, 30% C16, 5% C14), HT = hydrogenated tallow.

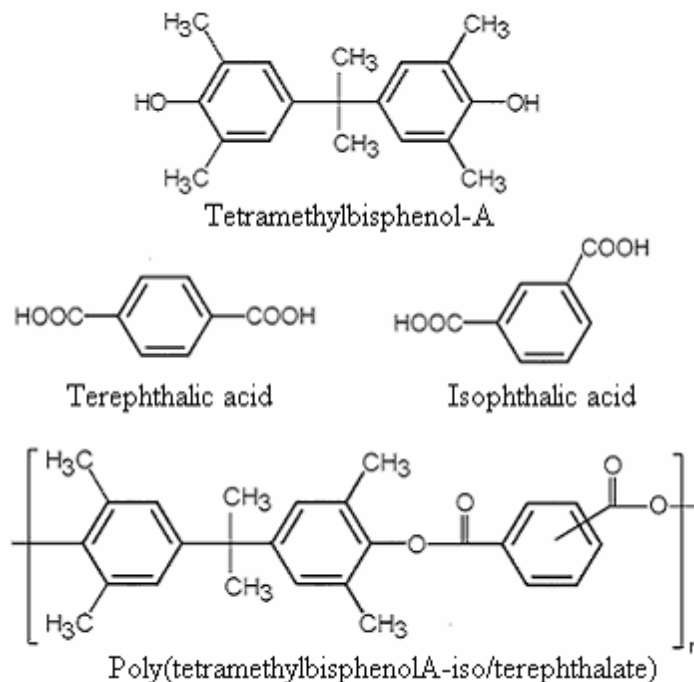


Figure 5.1.1 The structure of monomers and polymer used to prepare polyarylate-clay nanocomposites

5.1.3.2 Nanocomposite preparation

The solution intercalation approach was employed to prepare polyarylate-organoclay nanocomposites to obtain better dispersion. Toluene was selected as a solvent in which polyarylate (PA) showed good solubility and organically modified montmorillonite (10A and 6A) exhibited good dispersability. For comparison along with these two clays, unmodified clay (Cloisite Na⁺) was also used. Initially, 3 g of PA and varying amount of vacuum dried as received clay (3, 5 or 7 wt % of the polymer) was added to 45 ml of toluene and stirred for 12 hours. The obtained clear solution was poured on to a flat glass surface, allowing solvent evaporation at an ambient temperature and dry conditions. The formed film was peeled off and kept under vacuum at 60 °C for a week in order to ensure the complete removal of residual solvent. These films were transparent in nature. The nanocomposites based on 6A clay are abbreviated as PA-6A and that based on 10A clay are abbreviated as PA-10A, with suffix denoting the weight percent of clay loading as given in Table 5.1.2.

5.1.3.3 Characterizations

The X-ray diffraction studies of nanocomposites in the film form and that of clays in powder form (as received and toluene treated) were performed using Rigaku X-ray diffractometer (Dmax 2500) with Cu-K α radiation and were as given in Figure 5.1.2 and 5.1.3 (a-b) for clays and nanocomposites, respectively. The basal spacing of clays was estimated from the (001) peak in the XRD pattern. The average d -spacing value (d_{sp}) for the polymer peak (amorphous hollow) was calculated from the peak maxima using Bragg's equation. The dispersability of the intercalated clay particles in the nanocomposites matrix was also evaluated by means of transmission electron microscope (TEM, Jeol-1200 EX instrument), operated at an accelerating voltage of 80 kV (Figure 5.1.4). The TEM specimens were cut from 50 μ -nanocomposite films using ultramicrotome equipped with a diamond knife. The TGA of clay (as supplied and after dispersing in toluene for 12 hours, followed by oven dry at 60 °C for 3 days) was collected on Perkin Elmer TGA-7 at 20 °C.min⁻¹ under N₂ atmosphere from ambient to 700 °C. The dynamic mechanical analysis (DMA) was performed using Rheometrics DMTA III E, in the temperature range of ambient to 300 °C, at the frequency of 10 rads.sec⁻¹ and at 0.1 % strain using a film specimen. The intrinsic viscosity of polymer solutions containing clay was determined by graphical method at 35 °C using toluene as a solvent. The densities of nanocomposites in the film form were determined by flotation method using aqueous K₂CO₃ solutions at 40 °C. These density values were used to calculate the fractional free volume [Van Krevelen (1972)] of respective nanocomposites and were as given in Table 5.1.2.

5.1.3.4 Permeability determination

The pure gas permeability measurements for He, N₂, CH₄ and CO₂ were performed at 35 °C and at 10 atm upstream pressure (using variable volume method, as described in section 3.3.8.1) while maintaining the permeate side at ambient pressure. Measurements were repeated for three membrane samples prepared under identical conditions and results averaged. The permeability, expressed in Barrer, and selectivity (α , ratio of the respective gas permeability) were as given in Table 5.1.3.

5.1.4 Results and discussion

The physical properties of polyarylate-clay nanocomposites (based on 6A and 10A clay with different loading) were determined (Table 5.1.2) to assess and compare the nanocomposite formation as described in the following section. The gas permeation properties of these nanocomposites were compared with that of pristine polymer: poly(tetramethylbisphenolA-iso/terephthalate), PA.

Table 5.1.2 Physical properties of nanocomposites with varying percent loading of 6A and 10A clay

Nanocomposite abbreviation	Clay used, it's loading (wt. %)	d_{sp} (Å)	$[\eta]$ (dl.g ⁻¹)	Density of nanocomposites ρ (g.cm ⁻³)	v_f^a (cm ³ .cm ⁻³)	T_g (°C)
PA ₀	-	6.01	0.37	1.103	0.369	271
PA-6A ₃	6A, 3	5.76	0.44	1.111	0.365	263
PA-6A ₅	6A, 5	5.89	0.46	1.124	0.357	258
PA-6A ₇	6A, 7	5.75	0.53	1.135	0.351	256
PA-10A ₃	10A, 3	5.75	0.52	1.127	0.356	262
PA-10A ₅	10A, 5	5.47	0.57	1.133	0.352	258
PA-10A ₇	10A, 7	5.75	0.61	1.144	0.346	255

^a Fractional free volume ($v_f = 1 - V_w / V$) calculated using Van Krevelen's method [Van Krevelen (1972)]; ^b T_g was determine by DMA.

5.1.4.1 Method of Nanocomposite formation

The method of solution intercalation using toluene as a solvent was adopted in the present investigation. It is known to be one of the methods for preparing polymer-clay nanocomposites [Acharys (2006), Hsiao (2001), Manninen (2005)]. The TGA of toluene treated and as-received clay showed that 6A clay contained 3.63 wt. % excess surfactant, while 10A contained 0.51 % of the same at 400 °C. Thus, for the preparation of nanocomposites, as received clay was used. The selection of solvent, was based on solubility of the polymer and well dispersability of the clay in toluene. No agglomeration was observed when both the types of clay were suspended in toluene. It is said that high solubility of polymer and good dispersion of silicate are the primary criteria used in the solvent selection of good solution intercalation [Shen (2002)]. Toluene was reported to be

a solvent for solution intercalation of silicate-clays (MMT) [Shen (2002), Acharya (2006), Manninen (2005)].

5.1.4.2 X-Ray diffraction and TEM studies

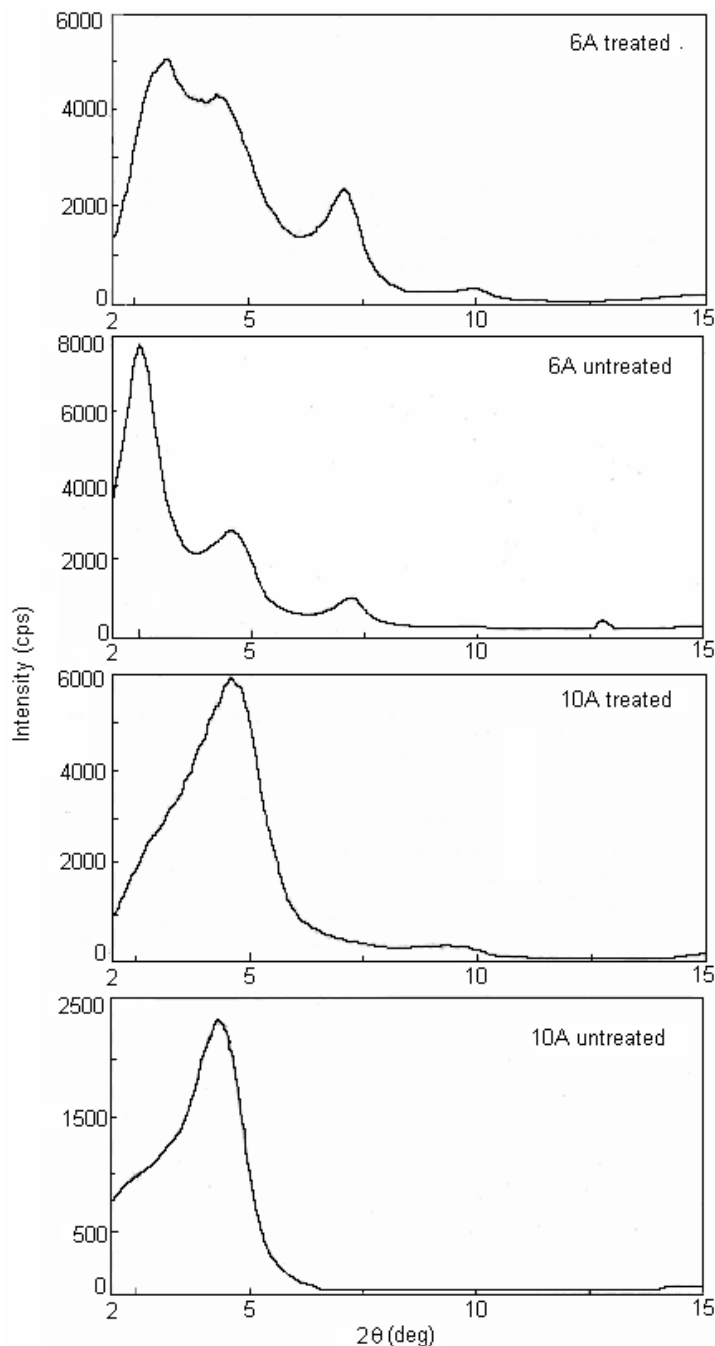


Figure 5.1.2 Wide angle X-ray diffraction spectra for treated and untreated clays

Organoclays (6A and 10A) used were layered silicates where the organic modifier was introduced by ion exchange. Due to natural defects/charge heterogeneity on the clay

plates, not all of the clay plates could be fully ion exchanged. Therefore, some of the organic surfactant could remain associated with the clay after ion exchange, but it would not be ionically bonded to the surface and remain only physically sorbed on to the surface. This excess surfactant (organic modifier) can be removed by solvent washes [Morgan (2003)]. The effect of excess surfactant on d-spacing of clay was investigated. Figure 5.1.2 presents the XRD scan of the as received and toluene treated clays. After toluene treatment, a decrease in d-spacing was observed in case of 6A. The d-spacing reduced from 3.44 nm to 2.75 nm. This indicated that the toluene treatment removed the excess organic modifier associated with the modified clay. For 10A clay, a marginal decrease of 0.1 nm in d-spacing was observed. The change in d-spacing could be due to the removal of excess surfactant on the clay surface. The thermogravimetric analysis of toluene treated and as-received clay showed that in case of 6A clay, 3.66 wt. % loss of surfactant and only 0.47 % loss of surfactant in case of 10A clay occurred.

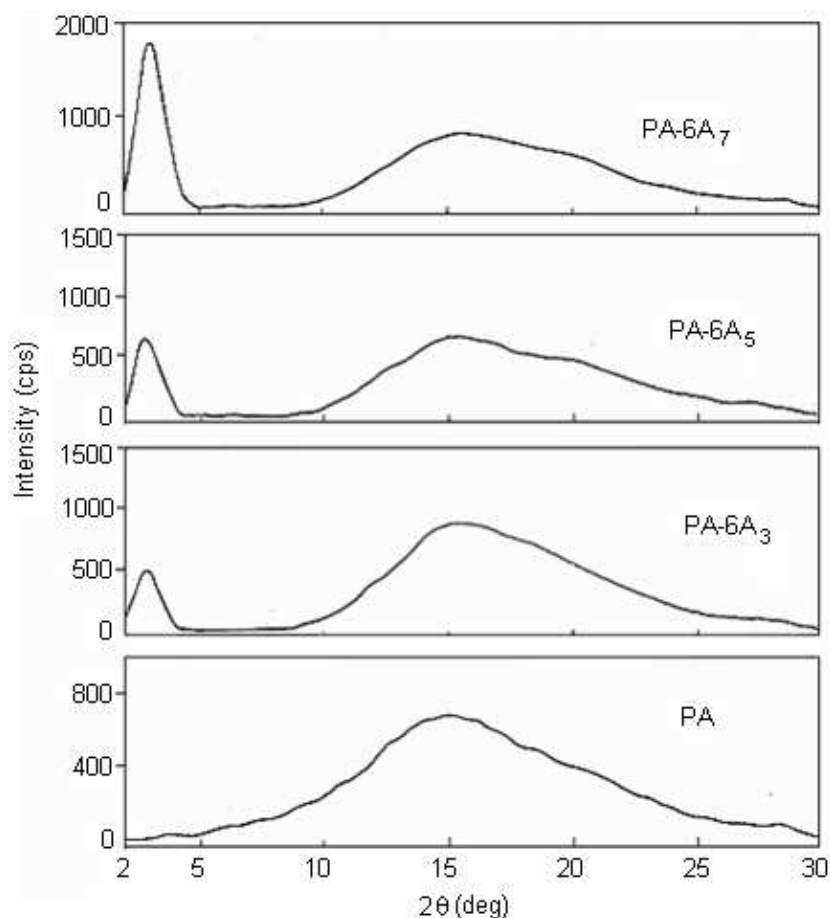


Figure 5.1.3a Wide angle X-ray diffraction spectra for polyarylate (PA) and nanocomposites based on 6A clay

Figure 5.1.3a shows X-ray diffraction spectra for 6A clay based nanocomposites. As can be seen from Figure 5.1.2, toluene treated 6A clay exhibited three well defined peaks with d_{001} peak having d-spacing of about 2.75 nm. However, in the case of nanocomposites, only one diffraction peak was observed at a higher d-spacing. The increase in d-spacing was about 0.33, 0.37 and 0.13 nm for 3, 5 and 7 % 6A-clay loading respectively. This indicated the intercalation of polymer resulted in a new set of diffraction planes. The increase in d-spacing is known to offer disordered intercalated structure of nanocomposites [Priya (2002), Viva (1997)].

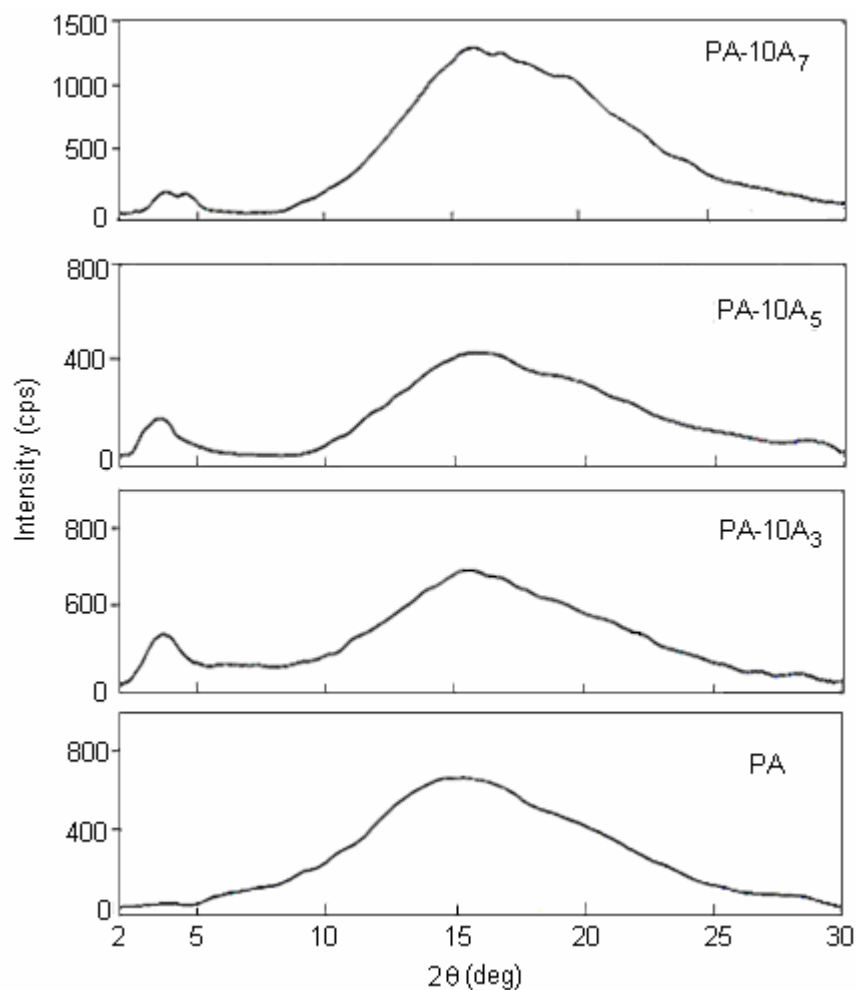


Figure 5.1.3b Wide angle X-ray diffraction spectra for polyarylate (PA) and nanocomposites based on 10A clay

Figure 5.1.3b shows X-ray diffraction patterns for 10A clay nanocomposites. The diffractogram for the nanocomposites showed shift in 2θ -value to the lower angle

indicating an increase in d-spacing of the clay. This increase was about 0.37 0.46 and 0.37 nm for the nanocomposites with 3, 5 and 7 % 10A-clay loading, respectively. This confirmed the disordered intercalation of the polymeric chains inside the clay galleries.

The nanocomposites formation was also confirmed by the transmission electron micrographs (TEM) analysis for both the types of clay loading in PA (Figure 5.1.4).

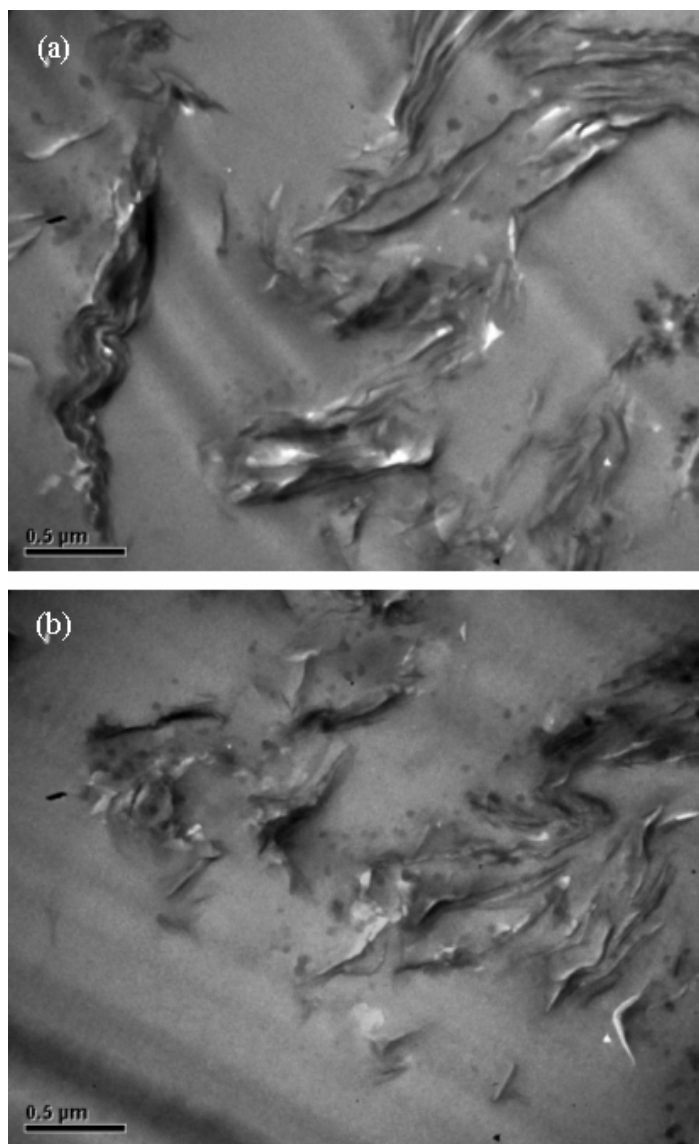


Figure 5.1.4 TEM images of nanocomposites; a: PA-6A₅ and b: PA-10A₅

5.1.4.3 *Dynamic mechanical analysis*

The dynamic mechanical analysis was carried out to study the effect of organically modified layered silicates on the glass transition temperature (as described by tan δ peak

temperature) of the polymer. The temperature dependence of $\tan \delta$ of the pristine polymer and the nanocomposites studied in this work is presented in Figure 5.1.5. The value of T_g (maximum of the $\tan \delta$ peak) was 271 °C for the pristine polymer, while it was reduced in case of nanocomposites with both the types of clays as the % clay loading increased (Table 5.1.2). The decrease in T_g followed the order of increasing clay loading for both the types of nanocomposites. This lowering of T_g could be attributed to the plasticization effect because of the organic modifier molecules of the layered silicates [Wang (2001)]. Similar reduction in T_g of the polyimide/clay nanocomposites were reported by Hsiao et al. [2001] attributed to the fact that the dodecyl groups in the organophilic clays provided a significant plasticizing effect, thus resulting in a reduction in the T_g . Wang et al. [2000] has reported that the ammonium compound in the interlayer of the clay can decrease the T_g of polymer-clay nanocomposites. The decrease in T_g was ascribed to plasticization from the organic ammonium compound in the gallery space of the clay.

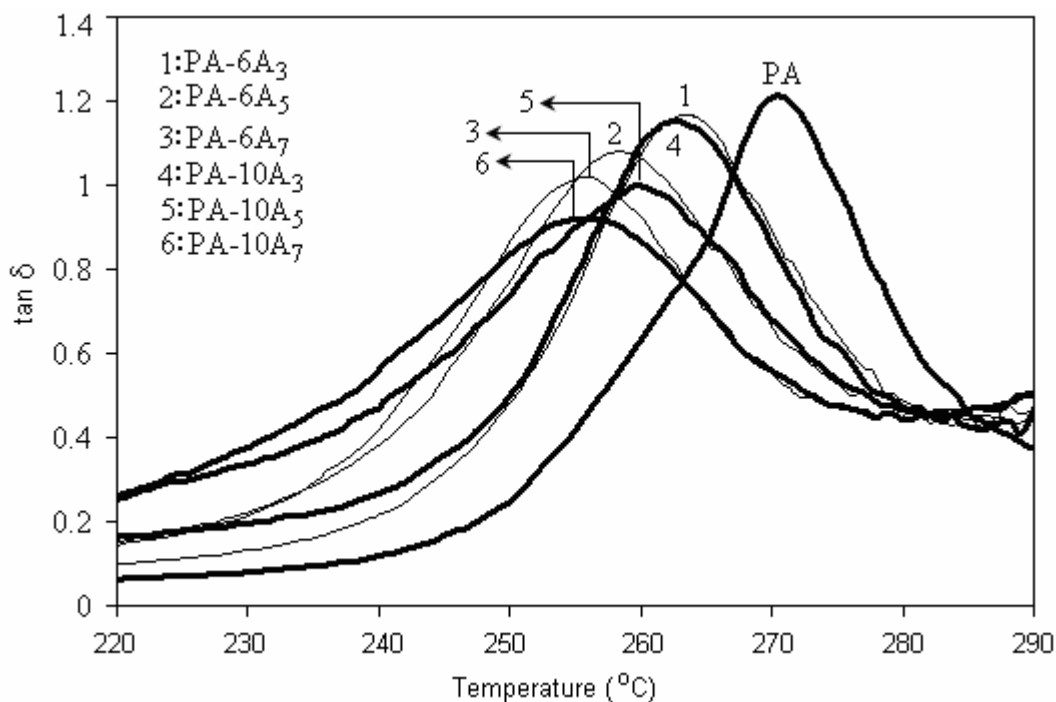


Figure 5.1.5 Tan δ curve by DMA of polyarylate (PA) and nanocomposites

5.1.4.4 Solution viscosity, nanocomposite density and free volume

The intrinsic viscosity data for PA solutions containing different 10A and 6A clay content is summarized in Table 5.1.2. A linear increase in viscosity with increasing clay loading was observed for solutions containing both the types of clay. This suggested that

even in solution phase, both, 6A and 10A clay had good interactions with polymer chains. For a particular percent loading, an increase in viscosity was found to be higher in the case of 10A than that for 6A, indicating better interactions of 10A clay with the polymer chains than that of 6A clay.

The experimental densities calculated by floatation method are given in the Table 5.1.2. The density for both the types of nanocomposite increased with an increase in the loading content, as anticipated. For 10A based nanocomposites, the density was higher than that for 6A based nanocomposites for the same level of loading. The fractional free volume (v_f) of a polymer can be estimated by the group contribution method [Van Krevelen (1972)]. As the clay content increased, a considerable decrease in v_f of the nanocomposites was observed. The extent of decrease in v_f was more in case of 10A based nanocomposites than for 6A based, for the same percent loading of clay. The lowering in v_f as a result of closer chain packing also indicated better dispersion and interactions of 10A clay than that of 6A clay with the polymer matrix.

5.1.4.5 Permeation properties

The gas permeability investigations of nanocomposites based on both types of clay was done with pure gases viz. He, N₂, CH₄ and CO₂ as summarized in Table 5.1.3.

Table 5.1.3 Permeability coefficient (P) and selectivities (α) for nanocomposites with different percent loading of clays

Gas	PA	6A clay			10A clay		
		3%	5%	7%	3%	5%	7%
He	43.7	31.8	28.1	21.4	29.4	26.4	16.1
N ₂	1.2	1.2	0.8	0.7	1.0	0.84	0.66
CH ₄	1.04	0.93	0.85	0.3	0.75	0.67	0.30
CO ₂	41.6	20	14.2	3.8	16.1	12.2	3.7
$\alpha(\text{He}/\text{N}_2)$	36.4	26.5	35.1	30.6	29.4	31.4	24.4
$\alpha(\text{He}/\text{CH}_4)$	42	34.2	33.1	71.3	39.2	39.4	53.7
$\alpha(\text{He}/\text{CO}_2)$	1.05	1.59	1.98	5.63	1.83	2.16	4.35
$\alpha(\text{CO}_2/\text{N}_2)$	34.7	16.7	17.8	5.4	16.1	14.5	5.6
$\alpha(\text{CO}_2/\text{CH}_4)$	40	21.5	16.7	12.7	21.5	18.2	12.3

For both the types of nanocomposites, an overall decrease in permeability was observed in comparison to that of pristine PA, for all the gases studied. This could be attributed to the closer chain packing in nanocomposites in comparison to the pristine polyarylate as revealed by lowering in d-spacing and the reduction in v_f . The platelet type morphology of clay particles embedded in a polymer matrix would increase diffusion path length by following a ‘tortuous path’ that retards the progress of the gas molecules through the matrix leading to lower permeability [Sinha (2003), Wang (2005)]. Increasing tortuosity path and restriction of chain mobilization due to the presence of MMT have more profound effect on the movement of larger size penetrant, N_2 , than O_2 and CO_2 [Ryu (2005)]. In the present work, the permeability of CO_2 was decreased to a greater extent (52-91 %) than for other gases studied.

The variation in relative permeability ($P_{nanocomposite} / P_{PA}$) with volume fraction of clay loading are presented in Figure 5.1.6 and 5.1.7, for both 6A and 10A clay based nanocomposites, respectively.

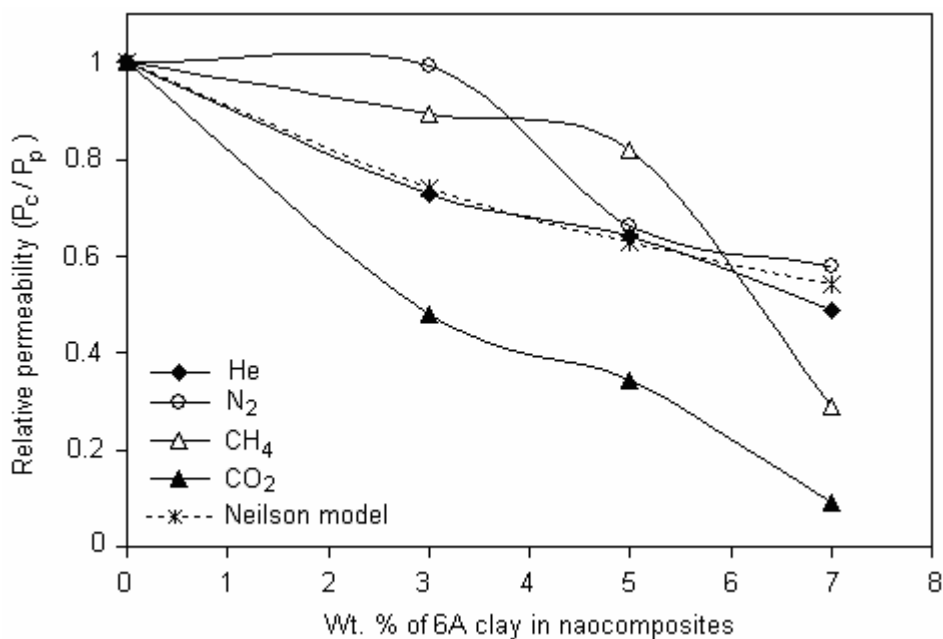


Figure 5.1.6 Variation of relative permeability (P_c/P_p) with volume fraction (ϕ_f) of 6A based nanocomposites

This ratio decreased with increased loading level and the extent of decrease in permeability was more rapid at higher clay loading (7%). Similar reduction in permeability for different gas molecules by loading of vermiculite in butyl rubber was

reported by Takahashi et al. [2006] The diffusion coefficients determined were reduced by two orders of magnitude at the highest loadings of vermiculite, whereas, the steady-state permeability coefficients were reduced by factors of 25 to 30 for different gases.

A decrease in permeability was slightly more in case of 10A based nanocomposites than in the case of 6A based nanocomposites at the same level of clay loading. This could be attributed to the lower available free volume in earlier cases at particular loading level as a result of better interaction of 10A clay with PA than that of 6A clay. This was also supported by observed higher density and solution viscosity of 10A based nanocomposites than for 6A based counterparts. In the present case, the clays were obtained with organic modifier having different groups. The modifier of 10A contain phenyl ring in the alkyl chain, while 6A does not contain phenyl ring. As a result, better interactions based dispersion of wholly aromatic polyarylate PA could be anticipated with earlier type. Similarly, in case of 6A and 10A clay based PBT nanocomposites demonstrated the extensive intercalation in case of 10A clay based nanocomposite attributed to the presence of benzyl group [Li (2001)]

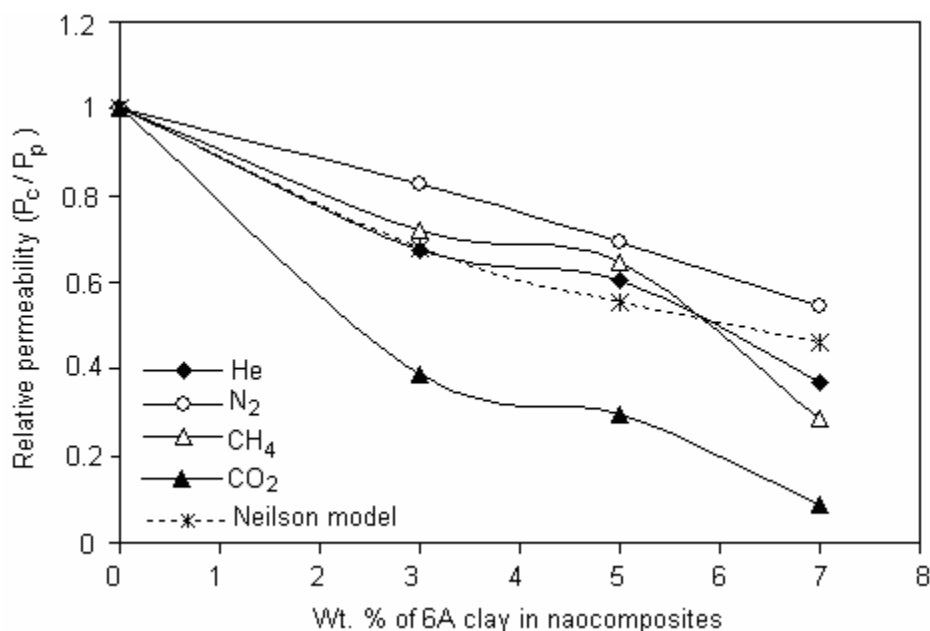


Figure 5.1.7 Variation of relative permeability (P_c/P_p) with volume fraction (ϕ_f) of 10A based nanocomposites

The variation in selectivity for various gas pairs in comparison to the selectivity of pristine PA showed a complex trend at different loading percent in 6A and 10A based nanocomposites. The He/CO₂ selectivity was increased, while, CO₂/N₂ and CO₂/CH₄

selectivity decreased at all the loading percent. The permeability reduction due to incorporation of tortuous path by clay can be anticipated to affect diffusivity of larger gases to a more extent. A larger decrease in permeability of CH₄ than for He, particularly at 7% loading led to considerable increase in He/CH₄ selectivity. The CO₂ based selectivities: $\alpha(\text{CO}_2/\text{N}_2)$ and $\alpha(\text{CO}_2/\text{CH}_4)$ were reduced dramatically as a result of larger drop in CO₂ permeability than for either N₂ or CH₄.

An increase in He/CH₄ selectivity could be affected only at 7 % loading indicating there could be a bare minimum requirement of a particular clay loading to affect selectivity favorably. This could be possible especially in view of the presence of long alkyl chain of organic modifier of the clay. Though such modifier is required to induce compatibility of clay with polymer chains, its nature (long chain alkyl) also induced plasticization as revealed by decrease in glass transition temperature by DMA analysis. This decrease in T_g could be anticipated to adversely affect the selectivity performance owing to poorer penetrant-discriminating ability due to plasticization. A smaller variation in He/CH₄ selectivity at 3-5 % loading suggested that probably this plasticization effect is more predominant than the tortuous path in controlling selectivity, while at 7 % loading, the tortuous path may be predominantly responsible to reduce permeability of larger gases leading to higher selectivity of He/CO₂ and He/CH₄. In order to effectively tune the selectivity favorably, it may be worth to properly choose the alkyl group modifier (intercalant/surfactant) that would have minimal plasticizing effect and maximum possible exfoliation while inducing compatibility of clay with polymer chains.

5.1.4.6 Determination of aspect ratio from permeability

From the trend obtained in reduction in He permeability (Figure 5.1.6 and 5.1.7) with filler content, the aspect ratio (α') was estimated by following Nielsen model (Eq. 5.1.1) developed for depicting barrier properties of composite materials containing platelet particles [Nielsen (1967)].

$$P_c = P_p \left(\frac{1 - \phi_f}{1 + \alpha' \phi_f / 2} \right) \quad (5.1.1)$$

where, P_c and P_p are the permeability of the composite medium and the pure polymer; while, ϕ_f and α' are volume fraction of the filler and the aspect ratio of platelets,

respectively. Helium gas was chosen to estimate the aspect ratio using Equation 5.1.1 in view of its non-interacting (inert) nature. Thus the transport of He would be diffusion controlled rather than sorption controlled. For nanocomposites based on 6A clay, the predicted α' was estimated to be 33, while in case of 10A clay based nanocomposites, the same was increased to 51. This clearly indicated the high level of dispersion in case of 10A clay based nanocomposites than 6A based. A nominal aspect ratio was generally calculated by fitting the relative permeability data as a function of clay content. Even if approximate, this nominal aspect ratio has proven to be a good indicator for the extent of clay exfoliation, with higher aspect ratios indicating better exfoliation/dispersion of the clay [Osman (2004)]. Higher reduction in v_f in case of 10A clay based nanocomposites also supported its high aspect ratio than that for 6A case. The above results were confirmed by the XRD and TEM analysis, which showed the better dispersion of 10A clay in the polymer matrix. Hotta et al. [2004] reported the gas permeability coefficients for O₂, N₂, and CO₂ in the nanocomposites relative to the corresponding value for pure LLDPE. Using Nielsen tortuous path model, aspect ratio was calculated. The experimental data closely matched the theoretical line for an aspect ratio of 5 [Hotta (2004)]. As seen from the Figure 5.1.6 and 5.1.7, the permeability prediction by Nielsen model fitted well for helium, while the nature of the curve varied considerably for other gases like CH₄ and CO₂. It could be anticipated that these gases have considerable interaction (sorption) with polymer matrix and thus Nielsen model could not be applied. Wang et al. [2005] has reported reduction in diffusion (59.5%) as well as in calculated solubility (22.9%) for N₂ in the rectorite/SBR composites. In present case, a larger effect on CH₄ diffusivity at higher loading level could be responsible for rapid decrease in relative permeability (Figure 5.1.6 and 5.1.7) of this gas; leading to higher He/CH₄ selectivity at this level of clay loading.

5.1.5 Conclusions

Polyarylate-clay nanocomposites were successfully prepared by solution intercalation method. In nanocomposites based on 6A and 10A, an increase in solution viscosity, increase in nanocomposite density than anticipated was observed by additivity rule. TEM analysis revealed that the clay layers were dispersed at nanometer scale in the polymer matrix. The attractive interaction as indicated by solution viscosity and density

behavior was more predominant in case of 10A clay based nanocomposites than that for 6A based cases.

An overall decrease in permeability for all the gases was observed for incremental loading of both types of the clay. A marked decrease in permeability of gases like CO₂ and CH₄, in comparison to the decrease in permeability of He gas was observed especially at higher clay loading. Though organic modifier of clay reduced glass transition temperature of formed nanocomposites, as revealed by DMA analysis, an increase in selectivity $\alpha(\text{He}/\text{CO}_2)$ and $\alpha(\text{He}/\text{CH}_4)$, especially at higher clay loading indicated the capability of nanocomposites to tune the selectivity behavior favorably. This suggested that nonplasticizing clay might prove more effective in improving selectivity. Predicted aspect ratio by Nielsen's model for both the nanocomposites was in agreement with the observed variation in physical properties of 6A and 10A based nanocomposites.

5.2. Poly(ionic liquid): Preparation, sorption analysis and composite membrane investigations

5.2.1 Introduction and Literature survey

In recent literature, CO₂ has been shown to be remarkably soluble in ionic liquids [Blanchard (1999), Blanchard (2001), Anthony (2002), Kamps (2003), Scovazzo (2004), Camper (2004)]. For instance, at 15 bar, CO₂ solubility in 1-butyl-3-methylimidazolium hexafluorophosphate ([bmim][PF₆]) is about 23 mol % [Blanchard (2001)]. The CO₂ solubility can be improved by structural modifications in cations and anions. The incorporation of fluorine-containing anions [Cadena (2004)] or cations [Baltus (2004)] and introduction of amine groups in cation [Bates (2002)] are known to improve CO₂ solubility in resulting ionic liquids. The room temperature ionic liquids (RTILs) are salts that are liquids at room temperatures and possesses negligible vapor pressures, high thermal stability, high ionic conductivity and are non-flammable [Scovazzo (2004)]. They dissolve a wide range of inorganic and organic compounds [Scovazzo (2004)]. Supported liquid membranes (SLM) containing ionic liquid are demonstrated to have high CO₂ selectivity and permeance [Scovazzo (2004)] and thus could be useful in its separation from other gases like N₂ and CH₄.

The limitations of SLM in commercial applicability could be overcome by incorporation of ionic liquid groups on polymer backbone. The direct polymerization of the ionic liquid monomer [Noda (2000), Tang (2005a)] and modification of the polymer by anion-exchange reaction has been reported [Marcilla (2004)]. Polymeric forms of ionic liquids are anticipated to have exceptional properties, such as stability, electrochemical activity and CO₂ absorption ability. Yoshizawa et al. [2002] found that polymers obtained from monomeric ionic liquids exhibited high ionic conductivity. Their polymer brushes and crosslinked polymers formed flexible and transparent films with excellent ionic conductivity [Tang (2005b)]. Ono et al. has used polymerized ionic liquids for photo electrochemical cell electrolytes [Ono (2001)]. Tang et al. [2005a] found that by making the ionic liquids into polymeric form, significant increase in CO₂ sorption capacity can be achieved in comparison to the monomeric ionic liquid. Polymers based on tetraalkylammonium-based ionic liquids have CO₂ sorption capacity of 6.0–7.6 times

than those of room temperature ionic liquids. The CO₂ sorption and desorption in polymeric solids were fast and desorption was shown to be completely reversible. These polymers could be prospective CO₂ sorbent and membrane materials. Though the sorption properties of poly(ionic liquid)s are reported in the literature, the CO₂ permeation performance in their membranes is lacking, probably owing to the inability to form a continuous membrane.

5.2.2 Objectives

The main objective of this work was to investigate performance of PIL based composite membranes for CO₂ permeation properties. The PIL preparation by a simple ion exchange method rather than the polymerization of ionic liquid monomers was explored. The chloride anion of a cheaper polymeric material possessing quaternized ammonium salt, viz., poly(vinylbenzyltrimethylammonium chloride) (PVBTMACl) was exchanged with promising anion (BF₄⁻). The anion exchange process was optimized by varying solvent composition, time duration and mole ratio. The composite membranes based on nafion and formed PIL - PVBTMABF₄ were prepared and gas permeability for CO₂ and N₂ were investigated. The gas sorption analysis of the precursor polymer (chloride salt) and formed PIL was also performed using N₂ and CO₂ to investigate effect of anion exchange on sorption properties.

5.2.3 Experimental

5.2.3.1 Materials

Poly(vinylbenzyltrimethylammonium chloride) was purchased from Scientific Polymer Products Inc. (USA) as a dry powder having molecular weight of 400,000. Sodium tetrafluoroborate (NaBF₄) and silver nitrate (AgNO₃) were obtained from Aldrich chemicals and used as received. A 20 wt. % nafion solutions (1100 eq. wt., sulfonic acid form) was procured from E. I. Dupont de Nemours & Co. (USA). *N,N*-dimethyl formamide (DMF), chloroform and acetonitrile were AR / LR grade and were obtained from S.D. Fine Chemicals, India. All these materials were used without further purification. The details of other polymers used for blending with PIL are discussed in section 5.2.5.1.

5.2.3.2 Anion exchange of PVBTMACl

A 15 g of PVBTMACl was dispersed in 250 ml mixture of acetonitrile and DMF (1:1), followed by addition of 5 molar excess of NaBF₄. After 10 minutes, the solution became turbid due to the precipitation of NaCl. The polymer dissolved gradually as the exchange reaction progressed. After continuous stirring for 72 hours at ambient conditions, the mixture was centrifuged, supernatant solution was separated and precipitated in chloroform. The obtained polymer was dried at 60 °C for 12 hours. Further purification was done by its dissolution in acetonitrile and reprecipitation into chloroform. The polymer was dried at 60 °C for 12 hours and finally under vacuum at the same temperature for 24 hours. 5 gm polymer was dispersed in 20 ml of de-ionized water in a conical flask at 4 °C for half an hour. The supernatant was decanted. This washing procedure was repeated trice at 4 °C to completely remove the excess of NaBF₄. The polymer was finally dried at 60 °C for 12 hours. The recovery of the polymer after water was 40 %. The solubility of this PIL in various solvents was as given in Table 5.2.2.

5.2.3.3 Characterization

The IR spectrum of PVBTMACl and PVBTMABF₄ were recorded in diffusive reflectance mode using Spectrum-1 spectrophotometer and were as shown in Figure 5.2.3. The glass transition temperature (T_g) was determined by differential scanning calorimetry on Thermal Instruments DSC-Q10 under N₂ atmosphere and at the heating rate of 10 °C/min. Wide-angle X-ray diffraction (WAXD) spectra of PVBTMACl, PVBTMABF₄ were recorded using Rigaku x-ray diffractometer (D-max 2500) with Cu-K_α radiation in 2θ range of 4-40° and were as shown in Figure 5.2.4. The average d-spacing (d_{sp}) for amorphous peak maximum was calculated using Bragg's equation. The reproducibility of the d_{sp} measurements was $\pm 0.05\text{Å}$. Electron spectroscopy for chemical analysis (ESCA) for PVBTMACl and PVBTMABF₄ were recorded on a V.G. Scientific (UK) ESCA 3000, using Al K as an X-ray source (1486.6 eV), operated at 250 W of power, 50 eV pass energy, 4 mm slit and a take-off angle of 30° in relation to the sample surface. The residual gas pressure in the spectrometer chamber during the data acquisition was less than 10⁻⁸ Torr. The ESCA spectra were referenced to the Cl 2p peak (201 eV) and were as shown in Figure 5.2.2. The scanning electron micrographs (SEM)

of nafion and nafion-PIL composite membranes were recorded with Leica, stereoscan-440 and were as shown in Figure 5.2.9. The surface analysis of the nafion and PIL-impregnated nafion membranes was done by attenuated total reflectance (ATR) spectroscopy (KRS crystal, Perkin-Elmer) at an angle of 45° . These spectra were as shown in Figure 5.2.10. Membrane surface roughness was analyzed by atomic force microscopy (AFM) with Multimode SPM - Veeco. The samples were analyzed in contact mode and the AFM images were as shown in Figure 5.2.11. The percent conversion of the Cl^- into BF_4^- was determined quantitatively by conductometric titration of dilute aqueous solution of PVBTMACl and PVBTMABF₄ (0.5 % w/v) with 0.05M aq. AgNO₃ solution.

5.2.3.4 Dense membrane preparation

The dense membrane preparation of PVBTMABF₄ was attempted using 2 % (w/v) solution of PVBTMABF₄ in acetonitrile. The solution was filtered through a 5- μm SS-filter and poured on to a flat glass surface. The solvent was allowed to evaporate at 40 °C under dry atmosphere. Continuous film of PIL could not be obtained; instead, it resulted in the flakes formation. These flakes were removed from the glass surface and vacuum dried at 60 °C for 3 days in order to ensure the complete removal of the solvent.

Nafion membranes were casted using 20 % (w/v) stock solution diluted with *n*-propanol to 5 % solution concentration. The solution was filtered through a 5- μm SS-filter and poured on to a flat glass surface. The solvent was allowed to evaporate at 60 °C under the dry atmosphere. The formed film was peeled off and vacuum dried at 45 °C for a week in order to ensure the complete removal of the solvent.

5.2.3.5 Equilibrium swelling studies

The swelling of casted nafion membranes in acetonitrile was determined at room temperature. The pre-weighted membrane samples (6 x 2 cm²) were dipped in acetonitrile for 12 hours. The swollen weights and dimensions of the membrane were determined immediately after blotting off the surface solvent with tissue paper. The solvent uptake was determined by the following equation [Hegazy (1999)]:

$$\text{Solvent uptake (\%)} = 100 \times (W_1 - W_0) / W_0$$

where W_0 is the weight of dry membrane and W_1 is the weight of swollen membrane. The variation in data for different coupons analyzed was within ± 7.5 %. The percent dimensional changes were calculated by the following equation [Kubota (2001)]:

$$\text{Dimensional change (\%)} = 100 \times (S_1 - S_0) / S_0$$

where S_0 is the initial length/width and S_1 is the final length/width. The variation in data for different coupons analyzed was within ± 4.5 %.

5.2.3.6 Preparation of blends

In an effort to prepare continuous dense film for gas permeation study, blends of PVBTMABF₄ with various polymers was attempted as detailed in Table 5.2.5. The film preparation was attempted by solvent casting method using a common solvent.

5.2.3.7 Preparation of Nafion-PVBTMABF₄ composite membranes

The composite membranes of PIL with nafion were prepared by dipping nafion membranes into the 6 % PIL solution in acetonitrile for different time intervals. After dipping for desired time period, the nafion membranes were removed from the solution, allowed to stand at ambient for 0.5 hour and then dried in vacuum oven at 60 °C for 3 days.

5.2.3.8 Determination of equilibrium gas sorption and permeation

The gas sorption analysis for N₂ and CO₂ were carried out at varying pressures, upto 16 atm absolute and at 35 °C. The gas solubility apparatus and procedure is already discussed in section 3.3.8.2. The resulting sorption isotherms were as given in Figure 5.2.5. The density of the PIL and its precursor polymer was determined in the sorption cell using He gas [Rutherford (2005)]. The volume of the sample chamber with the polymer present is determined by He expansion into a previously calibrated cell volume. This He expansion method assumes that a negligible amount of He is sorbed into the polymer over the time of exposure, which was confirmed by the absence of any observable pressure decay following expansion.

Gas permeability of the nafion-PIL composite membranes for N₂ and CO₂ were measured by the variable volume method at upstream gas pressure of 10 atm and at 35 °C

while maintaining the permeate side at the atmospheric pressure. The measurements were repeated at least for 3 membrane samples prepared with identical conditions. The average permeability and selectivity of different gas pairs were as summarized in Table 5.2.7.

5.2.4 Result and discussion

5.2.4.1 Preparation of poly(ionic liquid) (PVBTMABF₄)

Poly(ionic liquid) was prepared by ion exchange method using readily available polyelectrolyte, PVBTMACl, containing quaternary ammonium group. Its chloride anion was replaced by BF₄⁻ anion to obtain poly(ionic liquid), PVBTMABF₄ (Figure 5.2.1).

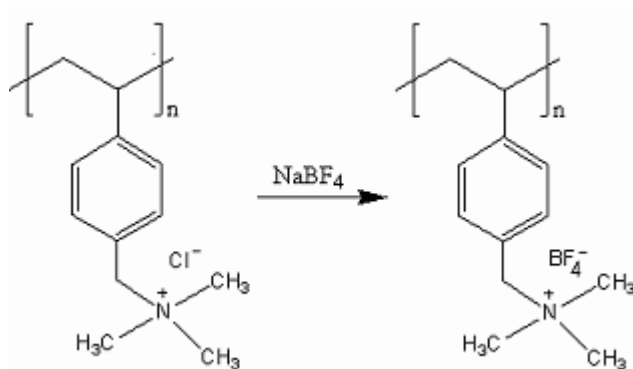


Figure 5.2.1 Preparation of poly(ionic liquid)

The ion exchange reaction was carried out in non-aqueous medium in view of insolubility of the byproduct, NaCl.

5.2.4.2 Purification of PIL

The synthesized PIL was purified by precipitating the acetonitrile solution of PIL into chloroform. The purification step was not sufficient to remove NaBF₄ completely. PIL was thus further purified by washing with cold water (4 °C). 5 gm of PIL was dispersed into 50 ml of water and allowed to stir for 0.5 hour at 4 °C. The dispersed PIL was allowed to settle down and supernatant liquid was decanted. The procedure was repeated thrice. The PIL was finally dried at 60 °C for 12 hours. The yield of this step was 40 %.

5.2.4.3 Physical properties of poly(ionic liquid)

The ESCA analysis of PVBTMACl and PVBTMABF₄ was performed to detect the chlorine and boron present in these materials, respectively. The spectra were as given in Figure 5.2.2 below.

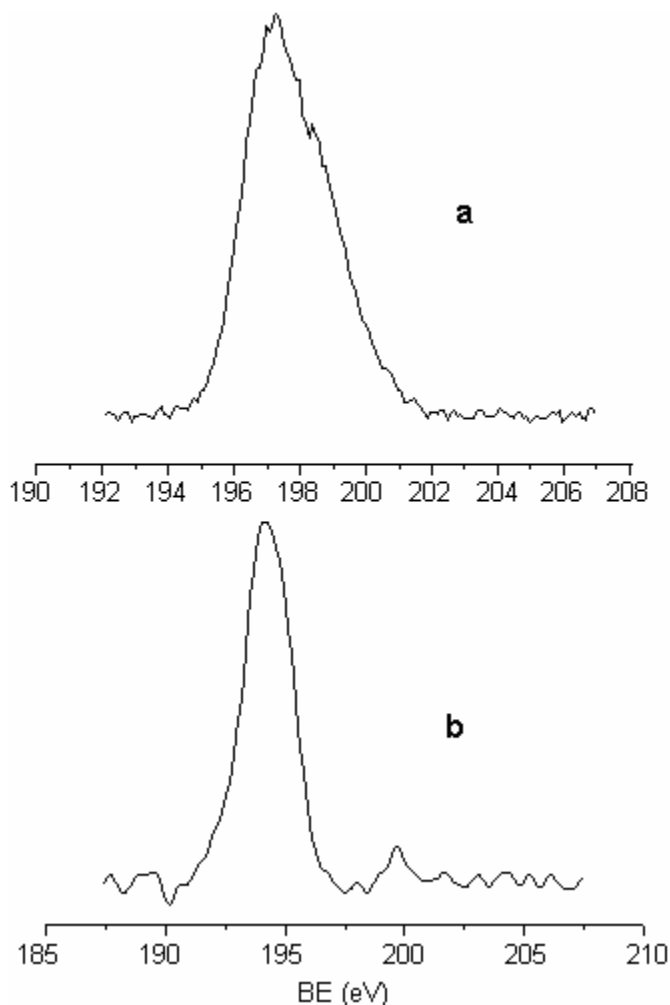


Figure 5.2.2 ESCA of a: PVBTMACl for occurrence of Cl⁻ in, b: PVBTMABF₄ for occurrence of boron

The binding energy of chlorine peak appears in the range of 197 to 210 eV; while in case of boron, it appears in the range of 186-195 eV [Wagner (1979)]. In precursor polymer, chloride peak appeared at 197.3 eV; while in case of PIL, it was absent. The boron peak in ESCA of PIL appeared at 194.3 eV. In comparison with B, F and Cl elements, Cl was 0.7 % on the surface, which shows almost all Cl⁻ was converted to BF₄⁻. Since ESCA is mainly surface property and may not completely represent the bulk

property, it was decided to perform conductivity based titration of PIL solution with aq. AgNO_3 .

The quantitative analysis of PIL for residual Cl^- was performed by conductometric titration and found to be 4.7 %. It may be further possible to achieve the complete conversion of Cl^- to BF_4^- by optimizing exchange conditions such as solvent, duration of exchange reaction, moles of NaBF_4 , etc. It was reported by Tang et al. [2005b] that the quaternization of *N*-butylimidazole with 4-vinylbenzyl chloride and subsequent anion-exchange reaction of chloride ions with BF_4^- or PF_6^- anions using NaBF_4 or KPF_6 , respectively, could not completely replace the chloride. Unfortunately, the detection method / amount replaced were not reported.

The IR spectrum of PVBTMACl and synthesized PVBTMABF_4 were as shown in Figure 5.2.3.

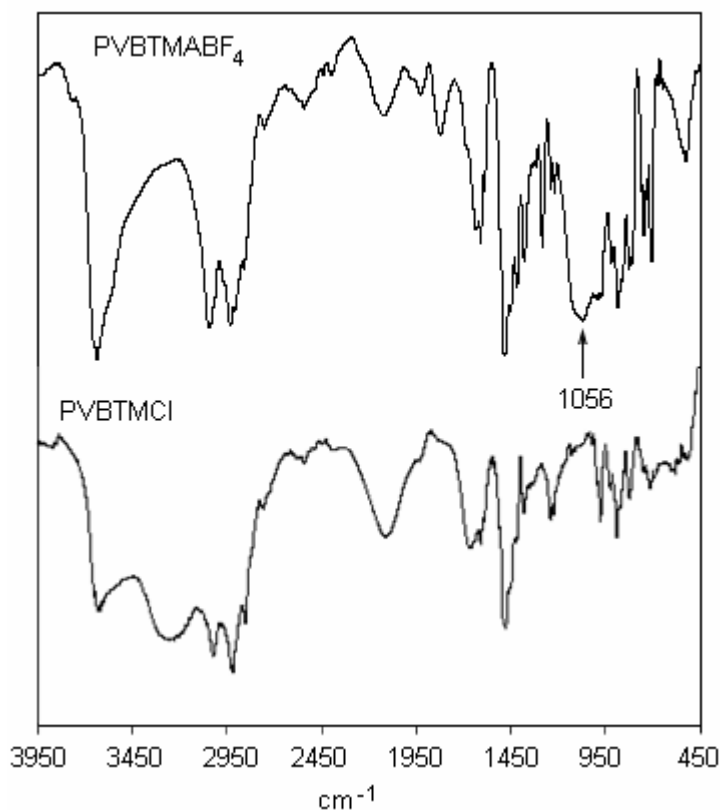


Figure 5.2.3 FTIR spectra of precursor polymer and PIL

The appearance of the peak at 1056 cm^{-1} , attributable to the characteristic B-F stretching vibration confirmed the conversion of Cl^- anion to BF_4^- [Suarez (1996)]. The peak at 1478 cm^{-1} in both the polymers ascribed to scissoring of methylene groups. The

peak at 888 cm^{-1} corresponds to out-of plane bending of aromatic-ring C-H bonds [Kumar (2006)]. The peak at 1377 cm^{-1} was attributed to stretching vibration of C–N of tertiary ammonium group [Domanska (2005)]. The other physical properties of the precursor polymer and PVBTMABF₄ were as given in Table 5.2.1.

Table 5.2.1 Physical properties of precursor polymer and PIL (PVBTMABF₄)

Polymer	d_{sp} Å	T_g (°C)	ρ (g/cm ³)
PVBTMACI	4.34	283	1.325
PVBTMABF ₄ (Powder)	4.63	238	1.406

^a: By conductometric titration

The WAXD spectra (Figure 5.2.4) showed that both, PVBTMACI and PVBTMABF₄ were amorphous in nature. The peak positions of amorphous maxima was used to calculate average chain d_{sp} and were as listed in Table 5.2.1.

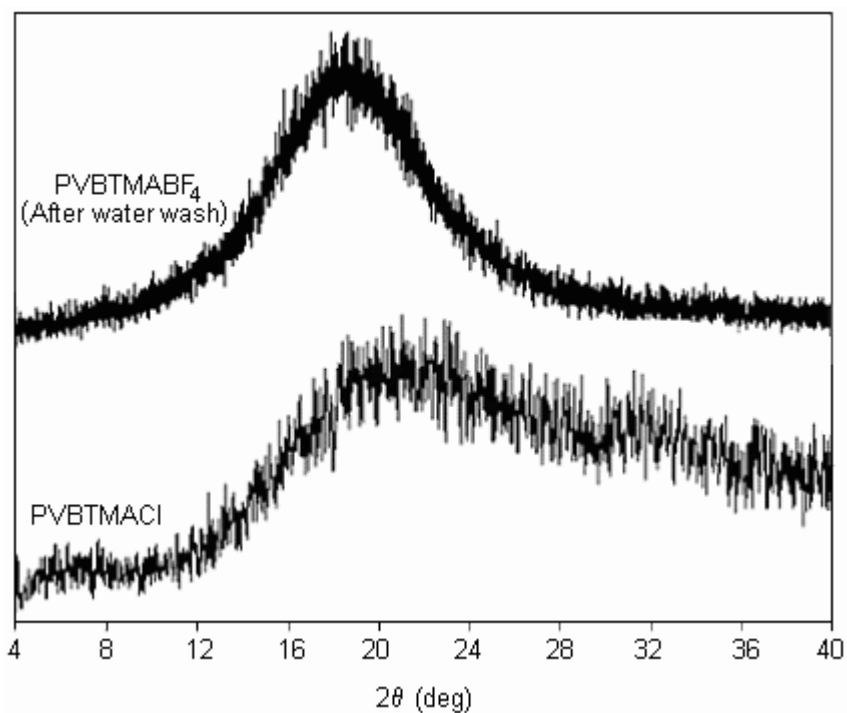


Figure 5.2.4 WAXD spectra of 1: PVBTMACI, 2: PVBTMABF₄ (After water wash)

PVBTMACI exhibited lower d_{sp} (4.34 Å) than that of PVBTMABF₄ (4.63 Å). Though the backbone of both polymers was same, the observed difference in d_{sp} might be

ascribed to the difference in size of the anions. The d_{sp} for the same poly(ionic liquid) observed by Tang et al. (synthesized by free radical polymerization of respective monomeric ionic liquid) was 4.79 Å. The exchange of Cl⁻ anion by BF₄⁻ led to increase in density as well.

The precursor polymer exhibited higher T_g (283 °C) than PIL (238 °C). Although PVBTMABF₄ may have strong interchain charge interactions, its T_g was lower than that of precursor polymer containing chloride anion. It was reported that anions in ionic liquids such as tetrafluoroborate anion have a strong plasticizing effect [Tang (2005b)]. These anions might improve the flexibility of polymer chains, facilitate the segmental motion, and consequently reduce the T_g of the polymer. The T_g of the same PIL reported by Tang et al. [2005a] was 215 °C.

5.2.4.4 Solvent solubility of PIL

The solubility of PVBTMACl and PVBTMABF₄ in various solvents was as presented in Table 5.2.2.

Table 5.2.2 Solubility of polymers in various solvents

Polymer	DMF	Acetonitrile	Water	Methanol	Chloroform	THF
PVBTMACl	+	-	+	-	-	-
PVBTMABF ₄	+	+	+	-	-	-

+: Soluble at ambient temperature, -: Insoluble

The precursor polymer and formed PIL were completely soluble in DMF as well in as water. The obtained PIL showed solubility in acetonitrile, while the precursor was insoluble in it.

5.2.4.5 Gas sorption study of poly(ionic liquid), PVBTMABF₄

The gas sorption analysis (N₂ and CO₂) of the precursor polymeric chloride salt, as well as BF₄⁻ exchanged PIL was performed using pressure decay method [Vieth (1966)]. The pure gas sorption isotherms were as shown in Figures 5.2.5. Both, the precursor (PVBTMACl) and the PIL (PVBTMABF₄) exhibited dual mode sorption as commonly observed for glassy polymers, and described by Equation 1.8. In both the polymers, CO₂ sorption was considerably higher than that of N₂, as commonly observed

for most of the polymeric materials. Noticeably, PIL showed significantly higher sorption than that of precursor, PVBTMACl. This indicates that the BF_4^- anion contributed to the increased CO_2 sorption in PIL.

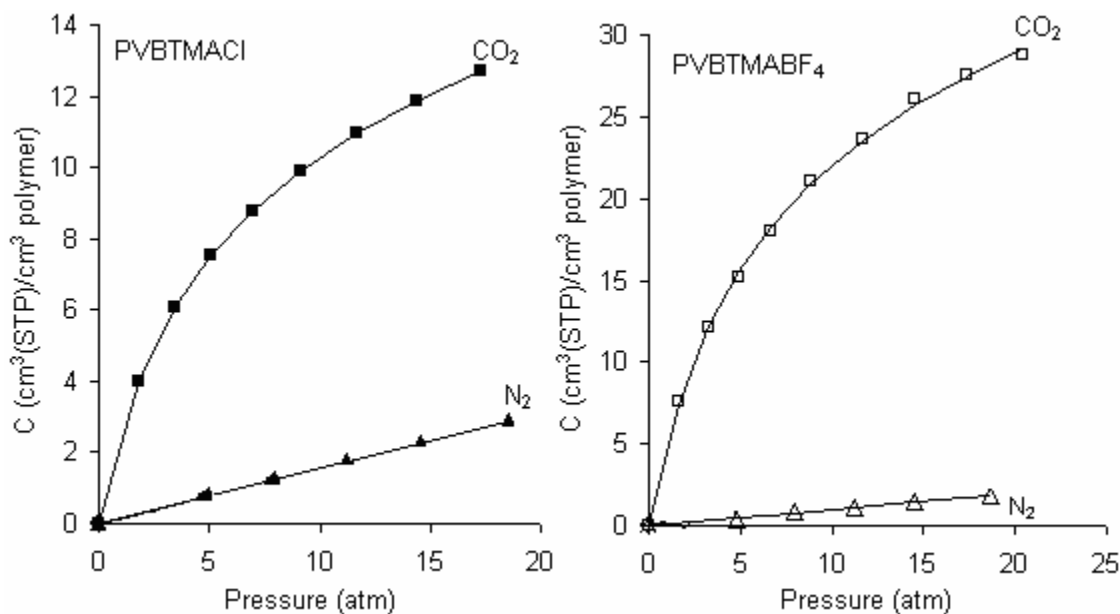


Figure 5.2.5 Gas sorption isotherms of precursor polymer and PIL

The dual mode sorption parameters were estimated from the nonlinear least-squares regression analysis using the genetic algorithm based on the observed gas sorption and were as given in Table 5.2.3. As the chain packing density decreased in the PIL (as indicated by increased d_{sp}), the C'_H for both the gases increased, the increase in C'_H for CO_2 being higher than that for N_2 . This could be due to the better interactions of BF_4^- anion with CO_2 . Such phenomenon of weak Lewis acid-base interaction between CO_2 and BF_4^- anion was reported in case of ionic liquids [Kazarian (2000), Anthony (2002)]. In comparison to precursor polymer, an increase in k_D for CO_2 and decrease in k_D for N_2 in PIL indicated the increased interaction of BF_4^- with CO_2 than for N_2 . The parameter 'b', termed as hole affinity constant, which is also related to rate of sorption desorption of gas [Vieth (1976)] was decreased for CO_2 in PIL, while that for N_2 , it was increased. This decrease in 'b' for CO_2 after PIL formation indicated delayed rate of desorption; probably because of better affinity of CO_2 with PIL than with precursor - PVBTMACl. In other words, CO_2 has greater tendency to remain sorbed in Langmuir sites of the PIL.

Table 5.2.3 Dual-mode sorption parameters for PIL and precursor polymer at 10 atm and at 35 °C

Polymer	Gas	k_D ($\text{cm}^3(\text{STP})/\text{cm}^3 \cdot \text{atm}$)	C'_H ($\text{cm}^3(\text{STP})/\text{cm}^3$ polymer)	b (1/atm)
PVBTMACl	CO ₂	0.16	12.37	0.23
	N ₂	0.15	0.42	0.0008
PVBTMABF ₄	CO ₂	0.31	28.53	0.20
	N ₂	0.1	0.95	0.001

The pressure dependency of solubility of gases and CO₂/N₂ solubility selectivity for precursor as well as PVBTMABF₄ was as shown in Figure 5.2.6.

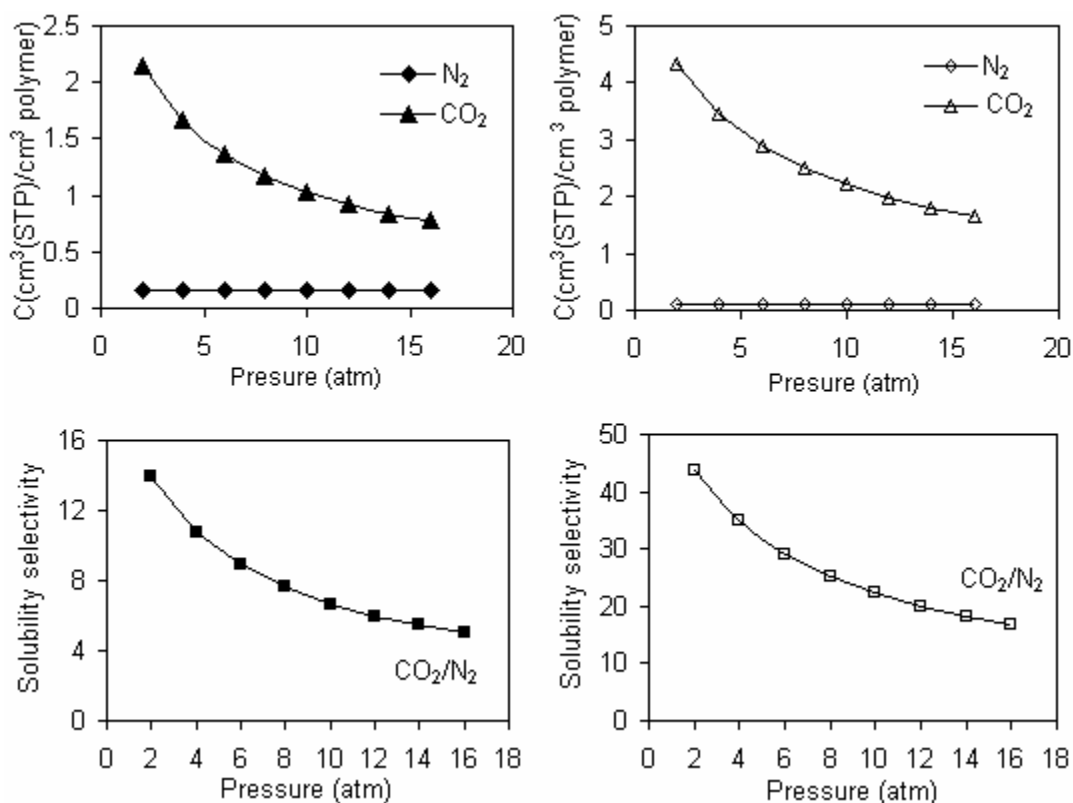


Figure 5.2.6 Change in solubility and solubility selectivity with respect to pressure

Both PVBTMACl and PVBTMABF₄ showed reduction in solubility selectivity with increasing pressure. Figure 5.2.6a and b showed negligible pressure dependency for solubility of N₂, while it was significant in case of CO₂, as typically observed in glassy polymers. The sorption selectivity for CO₂/N₂ was significantly higher in case of PIL

than that of PVBTMACl; depicting usefulness of BF_4^- anion in increasing CO_2 sorption in poly(ionic liquid)s.

CO_2 sorption capacity of the PIL obtained in the present work was compared with the sorption capacity of same polymer reported by Tang et al. in Figure 5.2.7 [Tang 2005a]. It was observed that at 10 atm, CO_2 sorption capacity in present case was 38 % than that for PIL reported by Tang et al. at the same pressure [Tang (2005a)].

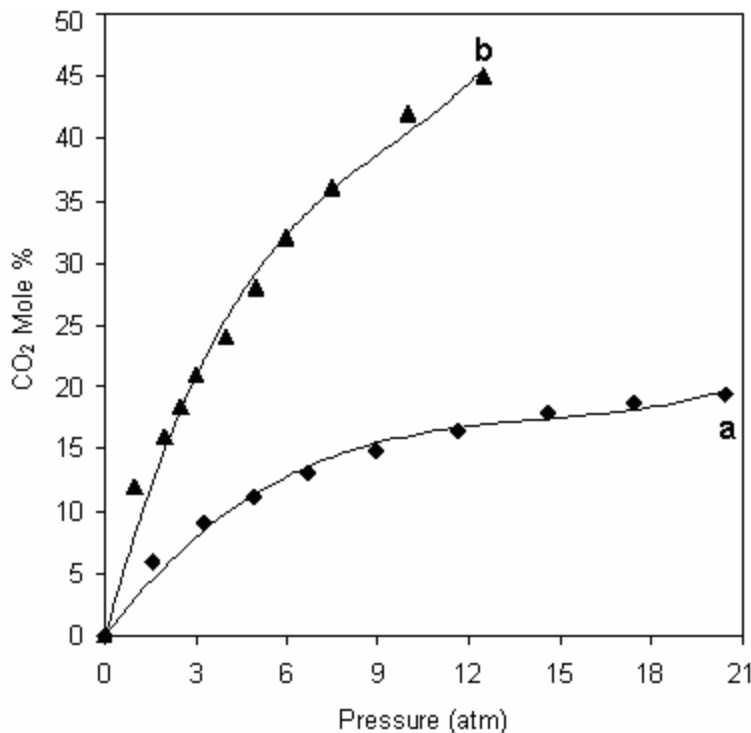


Figure 5.2.7 CO_2 sorption capacities of PVBTMABF₄ at different pressures a) present work at (at 35 °C) b) reported literature (at 22 °C)

The difference could be mainly stem from the temperature of sorption analysis. In the present case, the sorption was performed at 35 °C; while the temperature of sorption analysis by Tang et al. was 22 °C. It is reported that increased temperature generally lowers gas sorption in polymer [Costello (1995)] as well as in ionic liquids such as [emim][Tf₂N], [emmim][Tf₂N], [bmim][PF₆], [bmmim][PF₆], [bmim][BF₄] and [bmmim][BF₄] [Cadena (2004)]. Unfortunately, other physical properties (such as molecular weight of the polymer) were not reported by Tang et al. and could not be compared with that of present work. The method of PIL preparation used by Tang et al. was polymerization of BF_4^- containing monomers, while in present case; PIL was

obtained by anion exchange of precursor polymer containing Cl^- anion. The anion exchange obtained in the present case was 95.5 %; as deduced by conductivity titrations. Thus, though the conversion was not complete, its extent of conversion suggested that this may not be a reason for observed difference in sorption capacity.

5.2.4.6 Comparison of CO_2 sorption in PIL with other polymers

The utility of a polymeric material to be used as gas separation membrane material depends upon many factors such as intrinsic gas permeation properties (P , α , S and D), processability, capability to withstand operational conditions, etc. The basic requirement is to have high intrinsic gas permeability coupled with high selectivity for gas pair of interest.

Table 5.2.4 Comparison of solubility selectivity of PIL with other glassy polymers

Polymer	d_{sp} Å	ρ (g/cm^3)	$S(\text{CO}_2)$ At 10 atm	$S(\text{CO}_2/\text{N}_2)$ At 10 atm
Polyphenylene oxide (PPO) ^a	6.1	1.07	4.47	11.17
Polyphenylene oxide (PPO) ^b	6.95	1.05	3.33	5.47
Polyarylate (PA) ^c	4.8	1.2	2.18	6.85 ^g
Polycarbonate (PC) ^c	5.2	1.24	2.04	8.57 ^h
Polysulfone (PSF) ^c	5	1.21	2.03	14 ⁱ
PVBTMBF ₄ (PIL) ^c	4.6	1.37	2.20	22

^a Ref: [Vega (1993)], ^b Chapter 3, ^c Ref: [Barbari (1989)], ^e Present work, ^g Ref: [Pixton (1995)], ^h Ref: [McHattie (1992)], ⁱ Ref: [Hellums (1989)].

The present PIL showed high solubility selectivity for CO_2/N_2 in comparison to the other glassy polymers such as polycarbonates, polyarylates, polysulfones, etc. (Table 5.2.4). It was thus worth comparing sorption properties of PIL with other glassy polymeric materials. Glassy polymers generally have high diffusivity selectivity and low solubility selectivity. The high sorption selectivity for CO_2/N_2 in PIL stems from its interaction with CO_2 .

5.2.4.7 Membranes based on PIL

a) Blends of PIL with common polymers

Blending of PIL with various polymers were tried in order to obtain continuous film for gas permeation study of thus formed blend membranes. The blend preparation conditions and the observation with individual polymer were as given in Table 5.2.5.

Table 5.2.5 Observations of attempted blends of various polymers with PIL

Polymer	Solvent	Observation
PBI/Ultem/Polyarylate/ Polysulfone	DMF	Inhomogeneous blend, no continuous film could be casted
CA	DMF	Good films were casted till 20 % PIL content, but the formed films were brittle.
Nafion/Polyethylene oxide	DMF	Gel formation
Polyethyleneimine	Water	Sticky yellowish brawn film formed, but could not be removed from the glass surface.

The blends of poly(ionic liquid) with various glassy polymers such as PBI, Ultem, polyarylate and polysulfone were tried with varying proportions (5-20 % of PIL) by solution casting method using 2 wt. % polymer solution in DMF. The films formed with PBI, Ultem, polyarylate, PSF were inhomogeneous in nature and could not be pursued further. The dense film casting of PIL with Nafion or high molecular weight polyethylene oxide ($M_w = 50,00,000$) led to gel formation. PIL with polyethyleneimine though formed homogeneous solution in water; the solvent evaporation resulted in sticky yellow-brown film that could not be peeled off from the glass surface. In view of a continuous phase formation of PIL and PIL/PEO blend system, it may be worth to use these blends for thin film composite membrane (TFC) preparation, wherein the thin coating of blend can be supported on the porous ultrafiltration / microfiltration support. Thus it may be possible to overcome the observed limitations and draw an advantage of high anticipated CO_2 sorption in PIL to positively affect the gas permeation properties. This could not be attempted in the present work; alternatively, impregnation of PIL chains into suitable polymer matrix was attempted as discussed in following section.

b) *Preparation of Nafion-poly(ionic liquid) composites*

In view of inability of PIL to be converted into a thin film, it needs to be employed as a membrane material by following altogether different strategy. The TFC membrane, by definition, need to have a uniform coating of a polymer responsible for separation on the top of porous support. The coating of PIL on an ultrafiltration support would lead to cracked structure as observed during its film formation. Thus it was thought to anchor the PIL chains into the polymer matrix, rather than just coating on to the support membrane. In order to achieve such chain anchoring on support material surface, the polymer material that swells in a solvent, which is also a solvent for PIL needed to be chosen as a support material. It was found that nafion has a good swelling property in acetonitrile (AN). The average AN uptake was found to be 59.5 % and average dimensional changes along the length/width were 27 % after 12 hour dipping. Yeo et al. [1980] has reported the 54 % methanol uptake in nafion membrane of 1100 equivalent weight. Thus, nafion has good solvent uptake ability leading to membrane swelling that could be positively employed in the present case. This uptake is due to the unique structure of nafion (Figure 5.2.8), in which polymeric ions form clusters of dimensions of about 50 Å dispersed homogeneously in the fluorocarbon matrix [Sakai (1987)].

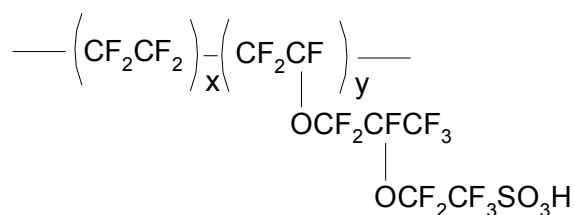


Figure 5.2.8 Chemical structure of Nafion

It is said that the degree of swelling of Nafion in a pure solvent is related to its polarity for both protic and aprotic solvents and in general, the uptake of polar solvents exceeds that of non-polar for the pure solvent cases [Elliott (2001)]. Because of this physical structure and chemical functionality, these membranes offer interesting opportunities for doping with additives that may lead to enhancement of the transport of one species relative to another. Previous reports suggested an approach of depositing silver into the structure of Dupont Nafion membrane to enhance the transport of oxygen

relative to that of nitrogen Sakai et al. [1987]. Dunkley-Timmerman [1988] loaded nafion membrane with ethylenediamine to increase the transport of CO_2 relative to other gases, e.g., CH_4 . Though the doping of the PIL into nafion solution was not possible due to gel formation (Table 5.2.5), the swelling capability of nafion was thought to be an alternative for this. The nafion membranes were dipped in 6 % PIL solution in acetonitrile for varying time (6, 12, 24 and 36 hours) at ambient conditions.

The morphology of as casted nafion membrane, acetonitrile dipped nafion membrane and PIL impregnated nafion membranes were analyzed by SEM and AFM as presented in Figure 5.2.9 and 5.2.11.

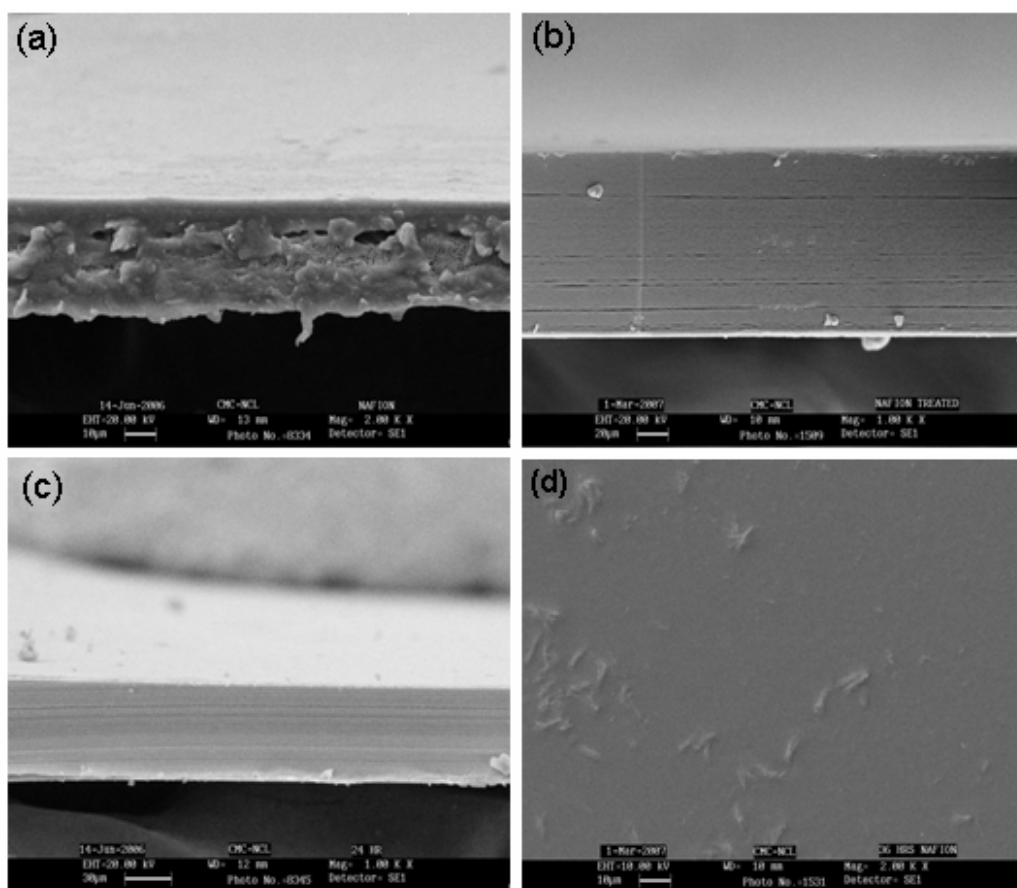


Figure 5.2.9 SEM of cross section of PIL impregnated nafion composite membranes a: Nafion, b: Solvent dipped, c: 24 hours dipped, d: surface image of 36 hours dipped membrane

The SEM of nafion membranes showed void formation in the membrane matrix during casting. These nafion membranes were prepared using as supplied 20 % Nafion

solution, which was diluted with *n*-propanol and then the films were casted at 60 °C. The solvents present in the 20 % stock solution contains 20.6 wt. % nafion dissolved in mixture of 20 wt. % water and 60 wt. % alcohols as solvent [Kawai (2005)]. Initially, volatile solvents (alcohols) may evaporate, leaving alcohol lean and water rich solvent behind. In these circumstances, phase separation of nafion in water rich phase (in which nafion is insoluble) might occur, leading to void formation (Figure 5.2.9a).

Similar phenomenon of void formation during CA membranes casted from its acetone or THF solution was reported [Kawakami (1982)]. In the present case, voids disappeared after these membranes were dipped into AN for 12 hours and subsequently dried at 60 °C (Figure 5.2.9b). This also indicated that, the Nafion chains in swollen state relaxed in favorable state, leading to collapse of these void volumes. These voids were also absent in Nafion membranes after dipping in PIL solution (6 wt. % in AN) for 24 hrs (Figure 5.2.9c). Figure 5.2.9d shows the surface image of nafion membrane impregnated in PIL solution for 36 hours, wherein clustering of PIL on the nafion surface could be seen.

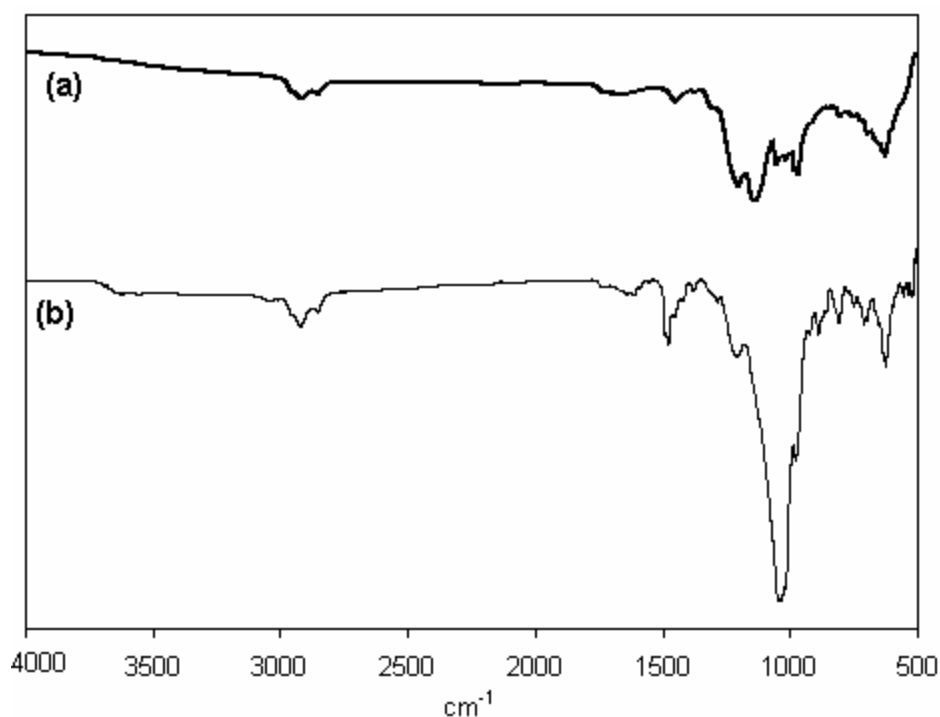


Figure 5.2.10 ATR image of (a) nafion and (b) nafion membrane impregnated with PIL for 36 hours

The ATR spectra of (Figure 5.2.10) showed a strong peak at 1030 cm^{-1} attributed to the B-F stretching vibration, confirming the presence of PIL on the membrane surface, which was dipped in PIL solution. Absence of this peak in case of nafion membrane confirmed the presence of PIL on the nafion surface.

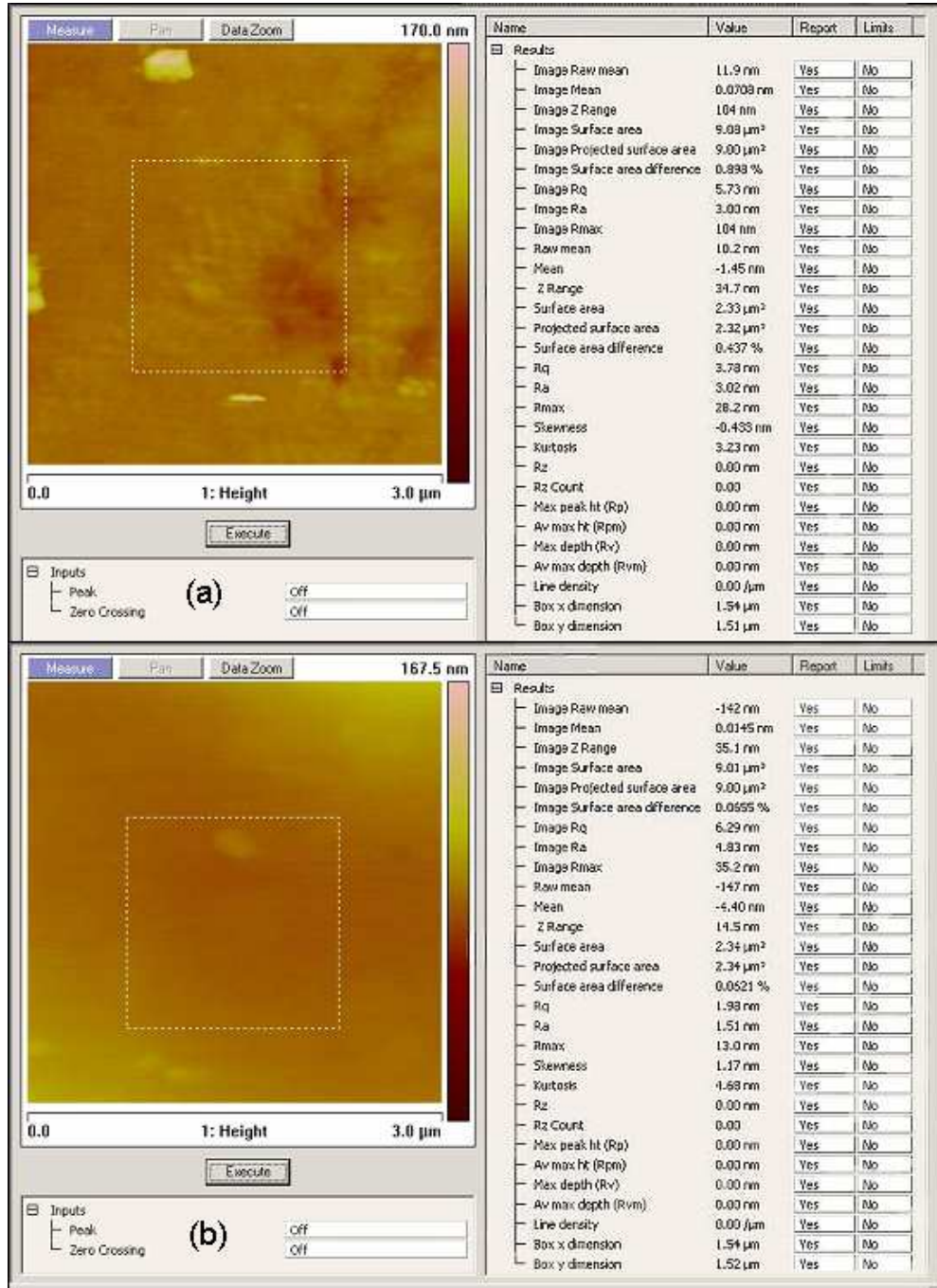


Figure 5.2.11 AFM surface image of a) Nafion b) nafion membrane impregnated with PIL for 36 hours

Figure 5.2.11 showed AFM image of the surface and image statistics for the nafion and PIL impregnated nafion membrane. After impregnation, the surface became smooth as compared to the surface of neat nafion membrane. R_q is the standard deviation of all the Z values (vertical distance) within the enclosed area, R_a is the mean roughness of the surface relative to the center plane and R_{max} is the difference in height between the highest and the lowest points on the surface relative to the mean plane [Fritzsche (1993)]. Surface roughness was analyzed for at least four different surface areas. The observed R_{max} for nafion membrane (28.2 nm) was reduced in case of PIL impregnated nafion membranes (13 nm). This indicated that the surface smoothening could be due to presence of PIL over nafion membrane surface.

The effect of PIL impregnation on weight and dimensional change of nafion membrane are presented in Table 5.2.6. After PIL impregnation, though membrane gained nominal weight (0.8 %), a 30 % increase in thickness and 14.4 % reduction in the membrane area were noted. The decrease in area by 14 % and an increase in volume by 11.2 % after dipping the nafion membrane into PIL solution are indicative of PIL-nafion interactions.

Table 5.2.6 Effect of PIL impregnation on weight and dimensional change of nafion membrane

% change			
Wight	Thickness	Area	Volume
0.8	30	-14.4	11.2

5.2.4.8 Permeation properties of nafion and composite membranes

The gas permeation performance for CO₂ and N₂ for the as casted nafion membranes, solvent treated nafion membrane and PIL impregnated composite membranes were as presented in Table 5.2.7. The permeation properties of the as casted nafion membrane were considerably different from that of solvent treated nafion membrane as well as the essentially dry commercial nafion membrane (Nafion 117). The comparison of these three types of nafion membranes were presented in Table 5.2.7. The as casted membrane were dipped into the acetonitrile for 12 hours to study the morphology by SEM as well as permeation properties of solvent treated nafion

membrane (as the PIL impregnated composite membranes were prepared using acetonitrile solution of PIL). The as casted nafion membrane showed highest permeability for both the gases, while almost 66 % reduction in permeability for both gases was resulted in the case of acetonitrile treated membranes without lose in CO₂/N₂ selectivity. The reported permeability of essentially dry nafion 117 membranes was lower by 96-97 % for both the gases than as casted nafion membrane [Chiou (1988)]. The trend observed in the permeation properties of these three types of nafion membranes may be attributed to the difference in the morphology of the membranes as observed by SEM (Figure 5.2.9) and possibility of water being present in the matrix. The as casted nafion membranes showed void structure (Figure 5.2.9a). Nafion is highly hygroscopic, and sorption of water can increase the permeability to gases by substantial amounts [Chiou (1988)]. The presence of void and moisture uptake may be combinely responsible for the observed high permeability than that of dry membranes reported by Chiou et al. [1988]. The lower permeability of the solvent treated nafion membrane than as casted nafion membrane could be anticipated after disappearance of void volumes. The selectivity of CO₂/N₂ for as casted as well as solvent treated nafion membrane was almost similar, though there was marked difference in permeability. This confirms that the void present in the casted nafion membranes were of closed type. The 31 % lower CO₂/N₂ selectivity of nafion 117 membrane than as casted or solvent treated nafion membrane may be due to the considerably lower CO₂ permeability of earlier type. The nafion 117 membrane was supposed to be essentially dry membrane and thus absence of water may be a reason for its lower permeability.

Table 5.2.7 Permeability and selectivity of nafion-PIL composite membranes

Gas	Nafion membrane			PIL impregnated membrane		
	As casted	Solvent treated	Essentially dry Nafion 117 ^a	6 hr	24 hr	36 hr
N ₂	8.4	2.81	0.26	0.50	0.43	0.5
CO ₂	133	44.8	2.85	9.1	8.91	13.8
CO ₂ /N ₂	15.8	15.94	10.96	18.14	20.69	27.6

^a: From [Chiou (1988)]

The composite membranes prepared by dipping as casted nafion membrane in PIL solution in acetonitrile for different time intervals demonstrated large drop in CO₂ and N₂ permeability with improved CO₂/N₂ selectivity in comparison to the as casted nafion membrane. Among 6 and 24 hours dipped membrane, almost no change in permeability of CO₂ and N₂ with slight increase in selectivity for the later case was noted. The 36 hours dipped membrane revealed high CO₂ permeability with similar N₂ permeability as that of 6 or 24 hour PIL-dipped membrane; which resulted into improved CO₂/N₂ selectivity for the former case. Thus, CO₂/N₂ selectivity increased with dip time while the improvement was 1.7 and 3 times higher than solvent treated and essentially dry nafion 117 membrane, respectively. The gas permeation study of these PIL impregnated composite membranes successfully demonstrated the usefulness of PIL to prepare composite membranes.

5.2.5 Conclusions

Poly(ionic liquid) was prepared by ion exchange method using readily available polyelectrolyte, PVBTMACl, containing quaternary ammonium group. The quantitative analysis of PIL for residual Cl⁻ was performed by conductometric titration, which was found to be 4.7 %. The appearance of the peak at 1056 cm⁻¹, in FTIR confirmed the conversion of Cl⁻ anion to BF₄⁻. The WAXD spectra showed that both, PVBTMACl and PVBTMABF₄ were amorphous in nature. PVBTMACl exhibited lower d_{sp} (4.34 Å) than that of PVBTMABF₄ (4.63 Å). Though the backbone of both polymers was same, the observed difference in d_{sp} might be ascribed to the difference in size of the anions. The precursor polymer exhibited higher T_g than PVBTMABF₄. The lower T_g in case of PVBTMABF₄ may be due to a strong plasticizing effect of tetrafluoroborate anions.

Both, the precursor (PVBTMACl) and the PIL (PVBTMABF₄) exhibited dual mode sorption. PIL showed significantly higher sorption for CO₂ than that of precursor, PVBTMACl. The sorption selectivity CO₂/N₂ was significantly higher in case of PIL than that of PVBTMACl. This indicated that the BF₄⁻ anion contributed to the increased CO₂ sorption in PIL. PIL showed high solubility selectivity for CO₂/N₂ in comparison to the same for other glassy polymers such as polycarbonates, polyarylates, polysulfones, etc.

In view of inability of PIL to be converted into a thin film, nafion-PIL composite membranes were prepared in order to achieve chain anchoring on nafion surface. The ATR and AFM study of these composite membranes confirmed the presence of PIL on the surface of nafion.

The permeation properties of the as casted nafion membrane were largely different from the solvent treated nafion membrane as well as the essentially dry commercial nafion membrane (Nafion 117). The trend observed in the permeation properties of these three types of nafion membranes may be attributed to the difference in the morphology of the membranes and water associated with the nafion membranes. The composite membranes exhibited lower permeability and improved CO₂/N₂ selectivity in comparison to the as casted nafion membrane.

References

- Acharya H., Srivastava S.K., Bhowmick A.K. *Polym. Engg. Sci.* (2006) 837-843.
- Anthony J.L., Maginn E.J., Brennecke J.F. *J. Phys. Chem. B* **106** (2002) 7315-7320.
- Baltus R.E., Culbertson B.H., Dai S., Luo H., DePaoli D.W. *J. Phys. Chem. B* **108** (2004) 721-727.
- Barbari T.A., Koros W.J., Paul D.R. *J. Membr. Sci.* **42** (1989) 69-86.
- Barrer R.M. In *Diffusion in Polymers* Crank J., Park G.S. (eds.), Academic Press: London 1968 pp 165-217.
- Bates E.D., Mayton R.D., Ntai Jr I., Davis J.H. *J. Am. Chem. Soc.* **124** (2002) 926-927.
- Blanchard L.A., Gu Z., Brennecke J.F. *J. Phys. Chem. B* **105** (2001) 2437-2444.
- Blanchard L.A., Hancu D., Beckman E.J., Brennecke J.F. *Nature* **399** (1999) 28-29.
- Cadena C., Anthony J.L., Shah J.K., Morrow T.I., Brennecke J.F., Maginn E.J. *J. Am. Chem. Soc.* **126** (2004) 5300-5308.
- Camper D., Scovazzo P., Koval C., Noble R. *Ind. Eng. Chem. Res.* **43** (2004) 3049-3054.
- Chang J., An Y.U., Sur G.S. *J. Polym. Sci., Part B: Polym. Phys.* **41** (2003) 94-103.
- Chiou J.S., Paul D.R. *Ind. Eng. Chem. Res.* **27** (1988) 2161-2164.
- Costello L.M., Koros W.J. *J. Polym. Sci., Part B: Polym. Phys.* **33** (1995) 135-146.
- Domanska U., Bogel-Lukasik R. *J. Phys. Chem. B* **109** (2005) 12124-12132.
- Dunkley-Timmerman T. Ph.D. Dissertation, The University of Texas at Austin, Austin, TX, 1988.
- Elliott J.A., Hanna S., Elliott A.M.S., Cooley G.E. *Polymer* **42** (2001) 2251-2253.
- Fritzsche A.K., Arevalo A.R., Moore M.D., O'Hara C. *J. Membr. Sci.* **81** (1993) 109-120.
- Ghosal K., Freeman B.D. *Polym. Adv. Tech.* **5** (1994) 673-697.
- Giannelis E.P. *Adv. Mater.* **8** (1996) 29-35.
- Giannelis E.P. *Appl. Organomet. Chem.* **12** (1998) 675-680.

- Hegazy E.A., Abd El-Rehim H.A., Khalifa N.A., El-Hag Ali A. *Radia. Phys. and Chem.* **55** (1999) 219-229.
- Hellums M.W., Koros W.J., Husk G.R., Paul D.R. *J. Membr. Sci.* **46** (1989) 93-112.
- Hotta S., Paul D.R. *Polymer* **45** (2004) 7639-7654.
- Hsiao S-H., Liou G-S., Chang L-M. *J. Appl. Polym. Sci.* **80** (2001) 2067–2072.
- Jeong H-K., Krych W., Ramanan H., Nair S., Marand E., Tsapatsis M. *Chem. Mater.* **16** (2004) 3838-3845.
- Kamps A.P-S., Tuma D., Xia T.J., Maurer G.J. *Chem. Eng. Data* **48** (2003) 746-749.
- Kawai J., Otsuki T., Kakuta M., Goto K., Kanaoka N., Asano Y, Takahashi R. US patent, 2005 US 2005/0106469 A1.
- Kawakami M., Iwanaga H., Hara Y., Iwamoto M., Kagawa S. *J. Appl. Polym. Sci.* **27** (1982) 2387-2393.
- Kazarian S.G., Briscoe B.J., Welton T. *Chem. Commun.* **20** (2000) 2047-2048.
- Kharul U.K., Kulkarni S.S., Kulkarni M.G., Houde A.Y., Charati S.G., Joshi S.G. *Polymer* **39** (1998) 2011-22.
- Khayankarn O., Magaraphan R., Schwank J.W. *J. Appl. Polym. Sci.* **89** (2003) 2875-2881.
- Kubota H., Suka I.G., Kuroda S-I., Kondo T. *Eur. Polym. J.* **37** (2001) 1367-1372.
- Kumar V., Bhardwaj Y.K., Jamdar S.N., Goel N.K., Sabharwal S. *J. Appl. Polym. Sci.* **102** (2006) 5512–5521.
- Lan T., Kaviratna P.D., Pinnavaia T. *Chem. Mater.* **6** (1994) 573-575.
- Li X., Kang T., Cho W.-J., Lee J.-K., Ha C.-S. *Macromol. Rapid Commun.* **22** (2001) 1306-1312.
- Manninen A.R., Naguib H.E., Nawaby A.V., Day M. *Polym. Engg. Sci.* (2005) 904-914.
- Marcilla R., Blazquez J.A., Rodriguez J., Pomposo J.A., Mecerreyes D. *J. Polym. Sci. Part A: Polym. Chem.* **42** (2004) 208–212.

- McHattie J.S., Koros W.J., Paul D.R. *Polymer* **33** (1992) 1701-1711.
- Merkel T.C., Freeman B.D., Spontak R.J., He Z., Pinnau I., Meakin P., Hill A.J. *Chem. Mater.* **15** (2003b) 109-123.
- Merkel T.C., He Z., Pinnau I., Freeman B.D., Meakin P., Hill A.J. *Macromolecules* **36** (2003a) 6844-6855.
- Messersmith P.B., Giannelis E.P. *J. Polym. Sci., Part A: Polym. Chem.* **33** (1995) 1047-1057.
- Morgan A.B., Harris J.D. *Polymer* **44** (2003) 2313-2320.
- Neilson L.E. *J. Macromol. Sci. (Chem.) A1* **5** (1967) 929.
- Noda A., Watanabe M. *Electrochimica Acta* **45** (2000) 1265-1270.
- Ono M., Kanagawa A.M. EP Patent (2001) EP1 116769 A2.
- Osman M.A., Mittal V., Lusti H.R. *Macromol. Rapid Commun.* **25** (2004) 1145-1149.
- Pixton M.R., Paul D.R. *Macromolecules* **28** (1995) 8277-8286.
- Priya L., Jog J.P. *J. Polym. Sci., Part B: Polym. Phy.* **40** (2002) 1682-1689.
- Puleo A.C., Paul D.R., Kelley S.S. *J. Membr. Sci.* **47** (1989) 301-332.
- Rutherford S.W., Kurtz R.E., Smith M.G., Honnell K.G., Coons J.E. *J. Membr. Sci.* **263** (2005) 57-65.
- Ryu S.H., Chang Y-W. *Polym. Bull.* **55** (2005) 385-392.
- Sakai, T.; Takenaka, H.; Torikai, E. *J. Membr. Sci.* **31** (1987) 227-234.
- Scovazzo P., Kieft J., Finan D.A., Koval C.D., DuBois L., Noble R.D. *J. Membr. Sci.* **238** (2004) 57-63.
- Shen Z., Simon G., Cheng Y-B. *Polymer* **43** (2002) 4251-4260.
- Shen Z., Simon G.P., Cheng Y-B. *Polymer* **43** (2002) 4251-4260.
- Sinha R.S., Yamada K., Okamoto M., Ogami A., Ueda K. *Chem. Mater.* **15** (2003) 1456-1465.
- Strawhecker K.E., Manias E. *Chem. Mater.* **12** (2000) 2943-2949.

- Suarez P.A.Z., Dullius J.E.L., Einloft S., Desouza R.F., Dupont J. *Polyhedron* **15** (1996) 1217-1219.
- Takahashi S., Goldberg H.A., Feeney C.A., Karim D.P., Farrell M., O'Leary K., Paul D.R. *Polymer* **47** (2006) 3083-3093.
- Tang J., Tang H., Ding S., Radosz M., Shen Y. *J. Polym. Sci., Part A: Polym. Chem.* **43** (2005b) 1432-1443.
- Tang J., Tang H., Sun W., Plancher H., Radosz M., Shen Y. *Chem. Commun.* **26** (2005a) 3325-3327.
- Vaia R.A., Giannelis E.P. *Macromolecules* **30** (1997) 8000-8009.
- van Amerongen G. J. *Rubber Chem. Technol.* **37** (1964) 1065.
- Van Krevelen D.W., Hoftyzer P.J. Properties of polymers: Correlation with chemical structure. Amsterdam: Elsevier Publishing Company 1972. pp.378.
- Vega A.M., Paul D.R. *J. Polym. Sci., Part B: Polym. Phys.* **31** (1993) 1577-1589.
- Vieth W R, Howell J.M. Hsieh J H. *J. Membr. Sci.* **1** (1976) 177-220.
- Vieth W.R., Tam P.M., Michaels A.S. *J. Colloid and Interface Sci.* **22** (1966) 360-370.
- Wagner C.D., Riggs W.M., Davis L.E., Moulder J.E., Muilenberg G.E. Handbook of X-ray Photoelectron Spectroscopy Published by Perkin-Elmer Corporation, 1979.
- Wang A., Pinnavaia T. *J. Polym. Mater. Sci. Eng.* **82** (2000) 274-275.
- Wang D., Paiuow D., Yao Q., Wilkie C.A. *J. Vinyl and additive tech.* **7** (2001) 203-213.
- Wang Z.F., Wang B., Qi N., Zhang H.F., Zhang L.Q. *Polymer* **46** (2005) 719-24.
- Xu R., Manias E., Snyder A.J., Runt J. *Macromolecules* **34** (2001) 337-339.
- Yano K., Usuki A., Okada A., Kurauchi T., Kamigaito O. *J. Polym. Sci., Part A: Polym. Chem.* **31** (1993) 2493-2498.
- Yeo R.S. *Polymer* **21** (1980) 432-435.
- Yoshizawa M., Ogihara W., Ohno H. *Polym. Adv. Technol.* **13** (2002) 589-594.

Chapter 6

Conclusions

The objective of the present thesis was to explore three potential methodologies, viz., polymer modification, monomer structure variations and composite membranes to improve gas permeation properties.

1. The backbone of highly permeable PPO was modified via Friedel-Craft benzoylation, nitration and amination. These PPO modifications rendered amorphous polymers in spite of the polar nature of introduced benzoyl, nitro and amino groups. The T_g was increased, while d-spacing, fractional free volume and thermal stability were decreased in comparison to PPO, owing to induced polarity. Increased packing density resulted into lower gas permeability than the unsubstituted PPO. Benzoylated PPO exhibited improved O_2/N_2 , Ar/N_2 and helium based selectivities. In these cases, an extent of decrease in permeability followed the trend of increasing molar mass of gases and not the kinetic diameter. Nitrated and aminated derivatives exhibited good improvement in CO_2 based selectivities. The gas sorption analysis revealed that the nitro group substitution was more effective in improving solubility selectivity, while amino group substitution was more effective in improving diffusivity selectivity.

2. The monomer level structural variations while varying nature (bulky/polar), site of substitution on bisphenol/diacid moiety of polyarylates was investigated for subsequent variations in gas permeation and related physical properties. The substitution of bulky isopropyl group on bisphenol in asymmetric manner offered the polymer with reduced packing density and T_g than its unsubstituted analogue. The lowering in T_g was ascribed to the plasticizing effect of isopropyl group. Polyarylates obtained with this bisphenol and varying dicarboxylic acid showed increased permeability and reduced selectivity than polyarylate with unsubstituted dicarboxylic acid. The selectivity could be improved by introducing polar group on dicarboxylic acid.

The substitution of bulky flat phenyl ring on bisphenol in asymmetric manner in DiPhBisA based polyarylates increased v_f than that of unsubstituted BisA-I+T. The

lowering in T_g in this case in spite rigid nature of the phenyl ring was attributed to the nature of substitution, which is asymmetric. The decreased permeability in DiPhBisA-I+T than for unsubstituted BisA-I+T was associated with increased selectivities for various gas pairs (except for $\alpha\text{CO}_2/\text{N}_2$), owing to the flat nature of phenyl ring. Polar group substitution on terephthalic acid moiety decreased permeability and increased selectivity. The effect of bulk of hexafluoroisopropyl group and *t*-butyl group present on acid moiety was reflected in increasing the permeability than DiPhBisA-I+T. The CO_2 based selectivities were improved in DiPhBisA-HFA.

The bridge substitution by 9,9'-fluorenylidene in bisphenol moiety increased chain stiffness of resulting polyarylates. The effects of this substitution on gas permeability and selectivity was more marked when the bisphenol rings were asymmetrically substituted. The asymmetric substitution by methyl group on bisphenol phenyl rings led to reduction in permeability, while asymmetric ring substitution by bromine and methyl group in DBrDMFBP based polyarylate though increased permeability, led to lowering in selectivity. This was attributed to the presence of flat 9,9'-fluorenylidene group at the bridge position.

The asymmetric bromine substitution on HFBisA increased packing density and lowered T_g , than the polyarylate based on HFBisA. Gas permeability though was reduced by 24-87 %, selectivities were enhanced up to 575 % attributed to the polar nature of bromine as well as its asymmetric type of substitution. The substitution on acid moiety of polyarylates based on DBrHFBisA improved solubility of gases and decreased diffusivity (in case of polar group substitution) as a consequence of increased chain interactions. This properly chosen substitution methodology led these polymers to lie on Robeson's upper bound. Polyarylates based on dibromoterephthalic acid enhanced the understanding towards effects of polarity.

3. Two approaches of composite membranes viz., polyarylate based nanocomposite membranes with clay and polyionic liquid-nafion membrane composite were investigated for gas permeation and related analyses. With varying clay loading in polyarylate, an increase in solution viscosity, nanocomposite density and reduction in the T_g of nanocomposites (associated with the plasticization effect) was observed. Due to the

addition of clay particles into the polymer matrix, though permeability of gases reduced as a consequence of induced tortuous path, after certain loading, an increase in selectivity indicated promises of this approach in improving selectivity.

A Simple and convenient ion exchange process was employed to obtain poly(ionic liquid). Though it exhibited improved CO₂ sorption capacity, efforts to utilize this material in conventional membrane form did not succeed. An altogether different approach of anchoring these PIL chains on swollen matrix of nafion membrane, followed by gas permeability investigations depicted the potential of this approach. The CO₂/N₂ selectivity was almost doubled due to PIL chain anchoring on nafion surface.

Synopsis of the thesis entitled

“Investigations on gas permeation and related physical properties of structurally architected aromatic polymers (polyphenylene oxides and polyarylates), polyarylate-clay nanocomposites and poly (ionic liquid)”

By

Y.S. Bhole

Polymer Science and Engineering Division, National Chemical Laboratory,
Dr. Homi Bhabha Road, Pune- 411 008

Introduction

An economic viability of gas separation process using polymeric membranes depends on intrinsic permeation characteristics of the polymer used for membrane preparation. Material research in this area is directed towards invention of newer polymers that would have simultaneous combination of high permeability, selectivity and ability to be processed into required membrane form. Basic understanding towards effects of variation in material properties following various methodologies (e.g. structural variation, blending, etc.) on gas permeation properties is essential to design materials with desired properties, which forms an objective of present thesis.

A study of structure-property relationship in glassy polymers has identified certain heuristic rules for the design of gas separation membrane material. Structural changes that inhibit packing of relatively rigid chains lead to increased permeability while maintaining permselectivity [1]. Furthermore, structural changes that reduce rotational mobility around flexible linkages in the polymer backbone lead to higher permselectivity without loss in permeability if intersegmental packing is not significantly affected [2]. Another observation is that unsymmetrical aromatic unit in the polymer backbone lead to higher permselectivity and lower permeability, which can be attributed

to higher packing density [3,4]. Such heuristic rules can be better strengthened by widening an understanding of structure-gas permeation property correlation.

The objective of this thesis was to investigate two strategies for improvement in gas permeation properties of polymeric materials; (a) basic structural variations and (b) composites containing one of the components that systematically affects intrinsic permeation properties. The effects of structural variations were addressed for two families of promising polymers: (i) polyphenylene oxide (PPO) and (ii) polyarylates. The PPO backbone was modified by substituents possessing simultaneous bulk and polarity; while, polyarylates were synthesized using monomers possessing select substituents. Two types of composite materials, one based on polyarylate-clay nanocomposite and another based on polyionic liquids were investigated to analyze their effects on selectivity. The thesis has been divided into following chapters:

Chapter 1: Gas permeation: Theoretical aspects and structure-property relationship

This chapter briefly reviews theoretical aspects of gas permeation in polymeric materials and the structure-property relationship aimed at improving permeation properties by adopting promising strategies/methodologies.

Chapter 2: Scope and objectives of the present work

This chapter discusses the scope and objectives of present work.

Chapter 3: Structural modifications in Polyphenylene oxide (PPO): Effects of substituents possessing simultaneous bulk and polarity

In this chapter, the effects of PPO backbone modifications by groups those are simultaneously bulky and polar on their physical and gas permeation properties are presented.

The PPO backbone was substituted with benzoyl, nitro, amine and amide functionality, possessing bulk and polarity. The highest possible degree of substitution was achieved by tuning reaction protocols for the substituted PPO in such a way that the dense membranes of which could sustain the applied gas pressure during permeability measurements. This was made possible in above mentioned cases, except for a PPO containing amide functionality. The gas sorption analysis was also performed in case of nitrated and aminated derivatives of PPO to explore effects of these substitutions on sorption of gases in the polymer matrix.

In case of benzoylated PPO, packing density was increased and thus the gas permeability was found to decrease. The helium and oxygen based selectivities were increased, while CO₂ based selectivities were decreased. This complex trend observed in the gas permeation properties is explained on the basis of nature of substituent and the degree of substitution.

Both, nitro and amino group substitution on PPO led to decrease in pure gas permeability and increased selectivity of various gas pairs; exhibiting distinct variation than benzoylation. The gas sorption analysis revealed that both, solubility selectivity and diffusivity selectivity were increased by these polar group substitutions. The nitro group substitution was more effective in improving solubility selectivity while amino group substitution was more effective in improving diffusivity selectivity.

Chapter 4: Investigations in polyarylates: Effect of asymmetric ring substitution on bisphenol and polar/bulky group substitution on acid

The effects of substitution on (i) bisphenol moiety in asymmetric manner by varying substituent type, (ii) varying bulk or polarity of the acid moiety and (iii) effects

of combination of these two substitution types in resulting polyarylates are addressed in this chapter. The synthetic aspects, physical and gas permeation properties of polyarylates with above types of substitution is categorized in the thesis as follows:

- Polyarylates based on asymmetrically substituted bisphenol (diisopropyl bisphenol-A, di-*t*-butyl bisphenol-A and diphenyl bisphenol-A) with dicarboxylic acids containing various substituents.
- Polyarylates based on systematically substituted fluorene bisphenol and dibromohexafluoro bisphenol-A; addressing combined effects of bridge and ring substitution with dicarboxylic acids containing various substituents.
- Polyarylates based on dibromoterephthalic acid, in which acid moiety was substituted by polar bromine.

All polyarylates synthesized in the present work were amorphous in nature, possessed good solvent solubility and moderately high glass transition temperature.

Polyarylates based on asymmetric, bulky group substituted diisopropyl bisphenol-A exhibited higher permeability for various gases in comparison to the polyarylate based on unsubstituted bisphenol-A. This was attributed to the increased v_f due to the bulky nature of the isopropyl substituent. Conversely, an asymmetric substitution by phenyl group owing to its planar geometry reduced gas permeability and increased selectivity than polyarylate based on unsubstituted bisphenol-A.

The bridge substitution by 9,9'-fluorenylidene in bisphenol moiety increased chain stiffness of resulting polyarylates. Effects of this group substitution on gas permeability and selectivity was more marked when the bisphenol rings were appropriately substituted. The asymmetric ring substitution by bromine and methyl group

in DBrDMFBP based polyarylate though increased permeability, showed lowering of selectivity. This was attributed to the presence of flat 9,9'-fluorenylidene group at the bridge position.

In case of polyarylates based on dibromohexafluorobisphenol-A, the substitution of polar bromine in asymmetric manner reduced gas permeability and increased selectivity to a great extent in comparison to unsubstituted hexafluorobisphenol-A based polyarylates obtained using the same dicarboxylic acid.

The presence of hexafluoroisopropylidene or bulky tert-butyl group in dicarboxylic acid moiety increased the permeability by almost two times while decreasing selectivity, whereas the presence of polar group on diacid moiety decreased the permeability with increase in selectivity, in comparison to polyarylate based on iso/terephthalic acid.

In case of dibromoterephthalic acid based polyarylates, the permeability decreased with increase in permselectivity for various gases in comparison to polyarylates based on terephthalic acid.

Chapter 5. Composite membrane materials: Tuning gas permeation properties by using organically modified clay and polyionic liquid

This chapter deals with exploration of potential of composite membrane materials to improve gas permeation properties favorably. Two different approaches were evaluated in membranes based on clay-polyarylate nanocomposites and use of polyionic liquid (PIL) that exhibited high CO₂ sorption capability. Gas permeation properties were studied and correlated with physical properties.

Polyarylate-clay nanocomposites: preparation, evaluation of physical properties and gas permeability

The MMT based clays in varying proportions were used to form nanocomposites with polyarylates by solution intercalation method. The physical and gas permeation properties of resulting nanocomposites were analyzed and correlated. An increase in disorder of the clay structure, an increased solution viscosity and nanocomposite density indicated polymer-clay interactions. Though a general decrease in gas permeability was observed, an increase in He/CH₄ selectivity at 7 % clay loading indicated the usefulness of forming nanocomposites towards improving gas selectivity. Based on measured He gas permeability of these nanocomposites, aspect ratio was estimated using Neilson's model. This aspect ratio correlated well with better observed dispersion in case of 10A based nanocomposites than 6A based.

Poly(ionic liquid): Preparation, sorption analysis and composite membrane investigations

In this chapter, the process for preparation of PIL and its use as an additive to form composite membrane is described. Tang et al. [5] proposed that transforming ionic liquids into polymeric form significantly enhance CO₂ sorption capacity. The objective of the present work was to explore the better route for PIL preparation and evaluate membrane performance. The chloride anion of poly(vinylbenzyltrimethylammonium chloride) (PVBTACl) was exchanged with promising anion, tetrafluoroborate (BF₄⁻) by a simple and convenient ion exchange method. Since PIL could not be transformed into dense membrane form, the composite membranes were attempted with an objective of improving CO₂ selectivity.

The gas sorption analysis of the precursor polymeric chloride salt, as well as BF_4^- exchanged PIL was done for CO_2 , N_2 and CH_4 using pressure decay method. Both the materials showed dual-mode sorption and the sorption parameters were evaluated to correlate with material properties. The composite membranes of PIL were prepared by dipping nafion membranes into the PIL solution. The gas permeation properties of these composite membranes for CO_2 and N_2 showed almost two fold increase in CO_2/N_2 selectivity in comparison to nafion membrane. Morphology of PIL-nafion composite membranes was studied by scanning electron microscopy.

Chapter 6. Conclusions

This chapter summarizes the results and conclusions of this work.

References

1. W.J. Koros, G.K. Fleming, *J. Membr. Sci.* **83** (1993) 1-80.
2. J.S. McHattie, W.J. Koros, D. Paul, *Polymer* **33** (1992) 1701-1711.
3. J.S. McHattie, W.J. Koros, D. Paul, *Polymer* **32** (1991) 840-850.
4. J.C. Schmidhauser, K.L. Longley, *J. Appl. Polym. Sci.* **39** (1990) 2083-2096.
5. J. Tang, H. Tang, W. Sun, H. Plancher, M. Radosz, Y. Shen, *Chem. Comm.* **26** (2005) 3325-3327.

List of publications

- 1) Y.S. Bhole, UK Kharul, 'Effect of fluorene-bisphenol ring substitution and bridge rigidity on physical and gas permeation properties of resulting polyarylates', *Polymer International*, 52 (2003) 1474-1479.
- 2) Y.S. Bhole, U.K. Kharul, S.P. Somani and S.C. Kumbharkar, 'Benzylation of Polyphenylene oxide: Characterization and gas permeability investigations', *European Polymer Journal*, 41(2005) 2461-2471.
- 3) Y.S. Bhole, P.B. Karadkar, U.K. Kharul, 'Nitration and Amination of polyphenylene oxide: preparation and gas permeation study', *European Polymer Journal*, 43 (2007) 1450-1459.
- 4) Y.S. Bhole, S.D. Wanjale, U.K. Kharul, J.P. Jog, 'Assessing feasibility of polyarylate-clay nanocomposites towards improvement of gas selectivity', to be Communicated.
- 5) Y.S. Bhole, P.B. Karadkar, U.K. Kharul, 'Effect of asymmetric polar bromine substitution in hexafluorobisphenol-A based polyarylates: Physical and gas permeation properties" to be Communicated.
- 6) Y.S. Bhole, U. K. Kharul, "Poly(ionic liquid) based membranes: Preparations and permeability investigations" to be Communicated.
- 7) Y.S. Bhole, U.K. Kharul, "Investigations on diisopropyl and diphenyl bisphenol based polyarylates for gas permeation analysis" to be Communicated.